

2010

Novel polythiophene materials for bionic applications

Robert Breukers
University of Wollongong

Recommended Citation

Breukers, Robert, Novel polythiophene materials for bionic applications, Doctor of Philosophy thesis, School of Chemistry, University of Wollongong, 2010. <http://ro.uow.edu.au/theses/3303>

Research Online is the open access institutional repository for the University of Wollongong. For further information contact Manager Repository Services: morgan@uow.edu.au.

UNIVERSITY OF WOLLONGONG

COPYRIGHT WARNING

You may print or download ONE copy of this document for the purpose of your own research or study. The University does not authorise you to copy, communicate or otherwise make available electronically to any other person any copyright material contained on this site. You are reminded of the following:

Copyright owners are entitled to take legal action against persons who infringe their copyright. A reproduction of material that is protected by copyright may be a copyright infringement. A court may impose penalties and award damages in relation to offences and infringements relating to copyright material. Higher penalties may apply, and higher damages may be awarded, for offences and infringements involving the conversion of material into digital or electronic form.

Novel Polythiophene Materials for Bionic Applications.

**A thesis submitted in fulfilment of the requirements for the
award of the degree**

Doctor of Philosophy

from

University of Wollongong

by

Robert Breukers, BSc (Hons)

School of Chemistry

September 2010

CERTIFICATION

I, Robert Breukers, declare that this thesis, submitted in fulfilment of the requirements for the award of Doctor of Philosophy, in the School of Chemistry, University of Wollongong, is wholly my own work unless otherwise referenced or acknowledged. The assistance of Dr Klaudia Wagner with electrochemistry, Dr Tony Romeo for SEM images and Dr Michael Higgins for AFM imaging are noted in the text in each case. The biocompatibility studies on my materials were performed by Dr Kerry Gilmore, Dr Anita Quigley, and Ms. Magdalena Kita this is also noted in the relevant section. The document has not been submitted for qualifications at any other academic institution.

Robert Breukers

September 2010

ABSTRACT

Bionics is the revolutionary area of medical research concerned with the interface between biology and electronics. For the next generation of bionic devices, new electromaterials need to be developed. Conducting polymers are excellent candidate electromaterials for these bionic devices. Due to their ease of synthesis and functionalisation, polythiophenes are one of the best candidate conducting polymers. Here the synthesis and optimisation of novel polythiophene materials for bionic applications was investigated. The research focused on four key properties that are desirable for bionic materials; functionality, biodegradability, processability and biocompatibility.

The introduction of functionality into polythiophene materials was demonstrated through the synthesis of several terthiophene building blocks. Functionalisation of these terthiophene building blocks was demonstrated by the attachment of amino acid, barbituric acid and spiropyran functionalities. The functionalised terthiophenes could be polymerised to yield functional polymers. Spiropyran functionalised polymers were of particular interest as conformational changes in these materials could be electrically induced.

The development of biodegradable conducting polymers was initially investigated with the development of conducting azomethine linked thiophene oligomers. The stability of azomethine materials was investigated and they were found to be susceptible to acid hydrolysis. Then the synthesis of several novel terthiophene and sexithiophene oligomers via Stille coupling as precursors to biodegradable conducting polymers was explored.

Films and aligned electrospun fibres of ester functionalised poly(octanoic acid 2-thiophen-3-yl ethyl ester) were fabricated. Further functionalisation of these structures was demonstrated through hydrolysis of the ester and functionalisation of the films and fibres with ferrocene acid chloride. The electrochemistry and surface properties of these structures was compared with the hydrolysed structures being more hydrophilic and showing a much greater electrochemical response in aqueous electrolyte.

The biocompatibility of several polythiophene materials was tested with C2C12 muscle cells, which were shown to be compatible with these materials. Smoother spin coated films were seen to be better scaffolds than rough electropolymerised films, for supporting cell differentiation of sensitive ROSA primary muscle cells. Aligned polythiophene fibre structures on gold Mylar were investigated for controlling the direction of ROSA cell differentiation. Fibres spaced between 15-100 μm apart gave the best directional cues to the cells and most efficiently promote alignment of myotubes. The insights and knowledge gained during this study will help in the development and application of conducting polymer materials for bionic applications.

ACKNOWLEDGEMENTS

I would like to thank my supervisors, Professor Gordon Wallace and Professor David Officer for all their guidance, help, ideas and support throughout my project. I appreciate the contributions and assistance of Dr Klaudia Wagner for electrochemistry, Dr Tony Romeo for SEM images and Dr Michael Higgins for AFM imaging. I am grateful to Dr Kerry Gilmore, Dr Anita Quigley, and Ms. Magdalena Kita for performing biocompatibility studies on my materials. I would also like to thank Dr Pawel Wagner, Dr Sanjeev Gambhir and Dr Syed Ashraf for advice on organic synthesis and supplying starting materials.

I am grateful to Professor Dermot Diamond and the research team of the National Centre for Sensor Research, Dublin City University for assistance with the spiropyran functionalised terthiophene studies, particularly Dr Robert Byrne for assistance with synthesis and Dr Fernando Benito-Lopez for the fabrication of the electrode chip. I would like to acknowledge the financial support of the Australian Research Council's Australian Postgraduate Award and Professor Gordon Wallace for my PhD scholarship.

I appreciate the help and friendship of the staff and students of the Intelligent Polymer Research Institute. In particular Simon Moulton, Scott McGovern, Dan Li, George Tsekouras, Grace Stevenson, Alberto Javier Granero Rodriguez, Shannon Little, Johana Mbere, David Harman, Adrian Gestos and Benjamin Mueller for helpful advice and interesting discussions. Finally, I would like to thank, my fiancée Jodi, my family and my friends for all their love and support.

PUBLICATIONS.

R. D. Breukers, K. J. Gilmore, M. Kita, K. K. Wagner, M. J. Higgins, S. E. Moulton, G. M. Clark, D. L. Officer, R. Kapsa, and G. G. Wallace. *Creating Conductive Structures for Cell Growth: Growth and Alignment of Myogenic Cell Types on Polythiophenes*, Journal of Biomedical Materials Research: Part A. (2010). 95A, 256-258.

K. Wagner, R. Byrne, M. Zanoni, S. Gambhir, L. Dennany, R. Breukers, M. Higgins, P. Wagner, D. Diamond, G. G. Wallace, D. L. Officer, *Multiswitchable poly(terthiophene) bearing a spiropyran functionality: understanding photo and electrochemical control*, Journal of the American Chemical Society. Accepted (2011).

CONFERENCE PRESENTATIONS.

The 2010 International Conference on Nanoscience and Nanotechnology, Sydney Convention Centre, Sydney, Australia, 22- 26th of February 2010. *Aligned Polythiophene Fibres for Tissue Engineering Applications.*

R. D. Breukers, K. J. Gilmore, M. Kita, K. K. Wagner, M. J. Higgins, S. E. Moulton, G. M. Clark, D. L. Officer, R. Kapsa, and G. G. Wallace.

Advanced Materials and Nanotechnology 4, University of Otago, New Zealand, 8-12th of February 2009. *Polythiophenes as scaffolds for cell growth.*

R. Breukers, K. Wagner, K. Gilmore, S. Moulton, D. Li, A. Quigley, R. Kapsa, M. Kita, D. Officer and G. Wallace.

The International Symposium on Functional Nanomaterials, Dublin City University, Dublin, Ireland, 10-11th of September 2009. *Polythiophenes as scaffolds for cell growth.* Robert Breukers, Klaudia Wagner, Kerry Gilmore, Simon Moulton, Anita Quigley, Robert Kapsa, Magdalena Kita, David Officer and Gordon Wallace.

The 2nd Alan MacDiarmid Symposium on Organic Conductors, Victoria University, Wellington, New Zealand, 14th April 2008. *Polythiophenes as scaffolds for cell growth.* Robert Breukers, David Officer and Gordon Wallace.

ABBREVIATIONS.

2,4-DNP	2,4-dinitrophenylhydrazine
3HT	3-hexylthiophene
AFM	atomic force microscopy
Ar	aromatic
ATR	attenuated total reflection
b.p.	boiling point
BOC	(<i>t</i> -butyloxy) carbamate
BSP	spiropyran
C2C12	mouse myoblast cell line
COD	1,5-cyclooctadiene
CV	cyclic voltammogram
DAPI	4',6-diamidino-2-phenylindole
DBU	1,8-diazabicycloundec-7-ene
DCC	N,N'-dicyclohexylcarbodiimide
DCM	dichloromethane
DCU	Dublin City University
DIPA	diisopropylamine
DIPEA	diisopropylethylamine
DMAP	4-dimethylaminopyridine
DMEM	Dulbecco's modified Eagle's medium
DMF	dimethylformamide
dppp	1,3-bis(diphenylphosphino)propane
DT	3-decylthiophene

EDOT	3,4-ethylenedioxythiophene
FBS	fetal bovine serum
FET	field-effect transistor
FTIR	Fourier transform infrared spectroscopy
GPC	gel permeation chromatography
GRIM	Grignard metathesis
HeLa	immortal cell line derived from the cervical cancer cells of Henrietta Lacks
Hep-2	human epidermoid larynx carcinoma cell line
ITO	indium tin oxide
LED	light emitting diode
M	mol/L
MALDI MS	matrix assisted laser desorption ionisation mass spectroscopy
MC	merocyanine
MN	multi nucleation
Mw	molecular weight
NBS	N-bromosuccinimide
NMP	N-methylpyrrolidone
NMR	nuclear magnetic resonance
OTE	octanoic acid 2-thiophen-3-yl ethyl ester
P3AT	poly(3-alkylthiophene)
P3HT	poly(3-hexylthiophene)
PBT	polybithiophene
PC-12	a cell line derived from a pheochromocytoma of the rat adrenal medulla

pd	polydispersity
PDDTTC _c	poly(decyl 4,4''-didecoxy-2,2':5',2''-terthiophene-3'-carboxylate) chemically polymerised
PDDTTC _e	poly(decyl 4,4''-didecoxy-2,2':5',2''-terthiophene-3'-carboxylate) electrochemically polymerised
PDOT _c	poly(3-decoxythiophene) chemically polymerised
PDOT _e	poly(3-decoxythiophene) electrochemically polymerised
PEDOT	poly(3,4-ethylenedioxythiophene)
PEO	polyethylene oxide
PFTE	poly(ferrocene carboxylate 2-thiophen-3-yl ethyl ester)
PHET	poly(3'-(2-hydroxyethyl)thiophene)
POP	poly(3-octylpyrrole)
POTE	poly(octanoic acid 2-thiophen-3-yl ethyl ester)
ppm	parts per million
PS	polystyrene
PTBEO	poly(2,2':5',2''-(terthiophene-3,3''-diyl)bis(ethane-2,1-diyl) dioctanoate)
PTTSPA	poly(2-(3',3'-dimethyl-6-nitrospiro[chromene-2,2'-indoline]-1'- yl)ethyl)-4,4''-didecoxy-2,2':5',2''-terthiophene-3'-acetate
PTTSPC	poly(2-(3',3'-dimethyl-6-nitrospiro[chromene-2,2'-indoline]-1'- yl)ethyl)-4,4''-didecoxy-2,2':5',2''-terthiophene-3'-carboxylate
Red-Al	sodium bis(2-methoxyethoxy)aluminumhydride
RO	reverse osmosis
ROSA	primary skeletal muscle myoblasts cell line from transgenic 129S4Gt 26 mice

rpm	revolutions per minute
r.t.	room temperature
SEM	scanning electron microscopy
TBAB	tetra-n-butylammonium bromide
TBAP	tetrabutylammonium perchlorate
TBApts	tetrabutylammonium <i>para</i> -toluenesulfonate
th	thiophene
THF	tetrahydrofuran
TLC	thin layer chromatography
TMS	trimethylsilane
TTSPA	(2-(3',3'-dimethyl-6-nitrospiro[chromene-2,2'-indoline]-1'-yl)ethyl)- 4,4''-didecoxy-2,2':5',2''-terthiophene-3'-acetate
TTSPC	(2-(3',3'-dimethyl-6-nitrospiro[chromene-2,2'-indoline]-1'-yl)ethyl)- 4,4''-didecoxy-2,2':5',2''-terthiophene-3'-carboxylate
UV	ultraviolet
wt	weight

TABLE OF CONTENTS

CERTIFICATION	i
ABSTRACT.....	ii
ACKNOWLEDGEMENTS	iv
PUBLICATIONS.....	v
CONFERENCE PRESENTATIONS.	vi
ABBREVIATIONS.	vii
TABLE OF CONTENTS	xi
LIST OF FIGURES	xiv
LIST OF TABLES	xxi
CHAPTER 1. INTRODUCTION.	1
1. 1 Introduction.....	1
1. 2 Conducting polymers.	3
1. 3 Conducting polymers in bionics.	5
1. 4 Polythiophenes in bionics.	7
1.4.1 Polythiophenes general introduction.....	7
1.4.2 Functionalised polythiophenes.....	13
1.4.3 Biodegradability.....	15
1. 5 Structure fabrication.....	17
1. 6 Overview of thesis.	20
1. 7 References.....	22
CHAPTER 2. EXPERIMENTAL.....	31
2. 1 General experimental details.....	31
2. 2 Synthetic procedures.	35

2.2.1	Chapter 3.	35
2.2.2	Chapter 4.	50
2.2.3	Chapter 5.	69
2.2.4	Chapter 6.	74
2.3	Electrochemical polymerisations.	78
2.4	Structure fabrications.	81
2.4.1	Spin coating of films.	81
2.4.2	Electrospinning of fibre mats.	81
2.5	Spectroscopic studies.	83
2.6	References.	86
CHAPTER 3. FUNCTIONALISED POLYTHIOPHENE MATERIALS THROUGH TERTHIOPHENE PRECURSORS.		89
3.1	Introduction.	89
3.2	Synthesis of functional terthiophenes.	92
3.3	Synthesis of functionalised terthiophene monomers.	97
3.3.1	Synthesis and polymerisation of barbituric acid functionalised terthiophene.	97
3.3.2	Amino acid functionalisation of terthiophenes.	100
3.3.3	Spiropyran functionalised terthiophenes.	107
3.4	Conclusions.	127
3.5	References.	129
CHAPTER 4. THIOPHENE-BASED OLIGOMER MATERIALS AS A SOURCE OF BIODEGRADABLE CONDUCTING POLYMERS.		133
4.1	Introduction.	133
4.2	Azomethines.	136

4. 3	Autopolymerisation.....	148
4. 4	Thiophene oligomers.....	153
4. 5	Conclusions.....	164
4. 6	References.....	165
CHAPTER 5. POLYTHIOPHENE SCAFFOLD FABRICATION.		169
5. 1	Introduction.....	169
5. 2	Polymer synthesis.	171
5. 3	Polymer film fabrication and characterisation.	174
5. 4	Fibre fabrication by electrospinning.	185
5.4.1	Electrospinning poly(3-hexylthiophene).....	185
5.4.2	Electrospinning of POTE.....	187
5.4.3	Hydrolysis and characterisation of POTE aligned electrospun fibres.	190
5. 5	Ferrocene functionalisation.....	193
5. 6	Conclusions.....	201
5. 7	References.....	202
CHAPTER 6. BIOCOMPATIBILITY OF POLYTHIOPHENE MATERIALS....		205
6. 1	Introduction.....	205
6. 2	Monomer synthesis and polymerisation.	208
6. 3	Biocompatibility results.	214
6. 4	Characterisation of polymer film properties.	221
6. 5	Conclusions.....	233
6. 6	References.....	234
CHAPTER 7. GENERAL CONCLUSIONS.....		237

LIST OF FIGURES

Figure 1.1. The structures of some common conducting polymers, a . polyacetylene, b . polypyrrole, c . polythiophene, d . polyaniline.....	3
Figure 1.2. Oxidation and reduction of polythiophene; a Polythiophene in the neutral undoped state; b Oxidation to the polaron form; c Further oxidation of the same segment causes loss of the unpaired electron and formation of a bipolaron.....	4
Figure 1.3. Example of a biodegradable conducting polymer. ^[30]	6
Figure 1.4. Oxidative polymerisation of a general thiophene monomer. The alpha and beta positions on the monomer are labelled. Polymerisation has proceeded through the α positions with the polymer shown in the oxidised state. A^- represents a counter ion.....	7
Figure 1.5. Regioisomeric couplings of singly substituted thiophene monomers.	9
Figure 1.6. The structure of a polyazomethine reported by Dubitsky <i>et al.</i> ^[96]	16
Figure 1.7. Schematic of electrospinning set up. ^[115]	19
Figure 3.1. General terthiophene structure.....	90
Figure 3.2. Reversible photo-induced isomerisation between benzospiropyran and merocyanine. Figure courtesy of Dr Robert Byrne. ^[33]	91
Figure 3.3. Structures of target terthiophene materials.	93
Figure 3.4. Planer β -(styryl)terthiophenes synthesised by Collis <i>et al.</i> ^[17]	97
Figure 3.5. Structure of acyl-serine methyl ester 20 and BOC-tyrosine methyl ester 21 for use in terthiophene functionalisation.....	100
Figure 3.6. ¹ H NMR spectra for 4,4''-didecoxy-2,2':5',2''-terthiophene-3'-carboxylic acid 15 (top) and (acyl-serine methyl ester)-4,4''-didecoxy-2,2':5',2''-terthiophene-3'-carboxylate 22 (bottom), note the appearance of additional	

peaks corresponding to the acyl-serine methyl ester at 4.90 ppm (CH), 4.66 ppm and 4.47 ppm (CH ₂), 3.75 ppm (COOCH ₃), and 2.03 ppm (COCH ₃).	102
Figure 3.7 . CV of polymer growth from (acyl-serine methyl ester)-4,4''-didecoxy-2,2':5',2''-terthiophene-3'-carboxylate 22 solution at 50 mVs ⁻¹ between -0.2 V and 1 V. The onset of monomer oxidation at 0.76 V is indicated by the arrow.	103
Figure 3.8 . CV of polymer film 24 grown at constant potential for 40 seconds at a scan rate of 50 mVs ⁻¹ between -0.3 V and 0.9 V.	104
Figure 3.9 . UV-visible absorbance spectra. a . TTSPA, b . TTSPC. For each terthiophene, spectrum 1 is the initial spectrum, 2 the spectrum after exposure to 1 minute of UV light and 3 the spectrum after subsequent exposure to white light.	111
Figure 3.10 . Kinetic curves at 25°C for the absorbance of the merocyanine at 570 nm. a . TTSPA, b . TTSPC.	113
Figure 3.11 . UV-visible spectra of terthiophene-spiropyran molecules in acetonitrile at concentration 0.05 mM, alone and with various analyte ions added. All spectra are of the mixtures after 1 minute of exposure to 254 nm UV radiation. a . TTSPA, b . TTSPC.	116
Figure 3.12 . CV's showing the growth of a polymer from a TTSPC growth solution (8 mM TTSPC, 0.1 M TBAP, 1:1 acetonitrile DCM, 50 mV/s, -0.3 V and 1 V).	119
Figure 3.13 . CV's showing the electrochemistry of polymer films at 50 mV/s in acetonitrile (0.1 M TBAP) electrolyte a . PTTSPA, b . PTTSPC.	120
Figure 3.14 . UV-visible spectroelectrochemistry PTTSPC film on ITO glass in 0.1 M TBAP acetonitrile, a . -300 mV to 600 mV, b . 600 mV to 950 mV.....	122

Figure 3.15. UV-visible spectroelectrochemistry PTTSPA film on ITO glass in 0.1 M TBAP acetonitrile, a. -300 mV to 600 mV, b. 600 mV to 950 mV.....	123
Figure 3.16. Schematic of ITO PET electrode chip.	124
Figure 3.17. PTTSPA films on electrode chips. The upper polymer film (A) has a potential of -0.3 V applied (reduced form), the lower oxidised film (B) has no applied voltage. The blue/grey colour is indicative of oxidised polymer with the spiropyran form attached.....	125
Figure 4.1. ¹ H NMR spectra of 34 and its breakdown products after acid hydrolysis. Top, bis((4-decoxythiophen-2-yl)methylene)benzene-1,4-diamine 34 . Middle, organic extract of reaction mixture, which corresponds to the spectrum of aldehyde 31 . Bottom, aqueous extract of reaction mixture, which corresponds to the spectrum of <i>p</i> -phenylenediamine dihydrochloride 37 (one phenylene singlet at 7.56 ppm, the peaks at 5.47, 5.38 and 4.78 ppm are due to water and DCM contamination). ^[33]	139
Figure 4.2. MALDI MS spectrum of poly(bis((4-decoxythiophen-2-yl)methylene)benzene-1,4-diamine) 40 . The main peaks at m/z 1373 (2Mer ⁺), 1979 (3Mer ⁺), 2586 (4Mer ⁺), and 3193 (5Mer ⁺) show the material is oligomeric.	141
Figure 4.3. CV's showing the electrochemistry of azomethine films on ITO glass in 0.1 M TBAP acetonitrile electrolyte at 50 mV/s scan rate. a. Non-acid catalysed azomethine 43 film. b. Acid catalysed azomethine 43 film.....	145
Figure 4.4. UV-visible absorption spectra of an acid catalysed azomethine 43 polymer film in acidic THF, showing the change in the spectra from before the acid was added to 7 hours after acid addition, illustrating film degradation. The arrow indicates the direction of the change in absorbance over time.	146

Figure 4.5. UV-visible spectrum of polymer 48 in reduced and oxidised forms.....	150
Figure 4.6. Proposed mechanism for the autopolymerisation of 2-bromo-3- alkoxythiophenes, courtesy of Dr Pawel Wagner. ^[18]	152
Figure 4.7. Cyclic voltammetric growth of PTBEO, scan rate 50 mV/s. The arrow indicates the growth in current with subsequent scans.	162
Figure 4.8. Post growth CV of PTBEO film grown at constant potential, scan rate 50 mV/s, -0.3 V to 1.0 V.....	162
Figure 5.1. FTIR spectra of POTE and PHET films.....	175
Figure 5.2. Schematic of POTE (left) and PHET (right) surfaces (cells attached to hydrophilic PHET surface).	176
Figure 5.3. SEM images of spin coated films a. POTE and b. PHET.....	177
Figure 5.4. AFM topographic images of POTE (a. and b.) and PHET (c. and d.). Polymers were scanned over 90 x 90 μm areas (a,c) and higher resolution images obtained from the same polymers over 10 x 10 μm areas (b,d).....	177
Figure 5.5. CV's of POTE and PHET films at 50 mV/s: a. acetonitrile electrolyte (0.1M TBAP) b. aqueous electrolyte (0.1M KNO ₃).....	179
Figure 5.6. UV-visible spectroelectrochemistry of polymer films in 0.1 M TBAP acetonitrile electrolyte, each spectrum is labelled with the applied potential: a. POTE film on ITO glass, b. PHET film on ITO glass.....	181
Figure 5.7. Water droplets on polymer films a. POTE film with contact angle 104° b. PHET film with contact angle 50°.....	182
Figure 5.8. Microscope images of P3HT electrospun fibres: a. P3HT fibres (spun from a 20 mg/mL soln.) b. P3HT fibres (spun from a 12.5 mg/mL soln.) The scale bar represents 20 μm	186

Figure 5.9. Microscope image of a POTE electrospun fibre mat. The scale bar represents 40 μm .	187
Figure 5.10. Aligned POTE fibres: a. microscope image, scale bar represents 20 μm ; b. SEM image, scale bar represents 10 μm .	188
Figure 5.11. Histogram showing the distribution of fibre angles for a POTE fibre mat aligned at 2000 rpm.	189
Figure 5.12. Microscope image of POTE fibres between platinum electrodes. Scale bar represents 100 μm .	191
Figure 5.13. CV's showing the electrochemistry at 50 mV/s in 0.1 M TBAP acetonitrile electrolyte of PHET and PFTE on gold Mylar electrodes: a. Polymer fibres, b. Polymer films.	196
Figure 5.14. CV showing the electrochemistry at 50 mV/s in 0.1 M TBAP acetonitrile electrolyte of PFTE fibres. A Oxidation and A' reduction peaks for ferrocene added to the electrolyte, B oxidation and B' reduction peaks for ferrocene bound to the fibres.	197
Figure 5.15. CV's comparing the electrochemistry at 50 mV/s, of PHET and PFTE films and fibres in aqueous 0.1 M KNO_3 electrolyte.	198
Figure 5.16. Comparison of the electrochemistry of PFTE films and fibres at different scan rates. a. The peak current (i_p) measured from the bound ferrocene peak versus scan rate for PFTE films and fibres. b. The difference between the peak voltage of bound and free ferrocene from the CV (ΔE_p) versus scan rate for PFTE films and fibres.	200
Figure 6.1. The structures of the polymers chosen for biocompatibility studies; poly(octanoic acid 2-thiophen-3-yl ethyl ester) (POTE), poly(3'-(2-hydroxyethyl) thiophene) (PHET), polybithiophene (PBT), poly(3-	

decoxythiophene) (PDOT), poly(decyl 4,4''-didecoxy-2,2':5',2''-terthiophene-3'-carboxylate) (PDDTTC) and poly(3-octylpyrrole) (POP).	209
Figure 6.2. Quantitation of C2C12 cell adhesion and proliferation on polymer films by absorbance measurements at three time intervals. Thio A: POP, Thio B: PBT, Thio C: PDOT _e , Thio D: PDDTTC _e , Thio E: POTE, Thio F: PHET, PS: polystyrene control, Au Mylar: gold Mylar control.....	215
Figure 6.3. Polymer films with ROSA cells after 3 days of differentiation, blue DAPI (nuclear stain), green desmin (myogenic protein): a. POP, b. PBT, c. PDOT _e , d. PDDTTC _e , e. POTE, f. PHET, g. gold Mylar control, h. polystyrene control. Scale bars represent 100 μm.	216
Figure 6.4. Quantitation of ROSA cell differentiation: a. percent multinucleation density, b. nuclei density per square millimetre. Pth A: POP, Pth B: PBT, Pth C: PDOT _e , Pth D: PDDTTC _e , Pth E: POTE, Pth F: PHET,	217
Figure 6.5. Quantitation of ROSA cell growth on PDDTTC _e and PDDTTC _c films at several time intervals compared to a gold Mylar control.....	218
Figure 6.6. Polymer films with ROSA cells after 3 days of differentiation, blue DAPI (nuclear stain), green phalloidin (stain which binds actin filaments in muscle cells): a. PDDTTC _e , b. PDDTTC _c , c. gold Mylar control. Scale bars represent 100 μm.	218
Figure 6.7. Calcein-stained C2C12 cells adhering and proliferating on a. POTE and b. PHET polymer fibres, c. underlying gold Mylar substrate. Scale bar represents 100 μm.	219
Figure 6.8. Fluorescence images of differentiated ROSA cells, stained with DAPI and desmin, aligned along medium (a. and b.) or low (c. and d.) densities of	

ester POTE (a. and c.) or hydroxyl PHET (b. and d.) fibres, or on gold Mylar in the absence of polymer fibres (e. and f.). Scale bars represent 80 μm	220
Figure 6.9. SEM images of polymer films: a. POP, b. PBT, c. PDOT, d. PDDTTC _e . Scale bars represent 10 μm	223
Figure 6.10. CV of a PDDTTC _c film on gold Mylar in 0.1 M TBAP acetonitrile electrolyte (50 mV/S scan rate). The arrow indicates the onset of oxidation. .	225
Figure 6.11. The UV-visible absorbance spectrum of a POTE fibre mat on ITO glass in 0.1 M TBAP acetonitrile, showing the spectrum at -300 mV, 900 mV and several time intervals after application of 900 mV to oxidise the fibres and leaving them in electrolyte.	226
Figure 6.12. UV-visible spectra showing the reduction of perchlorate doped polymer films over time in cell culture medium: a. POTE b. PHET. The arrows show the changes in the spectra over time between 1 minute and 1 hour with the dotted lines showing the spectra for the reduced form of the polymer.	228
Figure 6.13. UV-visible spectra showing the reduction of a perchlorate doped PDDTTC _c polymer film over time in cell culture medium. The arrow shows the change in the spectra over time between 1 minute and 1 hour, the spectrum after 24 hours is also shown, the dotted lines showing the spectrum for the reduced form of the polymer.	229
Figure 6.14. UV-visible spectra showing the reduction of <i>para</i> -toluenesulfonate doped polymer films over time in cell culture medium: a. POTE b. PHET. The arrows show the changes in the spectra over time between 1 minute and 1 hour with the dotted lines showing the spectra for the reduced form of the polymer.	231

LIST OF TABLES

Table 1.1. Advantages and disadvantages of polymerisation methods commonly used to synthesise polythiophenes.....	11
Table 1.2. Advantages and disadvantages of a range of fabrication techniques.....	18
Table 3.1. Physical properties of TTSPA and TTSPC, λ_{\max} for merocyanine (MC), A_e the absorbance of the merocyanine peak at equilibrium, K_e the equilibrium constant for the relaxation from the merocyanine form to the spiropyran form calculated from Equation 3.1, k (s^{-1}) the thermal relaxation constant for the closing of the merocyanine calculated from Equation 3.2.....	114
Table 3.2. Summary of the effect on the UV-visible spectra of adding metal ions to the TTSPA and TTSPC, before irradiation, after UV irradiation and after subsequent visible irradiation.....	117
Table 4.1. A comparison of the yields for 2-bromothiophene starting materials compared to literature yields.....	155
Table 6.1. Contact angles, onset potential from post growth CV's, morphology from SEM and biocompatibility (% multinucleation (MN) with ROSA cells) for polymer films. *Dr Klaudia Wagner is acknowledged for gathering this data.	221

CHAPTER 1. INTRODUCTION.

1. 1 Introduction.

Bionics, the area of research concerned with the interface between biology and electronics has revolutionised medical research,^[1] leading to the invention of new medical devices such as the bionic ear, which has been able to restore hearing to deaf people world wide.^[2] Other applications such as a bionic eye^[3] and devices to assist with spinal cord repair^[4] are currently being developed. Bionic devices rely on the effects created when an electronic device is implanted into a biological system as electrical fields have been shown to stimulate the healing of bone,^[5] cartilage,^[6] skin and connective tissue,^[7] and nerves.^[8]

Current bionic devices rely on conventional electronic materials such as metals, which are hard materials foreign to biological organisms.^[9] To improve such bionic devices and allow the fabrication of devices with new functionality, novel materials are needed that not only conduct electric signals but are tailored to specific applications within the biological environment. These materials must be biocompatible and non-toxic to the organism, able to be processed to form the necessary structures, and, in many cases, have surface functionality to promote cellular attachment, actuation capability to elicit movement, and have the ability to release drugs or other molecules upon the application of an external stimulus.^[10] For some applications it is desirable that materials are biodegradable since having fulfilled their function they need to degrade and be eluted from the body.^[11]

Conducting polymers are excellent candidate electromaterials for the next generation bionic devices as they have the advantage over conventional metal conductors that they are flexible, and, being organic molecules, are similar in nature to biological materials.^[9] The material and surface properties of conducting polymers can also be tailored to suit particular applications.^[8]

1.2 Conducting polymers.

The Nobel prize-winning discovery by Heeger, MacDiarmid, and Shirakawa^[12, 13] that doped polyacetylene is conducting, gave birth to a new class of materials; inherently conducting polymers.^[14] The structures of the reduced form of some of the more common classes of conducting polymers are shown below in Figure 1.1. Typically conducting polymers are made up of monomer units, with a structure containing a conjugated backbone made up of alternating double and single bonds.

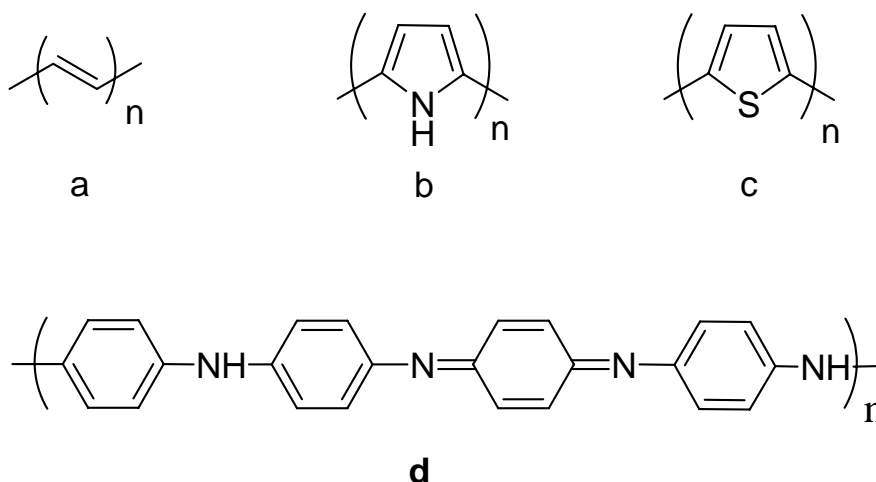


Figure 1.1. The structures of some common conducting polymers, **a.** polyacetylene, **b.** polypyrrole, **c.** polythiophene, **d.** polyaniline.

In their neutral state conjugated polymers are semi-conducting at best with conductivities typically ranging from 10^{-10} to 10^{-5} S/cm. However, after doping, either chemically or electrochemically, the conductivities of these materials approach that of some metals, typically in the range of $1-10^4$ S/cm.^[15] The oxidative doping of conducting polymers is generally a reversible process whereby the polymer becomes positively charged and is associated with an anionic counter ion or dopant (p-doped)

as shown in Figure 1.2.^[15] As the polymer becomes oxidised further, it undergoes a transition through a polaron state with radical cations to a bipolaron state when the unpaired electron is removed to leave a dication.^[11] The polaron and bipolaron act as charge carriers and give rise to the polymer's conductivity, the lower the band gap (the difference between the conduction band and valance band) of the polymer the more conductive it is.^[11] Conducting polymers can also become n-doped, however this is more difficult to achieve.^[16]

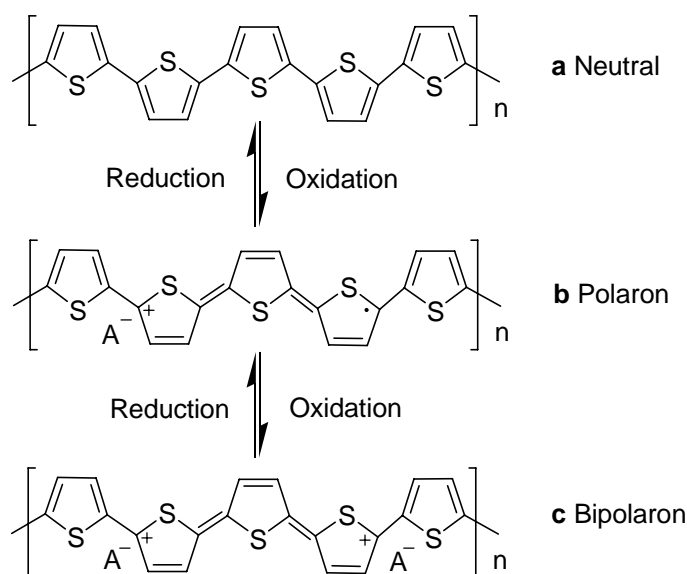


Figure 1.2. Oxidation and reduction of polythiophene; **a** Polythiophene in the neutral undoped state; **b** Oxidation to the polaron form; **c** Further oxidation of the same segment causes loss of the unpaired electron and formation of a bipolaron.

1.3 Conducting polymers in bionics.

While the initial interest in conducting polymers was in the intriguing structure and electronic properties, subsequent work has been driven by the diversity of their potential applications.^[17, 18] With recent research showing that electrical stimulation can aid in cell repair,^[8] bionics is becoming one of these areas of interest. Thus, the biocompatibility of conducting polymers has been the focus of several studies. Most research in this area has focused on the biocompatibility of polypyrroles and a range of cell types, dopants and structures have been investigated (see Guimard *et al.*^[11] for an excellent review on this area). Polypyrrole has been shown to be biocompatible with a wide range of cell types with nerve and muscle cells being of particular interest due to their excitable nature; for example, the nerve cells in the cochlear implant.^[19, 20] Polyaniline has been shown to be biocompatible with PC-12 cells^[21] as well as cardiac myoblasts^[22] but has not been as extensively studied. There are also reports that its biocompatibility is poor with certain cell lines and requires modification by peptides to increase it.^[23]

There have been limited reports on the biocompatibility of thiophene-based polymers. An oligosiloxane-modified polythiophene showed promising results supporting the growth of HeLa cells. However, the long siloxal chains insulated the cells from the thiophene backbone.^[24] A second report describes the successful growth of epithelial Hep-2 cells on PEDOT.^[25] A study by Da-Feng Li *et al.* reported good cell growth and proliferation of PC-12 cells on various poly-3-alkylthiophenes.^[26] These are very promising results, showing that polythiophene based materials have potential for bionic applications. However, the overall

biocompatibility of polythiophene materials is still a relatively unexplored area.^[11] In many bionic applications, implants are only needed temporarily, thus it would be desirable to develop a biodegradable conducting polymer material. To date, the development of biodegradable conducting polymers has centred around either composite materials in which the conducting polymer is associated with a non-conducting biodegradable polymer,^[27-29] or a polymer comprised of conducting polymer oligomer units linked by a biodegradable linkage such as an ester group (Figure 1.3).^[11, 30-32]

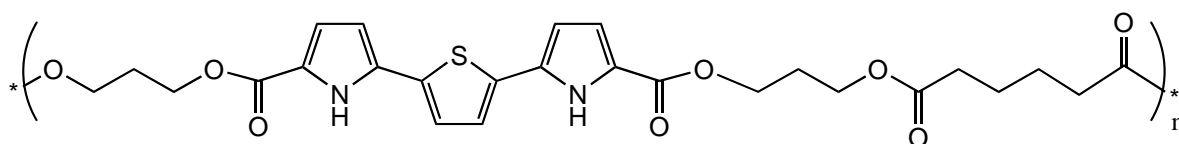


Figure 1.3. Example of a biodegradable conducting polymer.^[30]

Composite materials of polypyrrole and polylactide have conductivities which vary by six orders of magnitude depending on the polypyrrole content.^[27, 28] Their degradability depends on the ability of the body to clear remaining polypyrrole nanoparticles from the body. When using conductive oligomers with biodegradable linkers, conductivity is sacrificed for biodegradability. Polymers of this type have conductivities of 10^{-4} S/cm for the above example shown in Figure 1.3^[30] and 5×10^{-6} S/cm for a copolymer of polylactide and an aniline pentamer.^[31] With such materials the breakdown products need to be carefully screened to ensure they are non-toxic.^[33] As such, the synthesis and optimisation of materials that are biodegradable and conductive remains a significant challenge in the design of novel bionic materials.^[11]

1.4 Polythiophenes in bionics.

1.4.1 Polythiophenes general introduction.

Thiophenes have the advantage over other conducting polymer precursors in that they are highly stable to a wide range of reaction conditions as well as allowing a wide variety of functionality to be readily built on to the parent thiophene, bithiophene, or terthiophene monomers.^[16, 34, 35] Such functionality gives rise to the potential of tailoring material properties for a particular application and allows the incorporation of various linkers and other substituents.^[36] The general structure of a thiophene monomer and its oxidative polymerisation are shown below in Figure 1.4, the α and β positions on the thiophene ring are labelled. Polymerisation preferentially occurs through the two more activated α positions, resulting in a conducting polymer. Any α - β or β - β linkages are considered defects as they decrease the conductivity of the polythiophene by disrupting the highly ordered conjugated system.^[16]

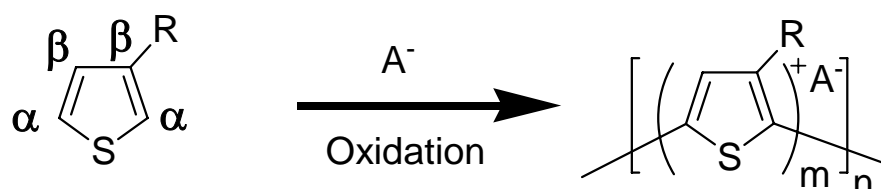


Figure 1.4. Oxidative polymerisation of a general thiophene monomer. The alpha and beta positions on the monomer are labelled. Polymerisation has proceeded through the α positions with the polymer shown in the oxidised state. A^- represents a counter ion.

Functionalisation of one or both of the beta positions can decrease the chances of undesirable α - β and β - β couplings, and can be used to change the polymer properties. For example, unsubstituted polythiophene itself is insoluble,^[37] however the attachment of alkyl chains to the beta position of the monomer gives organic-solvent

soluble polymers.^[38] Functionalisation gives the ability to tune the properties of a polythiophene for particular applications such as sensors,^[39, 40] FETs,^[41] LEDs,^[42] photovoltaics,^[43-45] and bionics.^[11]

There are many examples in the literature of the synthesis of covalently functionalised polythiophenes.^[16, 36] Generally covalent functionalisation of polythiophenes takes two forms; the synthesis of functionalised monomers or oligomers, which are subsequently polymerised,^[36] and the post-polymerisation functionalisation of polymers.^[46] Post-polymerisation functionalisation is useful for the introduction of polymerisation-sensitive functional groups and can be done both in solution if the polymer is soluble or on a polymer surface.^[47]

One issue that arises from the polymerisation of functionalised monomers and oligomers is that of regioregularity. When two monomers that have a single substituent in a beta position are coupled together they can couple in one of three ways (Figure 1.5), head-to-head, head-to-tail, or tail-to-tail. A polymer, which is made up of a random mixture of couplings, is referred to as regiorandom whilst one made up of a regular arrangement is termed regioregular.^[48] Regioregular polymers often have higher conductivities than regiorandom polymers as regiorandom linkages can cause twisting of the polymer backbone disrupting overlap of the *pi* orbitals.^[37]

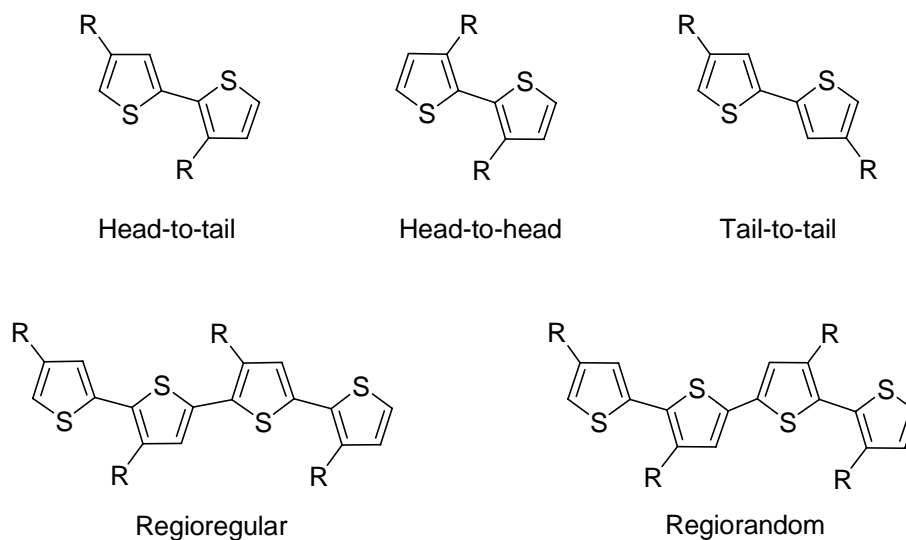


Figure 1.5. Regioisomeric couplings of singly substituted thiophene monomers.

To avoid regioregularity issues, symmetrical thiophene oligomers are often used as building blocks for polythiophenes.^[49] Due to their increased conjugation length thiophene oligomers have lower oxidation potentials than thiophene; thiophene has an oxidation potential of 1.70 V, bithiophene 1.15 V and terthiophene 0.95 V versus a Ag/AgCl reference electrode.^[50, 51] Bi- and ter-thiophenes, which have a lower oxidation potential, can still be polymerised when functionalised with electron withdrawing functionalities; such functionalities increase the oxidation potential of the monomer, and in the case of single thiophene monomers prevent polymerisation.^[16] The polymerisation of bi and terthiophene oligomers, however, is reported to generally give shorter polymers with lower conductivities than the equivalent thiophene monomer.^[52] The reason for the decrease in polymer length is thought to be due to the increased stability of the radical cations formed during the polymerisation. These can be more efficiently delocalised on longer oligomers^[16] and thus are less reactive to polymerisation.

Thiophene oligomers are generally synthesised by aryl-aryl bond forming reactions;^[53] Suzuki,^[52] Stille,^[43] Kumada,^[54] and Ullmann^[55] type reactions are commonly used. Thiophene oligomers with a range of functionalities ranging from alkyl chains to porphyrin groups have been synthesised.^[56] The particular coupling reaction used is dependent upon the functional groups present in the starting materials, Stille and Suzuki couplings are known to be tolerant to a wide range of functionalities.^[43, 52, 57]

The properties of thiophene-based polymers are dependent on the polymerization method used to make the polymer.^[58] The two simplest methods for producing polythiophenes are chemical oxidation and electrochemical oxidation,^[51] however polymers can also be made by other chemical methods.^[59, 60] The advantages and disadvantages of each method are outlined below in Table **1.1**. Generally the polymerisation conditions that are used to produce polythiophenes are dependent upon the monomers and the properties that are desired in the polymer.

Electrochemistry, as well as being a very useful characterisation technique, is also a good way of polymerising thiophene monomers and oligomers. Electrochemical polymerisation gives electrodes coated with polymer films, and presents the option of tuning the electrochemical growth conditions to give films with different surface properties and morphologies. For example polymer growth by cyclic voltammetry, constant current and constant potential all give films with slightly different morphologies.^[51]

Chemical oxidation of thiophene monomers is usually carried out using an iron chloride oxidant; chemical polymerisation can easily be scaled up and is able to produce large quantities of material relatively easily.^[61] In these oxidative polymerizations, the oxidation potential of the monomer needs to be below the potential of the chemical oxidant.^[16] If the polymer produced is soluble, it can be subsequently processed into complex structures such as fibres.^[62] Chemical methods also allow variation in the polymer form. Thus, polythiophene nanoparticles can be produced by using ionic liquids in the polymerization process.^[63] Vapour phase polymerisation can also be used to create polymer structures by exposing a film of oxidant to the monomer, this requires the monomer to be volatile.^[64]

Table 1.1. Advantages and disadvantages of polymerisation methods commonly used to synthesise polythiophenes.

Polymerisation Method.	Advantages	Disadvantages
Electrochemical Oxidation	-Good for producing polymer films. -Film properties can be controlled by varying current and voltage.	-Not useful for producing more complex structures. -Need a conducting substrate.
Chemical Oxidation	-Can vary polymer form, vapour phase, nano fibres and particles. -Often gives high molecular wt. -When polymer is soluble good for producing structures.	-Little control over regioregularity. -Oxidation potential of the monomer must be below that of oxidant.
Other Chemical methods.	-Can give more precise control over regioregularity and higher conductivities. -Useful on monomers with high oxidation potential.	-More difficult chemistries. -Lower molecular weights. -Not suitable with all functionalities.

While oxidative polymerization is useful for giving high molecular weight polymers, the regioregularity of these materials is generally lower than 90%.^[65] Other chemical polymerisation methods have been developed to give more regioregular polymers, the three most common of these being the McCullough,^[66] Rieke^[67] and Grignard metathesis (GRIM)^[59] polymerization methods. These methods involve more difficult and expensive chemistries than simple chemical oxidation but give more regioregular polymers with higher conductivities. Whilst the McCullough and Rieke methods require cryogenic temperatures and organolithium and highly reactive Rieke zinc respectively, the GRIM polymerisation method can be carried out at room temperature with simple Grignard reagents so is considered the more economical of the three methods.^[59] The GRIM and McCullough methods are unsuitable for use on monomers containing ester groups and other functionalities, which are sensitive to Grignard reagents and butyl lithium.^[48, 68] The copper catalysed Ullmann coupling of 2,5-dibromo-alkyl-thiophene-3-carboxylate monomers has also been investigated but generally this polymerisation results in low molecular weights.^[60]

Copolymerisation, where two or more monomers are polymerised together to give a polymer containing both monomers and thus the resulting polymer has a mixture of the properties of the monomers, is another technique that can be used to optimise the properties of polythiophenes.^[69] Copolymerisation is particularly useful where a functional monomer is needed in only relatively small quantities. Such a functional monomer can be combined with a second monomer like an alkyl thiophene in order to increase the solubility of the resulting material.^[69, 70] To be effective the monomers should have relatively similar oxidative reactivities so that they are both incorporated into the copolymer.^[71]

1.4.2 Functionalised polythiophenes.

To optimise the properties of polythiophene materials for bionic applications, a wide range of functionality can be incorporated into the monomer or polymer giving a wide diversity of material properties. For many applications, functionalities that increase the hydrophilicity and biocompatibility of the material are of interest and functionalities that increase the solubility and processability of the polymers are also important for bionic applications.^[11]

The literature reports the synthesis and polymerisation of thiophene monomers containing a wide range of functionalities, ranging from alkyl chains that increase solubility in organic solvents,^[37] fluorinated groups to make hydrophobic materials,^[72] esters,^[73] acids,^[73] alcohols,^[74] amines,^[75] and sulfonates.^[76] With such a wide range of functionalised materials previously reported, the properties of these materials needs to be compared to those required for bionic materials. In terms of solubility, bionic materials should be soluble in organic solvents to allow processing but insoluble in aqueous systems whilst still incorporating functionality to enhance bionic interactions. Polythiophenes functionalised by acid and sulfonate groups are reported to be water soluble and therefore are unsuitable as a scaffold for cell growth.^[73, 77] Alcohol-functionalised thiophene polymers are insoluble in both aqueous and organic media and therefore give rise to problems with processing.^[78] The use of ester groups to improve organic solvent solubility of alcohol polymers has previously been investigated.^[79] Ester groups can then be cleaved to leave a hydrophilic polymer.^[73] Additional possibilities to improve the material properties of the polymers are the use of hydrophobic copolymers^[80] to reduce the water

solubility of acids and sulfonates or bi/terthiophenes incorporating solubilising groups.^[52, 81]

To tailor polythiophene materials for particular bionic applications, often it is desirable to attach complex functionalities such as enzymes and cell growth factors. The attachment of more complex functionalities can be achieved relatively easily. Basic functionalities such as acids and alcohols are suitable for subsequent functionalisation through the use of esterification and other coupling reactions. There are many examples in the literature of functionalities that have been attached to thiophene monomers and to polythiophenes such as ferrocene, which has been coupled via a Wittig reaction,^[82] or the amino acid serine, which has been coupled to thiophene monomers through an ethyl linkage.^[83] Often large bulky substituents are coupled to terthiophene oligomers. Burrell *et al.* coupled several substituents including a porphyrin and crown ether via Wittig chemistry.^[56] More bulky groups such as the glucose oxidase enzyme have been covalently attached to polythiophene films using active ester chemistry.^[84] These are just some examples of the vast range of functionalities that have been attached to polythiophenes, the reader is referred to the handbook of conducting polymers^[48] for a more comprehensive review of the functionalisation of polythiophenes.

1.4.3 Biodegradability.

As previously outlined in Section 1.3 for many bionic applications, biodegradable conducting polymer materials would be desirable. The optimal biodegradable conducting polymer would be made up of conjugated units linked by conjugated yet degradable linkers. These degradable linkers would need to be stable enough to fulfil the polymers function, and then degrade upon the action of an enzyme or change in pH.

Such a polymer made up of oligomers would have a moderately high conductivity. Thiophene oligomers of 5 units and over are reported to have reasonable conductivities without the need to be polymerised. For example pentathiophenes have been reported to give conductivities of up to 0.4 S/cm.^[85] Thus, it is possible to link oligomers together by non conjugated or less conjugated linkers and still get a conductive polymer.^[85] This gives rise to the potential to create biodegradable conducting polymers.

Azomethine-linked thiophene oligomers (Figure 1.6) have the potential to be conductive yet degradable. Azomethines are known to be unstable under acidic conditions,^[86] this property could be exploited to tailor an azomethine material to biodegrade, such degradation would need to occur within the lysosomes of cells, which have a pH <5.^[87] Conductivities of up to 1 S/cm are reported for iodine doped polyazomethines.^[88] A range of electroactive azomethine polymers based on thiophene oligomers have previously been reported.^[89-96] These materials are known to be reversibly protonated on the nitrogen.^[95] and this could be exploited to give a

degradable polymer. Azomethines can be prepared by a simple coupling of aryl aldehydes and amines; the example shown in Figure 1.6 was prepared by coupling *p*-phenylenediamine with 2-thiophene carboxaldehyde.^[96]

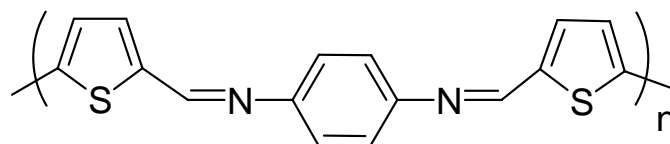


Figure 1.6. The structure of a polyazomethine reported by Dubitsky *et al.*^[96]

1.5 Structure fabrication.

The application of polythiophene materials for bionics requires the fabrication of polymer structures.^[27] There are a wide variety of fabrication techniques available; the particular technique that is used depends on the type of structure to be formed as well as the properties of the material.^[97] For the fabrication of polythiophene structures, solution based techniques are of most interest, utilising solutions of functionalised polythiophenes in organic solvents.^[98] These organic solvent-soluble polymers can be easily processed into various structures such as films and fibres.^[62, 99-101] In Table 1.2, a summary of the various fabrication methods for producing polymer films and fibres is given.

Polythiophene films have been readily produced by a range of methods such as dip coating,^[102] drop casting^[100] and spin coating.^[101] Of these methods spin coating is most suited to consistently producing uniform polymer films.^[103] This fabrication technique involves application of a polymer solution onto a rotating substrate, the polymer solution is then spread evenly over the substrate by the centrifugal force.^[103]

However, continuous polymer film structures are only of limited interest for bionics due to their flat structure. More complex patterns can be deposited relatively quickly by techniques such as inkjet printing.^[104] The inkjet printing of poly-3-alkylthiophenes has been reported,^[105] although the printing of polythiophenes is made difficult by the volatility of the solvents such as chloroform used to dissolve polythiophenes, causing clogging of the jets. This methodology also provides a way to create scaffolds for cell culturing.^[106]

Table 1.2. Advantages and disadvantages of a range of fabrication techniques.

Fabrication Technique.	Advantages.	Disadvantages.
Films –Drop casting	Quick and easy. Can produce relatively thick films.	Films are not uniform.
-Dip coating	Reasonably easy.	Can be slow and often gives tide lines.
-Spin coating	Fast method for reproducibly producing uniform films.	Films are often thin and may contain pin holes and defects.
Printing	Useful for producing complex patterns reproducibly.	Volatile organic solvents can cause clogging of nozzles.
Fibres –Wet spinning	Good for producing thick fibres.	Produces individual fibres often need to combine.
-Electrospinning.	Produces fibre mats with fibres of diameter 100 nm- 10 μm . Fibres can be patterned and aligned.	Several parameters need to be optimised to avoid defects and beading. Requires high molecular weights.

For bionic applications, fibrous structures are of particular interest, as electrically excitable cells are often arranged in fibrous aligned structures such as muscles. Therefore structures such as fibres are desirable as scaffolds for cell growth. Wet spinning is a process used to form fibres by injecting a polymer solution into a coagulant bath and can give fibres over 100 m in length^[107] with diameters generally between 10 μm and 100 μm .^[108] Wet spun fibres have been demonstrated as good scaffolds for supporting cell growth.^[109-111] Wet spun polythiophene fibres have not been reported in the literature but have been demonstrated in our laboratories.^[112]

Small fibres ranging from 0.01 microns to a few microns in diameter can be produced by electrospinning.^[113] Electrospun poly(lactic-co-glycolic acid) fibre mats have previously been reported to be useful scaffolds for cell growth.^[114] The high surface area and ability to align electrospun fibres gives advantages over conventional structures.^[113] Electrospinning is a relatively simple technique illustrated in Figure 1.7. It works by applying a potential, usually in the range of 1-30 kV, to a polymer solution that is being fed from a syringe at a constant rate by a syringe pump. The applied potential creates a Taylor cone within the polymer droplet as the charged polymer chains repel each other and the solvent evaporates, and fibres are formed, which are collected on a grounded target.^[113]

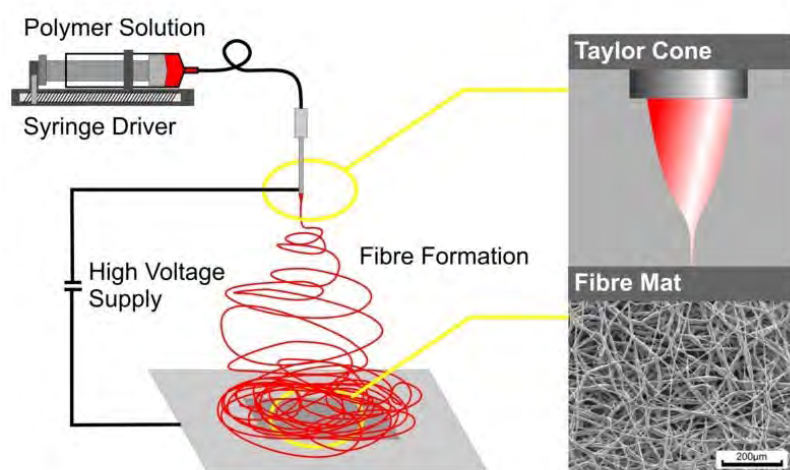


Figure 1.7. Schematic of electrospinning set up.^[115]

The electrospinning of polythiophenes, particularly poly-3-alkylthiophenes has been previously reported.^[62, 97-99, 116, 117] To increase the spin ability of polythiophene materials, they are often blended with PEO, as this high molecular weight polymer is reported to increase chain entanglements.^[97] The incorporation of insulating PEO decreases conductivity. However at low concentrations this effect is low.

1.6 Overview of thesis.

This project aimed to utilise the versatility and ease of synthesis of thiophene-based polymers to achieve the goal of producing novel conductive polythiophene scaffolds for the repair of damaged tissues and other bionic applications. To achieve this goal, this research focused on four main areas:

1. The synthesis of functionalised thiophene materials, containing functionalities that would facilitate and enhance bionic interactions. The synthesis of terthiophenes by Suzuki coupling was investigated and they were functionalised further by barbituric acid, amino acids and spiropyran molecules that are good hydrogen bonders and that are likely to facilitate increased interactions with bionic environments (Chapter 3).
2. The investigation of thiophene-based oligomers as a source of biodegradable conducting polymers. Thiophene-based azomethine polymers were investigated as these molecules are known to be acid sensitive. The synthesis of thiophene oligomers was also investigated as building blocks for degradable conducting polymers (Chapter 4).
3. The investigation of simple soluble polythiophenes and their fabrication into scaffold structures to support cell growth. Simple film and fibre structures were focused on as these can be produced relatively simply from soluble polymers by spin coating and electrospinning (Chapter 5).

4. The synthesis of a range of conducting polymer films and the comparison of their material properties and biocompatibility. The biocompatibility of a range of materials was tested with muscle cells as these cells are known to respond to electrical stimulation (Chapter 6).

This research has developed novel polythiophene materials for use in bionic applications and has demonstrated the utility of functionalised polythiophenes as scaffolds to support cell growth.

1. 7 References.

- [1] R. Zajtchuk, *Disease-a-month : DM* **1999**, 45, 449.
- [2] M. Clark Graeme, *Philosophical transactions of the Royal Society of London. Series B, Biological Sciences* **2006**, 361, 791.
- [3] Y. Wong, T., N. Dommel, P. Preston, L. Hallum, E., T. Lehmann, N. Lovell, H., G. Suaning, J., *IEEE transactions on neural systems and rehabilitation engineering : a publication of the IEEE Engineering in Medicine and Biology Society* **2007**, 15, 425.
- [4] M. E. Schwab, *Science (Washington, DC, United States)* **2002**, 295, 1029.
- [5] D. M. Ciombor, R. K. Aaron, *Journal of Cellular Biochemistr* **1993**, 52, 37.
- [6] R. K. Aaron, D. M. Ciombor, *Journal of Cellular Biochemistry* **1993**, 52, 42.
- [7] J. Y. Wong, R. Langer, D. E. Ingber, *Proceedings of the National Academy of Sciences of the United States of America* **1994**, 91, 3201.
- [8] G. G. Wallace, L. A. P. Kane-Maguire, *Advanced Materials (Weinheim, Germany)* **2002**, 14, 953.
- [9] G. G. Wallace, G. M. Spinks, *Chemical Engineering Progress* **2007**, 103, S18.
- [10] J. Kohn, *Nature Materials* **2004**, 3, 745.
- [11] N. K. Guimard, N. Gomez, C. E. Schmidt, *Progress in Polymer Science* **2007**, 32, 876.
- [12] C. K. Chiang, C. R. Fincher, Jr., Y. W. Park, A. J. Heeger, H. Shirakawa, E. J. Louis, S. C. Gau, A. G. MacDiarmid, *Physical Review Letters* **1977**, 39, 1098.

- [13] H. Shirakawa, E. J. Louis, A. G. MacDiarmid, C. K. Chiang, A. J. Heeger, *Journal of the Chemical Society, Chemical Communications* **1977**, 578.
- [14] H. S. Nalwa, Editor, *Handbook of Advanced Electronic and Photonic Materials and Devices, Volume 8: Conducting Polymers*, **2001**.
- [15] A. G. MacDiarmid, *Synthetic Metals* **2001**, 125, 11.
- [16] J. Roncali, *Chemical Reviews (Washington, DC, United States)* **1992**, 92, 711.
- [17] B. R. Hsieh, Y. Wei, *ACS Symposium Series* **1999**, 735, 1.
- [18] G. M. Spinks, P. C. Innis, T. W. Lewis, L. A. P. Kane-Maguire, G. G. Wallace, *Materials Forum* **2000**, 24, 125.
- [19] M. Martina, D. W. Hutmacher, *Polymer International* **2007**, 56, 145.
- [20] R. T. Richardson, B. Thompson, S. Moulton, C. Newbold, M. G. Lum, A. Cameron, G. Wallace, R. Kapsa, G. Clark, S. O'Leary, *Biomaterials* **2007**, 28, 513.
- [21] M.-Y. Li, P. Bidez, E. Guterman-Tretter, Y. Guo, A. G. MacDiarmid, P. I. Lelkes, X.-B. Yuan, X.-Y. Yuan, J. Sheng, H. Li, C.-X. Song, Y. Wei, *Chinese Journal of Polymer Science* **2007**, 25, 331.
- [22] P. R. Bidez, III, S. Li, A. G. MacDiarmid, E. C. Venancio, Y. Wei, P. I. Lelkes, *Journal of Biomaterials Science, Polymer Edition* **2006**, 17, 199.
- [23] E. Guterman, S. Cheng, K. Palouian, P. Bidez, P. Lelkes, Y. Wei, *Abstracts of Papers, 224th ACS National Meeting, Boston, MA, United States, August 18-22*, **2002**, 420.
- [24] M. Waugaman, B. Sannigrahi, P. McGeady, I. M. Khan, *European Polymer Journal* **2003**, 39, 1405.

- [25] L. J. del Valle, D. Aradilla, R. Oliver, F. Sepulcre, A. Gamez, E. Armelin, C. Aleman, F. Estrany, *European Polymer Journal* **2007**, *43*, 2342.
- [26] D.-F. Li, H.-J. Wang, J.-X. Fu, W. Wang, X.-S. Jia, J.-Y. Wang, *Journal of Physical Chemistry B* **2008**, *112*, 16290.
- [27] M. R. Abidian, D.-H. Kim, D. C. Martin, *Advanced Materials (Weinheim, Germany)* **2006**, *18*, 405.
- [28] G. Shi, M. Rouabhia, Z. Wang, L. H. Dao, Z. Zhang, *Biomaterials* **2004**, *25*, 2477.
- [29] G. Shustak, M. Gadzinowski, S. Slomkowski, A. J. Domb, D. Mandler, *New Journal of Chemistry* **2007**, *31*, 163.
- [30] T. J. Rivers, T. W. Hudson, C. E. Schmidt, *Advanced Functional Materials* **2002**, *12*, 33.
- [31] L. Huang, J. Hu, L. Lang, X. Wang, P. Zhang, X. Jing, X. Wang, X. Chen, P. I. Lelkes, A. G. MacDiarmid, Y. Wei, *Biomaterials* **2007**, *28*, 1741.
- [32] N. K. Guimard, J. L. Sessler, C. E. Schmidt, *Materials Research Society Symposium Proceedings* **2007**, *950E*, No pp given.
- [33] A. Treiber, P. M. Dansette, H. El Amri, J.-P. Girault, D. Ginderow, J.-P. Mornon, D. Mansuy, *Journal of the American Chemical Society* **1997**, *119*, 1565.
- [34] J. Roncali, *Journal of Materials Chemistry* **1999**, *9*, 1875.
- [35] G. E. Collis, A. K. Burrell, S. M. Scott, D. L. Officer, *Journal of Organic Chemistry* **2003**, *68*, 8974.
- [36] N. J. L. Guernion, W. Hayes, *Current Organic Chemistry* **2004**, *8*, 637.
- [37] I. Osaka, R. D. McCullough, *Accounts of Chemical Research* **2008**, *41*, 1202.

- [38] R. D. McCullough, S. P. Williams, S. Tristram-Nagle, M. Jayaraman, P. C. Ewbank, L. Miller, *Synthetic Metals* **1995**, *69*, 279.
- [39] L. An, L. Liu, S. Wang, *Biomacromolecules* **2009**, *10*, 454.
- [40] H.-C. Kim, S.-K. Lee, W. B. Jeon, H.-K. Lyu, S. W. Lee, S. W. Jeong, *Ultramicroscopy* **2008**, *108*, 1379.
- [41] H. Meng, J. Zheng, A. J. Lovinger, B.-C. Wang, P. G. Van Patten, Z. Bao, *Chemistry of Materials* **2003**, *15*, 1778.
- [42] W. Huang, H. Meng, W.-L. Yu, J. Pei, Z.-K. Chen, Y.-H. Lai, *Macromolecules* **1999**, *32*, 118.
- [43] F. C. Krebs, H. Spanggaard, *Solar Energy Materials & Solar Cells* **2005**, *88*, 363.
- [44] A. Iraqi, D. F. Pickup, *Polymer International* **2006**, *55*, 780.
- [45] J. Cremer, E. Mena-Osteritz, N. G. Pschierer, K. Muellen, P. Baeuerle, *Organic & Biomolecular Chemistry* **2005**, *3*, 985.
- [46] T. L. Benanti, A. Kalaydjian, D. Venkataraman, *Macromolecules (Washington, DC, United States)* **2008**, *41*, 8312.
- [47] M. A. Gauthier, M. I. Gibson, H.-A. Klok, *Angewandte Chemie, International Edition* **2009**, *48*, 48.
- [48] T. A. Skotheim, J. R. Reynolds, Editors, *Handbook of Conducting Polymers, Third Edition: Conjugated Polymers, Theory, Synthesis, Properties, and Characterization*, **2007**.
- [49] M. Pomerantz, Y. Cheng, R. K. Kasim, R. L. Elsenbaumer, *Synthetic Metals* **1999**, *101*, 162.
- [50] A. Galal, E. T. Lewis, O. Y. Ataman, H. Zimmer, H. B. Mark, Jr., *Journal of Polymer Science, Part A: Polymer Chemistry* **1989**, *27*, 1891.

- [51] J. Roncali, F. Garnier, M. Lemaire, R. Garreau, *Synthetic Metals* **1986**, *15*, 323.
- [52] S. Gambhir, K. Wagner, D. L. Officer, *Synthetic Metals* **2005**, *154*, 117.
- [53] E. Lukevics, P. Arsenyan, O. Pudova, *Heterocycles* **2003**, *60*, 663.
- [54] J. Kromer, P. Bauerle, *Tetrahedron* **2001**, *57*, 3785.
- [55] J. Hassan, C. Gozzi, E. Schulz, M. Lemaire, *Journal of Organometallic Chemistry* **2003**, *687*, 280.
- [56] A. K. Burrell, J. Chen, G. E. Collis, D. K. Grant, D. L. Officer, C. O. Too, G. G. Wallace, *Synthetic Metals* **2003**, *135-136*, 97.
- [57] T. Pinault, F. Cherioux, B. Therrien, G. Suess-Fink, *Heteroatom Chemistry* **2004**, *15*, 121.
- [58] G. Koeckelberghs, M. Vangheluwe, K. Van Doorselaere, E. Robijns, A. Persoons, T. Verbiest, *Macromolecular Rapid Communications* **2006**, *27*, 1920.
- [59] M. C. Iovu, E. E. Sheina, R. R. Gil, R. D. McCullough, *Macromolecules* **2005**, *38*, 8649.
- [60] M. Pomerantz, H. Yang, Y. Cheng, *Macromolecules* **1995**, *28*, 5706.
- [61] V. M. Niemi, P. Knuutila, J. E. Osterholm, J. Korvola, *Polymer* **1992**, *33*, 1559.
- [62] A. Babel, D. Li, Y. Xia, S. A. Jenekhe, *Macromolecules* **2005**, *38*, 4705.
- [63] J. M. Pringle, O. Ngamna, J. Chen, G. G. Wallace, M. Forsyth, D. R. MacFarlane, *Synthetic Metals* **2006**, *156*, 979.
- [64] S. Nair, E. Hsiao, S. H. Kim, *Chemistry of Materials* **2009**, *21*, 115.
- [65] M. Trznadel, A. Pron, M. Zagorska, R. Chrzaszcz, J. Pielichowski, *Macromolecules* **1998**, *31*, 5051.

- [66] R. D. McCullough, R. D. Lowe, *Journal of the Chemical Society, Chemical Communications* **1992**, 70.
- [67] T.-A. Chen, X. Wu, R. D. Rieke, *Journal of the American Chemical Society* **1995**, *117*, 233.
- [68] P. Vallat, J. P. Lamps, F. Schosseler, M. Rawiso, J. M. Catala, *Macromolecules (Washington, DC, United States)* **2007**, *40*, 2600.
- [69] A. Fraleoni-Morgera, C. Della-Casa, M. Lanzi, P. Costa-Bizzarri, *Macromolecules* **2003**, *36*, 8617.
- [70] C. Lee, K. J. Kim, S. B. Rhee, *Synthetic Metals* **1995**, *69*, 295.
- [71] K. Buga, R. Pokrop, A. Majkowska, M. Zagorska, J. Planes, F. Genoud, A. Pron, *Journal of Materials Chemistry* **2006**, *16*, 2150.
- [72] M. Nicolas, F. Guittard, S. Geribaldi, *Journal of Polymer Science, Part A: Polymer Chemistry* **2007**, *45*, 4707.
- [73] W.-S. Huang, *Polymer* **1994**, *35*, 4057.
- [74] C. Della Casa, E. Salatelli, F. Andreani, P. Costa Bizzarri, *Makromolekulare Chemie, Macromolecular Symposia* **1992**, *59*, 233.
- [75] P. C. Ewbank, G. Nuding, H. Suenaga, R. D. McCullough, S. Shinkai, *Tetrahedron Letters* **2001**, *42*, 155.
- [76] M. I. Arroyo-Villan, G. A. Diaz-Quijada, M. S. A. Abdou, S. Holdcroft, *Macromolecules* **1995**, *28*, 975.
- [77] B. Kim, L. Chen, J. Gong, Y. Osada, *Macromolecules* **1999**, *32*, 3964.
- [78] K. A. Murray, A. B. Holmes, S. C. Moratti, R. H. Friend, *Synthetic Metals* **1996**, *76*, 161.
- [79] P. Camurlu, A. Cirpan, L. Toppare, *Materials Chemistry and Physics* **2005**, *92*, 413.

- [80] J.-K. Lee, W.-S. Kim, H.-J. Lee, W. S. Shin, S.-H. Jin, W.-K. Lee, M.-R. Kim, *Polymers for Advanced Technologies* **2006**, *17*, 709.
- [81] F. Demanze, A. Yassar, F. Garnier, *Macromolecules* **1996**, *29*, 4267.
- [82] L. Tan, M. D. Curtis, A. H. Francis, *Macromolecules* **2002**, *35*, 4628.
- [83] M. Andersson, P. O. Ekeblad, T. Hjertberg, O. Wennerstroem, O. Inganaes, *Polymer Communications* **1991**, *32*, 546.
- [84] T. Kuwahara, K. Oshima, M. Shimomura, S. Miyauchi, *Synthetic Metals* **2005**, *152*, 29.
- [85] A. Donat-Bouillud, L. Mazerolle, P. Gagnon, L. Goldenberg, M. C. Petty, M. Leclerc, *Chemistry of Materials* **1997**, *9*, 2815.
- [86] M. Grigoras, O. Catanescu, C. I. Simionescu, *Revue Roumaine de Chimie* **2002**, *46*, 927.
- [87] G. M. Cooper, *The Cell : A Molecular Approach*, 5th ed., Sinauer Associates, , Sunderland, Mass., **2009**.
- [88] C. R. Hauer, G. S. King, E. L. McCool, W. B. Euler, J. D. Ferrara, W. J. Youngs, *Journal of the American Chemical Society* **1987**, *109*, 5760.
- [89] G. Zotti, A. Randi, S. Destri, W. Porzio, G. Schiavon, *Chemistry of Materials* **2002**, *14*, 4550.
- [90] S. Destri, I. A. Khotina, W. Porzio, C. Botta, *Optical Materials (Amsterdam)* **1998**, *9*, 411.
- [91] S. Destri, I. A. Khotina, W. Porzio, *Macromolecules* **1998**, *31*, 1079.
- [92] C. Botta, S. Destri, W. Porzio, L. Rossi, R. Tubino, *Synthetic Metals* **1998**, *95*, 53.
- [93] T. Olinga, S. Destri, W. Porzio, A. Selva, *Macromolecular Chemistry and Physics* **1997**, *198*, 1091.

- [94] S. Destri, W. Porzio, I. Khotina, T. E. Olinga, *Synthetic Metals* **1997**, *84*, 219.
- [95] C. Wang, S. Shieh, E. LeGoff, M. G. Kanatzidis, *Macromolecules* **1996**, *29*, 3147.
- [96] Y. A. Dubitsky, M. Catellani, A. Bolognesi, S. Destri, W. Porzio, *Synthetic Metals* **1993**, *55*, 1266.
- [97] A. Bianco, C. Bertarelli, S. Frisk, J. F. Rabolt, M. C. Gallazzi, G. Zerbi, *Synthetic Metals* **2007**, *157*, 276.
- [98] H. Liu, C. H. Reccius, H. G. Craighead, *Applied Physics Letters* **2005**, *87*, 253106/1.
- [99] D. Li, A. Babel, S. A. Jenekhe, Y. Xia, *Advanced Materials (Weinheim, Germany)* **2004**, *16*, 2062.
- [100] X. Wang, S. Ochiai, G. Sawa, Y. Uchida, K. Kojima, A. Ohashi, T. Mizutani, *Japanese Journal of Applied Physics, Part 1: Regular Papers, Brief Communications & Review Papers* **2007**, *46*, 1337.
- [101] J.-F. Chang, B. Sun, D. W. Breiby, M. M. Nielsen, T. I. Soelling, M. Giles, I. McCulloch, H. Sirringhaus, *Chemistry of Materials* **2004**, *16*, 4772.
- [102] C.-C. Liu, C.-M. Yang, W.-H. Liu, H.-H. Liao, S.-F. Horng, H.-F. Meng, *Synthetic Metals* **2009**, *159*, 1131.
- [103] K. Norrman, A. Ghanbari-Siahkali, N. B. Larsen, *Annual Reports on the Progress of Chemistry, Section C: Physical Chemistry* **2005**, *101*, 174.
- [104] T. A. Skotheim, J. R. Reynolds, Editors, *Handbook of Conducting Polymers, Third Edition. Conjugated Polymers Processing and Applications*, **2007**.
- [105] J. B. Chang, V. Liu, V. Subramanian, K. Sivula, C. Luscombe, A. Murphy, J. Liu, J. M. J. Frechet, *Journal of Applied Physics* **2006**, *100*, 014506/1.

- [106] P. G. Campbell, L. E. Weiss, *Expert Opinion on Biological Therapy* **2007**, *7*, 1123.
- [107] J. M. Razal, J. N. Coleman, E. Munoz, B. Lund, Y. Gogotsi, H. Ye, S. Collins, A. B. Dalton, R. H. Baughman, *Advanced Functional Materials* **2007**, *17*, 2918.
- [108] A. J. Granero Rodriguez, (Ed.: R. Breukers), Wollongong, **2010**.
- [109] L. P. Cheng, J. Zhang, Q. R. Wang, *Donghua Daxue Xuebao, Ziran Kexueban* **2006**, *32*, 102.
- [110] J. M. Razal, M. Kita, A. F. Quigley, E. Kennedy, S. E. Moulton, R. M. I. Kapsa, G. M. Clark, G. G. Wallace, *Advanced Functional Materials* **2009**, *19*, 3381.
- [111] A. F. Quigley, J. M. Razal, B. C. Thompson, S. E. Moulton, M. Kita, E. L. Kennedy, G. M. Clark, G. G. Wallace, R. M. I. Kapsa, *Advanced Materials (Weinheim, Germany)* **2009**, *21*, 4393.
- [112] R. Jalili, University of Wollongong, **2010**, unpublished results.
- [113] D. Li, Y. Xia, *Advanced Materials (Weinheim, Germany)* **2004**, *16*, 1151.
- [114] X. Zong, H. Bien, C.-Y. Chung, L. Yin, D. Fang, B. S. Hsiao, B. Chu, E. Entcheva, *Biomaterials* **2005**, *26*, 5330.
- [115] www.nanost.net/?viewthread-11586.html, **2008**.
- [116] R. Gonzalez, N. J. Pinto, *Synthetic Metals* **2005**, *151*, 275.
- [117] A. Laforgue, L. Robitaille, *Synthetic Metals* **2008**, *158*, 577.

CHAPTER 2. EXPERIMENTAL.

2.1 General experimental details.

Materials.

All reagents and chemicals were purchased from Aldrich (Sigma-Aldrich, Sydney, Australia) and were used without further purification unless otherwise stated. Ajax chloroform, DCM, ether, ethyl acetate and hexane were supplied by Lomb Scientific (Sydney, Australia), Scharlau methanol was obtained from Chem-Supply (Gillman, SA, Australia). Aldrich nitromethane and acetonitrile, and Sigma DMF were from Sigma-Aldrich (Sydney, Australia). Analytical TLC was performed on silica gel-coated plastic sheets (Merk 60) and visualised under UV light unless otherwise stated. Flash and column chromatography was performed using Kieselgel 60 as adsorbent. Anhydrous solvents were dried according to the procedures outlined in Perrin and Armarego.^[1] All reactions requiring anhydrous reagents were carried out under an inert atmosphere of argon or nitrogen. Solvents used for spectroscopy were analytical reagents.

Nuclear magnetic resonance.

Spectra were measured at 400 MHz (¹H), 100.6 MHz (¹³C) on a Bruker nuclear magnetic resonance (NMR) spectrometer. All NMR spectra were recorded in deuteriochloroform (CDCl₃) solution unless otherwise stated, with reference to tetramethylsilane (TMS).

Gel permeation chromatography.

The molecular weight of polymers was determined by GPC using THF as solvent and a Shimadzu LC-20AT gel chromatograph fitted with a Phenomenex phenogel column (10 μm x 600 mm) and a Sedex LT-ELSD 60 LT detector calibrated by polystyrene standards.

Fourier transform infrared spectroscopy.

Attenuated total reflectance FTIR spectra of polymer films and fibres were recorded using a Shimadzu IR prestige-21 spectrometer equipped with a Pike Technologies MiricleA germanium crystal ATR attachment.

Matrix assisted laser desorption ionisation (MALDI) mass spectroscopy.

The molecular weight of polymers, oligomers and monomers was determined on a Shimadzu-Biotech AXIMA Confidence MALDI MS using a dithranol matrix.

Electrochemical characterisation.

Cyclic voltammograms (CV's) were recorded using an eDAQ system controlled by EChem software. In either 0.1 M tetrabutylammonium perchlorate (TBAP) acetonitrile electrolyte, or in aqueous 0.1 M KNO_3 . The potential range -300 mV to $+900$ mV with a scan rate of 100 mVs^{-1} was used unless otherwise stated. The electrochemical cell consisted of the polymer-coated working electrode, a platinum mesh counter electrode and Ag/Ag^+ reference electrode for the acetonitrile system or Ag/AgCl for the aqueous system.

UV-visible spectroscopy.

Electronic spectra were recorded in chloroform unless otherwise stated using a Shimadzu UV-1601CE spectrometer.

UV-visible spectroelectrochemistry.

UV-visible spectroelectrochemistry was performed using the Shimadzu UV-1601CE spectrometer and eDAQ potentiostat system controlled by EChem software. Polymer films were characterised on ITO glass substrates using an ITO glass slide sputter coated with platinum as counter electrode and Ag/Ag⁺ reference electrode using 0.1 M TBAP acetonitrile electrolyte. Spectra of the polymer films were collected at every 0.1 V between -0.3 V and 1 V, the spectrum at each potential was applied for 1 minute prior to and during spectrum acquisition.

Contact angle measurements.

The wettability of the films was characterised using a DataPhysics OCA20 goniometer and the sessile drop technique^[2] with a 10 µL drop of RO water.

Conductivity measurements.

The conductivity of polymer films was measured in the oxidised state on drop cast films that had been oxidised in an iodine atmosphere. A Jandel-RM3 four point probe was used to take current measurements at a range of voltages. The thickness of the polymer films was measured by micrometer. The conductivity of the polymer films was then calculated.

Imaging.

Light microscope images were obtained on a Leica 2084 microscope. SEM images were obtained by Dr Tony Romeo on a JEOL JSM7500FA cold Field Emission Gun Scanning Electron Microscope, equipped with a JEOL hyper-minicup energy dispersive spectrometer, operated at an accelerating voltage of 5 kV, secondary electron images were taken with a semi in-lens detector. AFM images were obtained by Dr Michael Higgins on an Asylum Research MFP-3D AFM using a 0.29 Nm⁻¹ silicon nitride cantilever in contact mode with a scan rate of 0.5 Hz.

Biocompatibility analysis.

Biocompatibility studies were performed by Dr Kerry Gilmore, Dr Anita Quigley, and Ms. Magdalena Kita. Preliminary biocompatibility studies were performed using C2C12 cells cultured in Dulbecco's modified Eagle's medium (DMEM) containing 4 mM L-glutamine and 10% FBS. C2C12 cells were seeded at 15×10^3 per cm². Cell adhesion and proliferation was quantified using a Lactate Dehydrogenase assay.

Differentiation studies were performed using primary skeletal muscle myoblasts (ROSA cells), isolated from 5-6 weeks old male transgenic 129S4Gt (ROSA) 26 mice. ROSA cells were seeded at 30×10^3 cells per cm² in culture media, allowed to adhere for 24 hours before transferring to low serum differentiation media for a period of 3 - 4 days, with media changes every 48 hours. These cells were then immunostained using anti-Desmin antibody and counter stained with 1 $\mu\text{g mL}^{-1}$ 4',6-diamidino-2-phenylindole (DAPI). All biocompatibility studies were conducted in triplicate at 37°C, in a humidified, 5% CO₂ atmosphere, on polymer films that had been sterilised by ethanol and pre-soaked in cell culture media.

2.2 Synthetic procedures.

2.2.1 Chapter 3.

3-Methoxythiophene **7**.

3-Methoxythiophene **7** was prepared following the procedure of Zotti *et al.*^[3] Sodium methoxide (22.5 g, 0.42 mol) was dissolved in NMP (50 mL) and methanol (50 mL) the methanol was distilled off and the reaction cooled to 80°C. 3-Bromothiophene **8** (20 mL, 34.2 g, 0.21 mol) and copper bromide (3 g, 0.021 mol) were added and the reaction heated at 120°C for 2 hours then stirred overnight at room temperature. The reaction mixture was diluted with diethyl ether (50 mL), filtered through filter paper, washed with a saturated solution of NH₄Cl (100 mL), diluted with water (100 mL) and the organic phase extracted with diethyl ether (2 x 100 mL). The combined ether extracts were washed with water (50 mL) and dried (MgSO₄). The ether was distilled off then the product 3-methoxythiophene **7** was distilled under vacuum (b.p. 45°C, 0.2 mm Hg). Yield: 12 g, 50% (lit.^[3] 82%). ¹H NMR (400 MHz, CDCl₃) δ 7.17 (dd, 1H, *J*_{5,2}=3.2 Hz, *J*_{5,4}=5.2 Hz, H5); 6.75 (dd, 1H, *J*_{4,2}=1.6 Hz, *J*_{4,5}=5.2 Hz, H4); 6.25 (dd, 1H *J*_{2,4}=1.6 Hz, *J*_{2,5}=3.2 Hz, H2); 3.81 (s, 3H, OCH₃).

3-Decoxythiophene **9**.

The procedure of Zotti *et al.* for 3-pentylthiophene was modified for the formation of 3-decoxythiophene **9**.^[3] 3-Methoxythiophene **7** (12 g, 0.105 mol) was heated at 140°C with decanol (21.7 g, 0.137 mol), toluene (6 mL) and NaHSO₄ (0.573 g) as a catalyst for 2 hours using a fractionating column for later distillation. The toluene and methanol were distilled off up to a temperature of 110°C. The decanol was then removed using a vacuum pump (120°C, 0.05 mm Hg). 3-Decoxythiophene **9** was

then purified on a silica column using hexane as the eluent. Yield: 15.5 g, 62% (lit.^[4] 86%). ¹H NMR (400 MHz, CDCl₃) δ 7.16 (dd, 1H, *J*_{5,2}=3.2 Hz, *J*_{5,4}=5.2 Hz, H5); 6.75 (dd, 1H, *J*_{4,2}=1.6 Hz, *J*_{4,5}=5.2 Hz, H4); 6.25 (dd, 1H, *J*_{2,4}=1.6 *J*_{2,5}=3.2 Hz); 3.93 (t, 2H, *J*=6.4 OCH₂); 1.80-0.80 (8CH₂, CH₃).

3-Decoxythiophene-5-boronic acid 6.

The procedure of Zotti *et al.* for 3-pentylthiophene-5-boronic acid was modified for the formation of 3-decoxythiophene-5-boronic acid **6**.^[3] n-Butyl lithium (44.7 mL, 2.5 M in hexanes, 0.112 mol) was added to a solution of DIPA (10.96 g, 0.108 mol) in anhydrous THF (100 mL) at -78°C under argon. The reaction mixture was then warmed to 0°C for 10 min then cooled back to -78°C. At this temperature a solution of 3-decoxythiophene **9** (20 g, 0.083 mol) and triisopropyl borate (47.7 g, 0.25 mol) in anhydrous THF (20 mL) was slowly added to the cooled reaction. The reaction mixture was stirred at -78°C for 1 hour and then at room temperature overnight. The reaction mixture was poured onto cold 8% HCl (240 mL) and stirred for 1 hour. The organic layer was separated and the aqueous layer extracted with diethyl ether (2 x 200 mL) and the combined organic layers were washed with water (160 mL), then dried (MgSO₄). The solvent was removed leaving solid 3-decoxythiophene-5-boronic acid **6**, a slurry was formed with pentane (30 mL) the product was filtered and washed with more pentane (15 mL) leaving 3-decoxythiophene-5-boronic acid **6** as a light yellow solid. Yield: 14.8 g, 63%. ¹H NMR (400 MHz, CDCl₃) δ 7.17 (d, 1H, *J*_{3,5}=1.4, H3); 6.56 (d, 1H, *J*_{5,3}=1.4, H5); 3.95 (t, 2H, *J*=6.3, OCH₂); 1.8-0.8 (8CH₂ and CH₃). The ¹H NMR spectrum also showed peaks corresponding to the self anhydride consistent with literature.^[3]

2,5-Dibromothiophene 10.

NBS (8.98 g, 0.05 mol) was added to a solution of thiophene (2 g, 23.7 mmol) in THF (100 mL) and the reaction mixture was stirred overnight. After this time TLC revealed complete reaction. The solvent was removed, the crude product was washed by ether and filtered to remove the succinimide. The ether was removed and the product passed through a pad of silica using 50% DCM/hexane to remove any impurities. Yield: 4.69 g, 82% (lit.^[5] 72%). ¹H NMR (400 MHz, CDCl₃) δ 6.843 (s, 2H). The ¹H NMR of this well known compound agreed with the literature.^[5, 6]

2,5-Dibromo-3-cyanothiophene.

Procedure modified from that developed by Dr Sanjeev Gambhir.^[7] 2,5-Dibromo-3-carboxaldehyde thiophene (12 g, 44 mmol) was dissolved in THF (50 mL), a 28% solution of ammonium hydroxide (500 mL) was then added followed by iodine (12.432 g, 49 mmol). The reaction mixture was then stirred for 1.5 hours at room temperature. TLC using 2,4-DNP as indicator showed full conversion of the aldehyde. The product was obtained by extraction by DCM, dried (MgSO₄) and the solvent removed by rotary evaporator. The crude product was shown to be pure by ¹H NMR and taken for the next step. Yield: 11.7 g, 99% (lit.^[8] 97%). ¹H NMR (400 MHz, CDCl₃) δ 7.06 (s, 1H, H4).

2,5-Dibromothiophene-3-carboxylic acid.

Procedure modified from Dr Sanjeev Gambhir.^[7] 2,5-Dibromo-3-cyanothiophene (5 g, 18.7 mmol) was added to a solution of sodium hydroxide (10 g, 0.25 mol) in RO water (50 mL). The suspension was refluxed for 5 hours. Only a small quantity of

black material remained suspended after this time. The reaction mixture was diluted to 100mL with RO water and filtered through filter paper. The filtrate was then acidified with 10% HCl (150 mL). The white precipitate was collected by filtration and washed with ice cold water (50 mL). 2,5-Dibromothiophene-3-carboxylic acid was then dried overnight under vacuum. Yield: 4.35 g, 81% (lit.^[9] 87%). ¹H NMR (400 MHz, CDCl₃) δ 7.41(s, 1H, H4). Data is in agreement with the literature.^[9]

Methyl 2,5-dibromothiophene-3-carboxylate 11.

Procedure modified from Dr Sanjeev Gambhir.^[7] 2,5-Dibromothiophene-3-carboxylic acid (4 g, 14 mmol) was dissolved in methanol (50 mL). Conc. H₂SO₄ (1mL) was added and the solution refluxed overnight under argon. TLC showed reaction complete poured onto water (100 mL) and removed the methanol on a rotary evaporator. The ester **11** was extracted with DCM (3 x 50 mL) this was dried (MgSO₄) and neutralised (K₂CO₃). The solvent was removed under reduced pressure and residual solvent removed under vacuum. Yield: 2.6 g, 62% (lit.^[10] 59%). ¹H NMR (400 MHz, CDCl₃) δ 7.35 (s, 1H, H4), 3.87 (s, 3H, -COOCH₃). Data is in agreement with that of Dr Sanjeev Gambhir.^[7]

Decyl 2,5-dibromothiophene-3-carboxylate 12.

Procedure modified from Dr Sanjeev Gambhir.^[7] 2,5-Dibromothiophene-3-carboxylic acid (2.21 g, 7.8 mmol) was refluxed with stirring for 2 hours in thionyl chloride (18 mL). The thionyl chloride was then removed by a rotary evaporator. Decanol (11.6 mL) and pyridine (2 mL) were then added. The reaction mixture was stirred at 80°C for 3.5 hours under a nitrogen atmosphere. After this time TLC

showed the reaction was complete. The reaction mixture was worked up by pouring onto ice (10 g) adding ether (50 mL) then washing with 5% HCl (50 mL), water (50 mL), saturated potassium carbonate solution (50 mL), then water (50 mL). The organic phase was dried by magnesium sulfate and the ether removed by rotary evaporator. The decanol was then removed by vacuum distillation from an oil bath at 120°C. Yield: 2.5 g, 75%. ¹H NMR (400 MHz, CDCl₃) δ 7.35 (s, 1H, H4), 4.10 (t, 2H, J = 6.6, COOCH₂); 1.80-0.86 (8CH₂, 1CH₃). Data is in agreement with that of Dr Sanjeev Gambhir.^[7]

3-Thiophene acetic acid methyl ester.

3-Thiophene acetic acid (1 g, 7 mmol) was dissolved in methanol (40 mL), conc. H₂SO₄ (0.5 mL) was added and the reaction refluxed overnight under nitrogen. TLC analysis revealed the reaction was complete after this time, water was added and the ester was extracted by DCM, dried (MgSO₄) and then the solvent was removed. Yield: 1 g, 91%. ¹H NMR (400 MHz, CDCl₃) δ 7.27 (dd, 1H, J_{5,2}=3.1 Hz, J_{5,4}=5.3 Hz, H5), 7.13 (dd, 1H J_{2,4}=1.6 Hz, J_{2,5}=3.1 Hz, H2), 7.02 (dd, 1H, J_{4,2}=1.6 Hz, J_{4,5}=5.3 Hz, H4), 3.69 (s, 3H, CH₃), 3.64 (s, 2H, CH₂). The ¹H NMR of this known compound agrees with the literature.^[11]

Methyl 2,5-dibromothiophene-3-acetate 13.

NBS (2.34 g, 13 mmol) was added to a solution of 3-thiophene acetic acid methyl ester (1 g, 6.4 mmol) in THF (50 mL) and the reaction mixture was stirred overnight. After this time TLC revealed complete reaction. The solvent was removed; crude **13** was washed by ether and filtered to remove the succinimide. The ether was removed and the product passed through a short silica column using 50% DCM/hexane as

eluent. Yield: 1.82 g, 91%. $^1\text{H NMR}$ (400 MHz, CDCl_3) δ 7.12 (s, 1H, H4), 3.71 (s, 3H, CH_3), 3.65 (s, 2H, CH_2). Data is in agreement with that of Dr Sanjeev Gambhir.^[7]

Methyl 4,4''-didecoxy-2,2':5',2''-terthiophene-3'-carboxylate 1.

Procedure modified from Dr Sanjeev Gambhir.^[7] Methyl 2,5-dibromothiophene-3-carboxylate **11** (1 g, 3.3 mmol) was dissolved in dimethoxyethane (30 mL). To this was added a K_2CO_3 solution (1 M, 20 mL), 3-decoxy thiophene-5-boronic acid **6** (2.84 g, 0.01 mol) and $\text{Pd}(\text{PPh}_3)_4$ (0.25 g, 0.2 mmol). These were stirred together under argon at 65°C for 4 hours. TLC revealed the reaction was incomplete. Additional 3-Decoxy thiophene-5-boronic acid **6** (1.5 g, 5.3 mmol) and $\text{Pd}(\text{PPh}_3)_4$ (0.05 g, 0.04 mmol) were added. The reaction was continued overnight. TLC analysis showed that the reaction was complete. The product was extracted with DCM (2 x 25 mL) and dried (MgSO_4) then the solvent was removed. The crude **1** was diluted in 30% DCM/hexane and purified by column chromatography using 30% DCM/hexane as the eluent. Yield: 1.431 g, 70%. $^1\text{H NMR}$ (400 MHz, CDCl_3) δ 7.47 (s, 1H, H4'); 7.17 (d, 1H, $J = 1.75$ Hz, H3); 6.85 (d, 1H, $J = 1.7$ Hz, H3''); 6.33 (d, 1H, $J = 1.75$ Hz, H5); 6.16 (d, 1H, $J = 1.7$ Hz, H5''); 3.95 (m, 4H, 2OCH_2); 3.84 (s 3H, COOCH_3); 1.79-0.86 (16CH_2 , 2CH_3). UV-visible spectrum λ_{max} 372 nm. MALDI MS m/z 618.3 (M^+). $\nu_{\text{max}}/\text{cm}^{-1}$ 2922, 2852, 1716, 1527, 1456, 1369, 1246, 1170, 1029, 690. Data is in agreement with that of Dr Sanjeev Gambhir.^[7]

Methyl 4,4''-didecoxy-2,2':5',2''-terthiophene-3'-acetate 2.

Procedure modified from Dr Sanjeev Gambhir.^[7] Methyl 2,5-dibromothiophene-3-acetate **13** (1.8 g, 6 mmol) was dissolved in dimethoxyethane (50 mL). To this was

added a K_2CO_3 solution (1 M, 30 mL), 3-decoxy thiophene-5-boronic acid **6** (5 g, 17 mmol) and $Pd(PPh_3)_4$ (0.25 g, 0.2 mmol). These were stirred together under argon at $65^\circ C$ overnight. TLC showed the reaction was complete. The product was extracted with ethyl acetate (2 x 25 mL) and dried ($MgSO_4$), then the solvent was removed. Terthiophene **2** was diluted in 50% DCM/hexane and purified by column chromatography using 50% DCM/hexane as the eluent. Yield: 1.9 g, 51%. 1H NMR (400 MHz, $CDCl_3$) δ 7.06 (s, 1H, H4¹); 6.86 (d, 1H, J = 1.72 Hz, H3); 6.83 (d, 1H, J = 1.68 Hz, H3^{''}); 6.24 (d, 1H, J = 1.72 Hz, H5); 6.13 (d, 1H, J = 1.68 Hz, H5^{''}); 3.94 (m, 4H, 2OCH₂); 3.74 (s 3H, COOCH₃); 3.73 (s 2H, ArCH₂); 1.79-0.86 (16CH₂, 2CH₃). ν_{max}/cm^{-1} 2924, 2852, 1739, 1539, 1448, 1259, 1168, 1020, 692. Data is in agreement with that of Dr Sanjeev Gambhir.^[7]

Decyl 4,4''-didecoxy-2,2':5',2''-terthiophene-3'-carboxylate 3.

Procedure modified from Dr Sanjeev Gambhir.^[7] Decyl 2,5-dibromothiophene-3-carboxylate **12** (2.5 g, 5.9 mmol) was dissolved in dimethoxyethane (53 mL). To this was added a K_2CO_3 solution (1 M, 35 mL), 3-decoxythiophene-5-boronic acid **6** (4.9 g, 17 mmol) and $Pd(PPh_3)_4$ (0.25 g, 0.2 mmol). These were stirred together under argon at $65^\circ C$ overnight. TLC revealed the reaction was complete. The product was extracted with DCM (2 x 25 mL) and dried ($MgSO_4$) then the solvent was removed. The product **3** was diluted in 30% DCM/hexane and purified by column chromatography using 30% DCM/hexane as the eluent. Yield: 2.2 g, 50%. 1H NMR (400 MHz, $CDCl_3$) δ 7.38 (s, 1H, H4¹); 7.17 (d, 1H, J = 1.74 Hz, H3); 6.85 (d, 1H, J = 1.69 Hz, H3^{''}); 6.34 (d, 1H, J = 1.74 Hz, H5); 6.15 (d, 1H, J = 1.69 Hz, H5^{''}); 4.09 (t, 2H, J = 6.7, COOCH₂); 3.95 (m, 4H, 2OCH₂); 1.80-0.86 (24CH₂, 3CH₃). UV-

visible spectrum λ_{\max} 369 nm. MALDI MS m/z 744.2 (M^+). Data is in agreement with that of Dr Sanjeev Gambhir.^[7]

4,4''-Didecoxy-2,2':5',2''-terthiophene 4.

Procedure modified from Dr Sanjeev Gambhir.^[7] 2,5-dibromothiophene **10** (1.91 g, 8 mmol) was dissolved in dimethoxyethane (50 mL). To this was added a K_2CO_3 solution (1 M, 30 mL), 3-decoxy thiophene-5-boronic acid **6** (6.6 g, 23.5 mmol) and $Pd(PPh_3)_4$ (0.25 g, 0.2 mmol). These were stirred together under argon at 65°C for overnight. TLC analysis showed that the reaction was complete. The product was extracted with DCM (2 x 25 mL) washed by water and dried ($MgSO_4$) then the solvent was removed. The crude **4** was purified by column chromatography using 5% benzene/hexane as the eluent. Yield: 0.8 g, 20%. 1H NMR (400 MHz, $CDCl_3$) δ 7.03 (s, 2H, H3'); 6.83 (d, 2H, J = 1.68 Hz, H3); 6.12 (d, 2H, J = 1.68 Hz, H4); 3.94 (t, 4H, 2OCH₂); 1.8-0.86 (16CH₂, 2CH₃). UV-visible spectrum λ_{\max} 369 nm. MALDI MS m/z 560.4 (M^+). Data is in agreement with that of Dr Sanjeev Gambhir.^[7]

3',4'-Dihexyl-4,4''-didecoxy-2,2':5',2''-terthiophene 5.

Procedure modified from Wagner *et al.*^[12] 2,5-Dibromo-3,4-dihexylthiophene **14** (1.38 g, 3.2 mmol) was dissolved in dimethoxyethane (21 mL). To this was added a K_2CO_3 solution (1 M, 14 mL), 3-decoxy thiophene-5-boronic acid **6** (6.6g, 23.5 mmol) and $Pd(PPh_3)_4$ (0.15 g, 0.12 mmol). These were stirred together under argon at 65°C for overnight. TLC showed reaction complete. The product was extracted with DCM (2 x 25 mL) washed by water and dried ($MgSO_4$) then the solvent was removed. The crude **5** was purified by column chromatography using 90% hexane/DCM as the eluent, then washed twice by methanol (5 mL) to remove any

impurities. Yield: 2.17 g, 90% (lit.^[12] 72%). ¹H NMR (400 MHz, CDCl₃) δ 6.79 (d, 2H, J = 1.64 Hz, H3); 6.20 (d, 2H, J = 1.64 Hz, H4); 3.95 (t, 4H, 2OCH₂); 2.66 (t, 4H, 2Ar-CH₂); 1.82-0.81 (24CH₂, 4CH₃). UV-visible spectrum λ_{max} 325 nm. MALDI MS m/z 728.1 (M⁺). Data is in agreement with the literature.^[12]

4,4''-Didecoxy-2,2':5',2''-terthiophene-3'-carboxylic acid 15.

Procedure modified from Dr Sanjeev Gambhir.^[7] Methyl 4,4''-didecoxy-2,2':5',2''-terthiophene-3'-carboxylate **1** (0.98 g, 1.6 mmol) was added to a solution of potassium hydroxide (0.9 g, 15.8 mmol) in ethanol (95%, 30 mL) and water (3 mL). The reaction mixture was then heated to 80°C for 4 hours. After this time the solvent was removed and water (20 mL) and DCM (20 mL) were added. The reaction mixture was then acidified to pH 4 with dilute HCl. The product was extracted in the DCM layer, dried (MgSO₄) and the solvent removed. The crude acid **15** was then purified on a silica column using 3:7 ethyl acetate: DCM. Yield: 0.596 g, 62%. ¹H NMR (400 MHz, CDCl₃) δ 7.53 (s, 1H, H4'); 7.19 (d, 1H, J = 1.7 Hz, H3); 6.86 (d, 1H, J = 1.6 Hz, H3''); 6.34 (d, 1H, J = 1.6 Hz, H5); 6.18 (d, 1H, J = 1.6 Hz, H5''); 3.95 (m, 4H, 2OCH₂); 1.81-0.86 (16CH₂, 4CH₃). UV-visible spectrum λ_{max} 373 nm. MALDI MS m/z 604.5 (M⁺). ν_{max}/cm⁻¹ 2924, 2852, 1683, 1525, 1456, 1369, 1265, 1170, 1026, 688. Data is in agreement with that of Dr Sanjeev Gambhir.^[7]

4,4''-Didecoxy-2,2':5',2''-terthiophene-3'-acetic acid 16.

Procedure modified from Dr Sanjeev Gambhir.^[7] Methyl 4,4''-didecoxy-2,2':5',2''-terthiophene-3'-acetate **2** (1.15 g, 1.8 mmol) was added to a solution of potassium hydroxide (1 g, 17.9 mmol) in ethanol (95%, 40 mL) and water (4 mL). The

reaction mixture was then heated to 80°C for 4 hours. After this time the solvent was removed and water (25 mL) and DCM (25 mL) were added. The reaction mixture was then acidified to pH 4 with dilute HCl. The product was extracted in the DCM layer, dried (MgSO₄) and the solvent removed. The crude acid **16** was then purified on a silica column using 3:7 ethyl acetate: DCM. Yield: 0.79 g, 71%. ¹H NMR (400 MHz, CDCl₃) δ 7.08 (s, 1H, H4'); 6.86 (d, 1H, J = 1.68 Hz, H3); 6.83 (d, 1H, J = 1.72 Hz, H3''); 6.24 (d, 1H, J = 1.68 Hz, H5); 6.13 (d, 1H, J = 1.72 Hz, H5''); 3.99 (m, 4H, 2OCH₂); 3.78 (s 2H, ArCH₂); 1.8-0.86 (16CH₂, 2CH₃). UV-visible spectrum λ_{max} 353 nm. MALDI MS m/z 618.3 (M⁺). ν_{max}/cm⁻¹ 2924, 2852, 1714, 1533, 1456, 1363, 1259, 1168, 1022, 802, 688. Data is in agreement with that of Dr Sanjeev Gambhir.^[7]

4,4''-Didecoxy-3'-(5-allylidene-pyrimidine-2,4,6(1H,3H,5H)-trione)-2,2':5',2''terthiophene 18.

4,4''-Didecoxy-3'-propenal-2,2':5',2''terthiophene **17** (0.2 g, 0.3 mmol) and barbituric acid (64 mg, 0.5 mmol) were stirred together in DCM (15 mL) and ethanol (15 mL) for 12 hours. The crude was washed by water and extracted by DCM, dried (MgSO₄) and the solvent removed. The crude was then purified on a silica column using DCM to elute remaining starting material and THF to elute the pure 4,4''-didecoxy-3'-(5-allylidene-pyrimidine-2,4,6(1H,3H,5H)-trione)-2,2':5',2''terthiophene **18**. Yield: 0.150 g, 69%. ¹H NMR (400 MHz, CDCl₃) δ 9.67 (m, 2H, 2NH); 8.31 (m, 1H, CH-barbituric); 7.73 (m, 1H, H4'); 7.24 (m, 1H, H3); 6.85 (m, 1H, H3''); 6.56 (m, H5); 6.39 (m, 1H, H5''); 6.20 (m, 2H, 2CH); 3.98 (m, 4H, 2OCH₂); 1.8-0.86 (16CH₂, 2CH₃). MALDI MS m/z 725 (M⁺).

Poly(4,4''-didecoxy-3'-(5-allylidene)pyrimidine-2,4,6(1H,3H,5H)-trione)-2,2':5',2''terthiophene) 19.

To a stirred solution of 4,4''-didecoxy-3'-(5-allylidene)pyrimidine-2,4,6(1H,3H,5H)-trione)-2,2':5',2''terthiophene **18** (100 mg, 0.14 mmol) in chloroform (2 mL) under nitrogen was added dropwise a solution of anhydrous iron chloride (90 mg, 0.55 mmol) in nitromethane (1 mL), after 10 minutes the addition was complete and the reaction mixture was stirred at room temperature for 3 hours. After this time the reaction mixture was poured into methanol (20 mL) to precipitate the polymer. The polymer was then collected by filtration. A sample of the polymer was stirred with THF/hydrazine in an attempt to solubilise the material, however this was unsuccessful. Stirring in a chloroform acetic acid mix also failed to solubilise the *poly(4,4''-didecoxy-3'-(5-allylidene)pyrimidine-2,4,6(1H,3H,5H)-trione)-2,2':5',2''terthiophene) 19*. Yield: 95 mg, 95%. Due to the insoluble nature of **19** it could not be characterised by NMR or GPC.

(Acyl-serine methyl ester)-4,4''-didecoxy-2,2':5',2''-terthiophene-3'-carboxylate 22.

To a solution of 4,4''-didecoxy-2,2':5',2''-terthiophene-3'-carboxylic acid **15** (100 mg, 0.165 mmol) and DCC (60 mg) in THF (10 mL) was added DMAP (2 mg) and acyl-serine methyl ester **20** (50 mg 0.3 mmol) the reagents were stirred together overnight. TLC showed the reaction was complete and the product was extracted from water with DCM. The extract was dried by MgSO₄ and then the solvent removed by rotary evaporator. The crude *(acyl-serine methyl ester)-4,4''-didecoxy-2,2':5',2''-terthiophene-3'-carboxylate 22* was then purified by a silica column using 2% ethyl acetate in DCM. Yield: 60 mg, 49%. ¹H NMR (400 MHz, CDCl₃) δ 7.42 (s,

45

1H, H4'); 7.08 (d, 1H, J = 1.73 Hz, H3); 6.85 (d, 1H, J = 1.6 Hz, H3''); 6.35 (d, 1H, J = 1.73 Hz, H5); 6.18 (d, 1H, J = 1.6 Hz, H5''); 4.90 (dt, 1H, J = 7.8 Hz, J = 3.5 Hz, serine CH); 4.66 (dd, 1H, J = 11.6 Hz, J = 3.5 Hz, serine CH₂*); 4.47 (dd, 1H, J = 11.6 Hz, J = 3.5 Hz, serine CH₂*); 3.94 (m, 5H, serine NH, 2OCH₂); 3.75 (s 3H, serine COOCH₃); 2.03 (s 3H, serine COCH₃); 1.79-0.86 (16CH₂, 2CH₃). UV-visible spectrum λ_{\max} 369 nm. MALDI MS m/z 747 (M⁺).

(BOC-tyrosine methyl ester)-4,4''-didecoxy-2,2':5',2''-terthiophene-3'-carboxylate 23.

To a solution of 4,4''-didecoxy-2,2':5',2''-terthiophene-3'-carboxylic acid **15** (100 mg, 0.165 mmol) and DCC (60 mg) in THF (10 mL) was added DMAP (6 mg) and BOC-tyrosine methyl ester **21** (200 mg, 0.7 mmol). The reagents were stirred together overnight. TLC showed the reaction was complete and the product was extracted from water with DCM. The extract was dried by MgSO₄ and then the solvent removed by rotary evaporator. The crude (*BOC-tyrosine methyl ester*)-4,4''-didecoxy-2,2':5',2''-terthiophene-3'-carboxylate **23** was then purified by a silica column using 2% ethyl acetate in DCM. Yield: 100 mg, 69%. ¹H NMR (400 MHz, CDCl₃) δ 7.63 (s, 1H, H4'); 7.24 (d, 1H, J = 1.80 Hz, H3); 7.15 (m, 4H, tyrosine Ar); 6.89 (d, 1H, J = 1.61 Hz, H3''); 6.32 (d, 1H, J = 1.80 Hz, H5); 6.19 (d, 1H, J = 1.61 Hz, H5''); 4.98 (d, 1H, J = 7.5 Hz, tyrosine CH); 4.58 (d, 1H, J = 7.5 Hz, NH); 3.94 (m, 5H, serine NH, 2OCH₂); 3.72 (s 3H, tyrosine COOCH₃); 3.10 (m 2H, tyrosine CH₂); 1.81-0.86 (BOC-CH₃, 16CH₂, 2CH₃). MALDI MS m/z 882 (MH⁺).

Poly((acyl-serine methyl ester)-4,4''-didecoxy-2,2':5',2''-terthiophene-3'-carboxylate) 24.

To a dry flask containing anhydrous iron chloride (145 mg, 0.9 mmol) was added a solution of (acyl-serine methyl ester)-4,4''-didecoxy-2,2':5',2''-terthiophene-3'-carboxylate **22** (50 mg) in chloroform (5 mL). The reaction mixture was stirred under a nitrogen atmosphere for 24 hours. The polymer was precipitated by pouring the reaction solution onto methanol (50 mL). The precipitate was collected by filtration. The polymer was reduced by stirring in a solution of N,N-diethylhydroxylamine/THF. The reduced *poly((acyl-serine methyl ester)-4,4''-didecoxy-2,2':5',2''-terthiophene-3'-carboxylate) 24* was again precipitated by methanol and collected by filtration. Yield: 23 mg, 46%. $\nu_{\max}/\text{cm}^{-1}$ 2920, 2895, 2671, 1712, 1670, 1504, 1439, 1357, 1102, 765. Due to the low solubility of polymer **24** it could not be characterised by NMR spectroscopy or GPC.

Poly((BOC-tyrosine methyl ester)-4,4''-didecoxy-2,2':5',2''-terthiophene-3'-carboxylate) 25.

To a dry flask containing anhydrous iron chloride (200 mg, 1.2 mmol) was added a solution of (BOC-tyrosine methyl ester)-4,4''-didecoxy-2,2':5',2''-terthiophene-3'-carboxylate **23** (60 mg) in chloroform (6 mL). The reaction mixture was stirred under a nitrogen atmosphere for 24 hours. The polymer was precipitated by pouring the reaction solution onto methanol (50 mL). The precipitate was collected by filtration. The polymer was reduced by stirring the polymer in a solution of N,N-diethylhydroxylamine in THF. The reduced *poly((BOC-tyrosine methyl ester)-4,4''-didecoxy-2,2':5',2''-terthiophene-3'-carboxylate) 25* was again precipitated by methanol and collected by filtration. Yield: 42 mg, 70%. $\nu_{\max}/\text{cm}^{-1}$ 2916, 2847, 2793,

2677, 1728, 1504, 1411, 1365, 1165, 1056, 925, 740. Due to the low solubility of polymer **25** it could not be characterised by NMR spectroscopy or GPC.

Attempted synthesis of 6-(4,4''-Didecoxy-2,2':5',2''-terthiophene-3'-ylvinyl)-1',3',3'-trimethylspiro[chromene-2,2'-indoline] 28.

Diethyl 4,4''-didecoxy-2,2':5',2''-terthiophene-3'-ylmethylphosphonate **26** (64 mg, 0.09 mmol) was dissolved in dry THF (20 mL), LiCl (13 mg, 0.3 mmol) was then added followed by DBU (46 mg, 0.3 mmol). 1',3',3'-Trimethylspiro[chromene-2,2'-indoline]-6-carbaldehyde **27** (27.5 mg, 0.09 mmol) was then added and the reaction stirred at room temperature for 2 hours. After this time no reaction could be observed by TLC. The reaction mixture was then heated to reflux however this was also unsuccessful. The reaction was repeated using the same conditions in dry acetonitrile as solvent however this was also unsuccessful.

(2-(3',3'-Dimethyl-6-nitrospiro[chromene-2,2'-indoline]-1'-yl)ethyl)-4,4''-didecoxy-2,2':5',2''-terthiophene-3'-carboxylate (TTSPC).

Adapted from the method of Wagner *et al.*^[13] 4,4''-Didecoxy-2,2':5',2''-terthiophene-3'-carboxylic acid **15** (84 mg, 140 μ mol) was dissolved in dry DCM (20 mL). DCC (33 mg, 160 μ mol) was then added followed by 2-(3',3'-dimethyl-6-nitrospiro[chromene-2,2'-indoline]-1'-yl)ethanol **29** (42 mg, 120 μ mol) and DMAP (2 mg, 10 μ mol). The reaction mixture was then stirred under nitrogen at 50°C for 1.5 hours. TLC showed that the reaction was complete. The solvent was removed on a rotary evaporator and the (2-(3',3'-dimethyl-6-nitrospiro[chromene-2,2'-indoline]-1'-yl)ethyl)-4,4''-didecoxy-2,2':5',2''-terthiophene-3'-carboxylate was purified on a silica column using DCM as the eluent. Yield: 92 mg, 70%. ¹H NMR (400 MHz,

CDCl₃) δ 7.90 (dd, 1H, J= 2.7 Hz, J= 8.9 Hz, sp-Ar); 7.85 (d, 1H, J= 2.7 Hz, sp-Ar); 7.31 (s, 1H, th-H4'); 7.14 (t, 1H, J = 7.7 Hz, sp-Ar); 7.08 (d, 1H, J = 1.75 Hz, th-H3); 7.02 (d, 1H, J = 7.7 Hz, sp-Ar); 6.94 (d, 1H, J = 1.7 Hz, th-H3''); 6.80 (m, 1H, sp-Ar); 6.64 (m, 2H, 2sp-Ar); 6.59 (d, 1H, J = 7.7 Hz, sp-Ar); 6.25 (d, 1H, J = 1.75 Hz, th-H5); 6.11 (d, 1H, J = 1.7 Hz, th-H5''); 5.75 (d, 1H, J = 10.2 Hz, sp); 4.35 (m, 2H,); 3.90 (m, 4H, 2OCH₂); 3.51 (m, 4H,); 1.8-0.75 (all remaining CH₂ and CH₃). MALDI MS m/z 939.4 (MH⁺).

(2-(3',3'-Dimethyl-6-nitrospiro[chromene-2,2'-indoline]-1'-yl)ethyl)-4,4''-didecoxy-2,2':5',2''-terthiophene-3'-acetate (TTSPA).

Following the method of Wagner *et al.*,^[13] 4,4''-didecoxy-2,2':5',2''-terthiophene-3'-acetic acid **16** (51 mg, 82 μmol) was dissolved in dry DCM (10 mL), DCC (20 mg, 97 μmol) was then added followed by 2-(3',3'-dimethyl-6-nitrospiro[chromene-2,2'-indoline]-1'-yl)ethanol **29** (26 mg, 74 μmol) and DMAP (1 mg, 8.2 μmol). The reaction mixture was stirred under nitrogen at 50°C for 1.5 hours. TLC showed that the reaction was complete. The solvent was removed on a rotary evaporator and the product was purified on a silica column using DCM as the eluent. Yield: 60 mg, 77%. ¹H NMR (400 MHz, CDCl₃) δ 7.92 (dd, 1H, J= 2.8 Hz, J= 8.9 Hz, sp-Ar); 7.83 (d, 1H, J= 2.8 Hz, sp-Ar); 7.11 (t, 1H, J = 7.8 Hz, sp-Ar); 7.06 (s, 1H, th-H4'); 7.02 (d, 1H, J = 7.7 Hz, sp-Ar); 6.94 (d, 1H, J = 1.7 Hz, th-H3''); 6.86 (d, 1H, J = 1.8 Hz, th-H3); 6.82 (m, 2H, sp-Ar, th-H3''); 6.65 (m, 2H, 2sp-Ar); 6.55 (d, 1H, J = 7.7 Hz, sp-Ar); 6.14 (d, 1H, J = 1.8 Hz, th-H5); 6.07 (d, 1H, J = 1.5 Hz, th-H5''); 5.58 (d, 1H, J = 10.3 Hz, sp); 4.13 (m, 2H,); 3.90 (m, 4H, 2OCH₂); 3.78 (s, 2H, th-CH₂); 3.51 (m, 4H,); 1.8-0.75 (all remaining CH₂ and CH₃). MALDI MS m/z 953.4 (MH⁺).

2.2.2 Chapter 4.

4-Decoxythiophene-2-carbaldehyde **31** and 3-decoxythiophene-2-carbaldehyde **33**.

Following a modified procedure of Zoellner *et al.* for 4-hexoxythiophene-2-carbaldehyde,^[14] diisopropylamine (2.1 mL, 15 mmol) was dissolved in dry THF (30 mL) under a nitrogen atmosphere and cooled to -70°C with an acetone liquid nitrogen bath. n-Butyllithium (9.37 mL, 1.6 molar in hexane) was then added slowly and the reaction warmed to 0°C for 5 minutes. The reaction mixture was cooled back to -70°C and 3-decoxythiophene **9** (3 g, 12.5 mmol) dissolved in THF (5 mL) was added. The reaction mixture was warmed to 0°C for another 5 minutes. The reaction mixture was again cooled back to -70°C, dry DMF (2.9 mL, 37.5 mmol) was added and the reaction stirred at room temperature for 1 hour. The reaction mixture was then poured onto 5% HCl (200 mL) and the organic was extracted by ether, dried with MgSO₄ and the solvent removed. The product was purified on a silica column using 20% DCM/hexane as eluent. Kinetic and thermodynamic isomers were obtained 4-decoxythiophene-2-carbaldehyde **31**. Yield: 0.73 g, 22%. ¹H NMR (400 MHz, CDCl₃) δ 9.81 (s 1H, CHO); 7.41 (d, 1H, *J*=1.8 Hz, H3), 6.22 (d, 1H, *J*=1.8 Hz, H5), 3.97 (t, 2H, *J*=6.7 Hz, OCH₂), 1.83-0.86 (8CH₂ and CH₃). And 3-decoxythiophene-2-carbaldehyde **33**. Yield: 1.8 g, 54%. ¹H NMR (400 MHz, CDCl₃) δ 10.01 (s 1H, CHO); 7.61 (d, 1H, *J*=5.5 Hz, H4), 6.83 (d, 1H, *J*=5.5 Hz, H5), 4.15 (t, 2H, *J*=7 Hz, OCH₂), 1.83-0.86 (8CH₂ and CH₃). Data was as expected when compared to the similar 4-hexoxythiophene-2-carbaldehyde.^[14]

4-Decylthiophene-2-carbaldehyde 32.

3-Decylthiophene (5 g, 22.3 mmol) and diisopropylamine (3.34 g, 33 mmol) were dissolved in dry THF (60 mL) under a nitrogen atmosphere and cooled to -70°C with an acetone liquid nitrogen bath. n-Butyllithium (14 mL, 2.5 molar in hexane) was then added slowly and the reaction warmed to room temperature for 1 hour. The reaction mixture was cooled back to -70°C, dry DMF (5.1 mL, 66 mmol) was added and the reaction stirred at room temperature for overnight. The reaction mixture was poured onto 5% HCl (200 mL) and the organic was extracted by ether, dried with MgSO₄ and the solvent removed. The crude *4-decylthiophene-2-carbaldehyde* was passed through a pad of silica using 50% DCM/hexane as eluent. Yield: 5.28 g, 94%. ¹H NMR (400 MHz, CDCl₃) δ 9.87 (d 1H, *J*=1.2 Hz, CHO); 7.61 (d, 1H, *J*=1.2 Hz, H3), 7.37 (s, 1H, H5), 2.64 (t, 2H, *J*=7.8 Hz, Ar-CH₂), 1.66-0.86 (8CH₂ and CH₃).

Bis((4-decoxythiophen-2-yl)methylene)benzene-1,4-diamine 34.

4-Decoxythiophene-2-carbaldehyde **31** (0.8 g, 2.98 mmol) and *p*-phenylenediamine **30** (0.16 g, 1.49 mmol) were dissolved in ethanol (30 mL), acetic acid (0.8 mL) was added and the reaction stirred overnight at room temperature. After this time the yellow product, *bis*((4-decoxythiophen-2-yl)methylene)benzene-1,4-diamine **34** had precipitated, which was collected by filtration, washed with ethanol to remove any remaining reactants and dried under vacuum. Yield: 0.74 g, 82%. ¹H NMR (400 MHz, CDCl₃) δ 8.50 (s 2H, CHN); 7.25 (s, 4H, Ar); 7.14 (s, 2H, H5); 6.44 (s, 2H, H3); 3.97 (t, 4H, *J*=6.5 Hz, OCH₂); 1.80-0.87 (16CH₂ and 2CH₃). UV-visible

spectrum λ_{\max} 382 nm. MALDI MS m/z 609.4 (MH^+). Data was as expected when compared to the similar bis((thiophen-2-yl)methylene)benzene-1,4-diamine. ^[15]

Bis((4-decylthiophen-2-yl)methylene)benzene-1,4-diamine 35.

4-Decylthiophene-2-carbaldehyde **32** (0.5 g, 1.98 mmol) and *p*-phenylenediamine **30** (0.106 g, 0.98 mmol) were dissolved in ethanol (15 mL), acetic acid (0.4 mL) was added and the reaction stirred overnight at room temperature. After this time a yellow product **35** had precipitated. This *bis*((4-decylthiophen-2-yl)methylene)benzene-1,4-diamine **35** was collected by filtration, washed with ethanol to remove any remaining reactants and dried under vacuum. Yield: 0.38 g, 67%. ¹H NMR (400 MHz, CDCl₃) δ 8.55 (s, 2H, CHN); 7.33 (s, 2H, H5); 7.24 (s, 4H, Ar); 7.11 (s, 2H, H3); 2.62 (t, 4H, $J=7.5$ Hz, TH-CH₂); 1.65-0.87 (16CH₂ and 2CH₃). UV-visible spectrum λ_{\max} 375 nm. MALDI MS m/z 577.6 (MH^+). Data was as expected when compared to the similar bis((thiophen-2-yl)methylene)benzene-1,4-diamine. ^[15]

Bis((3-decoxythiophen-2-yl)methylene)benzene-1,4-diamine 36.

3-Decoxythiophene-2-carbaldehyde **33** (0.13 g, 0.49 mmol) and *p*-phenylenediamine **30** (26 mg, 0.24 mmol) were dissolved in ethanol (5 mL), acetic acid (0.1 mL) was added, and the reaction stirred overnight at room temperature. After this time the yellow product, *bis*((3-decoxythiophen-2-yl)methylene)benzene-1,4-diamine **36** had precipitated, which was collected by filtration, washed with ethanol to remove any remaining reactants and dried under vacuum. Yield: 87 mg, 60%. ¹H NMR (400 MHz, CDCl₃) δ 8.69 (s, 2H, CHN); 7.38 (d, 2H, $J=5.7$ Hz, H5); 7.23 (s, 4H, Ar); 6.83

(d, 2H, $J=5.7$ Hz, H4); 4.11 (t, 4H, $J=6.3$ Hz, OCH₂); 1.79-0.85 (16CH₂ and 2CH₃). UV-visible spectrum λ_{max} 385 nm. MALDI MS m/z 609.5 (MH⁺). Data was as expected when compared to the similar bis((thiophen-2-yl)methylene)benzene-1,4-diamine. ^[15]

Attempted synthesis of poly(bis((4-decoxythiophen-2-yl)methylene)benzene-1,4-diamine).

A solution of anhydrous iron chloride (53 mg, 0.33 mmol) in nitromethane (0.5 mL) was added dropwise to a stirred solution of bis((4-decoxythiophen-2-yl)methylene)benzene-1,4-diamine (50 mg, 0.08 mmol) in chloroform (1 mL) under nitrogen. The reaction mixture was stirred at room temperature for 4 hours, then poured onto methanol. Unfortunately a brown sludge formed and no polymer could be isolated. This is consistent with observations by Dubitsky *et al.* for bis((thiophen-2-yl)methylene)benzene-1,4-diamine where a complex between the monomer and the iron salt was observed to form. ^[15]

Bis((5-bromo-4-decoxythiophen-2-yl)methylene)benzene-1,4-diamine 38.

5-Bromo-4-decoxythiophene-2-carbaldehyde **39** (0.65 g, 1.87 mmol) and *p*-phenylenediamine (0.101 g, 0.94 mmol) were dissolved in ethanol (15 mL), acetic acid (0.4 mL) was added and the reaction stirred overnight at room temperature. After this time, the yellow *bis((5-bromo-4-decoxythiophen-2-yl)methylene)benzene-1,4-diamine 38* product had precipitated. The product was collected by filtration, washed with ethanol to remove any remaining reactants and dried under vacuum. Yield: 0.35 g, 49%. ¹H NMR (400 MHz, CDCl₃) δ 8.42 (s, 2H, CHN); 7.24 (s, 4H, Ar); 7.12 (s, 2H, H3); 4.07 (t, 4H, $J=6.5$ Hz, OCH₂); 1.80-0.85 (16CH₂ and 2CH₃).

2-Bromo-3-decoxythiophene-5-carbaldehyde 39.

4-Decoxythiophene-2-carbaldehyde **31** (0.5 g, 1.87 mmol) was dissolved in THF (10 mL), NBS (0.35 g, 1.96 mmol) was then added and the reaction mixture was stirred overnight at room temperature. The solvent was then removed, the product dissolved in ether and filtered. The ether was removed and the *2-bromo-3-decoxythiophene-5-carbaldehyde 39* purified on a silica column using 30% DCM/hexane as eluent.

Yield: 0.65 g, 99%. ^1H NMR (400 MHz, CDCl_3) δ 9.70 (s 1H, CHO); 7.36 (d, 1H, H4), 4.08 (t, 2H, $J=6.3$ Hz, OCH_2), 1.80-0.85 (8 CH_2 and CH_3).

Poly(bis((4-decoxythiophen-2-yl)methylene)benzene-1,4-diamine) 40.

Bis((5-bromo-4-decoxythiophen-2-yl)methylene)benzene-1,4-diamine **38** (0.35 g, 0.45 mmol) and 2,2'-bipyridyl (71 mg, 0.45 mmol) were dissolved in dry toluene (5 mL). $\text{Ni}(\text{COD})_2$ (0.124 g, 0.45 mmol) was added and the reaction refluxed under nitrogen overnight. The polymer was poured onto methanol to stop any further reaction and the solid polymer collected by filtration. *Poly(bis((4-decoxythiophen-2-yl)methylene)benzene-1,4-diamine) 40* was purified by Soxhlet extraction first with methanol then chloroform. Much of the polymer could not be solubilised. The yield of soluble material was 111 mg, 41%. ^1H NMR (400 MHz, CDCl_3) δ 8.45 (CHN); 7.30 (Ar); 7.12 (s, 2H, H3); 4.10 (OCH_2); 1.80-0.85 (16 CH_2 and 2 CH_3) The peaks in the ^1H NMR spectrum were broad, which is indicative of a mixture of oligomers. UV-visible spectrum λ_{max} 502 nm. GPC 1035 Da. MALDI MS m/z 1373 (2Mer $^+$), 1979 (3Mer $^+$), 2586 (4Mer $^+$).

Methyl 5,5''-diformyl-4,4''-didecoxy-2,2':5',2''-terthiophene-3'-carboxylate 41.

To a cooled (0°C) stirred flask containing dry DMF (1 mL) was added dropwise POCl₃ (0.8 mL, 5.2 mmol), and this Vilsmeier mixture was stirred under nitrogen for 20 minutes. A solution of methyl 4,4''-didecoxy-2,2':5',2''-terthiophene-3'-carboxylate **1** (0.11 g, 0.178 mmol) in 1,2 dichloroethane (10 mL) was then added to the Vilsmeier mixture. The reaction mixture was heated to 100°C for 2 hours, after this time the reaction mixture was worked up by pouring onto 5% HCl (50 mL), the product was extracted by DCM with care as an emulsion formed. The organic phase was washed by a saturated sodium bicarbonate solution followed by water. The organic phase was separated, dried (MgSO₄) and passed through a pad of silica to remove baseline impurities. The *methyl 5,5''-diformyl-4,4''-didecoxy-2,2':5',2''-terthiophene-3'-carboxylate 41* product was eluted by 2% methanol in chloroform. Yield: 40 mg, 33%. ¹H NMR (400 MHz, CDCl₃) δ 10.03 (s 1H, CHO); 9.99 (s 1H, CHO); 7.71 (s, 1H, H4'); 7.40 (s, 1H, H3); 6.94 (s, 1H, H3''); 4.21 (m, 4H, 2OCH₂); 3.89 (s 3H, COOCH₃); 1.89-0.85 (16CH₂, 2CH₃). UV-visible spectrum λ_{max} 405 nm. MALDI MS m/z 675.3 (MH⁺).

5,5''-Diformyl-4,4''-didecoxy-2,2':5',2''-terthiophene 42.

To a cooled (0°C) stirred flask containing dry DMF (1 mL) was added dropwise POCl₃ (0.8 mL, 5.2 mmol), and this Vilsmeier mixture was stirred under nitrogen for 20 minutes. A solution of 4,4''-didecoxy-2,2':5',2''-terthiophene **4** (0.1 g, 0.178 mmol) in 1,2 dichloroethane (10 mL) was added to this Vilsmeier mixture. The reaction mixture was heated to 100°C for 2 hours, after this time the reaction mixture was worked up by pouring onto 5% HCl (50 mL), the product was extracted by DCM with care as an emulsion formed. The organic extract was washed by a

saturated sodium bicarbonate solution followed by water. The organic phase was separated, dried (MgSO₄) and passed through a pad of silica to remove baseline impurities. The *5,5'*-diformyl-*4,4'*-didecoxy-*2,2':5',2''*-terthiophene **42** product was eluted by 2% methanol in chloroform. Yield: 64 mg, 58%. ¹H NMR (400 MHz, CDCl₃) δ 9.98 (s, 2H, 2CHO); 7.29 (s, 2H, 2H_{3'}); 6.92 (s, 2H, 2H₃); 4.19 (t, 4H, 2OCH₂); 1.9-0.86 (16CH₂, 2CH₃). UV-visible spectrum λ_{max} 427 nm.

Poly((methyl 5,5'-dimethylene -4,4''-didecoxy-2,2':5',2''-terthiophene-3'-carboxylate)benzene-1,4-diamine) 43.

Methyl 5,5''-diformyl-4,4''-didecoxy-2,2':5',2''-terthiophene-3'-carboxylate **41** (34 mg, 0.05 mmol) and *p*-phenylenediamine **30** (5.4 mg, 0.05 mmol) were dissolved in chloroform (5 mL). Acetic acid (0.05 mL) was added and the reaction stirred for 48 hours at room temperature. After this time the reaction mixture was poured onto methanol, the polymer was collected by filtration. Yield: 34 mg 91%. Unfortunately *Poly((methyl 5,5'-dimethylene -4,4''-didecoxy-2,2':5',2''-terthiophene-3'-carboxylate)benzene-1,4-diamine) 43* was found to only be sparingly soluble in common organic solvents and could not be characterised by NMR spectroscopy and GPC.

Surface polymerisation, poly((methyl 5,5'-dimethylene -4,4''-didecoxy-2,2':5',2''-terthiophene-3'-carboxylate)benzene-1,4-diamine) 43.

A solution of methyl 5,5''-diformyl-4,4''-didecoxy-2,2':5',2''-terthiophene-3'-carboxylate **41** (10 mg, 0.0148 mmol) and *p*-phenylenediamine **30** (1.6 mg, 0.0148 mmol) in chloroform (1 mL) was prepared. This solution was then spin coated at 800 rpm onto ITO glass substrates (1 cm x 5 cm) to give monomer films. These monomer

films were exposed to acetic acid vapour overnight and a colour change from red/orange to purple was observed. Monomer films not exposed to the acid changed colour less significantly.

Poly((5,5'-dimethylene -4,4''-didecoxy-2,2':5',2''-terthiophene)benzene-1,4-diamine) 44.

5,5''-Diformyl-4,4''-didecoxy-2,2':5',2''-terthiophene **42** (31 mg, 0.05 mmol) and *p*-phenylenediamine **30** (5.4 mg, 0.05 mmol) were dissolved in chloroform (5 mL). Acetic acid (0.05 mL) was added and the reaction stirred for 48 hours at room temperature. After this time the reaction mixture was poured onto methanol, the polymer was collected by filtration. Yield: 32 mg 90%. Unfortunately *poly*((5,5'-dimethylene -4,4''-didecoxy-2,2':5',2''-terthiophene)benzene-1,4-diamine) **44** was found to only be sparingly soluble in common organic solvents and could not be characterised by NMR spectroscopy and GPC.

5-Bromo-3',4'-dihexyl-4,4''-didecoxy-2,2':5',2''-terthiophene 45.

3',4'-Dihexyl-4,4''-didecoxy-2,2':5',2''-terthiophene **5** (0.64 g, 0.88 mmol) was dissolved in THF (20 mL), NBS (0.162 g, 0.9 mmol) was added and the reaction stirred overnight. The solvent was then removed and the crude *5-bromo-3',4'-dihexyl-4,4''-didecoxy-2,2':5',2''-terthiophene 45* was passed through a plug of silica using 50% DCM/hexane as eluent. The solvent was then removed to yield a neat oil. Unfortunately the oil was left overnight and polymerised to *poly*(3',4'-dihexyl-4,4''-didecoxy-2,2':5',2''-terthiophene) **47** evolving a white gas.

5-Bromo-4,4''-didecoxy-2,2':5',2''-terthiophene 46.

4,4''-Didecoxy-2,2':5',2''-terthiophene **4** (0.5 g, 0.89 mmol) was dissolved in THF (20 mL), NBS (0.16 g, 0.9 mmol) was added and the reaction stirred overnight. The solvent was removed and the crude product was passed through a plug of silica using 50% DCM/hexane as eluent. The solvent was again removed to yield a neat oil.

Unfortunately the oil was left overnight and polymerised to poly(4,4''-didecoxy-2,2':5',2''-terthiophene) **48** evolving a white gas. The reaction was therefore

repeated taking more care. 4,4''-Didecoxy-2,2':5',2''-terthiophene **4** (0.1 g, 0.18 mmol) was dissolved in THF (4 mL), NBS (32 mg, 0.18 mmol) was added and the reaction stirred overnight. The solvent was removed and the crude terthiophene was passed through a plug of silica using hexane as eluent. To avoid polymerisation 5-bromo-4,4''-didecoxy-2,2':5',2''-terthiophene **46** was stored in hexane at -20°C.

Yield: 94 mg, 82%. ¹H NMR (400 MHz, CDCl₃) δ 7.02 (d, 1H, J = 1.7 Hz, H3''); 6.98 (d, 1H, J = 1.7 Hz, H5''); 6.83 (s, 1H, H3'); 6.79 (s, 1H, H4'); 6.12 (s, 2H, H3); 4.05 (t, 2H, OCH₂); 3.94 (t, 2H, OCH₂); 1.8-0.86 (16CH₂, 2CH₃) this product was slightly impure containing traces of **4** and 5,5''-dibromo-4,4''-didecoxy-2,2':5',2''-terthiophene.

Autopolymerisation of 5-bromo-4,4''-didecoxy-2,2':5',2''-terthiophene 46.

A hexane solution containing 5-bromo-4,4''-didecoxy-2,2':5',2''-terthiophene **46** (20 mg, 31 μmol) was taken and the solvent removed, chloroform added and the reaction stirred at room temperature for 12 hours; it was observed to darken indicating polymerisation. The reaction mixture was worked up by washing the

polymer with water, extracting the chloroform and drying. The ^1H NMR spectrum contained broad overlapping peaks indicating random polymerisation.

A hexane solution containing 5-bromo-4,4''-didecoxy-2,2':5',2''-terthiophene **46** (20 mg, 31 μmol) was taken and the solvent removed, chloroform and a drop of HBr added and the reaction stirred at room temperature for 12 hours. The reaction mixture was observed to darken immediately indicating polymerisation. The reaction mixture was worked up by washing the poly(4,4''-didecoxy-2,2':5',2''-terthiophene) **48** with water extracting the chloroform and drying. The ^1H NMR spectrum again contained broad overlapping peaks indicating random polymerisation. UV analysis showed that this regioirregular polymer could be oxidised to give a free carrier tail.

2,5-Bis(tributylstannyl)thiophene 49.

Following the procedure of Hou *et al.*,^[16] thiophene (8.4 g, 0.1 mol) was dissolved in dry THF (60 mL). Under a nitrogen atmosphere, n-butyllithium (84 mL, 2.5 molar in hexane) was slowly added. The reaction mixture was refluxed for 2 hours, then cooled to room temperature. Tributyltin chloride (66.7 g, 0.205 mol) was added and the reaction stirred overnight. The reaction mixture was worked up by pouring onto water (100 mL) and extracting the product with ether (200 mL). The ether extract was dried (MgSO_4) and the solvent was removed on the rotary evaporator. The product was purified by distillation under reduced pressure (0.1 mm Hg), the 2-tributylstannylthiophene impurity was removed first up to 160°C. 36.5 g of the pure 2,5-bis(tributylstannyl)thiophene **49** was recovered at 180°C in 55% yield (lit.^[16] 53%). ^1H NMR (400 MHz, CDCl_3) δ 7.34 (s, 2H,); 1.56 (m, 12H, 6 CH_2); 1.33 (m, 12H, 6 CH_2); 1.09 (m, 12H, 6 CH_2); 0.89 (t, 18H, 6 CH_3). Data was consistent with the literature.^[16]

2-(2-Bromothiophen-3-yl)ethanol 51.

2-(Thiophen-3-yl)ethanol (10 g, 78 mmol) was dissolved in a mixture of chloroform (100 mL) and acetic acid (100 mL) and cooled to 0°C. NBS (14.2 g, 80 mmol) was added and the reaction stirred for 1 hour. The reaction mixture was worked up by pouring onto water (200 mL) and extracting the chloroform phase. The chloroform phase was washed by 10% KOH (100 mL) and water (100 mL), dried (MgSO₄), and the solvent was removed on the rotary evaporator. The product **51** was purified on a silica column using 50% DCM/hexane as the eluent followed by pure DCM. Yield: 12.37 g, 77% (lit.^[17] 98%). ¹H NMR (400 MHz, CDCl₃) δ 7.23 (d, 1H, J = 5.7 Hz, H5); 6.87 (d, 1H, J = 5.7 Hz, H4); 3.84 (t, 2H, J = 6.6 Hz, CH₂O); 2.86 (t, 2H, J = 6.6 Hz, th-CH₂); 1.53 (s, 1H, OH) Data was consistent with the literature.^[17]

(2-(2-Bromothiophen-3-yl)ethoxy)trimethylsilane 52.

2-(2-Bromothiophen-3-yl)ethanol **51** (10.6 g, 0.051 mol) was dissolved in dry THF (100 mL), freshly distilled triethylamine (6.1 g, 60 mmol) and trimethylsilyl chloride (5.8 g, 54 mmol) were then added. The reaction mixture was stirred for 4 hours, during this time a white precipitate formed, TLC showed complete protection of the alcohol. The precipitate was removed by filtration. Removal of the solvent by rotary evaporator yielded a pure product **52**. Yield: 13.7 g, 96% (lit.^[18] 92%). ¹H NMR (400 MHz, CDCl₃) δ 7.18 (d, 1H, J = 5.6 Hz, H5); 6.84 (d, 1H, J = 5.6 Hz, H4); 3.74 (t, 2H, J = 6.7 Hz, CH₂O); 2.81 (t, 2H, J = 6.7 Hz, th-CH₂); 0.08 (s, 9H, Si(CH₃)₃) Data was consistent with the literature.^[18]

2-(2-Bromothiophen-3-yl)ethyl octanoate 53.

2-(Thiophen-3-yl)ethyl octanoate (7.3 g, 28.7 mmol) was dissolved in THF (150 mL) and cooled to 0°C. NBS (5.37 g, 30 mmol) was added slowly and the reaction stirred at 0°C for 2 hours, then overnight at room temperature. The reaction mixture was worked up by pouring onto water (150 mL) and extracting the organic with DCM. The DCM extract was dried (MgSO₄) and the solvent removed. 2-(2-Bromothiophen-3-yl)ethyl octanoate **53** was then purified on a silica column using 20% DCM/hexane as eluent. Yield: 7.98 g, 83%. ¹H NMR (400 MHz, CDCl₃) δ 7.21 (d, 1H, J = 5.7 Hz, H5); 6.98 (d, 1H, J = 5.7 Hz, H4); 4.25 (t, 2H, J = 6.8 Hz, CH₂O); 2.92 (t, 2H, J = 6.8 Hz, th-CH₂); 2.29 (t, 2H, J = 7.6 Hz, OOCCH₂); 1.7-0.85 (5CH₂, CH₃). Data was as expected when compared to the spectrum of the similar 2-(2-bromothiophen-3-yl)ethyl acetate.^[19]

Ethyl 2-(2-bromothiophen-3-yl)acetate 54.

3-Thiophene acetic acid (2 g, 14 mmol) was dissolved in THF (25 mL) and cooled to 0°C. NBS (2.58 g, 14.5 mmol) was added slowly and the reaction mixture was stirred at 0°C for 4 hours, then overnight at room temperature. The solvent was removed, the product dissolved in ether and filtered to remove any succinimide. The ether was removed to yield crude 2-bromo-3-thiophene acetic acid. The crude 2-bromo-3-thiophene acetic acid was refluxed for 4 hours in absolute ethanol (75 mL) with conc. sulfuric acid (0.5 mL). TLC showed the reaction was complete the ester was poured onto water (200 mL), extracted with DCM (100 mL), the DCM extract was dried (MgSO₄), and the solvent was removed on a rotary evaporator. Ethyl 2-(2-bromothiophen-3-yl)acetate **54** was then purified on a silica column using 50% DCM/hexane as the eluent. Yield: 2.37 g, 53% (lit.^[20] 88%). ¹H NMR (400 MHz,

61

CDCl₃) δ 7.23 (d, 1H, J = 5.7 Hz, H5); 6.94 (d, 1H, J = 5.7 Hz, H4); 4.17 (q, 2H, J = 7.2 OCH₂); 3.61 (s, 2H, thCH₂); 1.27 (t, 3H, J = 7.2 CH₃). Data was consistent with the literature.^[20]

2-Bromo-3-hexylthiophene 55.

3-Hexylthiophene (2.36 g, 14 mmol) was dissolved in THF (25 mL) and cooled to 0°C. NBS (2.58 g, 14.5 mmol) was added slowly and the reaction stirred at 0°C for 4 hours, then overnight at room temperature. The solvent was removed, the product was dissolved in ether and filtered to remove any succinimide. The ether was removed and the product **55** purified on a silica column using hexane as eluent.

Yield: 3 g, 87% (lit.^[21] 81%). ¹H NMR (400 MHz, CDCl₃) δ 7.17 (d, 1H, J = 5.4 Hz, H5); 6.78 (d, 1H, J = 5.4 Hz, H4); 2.56 (t, 2H, J = 7.5 Hz, thCH₂); 1.6-0.85 (4CH₂, CH₃). Data was consistent with the literature.^[21]

3,3''-Dihexyl-2,2':5',2''-terthiophene 56.

2-Bromo-3-hexylthiophene **55** (1 g, 4 mmol) was dissolved in dry toluene (15 mL) and degassed by bubbling through nitrogen, Palladium tetrakis triphenylphosphine (50 mg) was added followed by 2,5-bis(tributylstannyl)thiophene **49** (1.32 g, 2 mmol) the reaction mixture refluxed overnight. The reaction mixture was worked up by washing with a saturated ammonium chloride solution and extracting the organic with ether, dried (MgSO₄), and the solvent was removed on the rotary evaporator. The product **56** was then purified on a silica column using hexane as the eluent.

Yield: 0.53 g, 32% (lit.^[22] 94%). ¹H NMR (400 MHz, CDCl₃) δ 7.17 (d, 2H, J = 5.3 Hz, 2H5); 7.05 (s, 2H, 2H3'); 6.93 (d, 2H, J = 5.3 Hz, 2H4); 2.78 (t, 4H, J = 7.7 Hz,

2th-CH₂); 1.7-0.85 (8CH₂, 2CH₃). UV-visible spectrum λ_{max} 338 nm. MALDI MS m/z 416 (M⁺). Data was consistent with the literature.^[22]

2,2':5',2''-(Terthiophene-3,3''-yl)ethanol 57.

2-(2-Bromothiophen-3-yl)ethanol **51** (2.1 g, 10 mmol) was dissolved in dry toluene (50 mL) and the solution degassed by bubbling nitrogen. Palladium tetrakis triphenylphosphine (50 mg) was added followed by 2,5-bis(tributylstannyl)thiophene **49** (3.3 g, 5 mmol), and the reaction refluxed overnight. The reaction mixture was worked up by washing with a saturated ammonium chloride solution, extracting the organic with ether and drying (MgSO₄). The solvent was removed on a rotary evaporator. The product was purified on a silica column using DCM/ethyl acetate as the eluent increasing the concentration of ethyl acetate from 1% to 20% gradually. Unfortunately purification proved difficult causing most of the product **57** to be lost. Yield: 50 mg, 2% (lit.^[23] 66%). ¹H NMR (400 MHz, CDCl₃) δ 7.22 (d, 2H, J = 5.4 Hz, 2H5); 7.10 (s, 2H, 2H3'); 6.98 (d, 2H, J = 5.4 Hz, 2H4); 3.89 (t, 4H, J = 6.7 Hz, 2CH₂O); 3.07 (t, 4H, J = 6.7 Hz, 2th-CH₂); 1.80 (br, 2H, 2OH).

2,2':5',2''-(Terthiophene-3,3''-yl)ethanol 57.

2,2':5',2''-(Terthiophene-3,3''-diyl)bis(ethane-2,1-diyl) dioctanoate **59** (1.33 g, 2.2 mmol) was added to a solution of potassium hydroxide (2 g, 35 mmol) in ethanol (95%, 40 mL) and water (10 mL). The reaction mixture was heated to 80°C for 4 hours. After this time the solvent was removed. Water (20 mL) was added and product **57** extracted by DCM (20 mL). The DCM extract was dried (MgSO₄) and the solvent removed. Yield: 0.57 g, 78% (lit.^[23] 66%). ¹H NMR (400 MHz, CDCl₃) δ

7.22 (d, 2H, J = 5.4 Hz, 2H5); 7.10 (s, 2H, 2H3'); 6.98 (d, 2H, J = 5.4 Hz, 2H4); 3.89 (t, 4H, J = 6.7 Hz, 2CH₂O); 3.07 (t, 4H, J = 6.7 Hz, 2th-CH₂); 1.80 (br, 2H, 2OH). UV-visible spectrum λ_{max} 338 nm. MALDI MS m/z 337.0 (MH⁺).

Attempted synthesis of 2,2':5',2''-(terthiophene-3,3''-yl)ethoxy)trimethylsilane 58.

(2-(2-Bromothiophen-3-yl)ethoxy)trimethylsilane **52** (2.8 g, 10 mmol) was dissolved in dry toluene (50 mL) and the solution degassed by bubbling nitrogen. Palladium tetrakis triphenylphosphine (50 mg) was added followed by 2,5-bis(tributylstannyl)thiophene **49** (3.3 g, 5 mmol) and the reaction refluxed overnight. The reaction mixture was worked up by washing with a saturated ammonium chloride solution and extracting the organic with ether, dried (MgSO₄), and the solvent was removed on the rotary evaporator. Unfortunately the TMS group appears to have been cleaved causing difficulty in purifying the product, as such no product was obtained.

2,2':5',2''-(Terthiophene-3,3''-yl)ethoxy)trimethylsilane 58.

2,2':5',2''-(Terthiophene-3,3''-yl)ethanol **57** (0.5 g, 1.5 mmol) was dissolved in dry THF (20 mL), freshly distilled triethylamine (1 mL) was added followed by trimethylsilyl chloride (1 g, 9 mmol). The reaction mixture was stirred for 4 hours, during which a white precipitate formed. TLC showed complete protection of the alcohol. The precipitate was removed by filtration. The solvent was removed by rotary evaporator yielding 2,2':5',2''-(*terthiophene-3,3''-yl*)ethoxy)trimethylsilane **58**. Yield: 0.69 g, 97%. ¹H NMR (400 MHz, CDCl₃) δ 7.19 (d, 2H, J = 5.2 Hz, 2H5); 7.10 (s, 2H, 2H3'); 6.97 (d, 2H, J = 5.2 Hz, 2H4); 3.81 (t, 4H, J = 7.0 Hz, 2CH₂O);

3.02 (t, 4H, J = 6.9 Hz, 2th-CH₂); 0.07 (s, 18H, 2Si(CH₃)₃). UV-visible spectrum λ_{\max} 325 nm. MALDI MS m/z 589 (MH⁺).

2,2':5',2''-(Terthiophene-3,3''-diyl)bis(ethane-2,1-diyl) dioctanoate 59.

2-(2-Bromothiophen-3-yl)ethyl octanoate **53** (1 g, 3 mmol) was dissolved in dry toluene (15 mL) and the solution degassed by nitrogen. Palladium tetrakis triphenylphosphine (50 mg) was added followed by 2,5-bis(tributylstannyl)thiophene **49** (1 g, 1.5 mmol) and the reaction refluxed overnight. The reaction mixture was worked up by washing with a saturated ammonium chloride solution and extracting with ether. The ether was dried (MgSO₄), and the solvent was removed on a rotary evaporator. The 2,2':5',2''-(*terthiophene-3,3''-diyl*)bis(*ethane-2,1-diyl*) dioctanoate **59** was then purified on a silica column using hexane/ethyl acetate as the eluent increasing the concentration of ethyl acetate from 1% to 5% gradually. Yield: 0.64 g, 36%. ¹H NMR (400 MHz, CDCl₃) δ 7.21 (d, 2H, J = 5.2 Hz, 2H5); 7.10 (s, 2H, 2H3'); 6.98 (d, 2H, J = 5.2 Hz, 2H4); 4.32 (t, 4H, J = 6.9 Hz, 2CH₂O); 3.12 (t, 4H, J = 6.9 Hz, 2th-CH₂); 2.28 (t, 4H, J = 7.7 Hz, 2OOCCH₂); 1.7-0.85 (10CH₂, 2CH₃). UV-visible spectrum λ_{\max} 330 nm. MALDI MS m/z 589 (MH⁺).

Diethyl 2,2':5',2''-(terthiophene-3,3''-diyl)diacetate 60.

Ethyl 2-(2-bromothiophen-3-yl)acetate **54** (2.37 g, 9.5 mmol) was dissolved in dry toluene (50 mL) and the solution degassed by nitrogen. Palladium tetrakis triphenylphosphine (90 mg) was added followed by 2,5-bis(tributylstannyl)thiophene **49** (3.16 g, 4.75 mmol) and the reaction refluxed overnight. The reaction mixture was worked up by washing with a saturated ammonium chloride solution and extracting with ether. The ether extract was dried (MgSO₄), and the solvent removed on a rotary

evaporator. *Diethyl 2,2':5',2''-(terthiophene-3,3''-diyl)diacetate* **60** was then purified on a silica column using 5% ethyl acetate/hexane as the eluent. Yield: 1.62 g, 41%. ¹H NMR (400 MHz, CDCl₃) δ 7.24 (d, 2H, J = 5.2 Hz, 2H5); 7.15 (s, 2H, 2H3'); 7.06 (d, 2H, J = 5.2 Hz, 2H4); 4.18 (q, 4H, J = 7.2 Hz, 2OCH₂); 3.77 (s, 4H, 2th-CH₂); 1.27 (t, 4H, J = 7.2 Hz, 2CH₃). UV-visible spectrum λ_{max} 325 nm. MALDI MS m/z 420.1 (M⁺).

5-Bromo-2,2':5',2''-(terthiophene-3,3''-diyl)bis(ethane-2,1-diyl) dioctanoate 61.

2,2':5',2''-(Terthiophene-3,3''-diyl)bis(ethane-2,1-diyl) dioctanoate **59** (0.45 g, 0.76 mmol) was dissolved in DMF (40 mL) and cooled to 4°C. NBS (0.143 g, 0.802 mmol) was then added and the reaction left for 72 hours at 4°C, after this time TLC showed complete reaction. The reaction mixture was worked up by pouring onto water and extracting by DCM, the solvent was removed and *5-bromo-2,2':5',2''-(terthiophene-3,3''-diyl)bis(ethane-2,1-diyl) dioctanoate* **61** purified by a silica column using 5% ethyl acetate/ hexane as the eluent. Yield: 0.4316 g, 84%. ¹H NMR (400 MHz, CDCl₃) δ 7.23 (d, 1H, J = 5.3 Hz, H5''); 7.09 (d, 1H, J = 3.8 Hz, H4'); 7.05 (d, 1H, J = 3.8 Hz, H3'); 6.98 (d, 1H, J = 5.3 Hz, H4''); 6.95 (s, 1H, H4); 4.28 (m, 4H, 2CH₂O); 3.11 (t, 2H, J = 7.0 Hz, th''-CH₂); 3.06 (t, 2H, J = 6.7 Hz, th-CH₂); 2.28 (m, 4H, 2OOCCH₂); 1.7-0.80 (10CH₂, 2CH₃).

5-Bromo-2,2':5',2''-(terthiophene-3,3''-yl)ethanol 62.

5-Bromo-2,2':5',2''-(terthiophene-3,3''-diyl)bis(ethane-2,1-diyl) dioctanoate **61** (0.41 g, 0.62 mmol) was added to a solution of potassium hydroxide (0.7 g, 12.2 mmol) in ethanol (95%, 15 mL) and water (3 mL). The reaction mixture was heated to 80°C

for 4 hours. After this time the solvent was removed. Water (20 mL) was added and product extracted by DCM (20 mL). The DCM extract was dried (MgSO₄) and the solvent removed. The crude *5-bromo-2,2':5',2''-(terthiophene-3,3''-yl)ethanol* **62** was then purified on a silica column using 10% ethyl acetate/DCM. Yield: 0.15 g, 58%. ¹H NMR (400 MHz, CDCl₃) δ 7.21 (d, 1H, J = 5.5 Hz, H5''); 7.09 (d, 1H, J = 3.7 Hz, H4'); 7.04 (d, 1H, J = 3.7 Hz, H3'); 6.97 (d, 1H, J = 5.5 Hz, H4''); 6.94 (s, 1H, H4); 3.89 (m, 4H, 2CH₂O); 3.07 (m, 4H, J = 7.0 Hz, 2th-CH₂); 2.05 (s, 2H, 2OH).

5-Bromo-2,2':5',2''-(terthiophene-3,3''-yl)ethoxy)trimethylsilane 63.

5-Bromo-2,2':5',2''-(terthiophene-3,3''-yl)ethanol **62** (0.15 g, 0.36 mmol) was dissolved in dry THF (5 mL), freshly distilled triethylamine (0.2 mL) was added followed by trimethylsilyl chloride (0.15 g, 1.4 mmol). The reaction mixture was stirred overnight, during this time a white precipitate formed. TLC showed complete protection of the alcohol. The precipitate was removed by filtration. The solvent was removed by rotary evaporator yielding *5-bromo-2,2':5',2''-(terthiophene-3,3''-yl)ethoxy)trimethylsilane* **63**. Yield: 0.192 g, 95%. ¹H NMR (400 MHz, CDCl₃) δ 7.20 (d, 1H, J = 5.4 Hz, H5''); 7.09 (d, 1H, J = 3.9 Hz, H4'); 7.05 (d, 1H, J = 3.9 Hz, H3'); 6.98 (d, 1H, J = 5.4 Hz, H4''); 6.95 (s, 1H, H4); 3.79 (m, 4H, 2CH₂O); 3.00 (t, 2H, J = 7.0 Hz, th''-CH₂); 2.94 (t, 2H, J = 6.2 Hz, th-CH₂); 0.07 (s, 18H, 2Si(CH₃)₃). UV-visible spectrum λ_{max} 343 nm.

Attempted synthesis of 2,2':5',2''-(terthiophene-3,3''-yl)ethoxy(trimethylsilane)-5-carboxylic acid 64.

n-Butyl lithium (0.53 mmol, 1.6 M in hexane) was added slowly to a solution of 2,2':5',2''-(terthiophene-3,3''-yl)ethoxy(trimethylsilane) **58** (257 mg, 0.53 mmol) and diisopropyl amine (69 mg, 68 mmol) in dry THF (25 mL) at -78°C under nitrogen. The reaction mixture was warmed to room temperature and stirred for 1 hour. After which carbon dioxide was bubbled through the reaction mixture. The reaction failed to give the desired product **64**.

Attempted synthesis of 5-formyl-2,2':5',2''-(terthiophene-3,3''-yl)ethoxy(trimethylsilane).

To a cooled (0°C) stirred flask containing dry DMF (1 mL), was added dropwise POCl₃ (0.5 mL, 3.3 mmol), and this Vilsmeier mixture was stirred under nitrogen for 20 minutes, after which a solution of 2,2':5',2''-(terthiophene-3,3''-yl)ethoxy(trimethylsilane) (0.1 g, 0.21 mmol) in DCM (10 mL) was added to it. The reaction mixture was stirred overnight at room temperature, and then the reaction mixture was worked up by pouring it onto 5% HCl (50 mL). The product was extracted by DCM. The DCM extract was washed by a saturated sodium bicarbonate solution followed by water. The DCM extract was dried (MgSO₄) and the solvent removed. The crude aldehyde was passed through a silica column using 10% DCM/hexane as eluent. Yield: 40 mg, 33%. MALDI MS showed masses of 364 (M⁺) 5-formyl-2,2':5',2''-(terthiophene-3,3''-yl)ethanol **65**, 392 (M⁺) 5,5''-diformyl-2,2':5',2''-(terthiophene-3,3''-yl)ethanol **66** and 336 (M⁺) 2,2':5',2''-(terthiophene-3,3''-yl)ethanol **57**. The mixture of products could not be purified by column chromatography.

**2,2':5',2'': 5'',2''': 5''',2''''': 5''''',2'''''''- (Sexithiophene-3,3'',4''',3'''''''-
tetrayl)tetrakis(ethane-2,1-diyl) tetraoctanoate **67**.**

5-Bromo-2,2':5',2'-(terthiophene-3,3''-diyl)bis(ethane-2,1-diyl) dioctanoate **61** (0.43 g, 0.65 mmol) was dissolved in dry DMF (25 mL), diisopropylethylamine (83 mg, 0.646 mmol) and tetra-n-butylammonium bromide (0.104 g, 0.323 mmol) were added, followed by palladium acetate (7 mg, 30 μ mol). The reaction mixture was heated at 110°C under nitrogen for 12 hours. The reaction mixture was worked up by pouring onto water (50 mL) and extracting with DCM. The DCM extract was dried (MgSO₄) and the solvent removed. 2,2':5',2'': 5'',2''': 5''',2''''': 5''''',2'''''''-

(Sexithiophene-3,3'',4''',3'''''''-tetrayl)tetrakis(ethane-2,1-diyl) tetraoctanoate **67** was purified on a silica column using 10% ethyl acetate/hexane. Yield: 0.103 g, 27%.

¹H NMR (400 MHz, CDCl₃) δ 7.23 (d, 2H, J = 5.3 Hz, 2H₅); 7.14 (d, 2H, J = 3.8 Hz, 2H_{3'}); 7.12 (d, 2H, J = 3.8 Hz, 2H_{4'}); 7.05 (s, 2H, 2H_{4''}); 6.99 (d, 2H, J = 5.3 Hz, 2H₄); 4.34 (m, 8H, 4CH₂O); 3.12 (m, 8H, 4th-CH₂); 2.29 (m, 8H, 4OOCCH₂); 1.7-0.80 (20CH₂, 4CH₃). UV-visible spectrum λ_{\max} 403 nm. MALDI MS m/z 1175 (M⁺).

2.2.3 Chapter 5.

2-(Thiophen-3-yl)ethyl octanoate (OTE).

Following the procedure of Camurlu *et al.*,^[24] 2-(thiophen-3-yl)ethanol **68** (5 g, 39 mmol) and triethylamine (5.44 mL, 39 mmol) were dissolved in DCM (50 mL) and cooled to 0°C under argon. Octanoyl chloride (8.02 mL, 46.8 mmol) was added dropwise to this cooled solution. TLC showed the reaction was complete. The crude ester was washed with 2 M HCl followed by 2 M NaOH and water. The DCM

extract was dried by MgSO_4 and the solvent removed. Yield: 9.47 g, 96% (lit.^[24] 86%). ^1H NMR (400 MHz, CDCl_3) δ 7.26 (dd, 1H, $J_{5,2}=3.0$ Hz, $J_{5,4}=4.9$ Hz, H5), 7.02 (m, 1H, H2), 6.97 (dd, 1H, $J_{4,2}=1.4$ Hz, $J_{4,5}=4.9$ Hz, H4), 4.29 (t, 2H, $J = 6.9$ Hz, CH_2O); 2.97 (t, 2H, $J = 6.9$ Hz, th- CH_2); 2.29 (t, 2H, $J = 7.5$ Hz, OOCCH_2); 1.65-0.85 (5CH_2 , CH_3). The ^1H NMR spectrum was in agreement with the literature.^[24]

3-Decylthiophene (DT).

Following a modified procedure from Pham *et al.*^[25] for the synthesis of 3-alkylthiophenes, oven dried magnesium turnings (4.8 g, 0.2 mol) were placed in a dry flask with anhydrous diethyl ether (40 mL) and a crystal of iodine. 1-Bromodecane (44.24 g, 0.2 mol) was dissolved in anhydrous diethyl ether (40 mL) and added dropwise to the magnesium turnings under argon. The iodine colour disappeared and the reaction began to reflux vigorously. The rate of addition of the 1-bromodecane solution was adjusted to control the rate of reaction. After addition was complete, the reaction mixture was refluxed for a further 2 hours, after which time nearly all the magnesium had disappeared. 3-Bromothiophene **8** (32.6 g, 0.2 mol) and Ni(dppp)Cl_2 (0.12 g) were added and the reaction refluxed overnight. Anhydrous diethyl ether (100 mL) was added to maintain the solvent level. The reaction was shown to be complete by TLC after this time. The reaction worked up by pouring onto 10% HCl (250 mL) on ice (250 g). The organic was extracted with diethyl ether (2 x 100 mL) dried (MgSO_4) and the solvent removed under reduced pressure. The crude 3-decylthiophene was purified by vacuum distillation (b.p. 100°C , 0.05 mm Hg) Yield: 21.5 g, 47.9% (lit.^[26] 76%). ^1H NMR (400 MHz, CDCl_3) δ 7.23 (dd, 1H, $J_{5,2}=3.0$ Hz, $J_{5,4}=5.1$ Hz, H5), 6.93 (dd, 1H, $J_{4,2}=1.2$ Hz, $J_{4,5}=5.1$ Hz,

H4), 6.92(m, 1H, H2), 2.62 (t, 2H, $J=7.7$ Hz th-CH₂), 1.7-0.8 (8CH₂, CH₃). Data is in agreement with the literature.^[26]

Poly(octanoic acid 2-thiophen-3-yl-ethyl ester) (POTE).

To a stirred solution of 2-(thiophen-3-yl)ethyl octanoate (3 g, 12 mmol) in chloroform (120 mL), under nitrogen, was added dropwise anhydrous iron chloride (7.67 g, 47 mmol) in nitromethane (48 mL). The reaction proceeded with stirring for 3 hours at room temperature. The polymer was precipitated by pouring into methanol (500 mL) and collected by vacuum filtration. The polymer was reduced overnight using 10% solution of hydrazine in THF (100 mL). The reduced polymer was precipitated by pouring onto methanol, collected by filtration and washed with methanol. The reduced POTE was purified by Soxhlet extraction with methanol and hexane. With the main fraction extracted by chloroform. Yield: 1.24 g, 42%. GPC Mw 61 kDa pd 1.44. ¹H NMR (400 MHz, CDCl₃) δ 7.14 (br, 1H, H4), 4.28 (br, 2H, CH₂O); 2.91 (br, 2H, th-CH₂); 2.31 (br, 2H, OOCCH₂); 1.7-0.85 (5CH₂, CH₃). UV-visible spectrum λ_{\max} 420 nm. $\nu_{\max}/\text{cm}^{-1}$ 2954, 2927, 2854, 1735, 1650, 1163, 1103.

Poly(3-decylthiophene)-co-(octanoic acid 2-thiophen-3-yl-ethyl ester)

(POTEcoDT).

To a stirred solution of 3-decylthiophene (0.5 g, 2.2 mmol) and 2-(thiophen-3-yl)ethyl octanoate (0.56 g, 2.2 mmol) in chloroform (50 mL), under nitrogen, was added dropwise anhydrous iron chloride (2.85 g, 4.8 mmol) in nitromethane (20 mL). The reaction proceeded with stirring for 3 hours at room temperature. The polymer was precipitated by pouring into methanol (200 mL) and collected by vacuum filtration. The polymer was reduced overnight using 10% solution of hydrazine in

THF (20 mL). The reduced polymer was precipitated by pouring onto methanol, collected by filtration and washed with methanol. The reduced POTEcoDT was purified by Soxhlet extraction with methanol and hexane and the main fraction was collected in chloroform. Yield: 0.12 g, 12%. GPC Mw 61 kDa pd 1.4. ^1H NMR (400 MHz, CDCl_3) δ 7.14 (br, 1H, est-H4), 6.98 (br, 1H, dec-H4); 4.29 (br, 2H, CH_2O); 2.91 (br, 2H, estth- CH_2); 2.80 (br, 2H, decth- CH_2), 2.30 (br, 2H, OOCCH_2); 1.70-0.85 (13CH_2 , 2CH_3). UV-visible spectrum λ_{max} 432 nm.

3-Hexylthiophene (3HT).

Following the procedure of Pham *et al.*,^[25] oven dried magnesium turnings (3.6 g, 0.15 mol) were placed in a dry flask with anhydrous diethyl ether (20 mL) and a crystal of iodine. 1-Bromohexane (24.8 g, 0.15 mol) was dissolved in anhydrous diethyl ether (30 mL) and added dropwise to the magnesium turnings under argon. The iodine colour disappeared and the reaction began to reflux vigorously. The rate of addition of the 1-bromohexane solution was adjusted to control the rate of reaction. After addition was complete, the reaction mixture was refluxed for a further 2 hours, after which time nearly all the magnesium had disappeared. 3-Bromothiophene **8** (24.5 g, 0.15 mol) and Ni(dppp)Cl_2 (0.09 g) were added and the reaction refluxed overnight. Anhydrous diethyl ether (80 mL) was added to maintain the solvent level. The reaction was shown to be complete by TLC after this time. The reaction worked up by pouring onto 10% HCl (200 mL) on ice (200 g). The organic was extracted with diethyl ether (2 x 100 mL) dried (MgSO_4) and the solvent removed under reduced pressure. The product was purified by vacuum distillation (boiling point, 65°C at 0.04 mm Hg) Yield: 13.4 g, 53% (lit. ^[25]79%). ^1H NMR (400 MHz, CDCl_3) δ 7.22 (dd, 1H, $J_{5,2}=2.9$ Hz, $J_{5,4}=4.9$ Hz, H5), 6.92 (m, 2H, H2,H4),

2.62 (t, 2H, $J=8.1$ Hz th-CH₂), 1.65-0.85 (4CH₂, CH₃). Data is in agreement with the literature. [25]

Poly(3-hexylthiophene) (P3HT).

To a stirred solution of 3-hexylthiophene (0.2 g, 1.2 mmol) in chloroform (12 mL), under nitrogen, was added dropwise anhydrous iron chloride (0.78 g, 4.8 mmol) in nitromethane (5 mL). The reaction proceeded with stirring for 3 hours at room temperature. The polymer was precipitated by pouring into methanol (100 mL) and collected by vacuum filtration. The polymer was reduced overnight using a 10% solution of hydrazine in THF (10 mL). The reduced polymer was precipitated by pouring onto methanol, collected by filtration and washed with methanol. The reduced polymer was purified by Soxhlet extraction. First methanol and hexane were used to remove impurities, then chloroform was then used to extract the product. Yield: 0.11 g, 55%. GPC Mw 89 kDa pd 1.85. ¹H NMR (400 MHz, CDCl₃) δ 6.98 (br, 1H, H4); 2.65 (br, 2H, th-CH₂), 1.65-0.85 (4CH₂, CH₃).

Poly(2-(thiophen-3-yl)ethanol) (PHET).

Poly(octanoic acid 2-thiophen-3-yl-ethyl ester) films and fibres were hydrolysed in a saturated solution of NaOH in methanol for 1 hour. Following this, they were washed by methanol, water, and methanol. The hydrolysis of the ester to yield alcohol functionalised PHET materials was confirmed by FTIR. $\nu_{\max}/\text{cm}^{-1}$ 3300, 2929, 1593, 1354, 1048, 795.

Ferrocene acid chloride.

Following the procedure of Rolfes *et al.*,^[27] to a solution of ferrocene carboxylic acid (0.23 g, 1 mmol) and 4-dimethylaminopyridine (1 mg) in toluene (5 mL), was added oxalyl chloride (0.165 g, 1.3 mmol). The reaction mixture was then stirred under nitrogen for 30 minutes at room temperature before being heated to 80°C for 5 minutes. The solvent was then removed on the rotary evaporator. The product was then dissolved in hexane (4 mL) and filtered, the solution was then reduced to 1 mL then placed in the freezer to crystallise. The crystals were then collected and dried under vacuum. Yield: 175 mg, 70% (lit.^[27] 68%).

Poly(ferrocene carboxylic acid 2-thiophen-3-yl-ethyl ester) (PFTE).

Ferrocene acid chloride (5mg) and 1 drop of pyridine were dissolved in ether (10ml), poly(2-(thiophen-3-yl)ethanol) structures were then immersed in the reaction solution and allowed to react for 12hrs. After this time the polymer functionalisation was complete as evidenced by FTIR and electrochemistry. The *poly(ferrocene carboxylic acid 2-thiophen-3-yl-ethyl ester)* sample was removed from the solution and washed by ether, water and acetonitrile. The sample was then dried and taken for characterisation. $\nu_{\max}/\text{cm}^{-1}$ 2947, 1706, 1563, 1395, 1348, 1129, 1046, 810.

2.2.4 Chapter 6.

1-(Phenylsulfonyl)-pyrrole.

Following the procedure of Ashraf *et al.*,^[28] pyrrole (59.4 g, 0.88 mol) and tetrabutylammonium hydrogen sulfate (26 g, 0.77 mol) were dissolved in DCM (320 mL) and a solution of sodium hydroxide (280 g) in water (340 mL) was added. To

this mixture, was added slowly a solution of benzenesulfonyl chloride (223 g, 1.26 mol) in DCM (120 mL) (the addition rate was adjusted to maintain a gentle reflux). After the addition was complete, the reaction mixture was stirred overnight before being worked up by adding water (1.2 L) and extracting with chloroform three times. The chloroform phase was washed by water twice, dried (MgSO₄) and the solvent removed. The product was then purified by recrystallisation from methanol. Yield: 145 g, 77%. ¹H NMR (400 MHz, CDCl₃) δ 7.86 (2H, Ph-ortho); 7.59 (1H, Ph-para), 7.51 (2H, Ph-meta), 7.16 (2H, H2), 6.49 (2H, H3).

1-(1-(Phenylsulfonyl)-pyrrol-3-yl)octan-1-one.

Following the procedure of Ashraf *et al.*^[28] octanoyl chloride (45 g) was added to a suspension of aluminium chloride (50.4 g) in DCM (1 L). The mixture was stirred for 30 minutes at room temperature under nitrogen. The mixture was then cooled on an ice bath and 1-(phenylsulfonyl)-pyrrole (50 g, 0.24 mol) dissolved in DCM (300 mL) was added slowly as to maintain the temperature below 5°C. The reaction mixture was then stirred for 1.5 hours at room temperature before being quenched carefully by ice water. The organic phase was separated, dried (MgSO₄) and the solvent was removed. The crude oil was used without further purification. Yield: 80 g.

1-(Pyrrol-3-yl)octan-1-one.

Following the procedure of Ashraf *et al.*,^[28] 1-(1-(phenylsulfonyl)-pyrrol-3-yl)octan-1-one (80 g) was dissolved in dioxane (350 mL), a sodium hydroxide solution (5 mol/L 850 mL) added and the reaction refluxed overnight. The reaction mixture was cooled and the organic layer separated and washed with brine. The organic extract

was dried (MgSO_4) and the solvent was removed. The residue was then purified by recrystallisation from hexane. Yield: 36.8 g. $^1\text{H NMR}$ (400 MHz, CDCl_3) δ 8.70 (br, 1H, NH); 7.43 (d, 1H, $J=1.5$ Hz, H5), 6.78 (s, 1H, H2), 6.67 (d, 1H, $J=1.5$ Hz, H4), 2.74 (t, 2H, $J=7.5$ Hz, COCH_2), 1.80-0.80 (5CH_2 , CH_3).

3-Octylpyrrole 69.

Following the procedure of Ashraf *et al.*,^[28] 1-(pyrrol-3-yl)octan-1-one (36.8 g, 0.19 mol) was dissolved in dry THF (750 mL) under nitrogen and cooled to 0°C . Red-Al (121.3 g, 0.39 mol) was added slowly, the solution stirred at room temperature for 3 hours, before being heated to 50°C for 1 hour. The product was hydrolysed by slow addition of water. The THF layer was separated and remaining product extracted from the water layer with ether. The combined organic extracts were dried (MgSO_4) and the solvent was removed. The product **69** was then purified by vacuum distillation (b.p. 86°C , 0.05 mm Hg). Yield: 20 g, 59%. $^1\text{H NMR}$ (400 MHz, CDCl_3) δ 8.00 (br, 1H, NH); 6.71 (s, 1H, H5), 6.57 (s, 1H, H2), 6.09 (s, 1H, H4), 2.47 (t, 2H, $J=8.0$ Hz py- CH_2), 1.70-0.85 (6CH_2 , CH_3).

Poly(3-decoxythiophene) (PDOT_c).

To a stirred solution of 3-decoxythiophene **9** (0.75 g, 3 mmol) in chloroform (30mL), under nitrogen, was added dropwise a solution of anhydrous iron chloride (2.02 g, 12.5 mmol) in nitromethane (12 mL). The reaction proceeded with stirring for 24 hours at room temperature. The polymer was precipitated by pouring into methanol (50 mL) and collected by vacuum filtration. The polymer was reduced overnight using 10% solution of hydrazine in THF (100 mL). The reduced polymer was precipitated by pouring onto methanol, collected by filtration and washed with

methanol. The reduced PDOT_c was purified by Soxhlet extraction with methanol, with the main fraction extracted by chloroform. Yield: 149 mg, 20%. The molecular mass, as determined by GPC was 2 kDa with a polydispersity of 1.7. ¹H NMR (400 MHz, CDCl₃) δ 7.04 (br, 1H, H₄), 4.16 (br, 2H, OCH₂); 2.0-0.85 (8CH₂, CH₃). UV-visible spectrum λ_{max} 466 nm.

Poly(decyl 4,4''-didecoxy-2,2':5',2''-terthiophene-3'-carboxylate) (PDDTTC_c).

To a stirred solution of decyl 4,4''-didecoxy-2,2':5',2''-terthiophene-3'-carboxylate **3** (0.2 g, 0.27 mmol) in chloroform (9mL), under nitrogen, was added dropwise a solution of anhydrous iron chloride (0.162 g, 1 mmol) in nitromethane (3 mL). The reaction proceeded with stirring for 24 hours at room temperature. The polymer was precipitated by pouring into methanol (50 mL) and collected by vacuum filtration. The polymer was reduced overnight using 10% solution of hydrazine in THF (100 mL). The reduced polymer was precipitated by pouring onto methanol, collected by filtration and washed with methanol. The reduced PDDTTC_c was purified by Soxhlet extraction with methanol and the main fraction was collected in chloroform. Yield: 150 mg, 75%. The molecular mass, as determined by GPC was 125 kDa with a polydispersity of 1.13. ¹H NMR (400 MHz, CDCl₃) δ 7.37 (br, 1H, H₄[']); 7.15 (br, 1H, H₃); 6.83 (br, 1H, H₃^{''}); 4.08 (br, 2H, COOCH₂); 3.96 (br, 4H, 2OCH₂); 4.08 (br, 2H, COOCH₂); 1.9-0.80 (24CH₂, 3CH₃). UV-visible spectrum λ_{max} 549 nm. ν_{max}/cm⁻¹ 2924, 2854, 1713, 1512, 1466, 1350, 11.80, 1072, 772.

2.3 Electrochemical polymerisations.

General

Polymers were grown from monomer solutions containing 0.1 M TBAP. The polymers were grown onto clean ITO glass or gold Mylar electrodes with an area of 1 cm² using; a platinum mesh counter electrode, a Ag/Ag⁺ reference electrode, and an eDAQ system controlled by EChem software. Generally first the polymerisation was studied by cyclic voltammetry scanning from a potential range -0.2 V to 1 V at a scan rate of 50 mV/s. Polymer films were grown at constant current by applying 1 mA/cm², or constant potential depending on which method gave best quality films.

Poly((Acyl-serine methyl ester)-4,4''-didecoxy-2,2':5',2''-terthiophene-3'-carboxylate) 24.

A 20 mmol/L monomer **22** solution in 1:1 DCM acetonitrile was used. Cyclic voltammetric growth at 50 mV/s between -0.2 V and 1 V showed the onset of oxidation for this monomer at 0.76 V. Films were then grown at both constant current of 1 mA/cm² and constant potential of 0.85 V. The **24** films grown at constant current were even in appearance and so several films were grown by this method and taken for further studies. $\nu_{\max}/\text{cm}^{-1}$ 3255, 2947, 2669, 1734, 1643, 1551, 1497, 1250, 1142.

Poly((BOC-tyrosine methyl ester)-4,4''-didecoxy-2,2':5',2''-terthiophene-3'-carboxylate) 25.

A 20 mmol/L monomer **23** solution in 1:1 DCM acetonitrile was used. Cyclic voltammetric growth at 50 mV/s between -0.2 V and 1 V showed the onset of

oxidation for this monomer at 0.73 V. Films were then grown at both constant current of 1 mA/cm² and constant potential of 0.85 V. The **25** films grown at constant current were even in appearance and so several films were grown by this method and taken for further studies.

Poly((2-(3',3'-dimethyl-6-nitrospiro[chromene-2,2'-indoline]-1'-yl)ethyl)-4,4''-didecoxy-2,2':5',2''-terthiophene-3'-carboxylate) (PTTSPC).

An 8 mmol/L solution of the monomer TTSPC in 0.1 M TBAP 1:1 acetonitrile DCM was prepared. Polymerisation was initially studied by cyclic voltammetric growth at 50 mV/s between -0.3 V and 1 V on an ITO glass electrode showing an onset of oxidation of 0.8 V. The PTTSPC films were then grown at constant potential of 0.9 V for 40 seconds this gave nice looking uniform films that were still transparent.

Poly((2-(3',3'-dimethyl-6-nitrospiro[chromene-2,2'-indoline]-1'-yl)ethyl)-4,4''-didecoxy-2,2':5',2''-terthiophene-3'-acetate) (PTTSPA).

An 8 mmol/L solution of the monomer TTSPA in 0.1 M TBAP 1:1 acetonitrile:DCM was prepared. Polymerisation was initially studied by cyclic voltammetric growth at 50 mV/s between -0.3 V and 1 V on an ITO glass electrode showing an onset of oxidation of 0.8 V. The PTTSPA films were then grown at constant potential of 0.9 V for 40 seconds this gave nice looking uniform films that were still transparent.

Poly(2,2':5',2''-(terthiophene-3,3''-diyl)bis(ethane-2,1-diyl) dioctanoate) (PTBEO).

A 20 mmol/L monomer **59** solution in acetonitrile was used. Cyclic voltammetric growth at 50 mV/s between -0.2 V and 0.9 V showed the onset of oxidation for this

monomer at 0.7 V. Polymer growth at a constant potential of 0.8 V for 40 seconds was found to give even looking PTBEO films.

Poly(2,5'-bithiophene) (PBT).

A 0.1 mol/L solution of bithiophene in 0.1M TBAP acetonitrile was prepared. Films were then grown at constant current 1mA/cm² for 40 seconds. The PBT films looked uniform and gave a good electrical response by CV. $\nu_{\max}/\text{cm}^{-1}$ 2677, 1674, 1535,1319,1210, 1095, 1026.

Poly(decyl 4,4''-didecoxy-2,2':5',2''-terthiophene-3'-carboxylate) (PDDTTC_e).

A 20 mmol/L monomer **3** solution in 1:1 DCM acetonitrile was used. Films were grown at constant current of 1 mA/cm². The PDDTTC_e films looked uniform and gave a good electrical response by CV. ^[29] $\nu_{\max}/\text{cm}^{-1}$ 2677, 1712, 1512,1327, 1172, 1088, 740.

2.4 Structure fabrications.

2.4.1 Spin coating of films.

Polymer solutions were prepared for spin coating by dissolving polymer (50 mg) in chloroform (5 mL) and filtering to remove any solid impurities. The substrates (gold-coated mylar, ITO-coated glass and glass) were cut into 5 x 1 cm pieces and thoroughly washed using detergent, water, isopropanol and methanol. The polymer films were spin coated onto the substrates at 1000 rpm for 20 seconds using a Laurell WS-400B-6NPP/LITE spin coater.

2.4.2 Electrospinning of fibre mats.

Electrospinning was performed in a box flushed with dry air, using a Gamma ES30P-5W HV power supply and a Kd Scientific KDS 100 CE syringe pump to control the flow rate of polymer solution. The fibres were collected on a grounded target at a distance of 15 cm.

Poly(3-hexylthiophene) fibres.

A stock spinning solution was prepared by dissolving poly(3-hexylthiophene) (38 mg) and polyethylene oxide (Mw 5×10^3 kDa, 2 mg) in chloroform (1 mL). This solution was spun starting at flow rate 1 mL/hr observing the jet and varying the applied voltage until the jet stabilised this was found to occur at 5 kV. The fibres however looked very clumpy when observed under a microscope. The flow rate was gradually reduced, however no improvement in fibre morphology was observed. To improve fibre morphology the polymer concentration was halved by diluting 0.5 mL

of the stock solution with 0.5 mL of chloroform. This 19 mg/mL P3HT solution was observed to form a stable jet at 5 kV. The flow rate was slowly reduced and the fibre morphology was observed to be optimal at 0.5 mL/hour where the fibres were smooth and unbeaded. Reducing the concentration further to 10 mg/mL, resulted in fibre beading. A polymer concentration of 12.5 mg/mL was also observed to give good fibres at a flow rate of 0.3 mL/hour and applied potential of 5 kV.

Poly(octanoic acid 2-thiophen-3-yl-ethyl ester) fibres.

A spinning solution was prepared by dissolving poly(octanoic acid 2-thiophen-3-yl-ethyl ester) (19 mg) and polyethylene oxide (Mw 5×10^3 kDa, 1 mg) in chloroform (0.9 mL) and DMF (0.1 mL), followed by filtration. The solution was electrospun with the optimal flow rate of 0.5 mL/hour at an applied voltage of 5 kV with 15 cm separation between needle and collector. The fibres were collected for a 2 min period onto a gold Mylar substrate attached to the target.

Poly(octanoic acid 2-thiophen-3-yl-ethyl ester) aligned fibres.

Aligned fibre mats were formed using the same spinning conditions as above for the poly(octanoic acid 2-thiophen-3-yl-ethyl ester) non-aligned fibre mats. The fibres were collected on a rotating drum of 5 cm diameter at a rotation speed varying from 500 rpm to 2000 rpm. The fibres were collected for a 2 min period onto gold Mylar attached to the rotating drum target. The alignment of electrospun fibres was quantitated from phase contrast images using the Image Pro Plus program (Media Cybernetics, Inc.).

2.5 Spectroscopic studies.

TTSPC and TTSPA interactions with metal ions.

A stock 0.1 mmol/L solution of (2-(3',3'-dimethyl-6-nitrospiro[chromene-2,2'-indoline]-1'-yl)ethyl)-4,4''-didecoxy-2,2':5',2''-terthiophene-3'-acetate in acetonitrile was prepared and 1.5 mL of the solution was placed in a cuvette and diluted with 1.5 mL acetonitrile. The spectrum of this solution was taken on a Shimadzu UV-1601CE spectrometer in a quartz cuvette. The solution was then illuminated by 254 nm UV light for 1 minute to open the spiropyran moiety, the spectrum was immediately taken. The solution was exposed to white light for 1 minute to close the spiropyran and the spectrum again taken. The interaction of the spiropyran terthiophene with various metal ions was studied by repeating the above with the addition of 1.5 mL of stock solution and 1.5 mL of metal ion solution 0.1 mmol/L in acetonitrile. $\text{Co}(\text{NO}_3)_2$, $\text{Cu}(\text{NO}_3)_2$, $\text{Cd}(\text{NO}_3)_2$, were used to make up the metal ion solutions, a solution of 0.1M HCl) 0.1 mL in 1.4 mL acetonitrile was also used to investigate the interaction with acid. The kinetics of the closing of the spiropyran was also investigated by opening the molecule with UV light for 1 minute before monitoring the absorbance at 570 nm keeping the cuvette at 25°C.

The studies were repeated on a 0.1 mmol/L stock solution of the second monomer (2-(3',3'-dimethyl-6-nitrospiro[chromene-2,2'-indoline]-1'-yl)ethyl)-4,4''-didecoxy-2,2':5',2''-terthiophene-3'-carboxylate.

Degradation of bis((4-decoxythiophen-2-yl)methylene)benzene-1,4-diamine 34.

Preliminary degradation studies were performed by dissolving bis((4-decoxythiophen-2-yl)methylene)benzene-1,4-diamine **34** (5 mg) in THF and adding a drop of HCl to the solution. The colour of the solution was monitored and degradation was observed. The degradation was monitored by NMR spectroscopy. Bis((4-decoxythiophen-2-yl)methylene)benzene-1,4-diamine **34** (10 mg) was dissolved in 1 mL d_6 -THF. A ^1H NMR spectrum was taken, HCl (0.05 mL) was then added and several ^1H NMR spectrums were taken to monitor the degradation. A precipitate was observed to form broadening the spectrum, which showed the appearance of a characteristic aldehyde peak. After leaving overnight, a white precipitate was collected, which was identified as *p*-phenylenediamine dihydrochloride **37** (^1H NMR (400 MHz, D_2O) δ 7.56 (s, 4H, Ar)).^[6] The NMR spectrum of the filtrate, ^1H NMR (400 MHz, d_6 -THF) δ 9.76 (s 1H, CHO); 7.45 (d, 1H, $J=1.9$ Hz, H3), 6.92 (d, 1H, $J=1.9$ Hz, H5), 3.97 (t, 2H, $J=6.7$ Hz, OCH_2), 1.83-0.86 (8CH_2 and CH_3) was consistent with 4-decoxythiophene-2-carbaldehyde **31**.

Degradation of poly((methyl 5,5'-dimethylene -4,4''-didecoxy-2,2':5',2''-terthiophene-3'-carboxylate)benzene-1,4-diamine) 43.

The degradation of poly((methyl 5,5'-dimethylene -4,4''-didecoxy-2,2':5',2''-terthiophene-3'-carboxylate)benzene-1,4-diamine) **43** films was monitored by UV-visible spectroscopy. A poly((methyl 5,5'-dimethylene -4,4''-didecoxy-2,2':5',2''-terthiophene-3'-carboxylate)benzene-1,4-diamine) **43** film on a ITO glass slide was placed in a cuvette containing THF, a spectrum collected, HCl (0.05 mL, 32%) was added and spectra taken at regular intervals. The spectra showed degradation of the

polymer film. A polymer **43** film was placed in pH 7.3 phosphate buffer. At this pH, the film was stable for several weeks with no change observed in the UV-visible spectrum. A polymer **43** film was then placed into a dilute HCl solution (pH 1) here the film was observed to undergo protonation and change colour, however the film was still present after 2 weeks.

Auto reduction of POTE, PHET and PDDTTC_c films.

The auto reduction of POTE, PHET and PDDTTC_c films on ITO glass was studied by UV-visible spectroscopy. The spectrum of the reduced film on ITO glass was taken, the film was electrochemically oxidised by applying a constant potential of 0.8 V for 2 minutes in 0.1 M TBAP/acetonitrile. The film was then quickly washed then placed in a cuvette containing cell culture media and the UV-visible spectrum monitored. This was also repeated for POTE and PHET films in TBApts electrolyte.

2.6 References.

- [1] D. D. Perrin, W. L. F. Armarego, *Purification of Laboratory Chemicals.*, 3 ed., Pergamon Press., England, **1988**.
- [2] C. D. Bain, G. M. Whitesides, *Science (Washington, DC, United States)* **1988**, 240, 62.
- [3] G. Zotti, M. C. Gallazzi, G. Zerbi, S. V. Meille, *Synthetic Metals* **1995**, 73, 217.
- [4] C. Shi, Y. Yao, Y. Yang, Q. Pei, *Journal of the American Chemical Society* **2006**, 128, 8980.
- [5] S. A. Ponomarenko, A. M. Muzafarov, O. V. Borshchev, E. A. Vodopyanov, N. V. Demchenko, V. D. Myakushev, *Russian Chemical Bulletin* **2005**, 54, 684.
- [6] <http://riodb01.ibase.aist.go.jp/sdbs/> T. Yamaji, T. Saito, K. Hayamizu, M. Yanagisawa, O. Yamamoto, *Vol. 2010*, National Institute of Advanced Industrial Science and Technology, Japan, **2010**.
- [7] S. Gambhir, Massey University, **2006**, unpublished results.
- [8] B. Pal, W.-C. Yen, J.-S. Yang, W.-F. Su, *Macromolecules (Washington, DC, United States)* **2007**, 40, 8189.
- [9] L. Huo, T. L. Chen, Y. Zhou, J. Hou, H.-Y. Chen, Y. Yang, Y. Li, *Macromolecules (Washington, DC, United States)* **2009**, 42, 4377.
- [10] S. Nishimura, A. Sakumoto, E. Imoto, *Nippon Kagaku Zasshi* **1961**, 82, 1540.
- [11] B. Kim, L. Chen, J. Gong, Y. Osada, *Macromolecules* **1999**, 32, 3964.

- [12] K. Wagner, L. L. Crowe, P. Wagner, S. Gambhir, A. C. Partridge, J. C. Earles, T. M. Clarke, K. C. Gordon, D. L. Officer, *Macromolecules (Washington, DC, United States)* **2010**, *43*, 3817.
- [13] K. Wagner, R. Byrne, M. Zanoni, S. Gambhir, L. Dennany, R. Breukers, M. Higgins, P. Wagner, D. Diamond, G. G. Wallace, D. L. Officer, *Journal of the American Chemical Society* **2010**, submitted for publication.
- [14] M. J. Zoellner, U. Jahn, E. Becker, W. Kowalsky, H.-H. Johannes, *Chemical Communications (Cambridge, United Kingdom)* **2009**, 565.
- [15] Y. A. Dubitsky, M. Catellani, A. Bolognesi, S. Destri, W. Porzio, *Synthetic Metals* **1993**, *55*, 1266.
- [16] J. Hou, Z. a. Tan, Y. Yan, Y. He, C. Yang, Y. Li, *Journal of the American Chemical Society* **2006**, *128*, 4911.
- [17] J. Yu, S. Holdcroft, *Macromolecules* **2000**, *33*, 5073.
- [18] P. J. Costanzo, K. K. Stokes, *Macromolecules* **2002**, *35*, 6804.
- [19] S. Zrig, P. Remy, B. Andrioletti, E. Rose, I. Asselberghs, K. Clays, *The Journal of Organic Chemistry* **2008**, *73*, 1563.
- [20] S.-Y. Jang, G. A. Sotzing, M. Marquez, *Macromolecules* **2004**, *37*, 4351.
- [21] T. Dohi, M. Ito, N. Yamaoka, K. Morimoto, H. Fujioka, Y. Kita, *Tetrahedron* **2009**, *65*, 10797.
- [22] T. Olinga, S. Destri, W. Porzio, A. Selva, *Macromolecular Chemistry and Physics* **1997**, *198*, 1091.
- [23] K. P. R. Nilsson, A. Aslund, I. Berg, S. Nystroem, P. Konradsson, A. Herland, O. Inganaes, F. Stabo-Eeg, M. Lindgren, G. T. Westermark, L. Lannfelt, L. N. G. Nilsson, P. Hammarstroem, *ACS Chemical Biology* **2007**, *2*, 553.

- [24] P. Camurlu, A. Cirpan, L. Toppare, *Materials Chemistry and Physics* **2005**, 92, 413.
- [25] C. V. Pham, H. B. Mark, Jr., H. Zimmer, *Synthetic Communications* **1986**, 16, 689.
- [26] M. He, T. M. Leslie, J. A. Sinicropi, *Chemistry of Materials* **2002**, 14, 4662.
- [27] J. Rolfes, J. T. Andersson, *Analytical Communications* **1996**, 33, 429.
- [28] S. A. Ashraf, F. Chen, C. O. Too, G. G. Wallace, *Polymer* **1996**, 37, 2811.
- [29] S. Gambhir, K. Wagner, D. L. Officer, *Synthetic Metals* **2005**, 154, 117.

CHAPTER 3. FUNCTIONALISED POLYTHIOPHENE MATERIALS THROUGH TERTHIOPHENE PRECURSORS.

3.1 Introduction.

Functionalisation gives the ability to tune the properties of a thiophene-based polymer for particular applications such as sensors,^[1, 2] FETs,^[3] LEDs,^[4] photovoltaics,^[5-7] and bionics.^[8] Functionalisation of conducting polymers can be achieved by incorporating a functional dopant as well as by covalent modification.^[9] Covalent functionalisation of polythiophenes is of particular interest as the functionality can be conjugated through the polymer structure allowing changes to the functionality to be sensed as changes to the polymer. Covalent functionalisation is also more chemically stable than the incorporation of functional dopants.^[9]

Terthiophene molecules are convenient building blocks for conducting polymers and are a useful base for the incorporation of functionalisation into conducting polymer materials. The increased conjugation length of terthiophene molecules gives a reduction in oxidation potential when compared to single thiophenes and bithiophenes.^[10] Our research group has extensive experience with the synthesis of functional terthiophene derivatives.^[11-19] A range of terthiophene materials have been synthesised (Figure 3.1) containing hexoxy and decoxy chains as well as a range of other functional groups on the central thiophene.^[16] The alkoxy chains have the

benefit of decreasing the oxidation potential and increasing the solubility of the monomers in organic solvents.^[20]

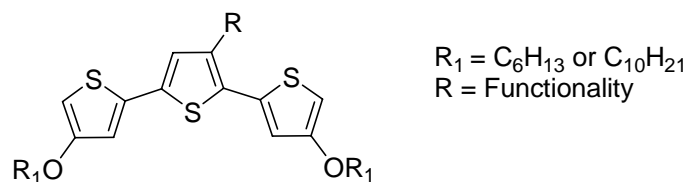


Figure 3.1. General terthiophene structure.

Here, the further functionalisation of these basic terthiophene building blocks is investigated. We are interested in functionalities that facilitate interactions (such as hydrogen bonding) between biological systems and the polymer. Such interactions are desirable for bionic applications such as cell growth scaffolds. Thus several functionalities, which are candidates for increasing the biocompatibility and tailoring materials for bionic applications, were investigated. One such molecule is barbituric acid, a molecule well known to form strong hydrogen bonds.^[21] Thus, coupling this to terthiophenes could be used to increase the ability of the materials to hydrogen bond and interact with biological environments, as could amino acids the basic building blocks of all proteins and peptides that are a major component of all living organisms.^[9] Many cell growth factors are made up of amino acids building blocks. Thus the attachment of amino acids is a model for the attachment of longer peptides. Such peptides and proteins are relatively expensive and thus unsuitable for preliminary investigations. Consequently, it may be beneficial to use copolymerisation to incorporate only small quantities of the more expensive functional monomers into the conducting polymer scaffolds.

A third class of functional molecules that offer a multitude of possibilities for functionalised polythiophenes are the spiropyrans. Spiropyrans are an interesting class of molecules, which have the unique property of being able to reversibly change conformation with the application of light (Figure 3.2). Exposing the benzospiropyran form to UV light causes the molecule to open up to a charged merocyanine form, which can be reversed by the application of visible light.^[22] The merocyanine is well known to complex various metal ions,^[23-28] DNA,^[29] and amino acids.^[30-32] A spiropyran-coupled polythiophene offers the potential of signal transduction, where changes to the spiropyran conformation are manifested as changes in the resistance of the polymer. Such a material would be ideal in sensor or bionic applications.

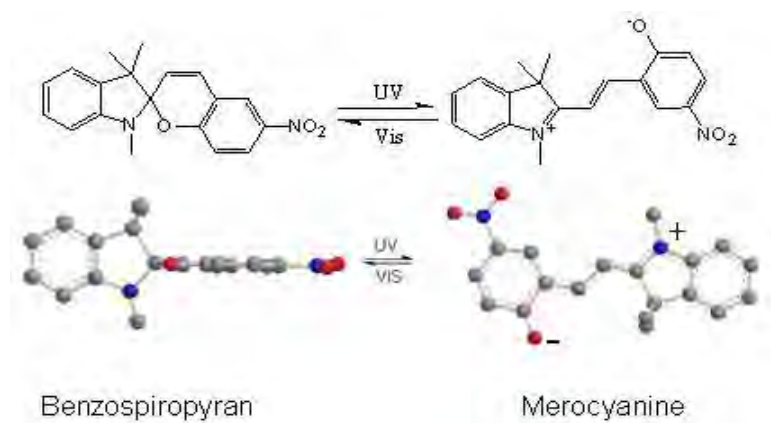


Figure 3.2. Reversible photo-induced isomerisation between benzospiropyran and merocyanine. Figure courtesy of Dr Robert Byrne.^[33]

The polymerisation of the functionalised terthiophene monomers will be achieved using one of the two simplest methods for producing polythiophenes, chemical oxidation and electrochemical oxidation.^[10] As every monomer has a different oxidation potential and solubility, both methods were investigated for the synthesis of polymers and the resulting functional polymers characterised.

3.2 Synthesis of functional terthiophenes.

Our research group has extensive experience with the synthesis of terthiophene materials incorporating a diverse range of functional groups.^[16] The aim here was to utilise this experience to synthesise functional monomers containing carboxylic acid groups as they can easily be functionalised further. The synthetic approach that has been developed by our research group uses palladium catalysed Suzuki coupling of two molecules of 3-alkoxythiophene-5-boronic acid with functionalised 2, 5-dibromothiophene derivatives (for example, see Scheme 3.2). This building block approach to terthiophene synthesis is a simple method, which can be used to synthesise terthiophenes with a multitude of functional groups. A range of boronic acids incorporating different length alkyl and alkoxy chains for solubility can be used or they can be unfunctionalised if solubility is not so important. The relatively mild conditions used in the Suzuki coupling reaction allow a diversity of functionality to potentially be incorporated.^[34]

Many functional terthiophenes can potentially be synthesised by this Suzuki coupling method. Our goal was to synthesise monomers containing decoxy chains for improved solubility and ester groups that could be hydrolysed to give free carboxylic acids for further functionalisation. Thus, simple esters methyl 4,4''-didecoxy-2,2':5',2''-terthiophene-3'-carboxylate **1** and methyl 4,4''-didecoxy-2,2':5',2''-terthiophene-3'-acetate **2** were chosen for synthesis (Figure 3.3). These terthiophene esters differ by a methylene spacer. This allows the synthesis of functionalised polymers with the functionality at slightly different distances from the polymer backbone. Closer spacing may allow for better signal transduction between the

polymer and the functionality. A slightly longer spacing gives greater flexibility and could allow the functionality to interact more closely with the environment.

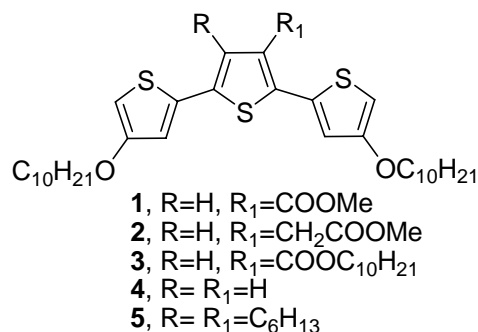
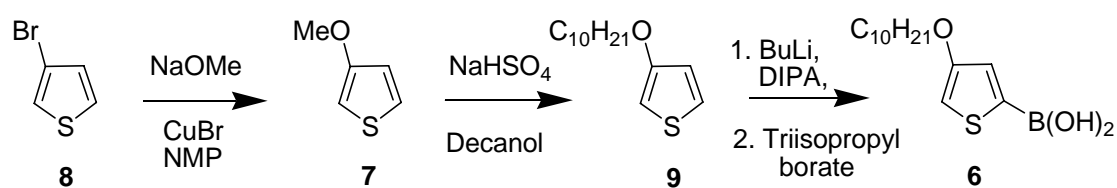


Figure 3.3. Structures of target terthiophene materials.

Several other functional terthiophenes were also chosen as useful starting materials for polymer synthesis such as (decyl 4,4''-didecoxy-2,2':5',2''-terthiophene-3'-carboxylate **3**, 4,4''-didecoxy-2,2':5',2''-terthiophene **4** and 3',4'-dihexyl-4,4''-didecoxy-2,2':5',2''-terthiophene **5**), which all contain decoxy chains as well as other solubilising groups (Figure 3.3). The utility of these materials as precursors for degradable conducting polymers and the biocompatibility of the resulting polymers will be further investigated in Chapters 4 and 6.

The 3-decoxythiophene-5-boronic acid **6** starting material required to make these terthiophenes and improve their solubility, was synthesised by modification of the method of Zotti *et al.*^[20] for the analogous 3-pentoxythiophene-5-boronic acid (Scheme 3.1). 3-Methoxythiophene **7** was synthesised by coupling of 3-bromothiophene **8** with sodium methoxide and purified by distillation under reduced pressure. The 3-methoxythiophene **7** was then reacted with decanol (direct reaction of 3-bromothiophene **8** with sodium and decanol is known to give a low yield^[20]).

The 3-decoxythiophene-5-boronic acid **6** was then synthesised by lithiation of the 3-decoxythiophene **9**, followed by reaction with triisopropyl borate. The ^1H NMR of 3-decoxy thiophene-5-boronic acid **6** was as expected when compared to literature data for 3-pentoxythiophene-5-boronic acid showing doublets at 7.17 ppm and 6.56 ppm corresponding to the thiophene protons and a triplet at 3.95 ppm corresponding to the alkoxy CH_2 .^[20]

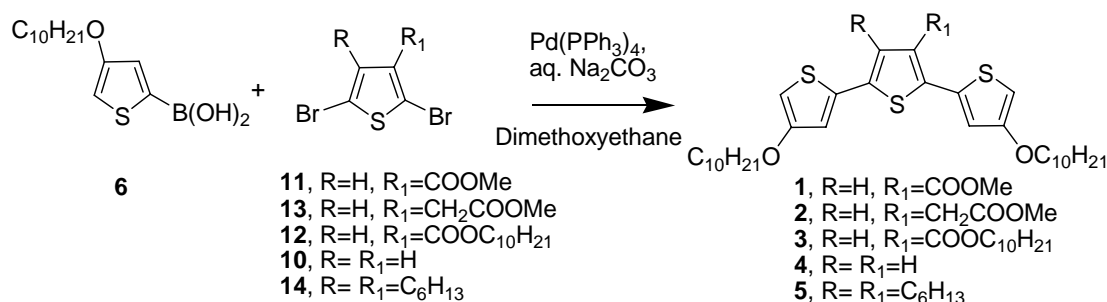


Scheme 3.1.

The other starting materials for the synthesis of terthiophenes by Suzuki coupling are 2,5-dibromothiophene derivatives. Several of these were synthesised so that functional terthiophenes could be prepared (Scheme 3.2). The well known 2,5-dibromothiophene **10** was easily synthesised by brominating thiophene with 2 equivalents of NBS in THF. Ester starting materials; such as methyl 2,5-dibromothiophene-3-carboxylate **11**, decyl 2,5-dibromothiophene-3-carboxylate **12** and methyl 2,5-dibromothiophene-3-acetate **13** were then synthesised following the procedure of Gambhir *et al.*^[16] 2,5-Dibromo-3,4-dihexylthiophene **14** was kindly supplied by Dr Sanjeev Gambhir.

Terthiophenes were then synthesised by Suzuki coupling using tetrakis (triphenylphosphine) palladium(0) catalyst following a procedure modified from

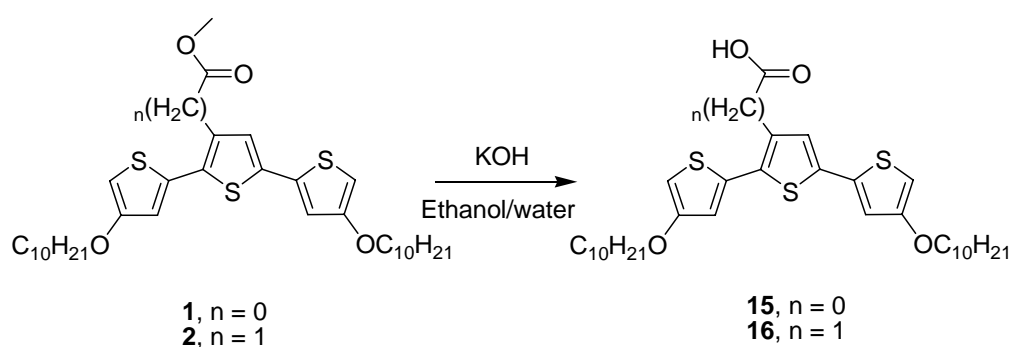
Gambhir *et al.*^[16] The synthesis of these terthiophene materials is outlined in Scheme 3.2 and the experimental details for these reactions can be found in Chapter 2. The purity of these known terthiophene monomers was confirmed by ¹H NMR spectroscopy with 5 aromatic thiophene peaks observed between 7.5 ppm and 6.15 ppm for the non-symmetrical terthiophenes **1-3**, and for the symmetrical terthiophenes **4** and **5**, only 3 and 2 aromatic proton peaks were observed respectively, the position of these peaks was consistent with data supplied by Dr Sanjeev Gambhir.^[35]



Scheme 3.2.

To be useful for further functionalisation, the ester terthiophene molecules **1** and **2** needed to be hydrolysed to their free acid forms. As shown in Scheme 3.3 the terthiophene acids 4,4''-didecoxy-2,2':5',2''-terthiophene-3'-carboxylic acid **15** and 4,4''-didecoxy-2,2':5',2''-terthiophene-3'-acetic acid **16** were obtained by the treating the methyl esters **1** and **2** with potassium hydroxide in a mixture of ethanol and water at 80°C for 4 hours, after which time there was no ester apparent on TLC. Crude acids **15** and **16** were obtained after acidification by dilute HCl, and extraction of the solid acid with DCM. The crude acid was purified by column chromatography using 3:7 ethyl acetate: DCM as the eluent. For 4,4''-didecoxy-2,2':5',2''-

terthiophene-3'-carboxylic acid **15** the hydrolysis was confirmed by the absence of the singlet at 3.84 ppm, which corresponds to the ester methyl group in the ^1H NMR spectrum and the FTIR spectrum showed a shift in the C=O peak from 1716 cm^{-1} for the ester to 1683 cm^{-1} for the acid. Similarly for the 4,4''-didecoxy-2,2':5',2''-terthiophene-3'-acetic acid **16**, the hydrolysis was confirmed by the absence of the singlet at 3.74 ppm, which corresponds to the ester methyl group in the ^1H NMR spectrum and the FTIR spectrum showed a shift in the C=O peak from 1739 cm^{-1} for the ester to 1714 cm^{-1} for the acid. The pure acids **15** and **16** were then used for the attachment of several functionalities through esterification.



Scheme 3.3.

3.3 Synthesis of functionalised terthiophene monomers.

With the required acids **15** and **16** and other suitable terthiophenes in hand, the synthesis of a number of materials with hydrogen bonding and further functionality to optimise the materials for bionic applications was undertaken.

3.3.1 Synthesis and polymerisation of barbituric acid functionalised terthiophene.

Barbituric acid is known to be a strong hydrogen bond donor.^[21] A polymer incorporating such functionality may have strong interactions with cells and this may give the ability to control the growth of certain cell types on polymer structures, which would be interesting for bionic applications.

Previously novel β -(styryl)terthiophenes (Figure **3.4**) have been synthesised by Collis *et al.*^[17] These molecules are of interest as the planar functionality is conjugated to the terthiophene giving rise to advantageous electronic properties. An analogous planar system with a terthiophene attached through a conjugated linker to a barbituric acid group was thus the goal of this work.

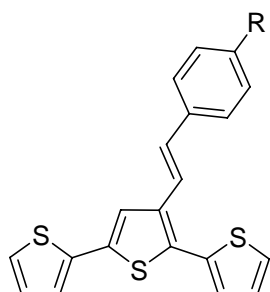


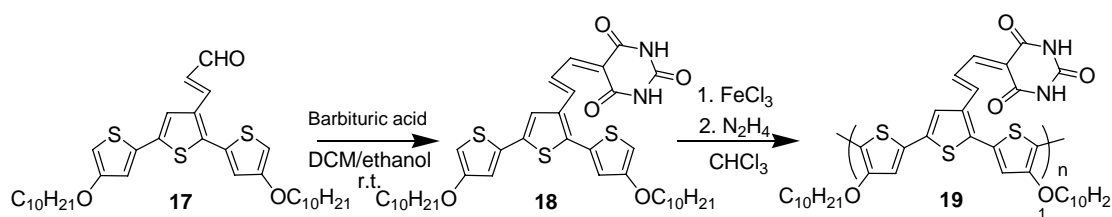
Figure **3.4**. Planar β -(styryl)terthiophenes synthesised by Collis *et al.*^[17]

Barbituric acid condenses readily with aldehydes to give alkene linkages^[36] and, thus, the condensation of barbituric acid with a terthiophene aldehyde was deemed a simple approach to the conjugated planar precursor of a barbituric acid-functionalised polymer. 4,4''-Didecoxy-3'-propenal-2,2':5',2''terthiophene **17** was generously supplied by Dr Pawel Wagner. The coupling reaction (Scheme **3.4**) was undertaken in a DCM ethanol mix at room temperature overnight. After washing of the material by water and extraction by DCM, the product was purified by column chromatography on silica. The 4,4''-didecoxy-3'-(5-allylidenepyrimidine-2,4,6(1H,3H,5H)-trione)-2,2':5',2''-terthiophene **18** product was analysed by mass spectrometry, which gave a mass of 725, that was the mass of the expected product.

One of the easiest and most commonly utilised methods for the oxidative polymerisation of thiophene monomers and oligomers is chemical oxidation by anhydrous iron chloride.^[37] This method typically involves the addition of a monomer solution to a slurry containing four equivalents of the iron chloride oxidant in a solvent, such as chloroform. Typically the polymerisation solution darkens as the polymer forms, the resulting polymer is in its oxidised and is insoluble until it is reduced, this is typically performed by a base such as hydrazine.

The functionalised monomer **18** was polymerised by this iron chloride oxidation method (Scheme **3.4**), the polymerisation solution darkened indicating formation of poly(4,4''-didecoxy-3'-(5-allylidenepyrimidine-2,4,6(1H,3H,5H)-trione)-2,2':5',2''terthiophene) **19**, after 12 hours this polymerisation solution was poured onto methanol to remove the remaining iron chloride as polythiophenes are generally insoluble in methanol. The polymer in its oxidised state was collected by filtration,

samples of the polymer **19** in THF were treated with the bases hydrazine and the less harsh N,N-diethylhydroxylamine. Nonetheless, treatment of samples of the black oxidised polymer **19** with these bases was unsuccessful in reducing and solubilising the polymer. The polymer remained as a black insoluble solid indicating it had not been reduced. It was unclear whether this was due to the bases reacting with the polymer or strong hydrogen bonds within the polymer. It was hypothesised that the barbituric acid moiety may have been deprotonated by base treatment thus causing the insolubility of the polymer. Stirring the samples of **19** in an acetic acid chloroform mixture after base treatment was unsuccessful in solubilisation of the polymer by protonation.



Scheme 3.4

As the barbituric acid-functionalised polymer **19** could not be solubilised processing the polymer into structures for use in bionic applications could not be achieved. This result highlights the importance of solubility of novel polymeric materials. Solubility allows materials to be easily characterised and fabricated into structures. The investigation of other novel thiophene materials containing barbituric acids was considered however the desirable conjugated planar structure is likely to be one of the reasons for the insolubility. The decision was thus made to investigate the more biologically relevant amino acids instead of planar conjugated hydrogen bonding systems.

3.3.2 Amino acid functionalisation of terthiophenes.

Amino acids are one of the basic building blocks of life. Thus the incorporation amino acid functionality onto a conducting polymer is of interest to increase the biocompatibility of these materials. Overall the attachment of cell growth factors such as laminin and fibronectin, which are known to stimulate cell growth,^[38] to polythiophene films would be optimal. However, to simplify the synthesis and characterisation of the monomers and polymers, single amino acids were chosen as model compounds for optimisation of the chemistry. Amino acids and peptides have multiple functional groups, which can often interfere with reactions, causing lower yields and unwanted side products. This can be avoided by using protected amino acids, of which there is a wide range available.

Protected amino acids, serine **20** and tyrosine **21** (Figure 3.5), purchased from Aldrich, were chosen for preliminary experiments as these amino acids have alcohol functionalities, which can be coupled to 4,4''-didecoxy-2,2':5',2''-terthiophene-3'-carboxylic acid **15** via a simple DCC mediated esterification. The DCC coupling method is a convenient method of esterification that proceeds under mild conditions. By protecting the acid and amino groups in the amino acids, side reactions could be minimised and homo coupling prevented.

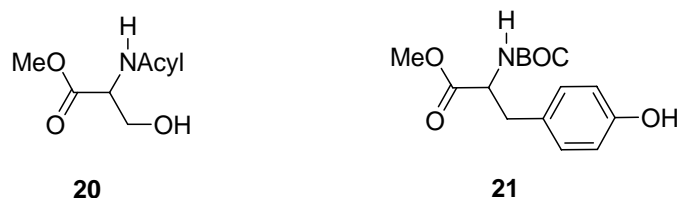
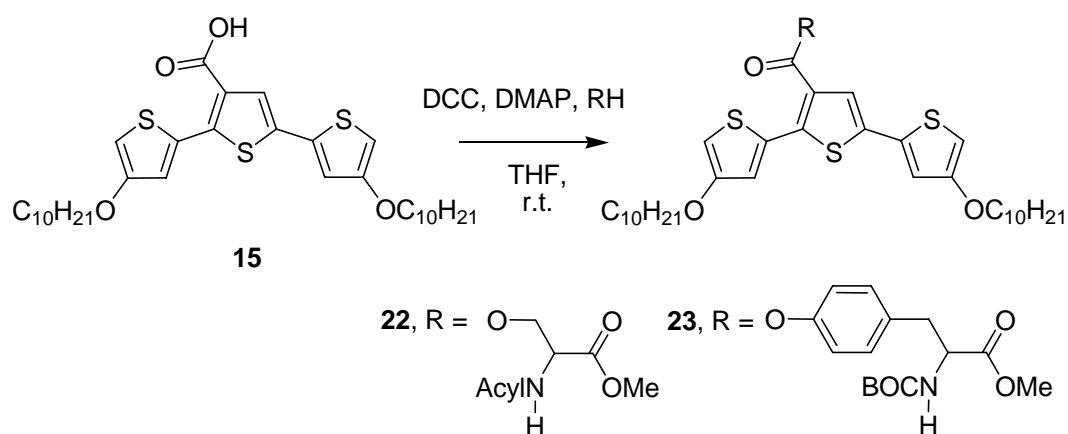


Figure 3.5. Structure of acyl-serine methyl ester **20** and BOC-tyrosine methyl ester **21** for use in terthiophene functionalisation.

The coupling reactions were carried out at room temperature with DCC coupling agent and DMAP as a base (Scheme 3.5). The reactions were monitored by TLC and shown to be complete after stirring overnight. The products were then purified by column chromatography. The coupling products, characterised by mass spectrometry, gave masses of 747 and 882 for the two compounds (acyl-serine methyl ester)-4,4''-didecoxy-2,2':5',2''-terthiophene-3'-carboxylate **22** and (BOC-tyrosine methyl ester)-4,4''-didecoxy-2,2':5',2''-terthiophene-3'-carboxylate **23**, respectively, which were as expected. The ¹H NMR spectra showed peaks corresponding to both the amino acid groups as well as the terthiophene. The spectrum of **22** is shown as the bottom spectrum in Figure 3.6, it contains peaks consistent with the terthiophene **15** (shown as the top spectrum in Figure 3.6) as well as peaks corresponding to the acyl-serine methyl ester at 4.90 ppm (CH), 4.66 ppm and 4.47 ppm (CH₂), 3.75 ppm (COOCH₃), and 2.03 ppm (COCH₃).



Scheme 3.5.

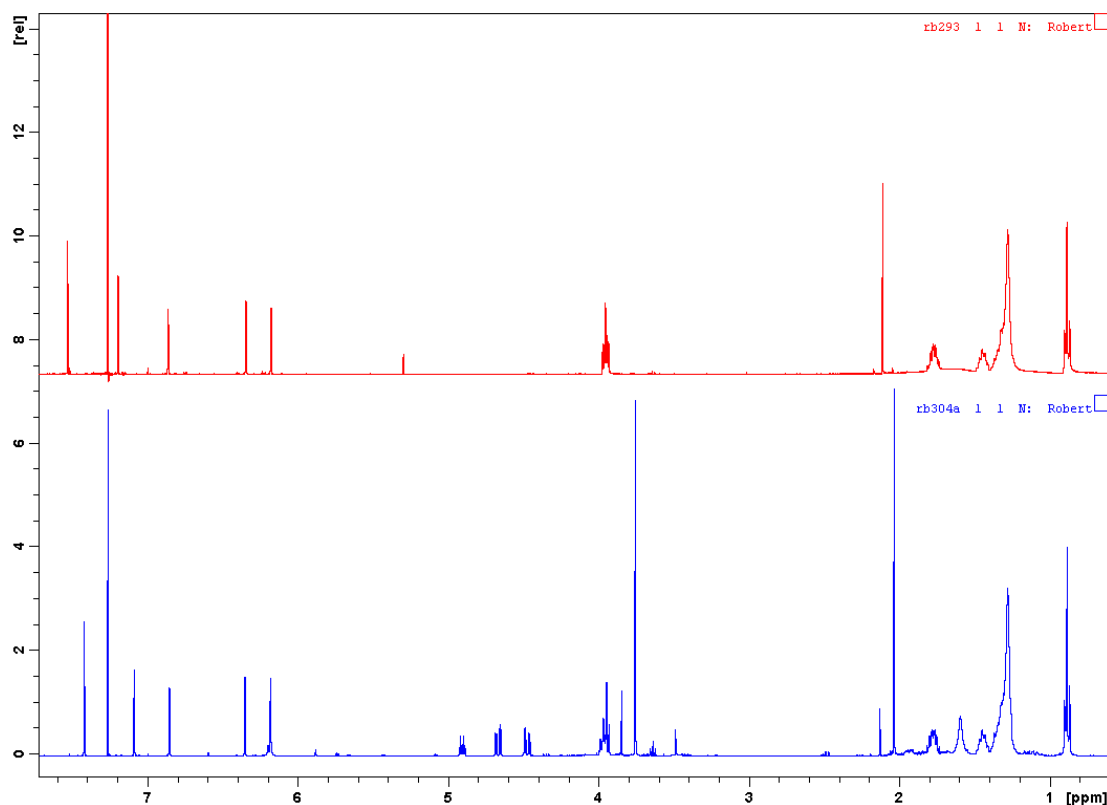


Figure 3.6. ^1H NMR spectra for 4,4''-didecoxy-2,2':5',2''-terthiophene-3'-carboxylic acid **15** (top) and (acyl-serine methyl ester)-4,4''-didecoxy-2,2':5',2''-terthiophene-3'-carboxylate **22** (bottom). Note the appearance of additional peaks corresponding to the acyl-serine methyl ester at 4.90 ppm (CH), 4.66 ppm and 4.47 ppm (CH_2), 3.75 ppm (COOCH_3), and 2.03 ppm (COCH_3).

Once the functionalised monomers had been synthesised their polymerisation was studied. Firstly electrochemical polymerisation was investigated. Gold Mylar working electrodes with surface area 1 cm^2 were used. Gold Mylar is flexible and conductive so a good substrate for investigating bionic applications. Monomer solutions (20 mmol/L) were prepared, in 1:1 DCM acetonitrile with TBAP 0.1 M. Polymers were then grown on gold Mylar by cyclic voltammetry at 50 mV/s between -0.2 V and 1 V. The CV for (acyl-serine methyl ester)-4,4''-didecoxy-2,2':5',2''-terthiophene-3'-carboxylate **22** (Figure 3.7) shows the onset of monomer oxidation at 0.76 V and current growth over subsequent scan indicating polymer deposition. Films of **22** were then grown at both constant current of 1 mA/cm^2 and constant

potential of 0.85 V. The appearance of films grown by both methods was compared. The films grown at constant potential had even coverage of the working electrode whilst the films grown at constant current gave more uneven electrode coverage. Therefore several films were grown by the constant potential method to take for characterisation. The second monomer (BOC-tyrosine methyl ester)-4,4''-didecoxy-2,2':5',2''-terthiophene-3'-carboxylate **23** was similarly polymerised by cyclic voltammetry and showed an onset of oxidation at 0.73 V, films were then grown at constant current of 1 mA/cm² and were even in appearance.

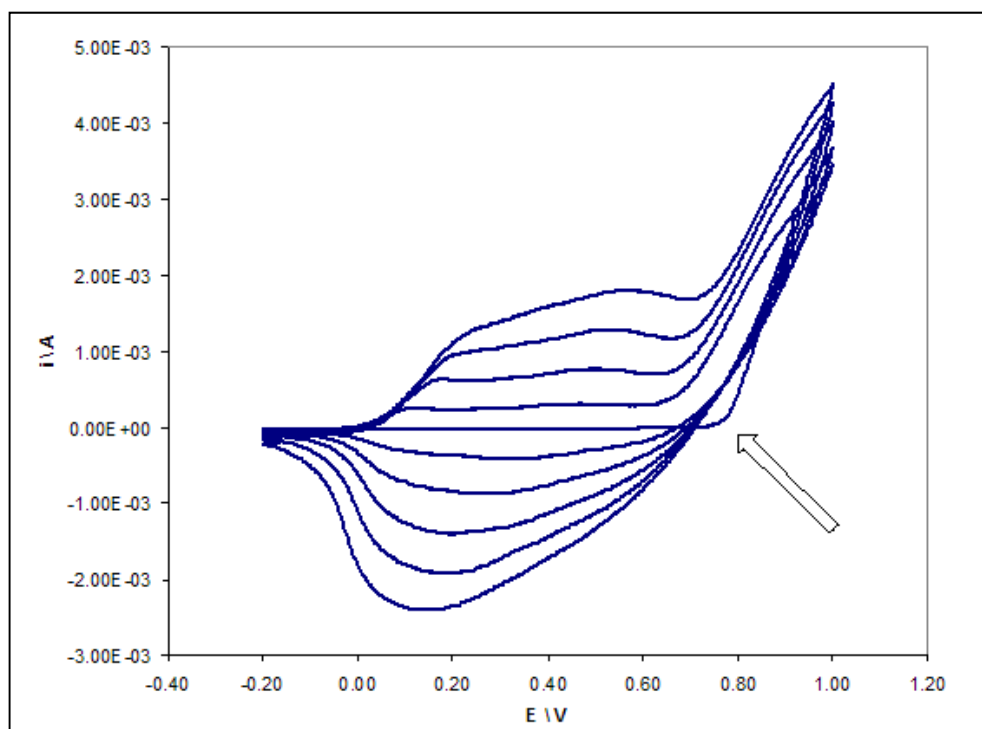


Figure 3.7. CV of polymer growth from (acyl-serine methyl ester)-4,4''-didecoxy-2,2':5',2''-terthiophene-3'-carboxylate **22** solution at 50 mVs⁻¹ between -0.2 V and 1 V. The onset of monomer oxidation at 0.76 V is indicated by the arrow.

A CV for a film of poly((acyl-serine methyl ester)-4,4''-didecoxy-2,2':5',2''-terthiophene-3'-carboxylate) **24** grown at constant potential is shown below in Figure 3.8, this CV was conducted at 50 mVs⁻¹ between -0.2 V and 1 V. The CV for

polymer **24** was stable over 5 scans, and showed an oxidation peak at 0.56 V and a reduction peak at 0.2 V, the CV is indicative of a conducting polymer as it shows a capacitive response.

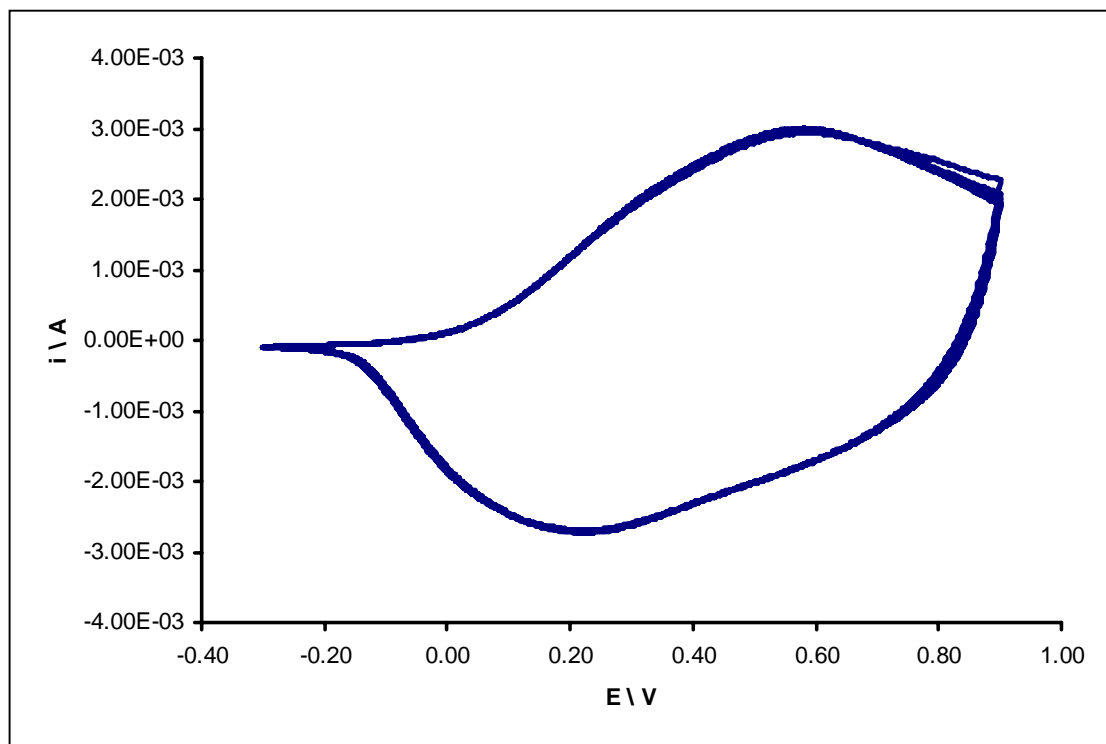
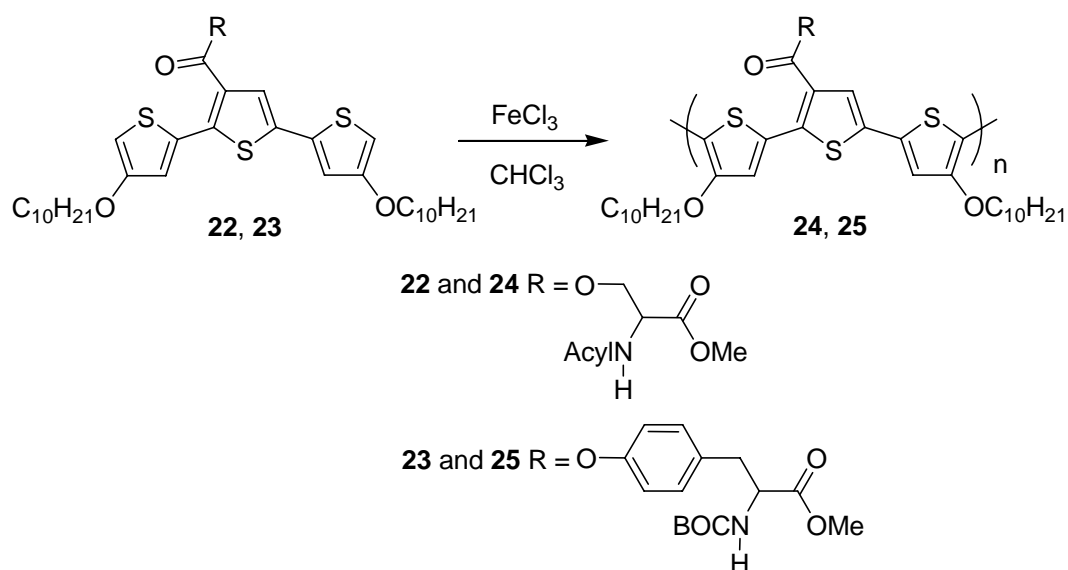


Figure 3.8. CV of polymer film **24** grown at constant potential for 40 seconds at a scan rate of 50 mVs^{-1} between -0.3 V and 0.9 V .

As electrochemistry is limited to producing polymer films on conductive substrates, chemical polymerisation of the amino acid functionalised monomers was investigated as a means of producing soluble polymers that could be fabricated into more complex structures. The polymers were prepared by adding a monomer solution in chloroform to a slurry of iron chloride in chloroform (Scheme 3.6). For both monomers the solutions immediately darkened indicating oligomer formation. The reactions were then stirred at room temperature under nitrogen atmosphere for 24 hours and worked up by pouring onto methanol.



Scheme 3.6.

The resulting chemically produced polymers had relatively low solubility and thus were difficult to characterise by NMR spectroscopy and GPC. The poly((acyl-serine methyl ester)-4,4''-didecoxy-2,2':5',2''-terthiophene-3'-carboxylate) **24** is sparingly soluble and poly(BOC-tyrosine methyl ester)-4,4''-didecoxy-2,2':5',2''-terthiophene-3'-carboxylate **25** is insoluble. The low solubility of these materials is likely due to the polymerisation conditions causing cleavage of the protecting groups. The BOC group is cleaved by acidic conditions^[39] thus HCl produced as a by-product of the polymerisation has caused deprotection of this group. The acyl protecting group is deprotected by basic conditions^[39] thus it has likely been cleaved by the base diethylhydroxylamine used to reduce the polymer. The low solubility of these materials means they are unsuitable for structure fabrication.

We have shown here that amino acid-functionalised terthiophene monomers can be synthesised and electrochemically polymerised to give smooth electro active films.

The chemical polymerisation of these materials unfortunately resulted in sparingly soluble materials. These results pave the way for the functionalisation of polymers with peptides and proteins. In future, more attention should be given to the selection of the protecting groups used to protect the amino acids as here the protecting groups were unable to withstand the chemical polymerisation conditions. Electrochemical polymerisation looks to be a more appropriate method for producing functionalised polymers as the conditions used are less harsh on sensitive functional groups.

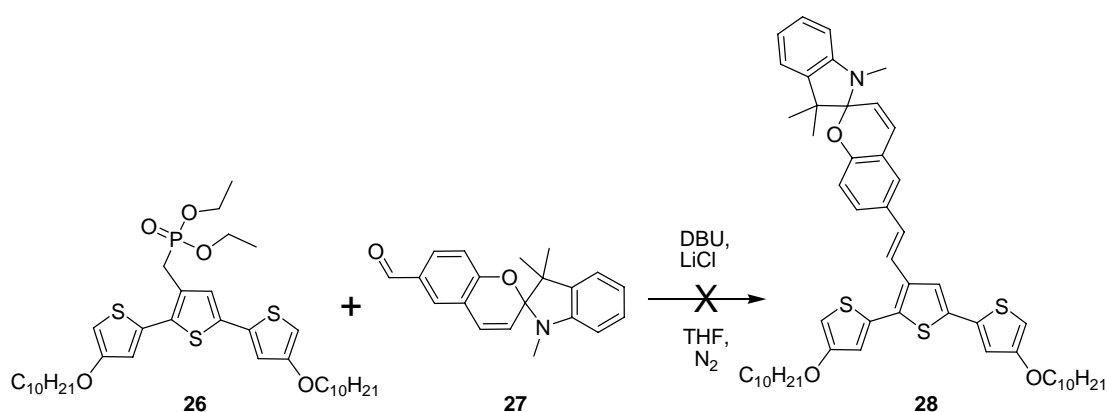
3.3.3 Spiropyran functionalised terthiophenes.

In addition to being very useful in potential sensor applications^[22] spiropyrans have been shown to bind amino acids.^[30-32] This property is of particular interest when combined with the ability of the molecules to reversibly switch from a closed form to an open charged merocyanine form (Figure 3.2), which binds charged amino acids and proteins. Switching from the merocyanine to the spiropyran through electrical signals from the polythiophene offers the tantalising possibility of controlled release of growth factors. Therefore, we have synthesised spiropyran functionalised terthiophene monomers and used them to create functional polythiophenes.

This work was carried out as a joint collaboration between our research group and the research team of the National Centre for Sensor Research, Dublin City University (DCU), combining our expertise in the area of polythiophene materials, with their experience working with spiropyran molecules. As part of this collaboration I was able to visit DCU and carry out research in their laboratories.

As the synthesis of terthiophenes with spiropyrans attached via ester linkages was already under active investigation in our combined laboratories,^[40] we decide to investigate the attachment of a spiropyran molecule through a conjugated linker. Our proposed route involved a Horner-Emmons coupling reaction between an aldehyde functionalised spiropyran and a phosphonate functionalised terthiophene (Scheme 3.7). Diethyl 4,4''-didecoxy-2,2':5',2''-terthiophene-3'-ylmethylphosphonate **26** was kindly supplied by Dr Sanjeev Gambhir, and 1',3',3'-trimethylspiro[chromene-2,2'-indoline]-6-carbaldehyde **27** supplied by Dr Robert Byrne and these starting

materials were combined and reacted together. Unfortunately, this reaction was unsuccessful and no 6-(4,4''-didecoxy-2,2':5',2''-terthiophene-3'-ylvinyl)-1',3',3'-trimethylspiro[chromene-2,2'-indoline] **28** was obtained after several attempts trying different solvents and reaction conditions. It is likely that the reactivity of the aldehyde group is significantly reduced as a result of the electron donating pyran oxygen. As the esterification route to spiroopyran functionalised terthiophenes was already known to work well for the synthesis of (2-(3',3'-dimethyl-6-nitrospiro[chromene-2,2'-indoline]-1'-yl)ethyl)-4,4''-didecoxy-2,2':5',2''-terthiophene-3'-acetate (TTSPA)^[40] further investigation of this route was undertaken.

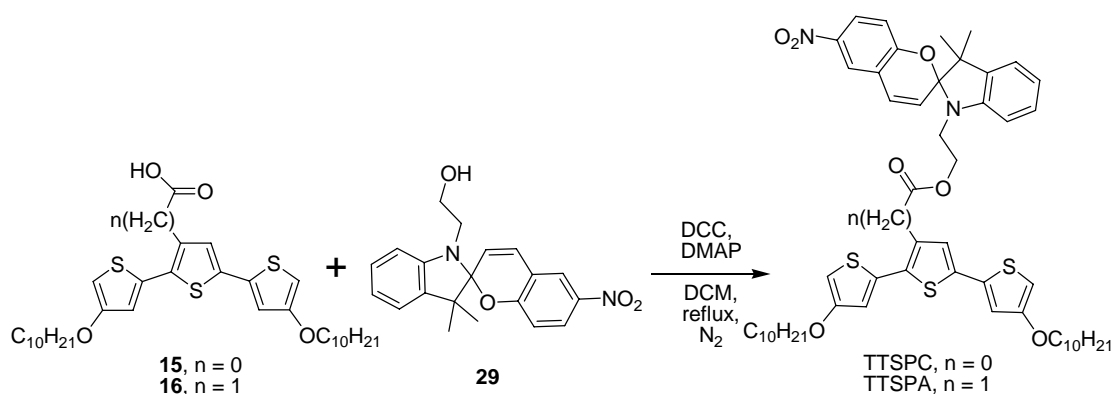


Scheme 3.7.

TTSPA had already been synthesised in our laboratories and the electrochemistry of this monomer and its subsequent polymer studied.^[40] Here we decided to further this study in the context of biological applications, thus we synthesised TTSPA as well as (2-(3',3'-dimethyl-6-nitrospiro[chromene-2,2'-indoline]-1'-yl)ethyl)-4,4''-didecoxy-2,2':5',2''-terthiophene-3'-carboxylate (TTSPC) (Scheme 3.8). We then went on to compare these two monomers and study the interaction of both monomers with metal

ions. Terthiophene monomers TTSPA and TTSPC were subsequently polymerised and their polymers investigated.

The functionalisation reactions were relatively straight forward following the method of Wagner *et al.* (Scheme 3.8).^[40] 2-(3',3'-Dimethyl-6-nitrospiro[chromene-2,2'-indoline]-1'-yl)ethanol (**29**), DCC and DMAP were added to solutions of terthiophene acids **15** and **16** in dry DCM and the reactions stirred at reflux under a nitrogen atmosphere. After 1.5 hours, TLC showed complete reaction. The solvent was removed and the functionalised terthiophene esters purified by chromatography on silica using DCM as eluent. These DCC esterifications worked well and gave yields of 70% for TTSPC and 77% for TTSPA. Mass spectrometry gave masses of 939.4 for TTSPC and 953.4 for TTSPA, which were as expected for MH^+ . The 1H NMR spectrum of the TTSPA was consistent with that of Wagner *et al.*^[40] showing proton peaks corresponding to both the terthiophene and spiropyran. The TTSPC 1H NMR spectrum also showed peaks corresponding to both the terthiophene and spiropyran, only the acyl peak at 3.78 ppm was no longer apparent.



Scheme 3.8.

The functionalised materials were initially studied by UV-visible spectroscopy without analyte molecules (Figure **3.9**). The switching of these molecules can be achieved by UV light (which opens the molecule to the merocyanine) and visible light (which closes the molecule to the spiropyran form). Therefore, a set of three spectra was taken for each sample, an initial spectrum (1), a spectrum after exposure to 254 nm UV light for 1 minute (2), then a final spectrum after exposure to 1 minute of white light (3). When the TTSPA sample was illuminated with 254 nm UV light, an absorbance peak at 568 nm appeared corresponding to a switch from the closed spiropyran form to the open merocyanine form. This peak then disappeared after illumination by white light and the original spectrum was regenerated (Figure **3.9a**). The TTSPC (Figure **3.9b**) showed a very similar response however the merocyanine absorbance peak shifted to 575 nm.

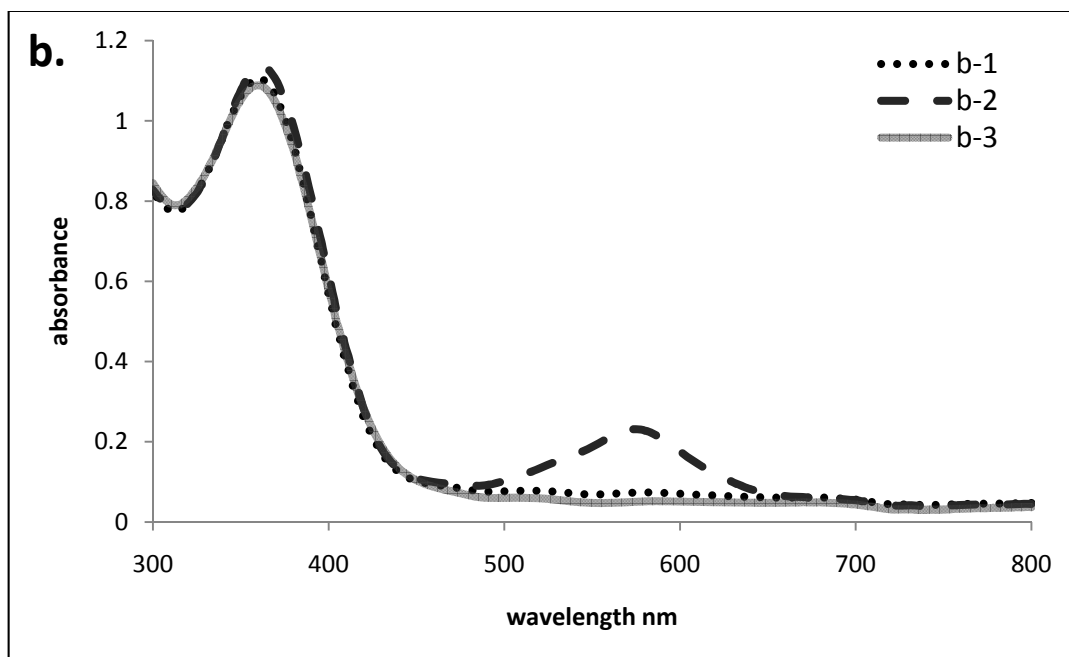
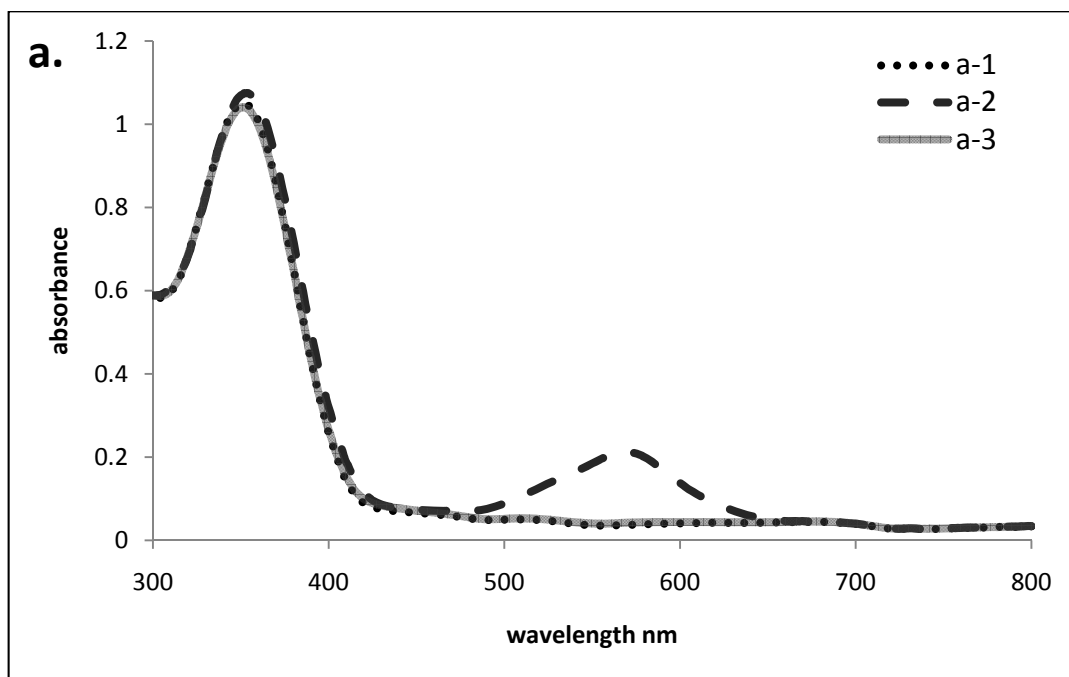


Figure 3.9. UV-visible absorbance spectra. **a.** TTSPA, **b.** TTSPC. For each terthiophene, spectrum **1** is the initial spectrum, **2** the spectrum after exposure to 1 minute of UV light and **3** the spectrum after subsequent exposure to white light.

It is known that the merocyanine will relax back to the closed form in the absence of UV light. This relaxation has been shown to be strongly solvent dependent with more polar solvents stabilising the merocyanine form.^[24] An equilibrium constant for this relaxation (K_e) can be calculated from Equation **3.1** by taking the merocyanine absorbance measured after 15 hours in the dark.^[24] This and other physical properties of the molecules are shown in Table **3.1**.

$$K_e = \frac{[MC]}{[BSP]} = \frac{A}{3.5 \times 10^4 \times C - A} \quad \text{Equation 3.1}$$

where K_e is the equilibrium constant between the spiropyran form (BSP) and the merocyanine (MC) using Beer's law, A is the equilibrium absorbance at the absorbance maximum, C is the concentration of spiropyran initially dissolved and $3.5 \times 10^4 \text{ M}^{-1} \text{ cm}^{-1}$ is the value of ϵ_{MC} . Equation taken from Byrne *et al.*^[24]

The kinetics of the merocyanine closing was studied by opening the molecule by UV light and then monitoring the absorbance at 570 nm (Figure **3.10**). The merocyanine absorbance was observed to decrease towards baseline over a period of 5 minutes, indicating the spiropyran when coupled to terthiophene prefers to be in the closed form. Using Equation **3.2**, a thermal relaxation constant was calculated from a kinetic curve at 25°C for the absorbance of the merocyanine peak.

$$y = ae^{-kt} + b \quad \text{Equation 3.2}$$

where y is the absorbance value at λ_{max} , a is the absorbance at t = 0, k is the rate constant, t is the time in seconds and b is the asymptotic value. This equation taken

from Byrne *et al.*,^[24] was used to determine the rate constant for the thermal isomerisation.

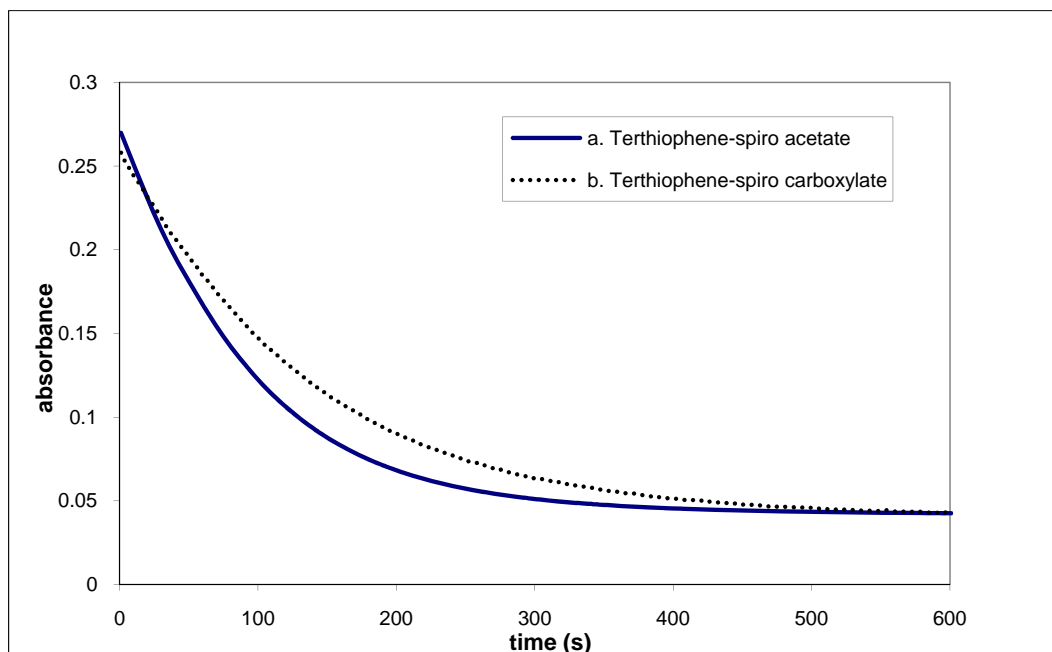


Figure 3.10. Kinetic curves at 25°C for the absorbance of the merocyanine at 570 nm. **a.** TTSPA, **b.** TTSPC.

The calculated K_e and rate constants for the closing of the merocyanines are compared below in Table 3.1 for both the molecules along with the position of the merocyanine peak and the equilibrium absorbance of this merocyanine peak. There is little difference between the two molecules with them both having similar very low K_e values indicating these molecules very much prefer the closed spiropyran form. The TTSPA has got a higher rate constant, which shows that it is able to relax back to the closed form faster possibly due to the greater flexibility imparted by the extra carbon atom in the linker. The rate constants for both molecules however are 4 times faster than that of similar unbound spiropyrans in acetonitrile^[41] indicating that the presence of the terthiophene promotes the spiropyran form over the merocyanine.

This increased stability can be explained by the thiophene disrupting aggregation of the merocyanine form and therefore promoting the spiropyran form.

Table **3.1**. Physical properties of TTSPA and TTSPC, λ_{max} for merocyanine (MC), A_e the absorbance of the merocyanine peak at equilibrium, K_e the equilibrium constant for the relaxation from the merocyanine form to the spiropyran form calculated from Equation **3.1**, k (s^{-1}) the thermal relaxation constant for the closing of the merocyanine calculated from Equation **3.2**.

Molecule	λ_{max} for MC	A_e	K_e	k s^{-1}
TTSPA	568 nm	0.042	0.025	0.010
TTSPC	575 nm	0.046	0.027	0.0074

As the open charged merocyanine is able to bind molecules such as metal ions and amino acids, this property could possibly be used in sensor applications or to bind and release molecules of interest such as growth factors. Therefore, we sought to investigate the interaction of several metal ions with the two spiropyran terthiophenes. These interactions were investigated by UV-visible spectroscopy since there is a change in the electronic spectrum when an ion binds the merocyanine.^[26] Acid is also known to cause changes to the spectrum^[23] and thus the effect of adding HCl was also assessed for comparison. Here the metal ions Co, Cu and Cd metal ions were used for the binding studies and the details of the study are given in the experimental (Chapter 2). A set of three spectra were taken for the molecules with each ion; before UV light irradiation, after UV and after subsequent irradiation by visible light. These spectra were then used to assess the effect of the binding of the ions. The spectra of the UV irradiated samples are shown in Figure **3.11** below as this is where the most significant changes were observed. The effect on the samples

before the irradiation and after the visible light is summarised in Table 3.2. Attempts were also made to analyse the interaction of these monomers with amino acids, however the amino acids we trialled (glycine, tyrosine, aspartic acid) were not compatible in our solvent system (amino acids were insoluble in the acetonitrile used for these studies).

Overall the changes to the UV-visible spectra upon the addition of metal ions were not large however there were significant differences between the different ions and the different molecules. As expected the addition of HCl caused a change in the spectra with a broad shoulder forming at 450 nm, this is evidence that the acid is protonating the merocyanine, visible light gave only partial recovery showing this protonation is not easily reversible. Similar protonation of the merocyanine has been observed by Angiolini *et al.* where a broad peak from 400 to 500 nm was observed.^[42]

Of the metal ions the addition of cobalt and irradiation by UV light caused the appearance of new peaks around 500 nm for both molecules, which were very broad and could not be fully reversed by white light indicating strong binding. Copper gave very little change to the spectra of the TTSPC but caused a shoulder to form at 450 nm in the TTSPA, which could not be recovered upon irradiation with white light. The difference in the copper affinity between these two molecules is interesting and must be due to the greater flexibility in the acetate linker. Previous studies have shown merocyanine to interact more strongly with cobalt than copper.^[23] Cadmium showed some binding with both molecules as evidenced by the appearance of the peak at 520 nm after UV irradiation (this is a shift from the merocyanine peak with

no metal ions present), this peak disappeared after irradiation with visible light indicating this is a reversible binding. This result is consistent with Chibisov *et al.* who observed a peak 495 nm upon cadmium binding, which could be reversed upon white light irradiation.^[43]

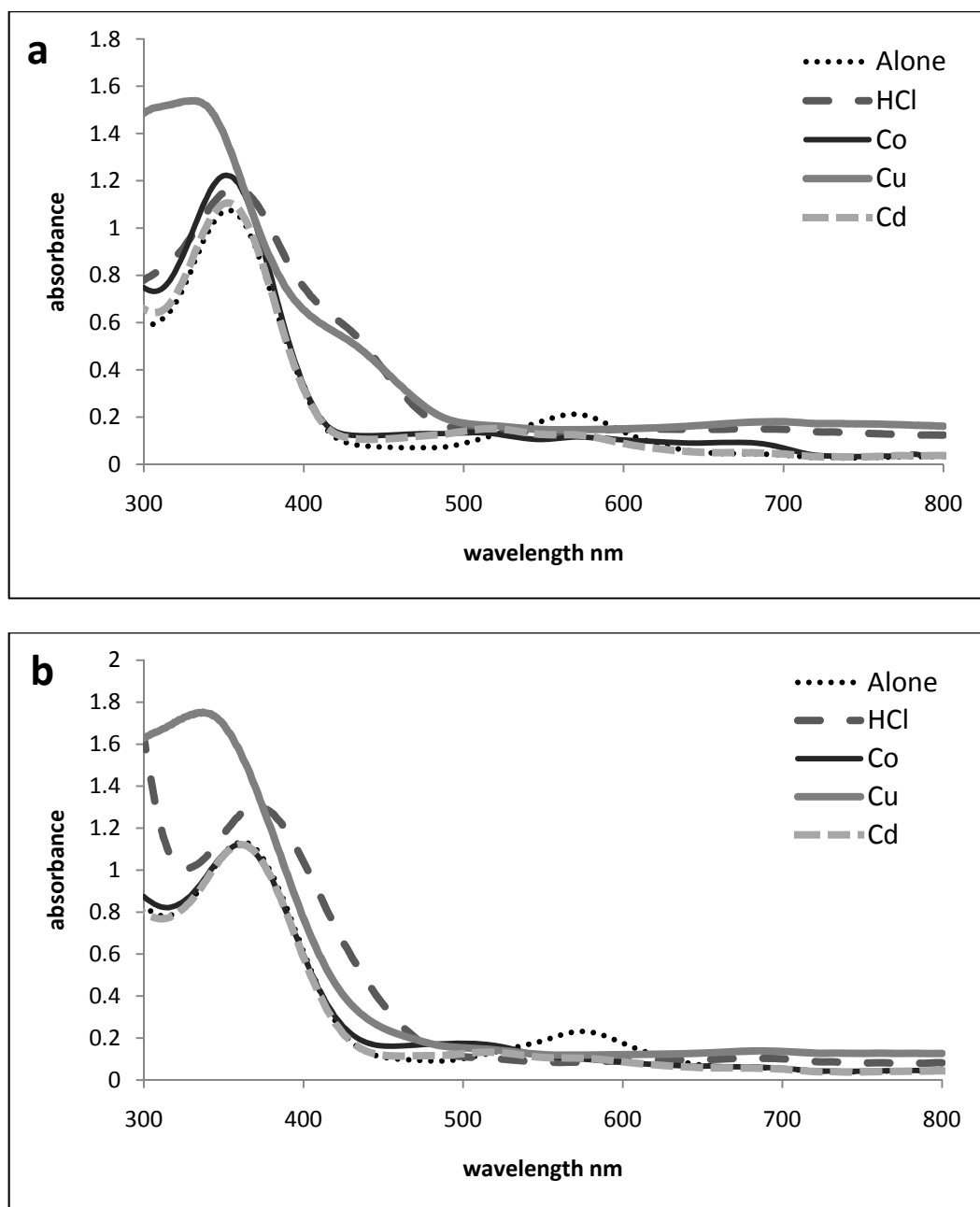


Figure 3.11. UV-visible spectra of terthiophene-spiropyran molecules in acetonitrile at concentration 0.05 mM, alone and with various analyte ions added. All spectra are of the mixtures after 1 minute of exposure to 254 nm UV radiation. **a.** TTSPA, **b.** TTSPC.

Table 3.2. Summary of the effect on the UV-visible spectra of adding metal ions to the TTSPA and TTSPC, before irradiation, after UV irradiation and after subsequent visible irradiation.

Sample.	Before irradiation.	After UV irradiation.	After visible irradiation.
TTSPA - alone	Peak at 360 nm.	New peak appears at 568 nm.	Spectrum returns to that of closed form.
TTSPA - HCl	Same as TTSPA-alone.	Shoulder out to 480 nm appears.	Returns to closed form with slight shoulder.
TTSPA-Co	Same as TTSPA-alone.	Very weak peaks at 450 nm and 570 nm.	Weak peak at 570 nm still slightly present.
TTSPA-Cu	Increased absorbance at 360 nm due to copper.	Shoulder out to 470 nm appears.	Shoulder out to 470 nm still present.
TTSPA-Cd	Same as TTSPA-alone.	Peaks at 520 nm and 570 nm.	Spectrum returns to that of closed form.
TTSPC- alone	Peak at 360 nm.	New peak appears at 574 nm.	Spectrum returns to that of closed form.
TTSPC- HCl	Same as TTSPC-alone.	Slight shoulder out to 450 nm appears.	Returns to closed form with slight shoulder.
TTSPC-Co	Same as TTSPC-alone.	Weak peaks at 500 nm.	Weak peak at 500 nm reduces, still slightly present.
TTSPC-Cu	Increased absorbance at 360 nm due to copper.	Very little change observed.	Very little change observed.
TTSPC-Cd	Same as TTSPC-alone.	Peaks at 510 nm and 570 nm.	Spectrum returns to that of closed form.

The differences in binding of various metal ions shows how the spiropyran is able to be selective, such selectivity is necessary for sensor applications. This reversible binding of the cadmium is a very promising result as it highlights the utility of the system whereby molecules can be bound and released in a controllable fashion.

Once the spiropyran terthiophene monomers had been studied and their interactions with various analyte molecules assessed, the materials needed to be polymerised to give functional spiropyran polymer materials. To avoid the solubility difficulties associated with chemical polymerisation as previously encountered in sections **3.3.1** and **3.3.2** (for barbituric acid and amino acid functionalised polymers), electrochemical polymerisation was chosen as a convenient method for the fabrication of polymer films. Polymer films can be grown on a range of electrodes, although transparent electrodes were used for this study as they were required for spectroscopy. ITO glass electrodes were thus chosen as these are both transparent and conductive.

The electrochemical polymerisation of the monomers was then investigated. Solutions of the monomers (8 mmol/L) in 0.1M TBAP 1:1 acetonitrile:DCM were prepared. Polymerisation was initially studied by cyclic voltammetric growth at 50 mV/s between -0.3 V and 1 V on 1 cm² ITO glass electrodes (Figure **3.12**) the onset of oxidation was 0.76 V for TTSPA and 0.78 V for TTSPC. Poly(2-(3',3'-dimethyl-6-nitrospiro[chromene-2,2'-indoline]-1'-yl)ethyl)-4,4''-didecoxy-2,2':5',2''-terthiophene-3'-carboxylate (PTTSPC) films were then grown at constant potential of 0.9 V for 40 seconds this gave nice looking uniform films that were still transparent. Poly(2-(3',3'-dimethyl-6-nitrospiro[chromene-2,2'-indoline]-1'-yl)ethyl)-

4,4''-didecoxy-2,2':5',2''-terthiophene-3'-acetate (PTTSPA) films could also be grown at constant potential of 0.9 V, these films were grown for 90 seconds, which gave good looking even films (a 40 second growth time gave very thin films for the TTSPA monomer).

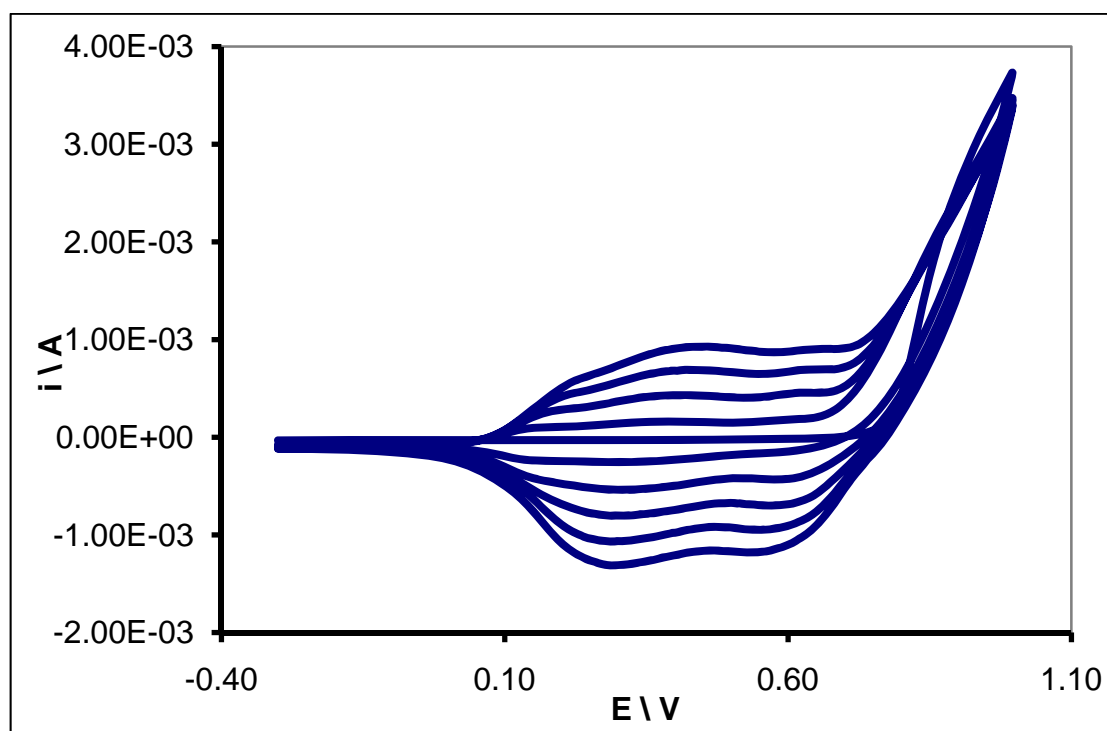


Figure 3.12. CV's showing the growth of a polymer from a TTSPC growth solution (8 mM TTSPC, 0.1 M TBAP, 1:1 acetonitrile DCM, 50 mV/s, -0.3 V and 1 V).

The electrochemistry of the PTTSPA (Figure 3.13 a.) and PTTSPC (Figure 3.13 b.) polymer films was then studied by running post growth CV's. The CV's of both materials are indicative of conducting polymers, however the first scan of these CV's showed a strong oxidation between 0.8 V and 0.9 V, this oxidation was not apparent in subsequent scans. This observation is consistent with the studies by Wagner *et al.* within our laboratories of PTTSPA^[40] and is likely due to the irreversible oxidation of the spiropyran to the merocyanine form.

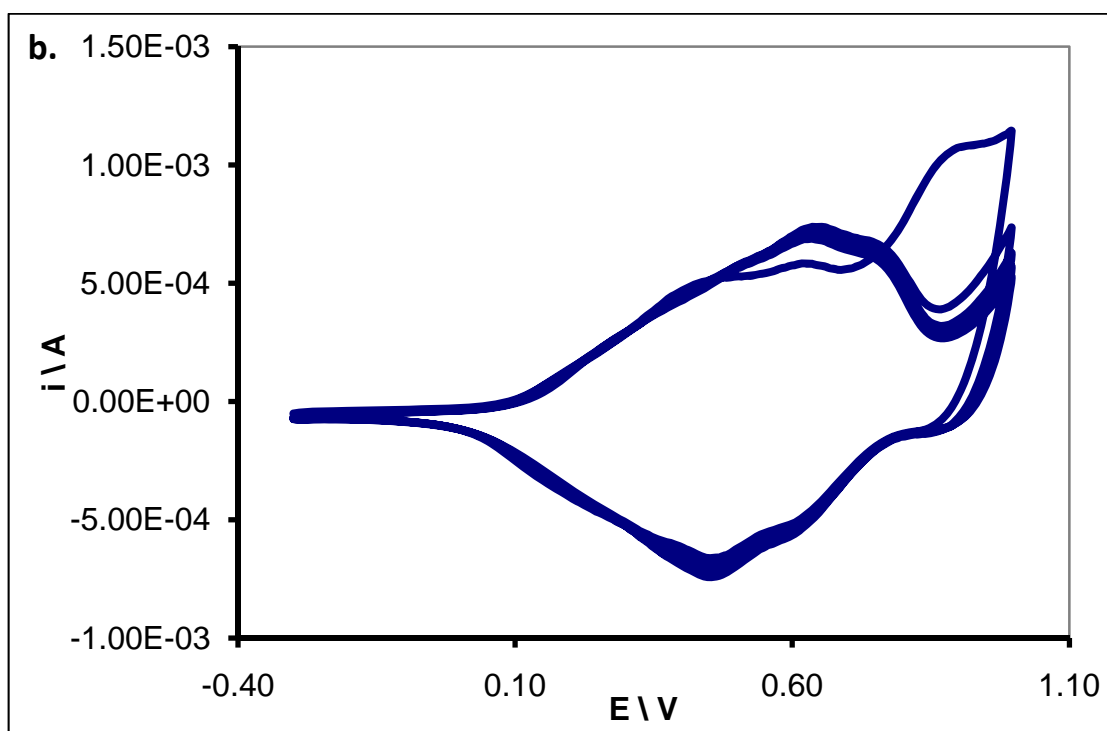
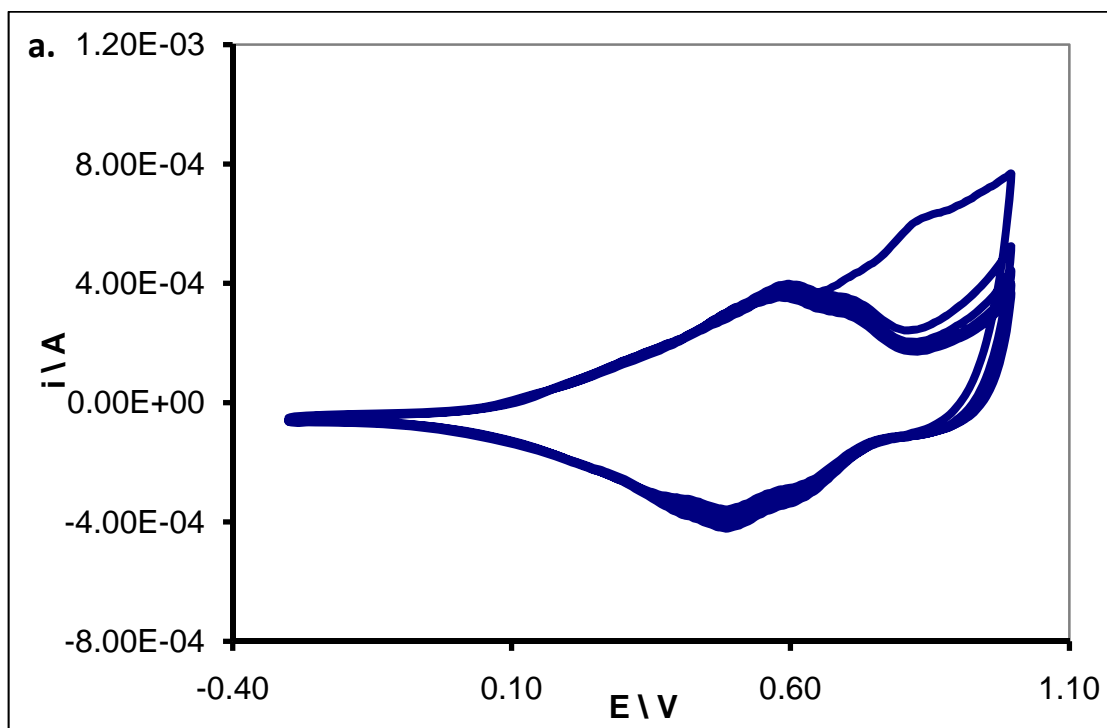


Figure 3.13. CV's showing the electrochemistry of polymer films at 50 mV/s in acetonitrile (0.1 M TBAP) electrolyte **a.** PTTSPA, **b.** PTTSPC.

The studies within our laboratories by Wagner *et al.* on PTTSPA had also shown that this material gave a unique spectroelectrochemical response where at higher voltages a peak due to the merocyanine was observed.^[40] The spectroelectrochemistry of the PTTSPA was thus repeated and the response compared to that of the PTTSPC (Figure 3.14). The initial spectroelectrochemistry of PTTSPC is typical of a polythiophene (Figure 3.14a). At -300 mV the spectrum is that of a reduced polythiophene with a peak at 550 nm characteristic of the polythiophene backbone. Between 100 mV and 600 mV this peak is seen to reduce and a free carrier tail develops out to the red. In the 600 mV spectrum, two additional peaks become apparent at ~860 and ~970 nm, which have previously been assigned to merocyanine π -radical cation dimmers,^[44] supporting the electrochemical oxidation and isomerisation of the spiropyran. Above 600 mV, a new peak at 540 nm is observed to grow as the potential increases from 600 mV to 950 mV (Figure 3.14b). This peak is believed to be due to oxidised merocyanine. The same changes were observed for the PTTSPA spectra (Figure 3.15) and these are consistent with the observations of Wagner *et al.*^[40]

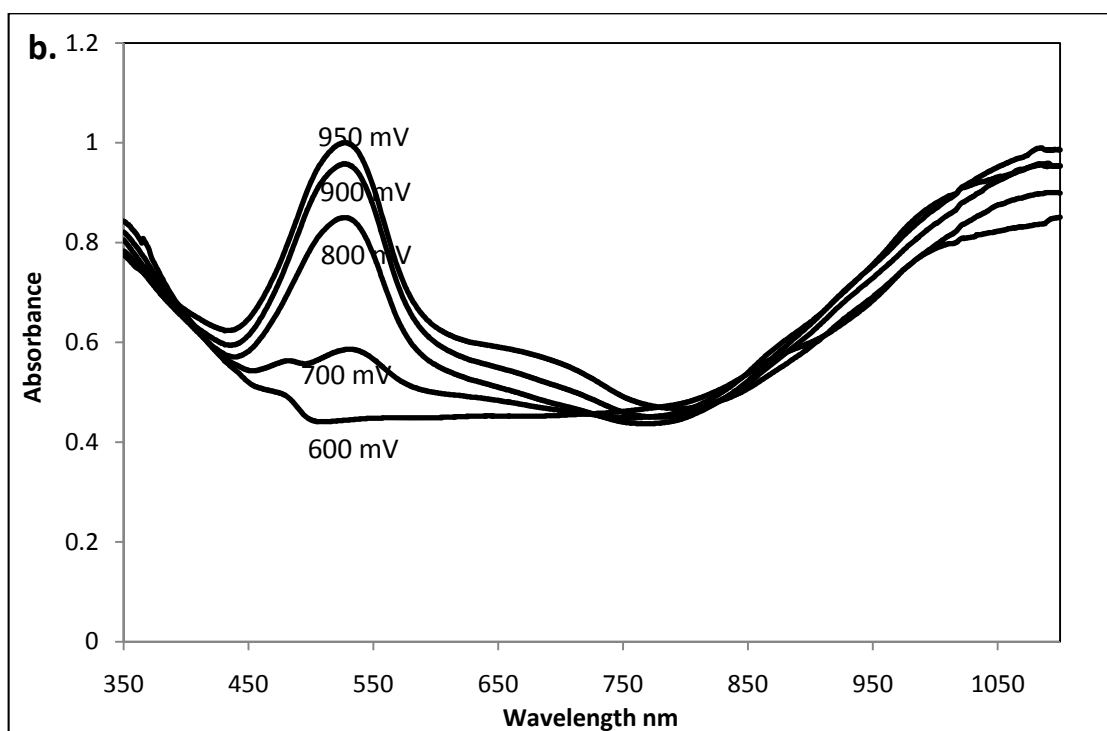
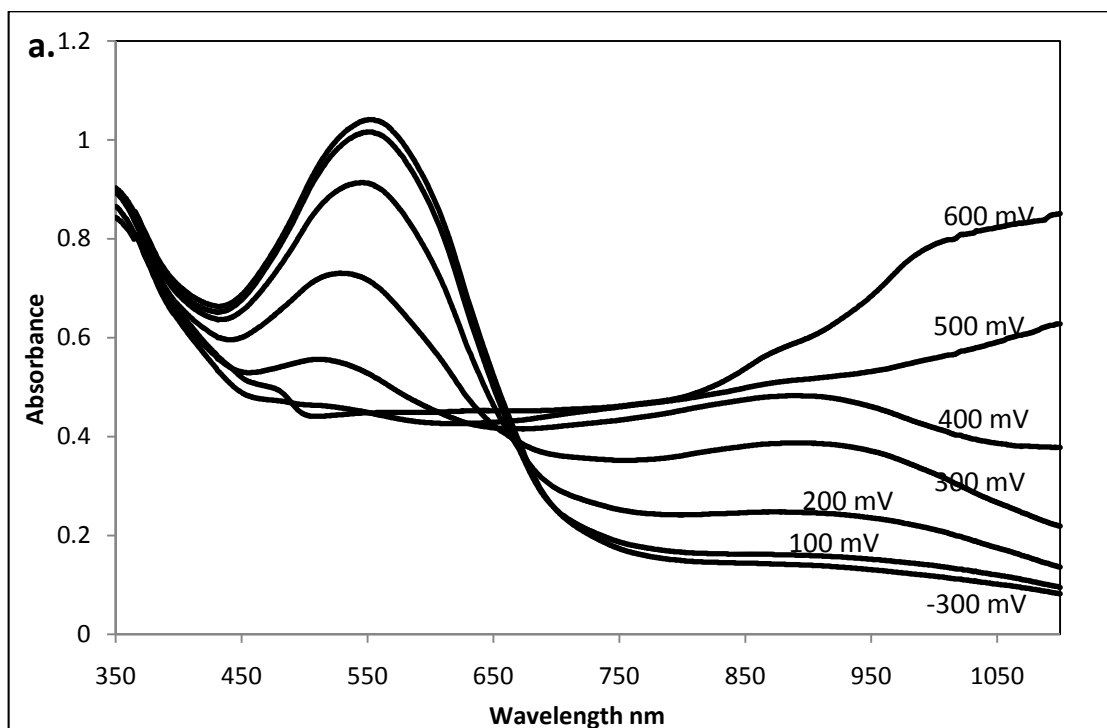


Figure 3.14. UV-visible spectroelectrochemistry of PTTSPC film on ITO glass in 0.1 M TBAP acetonitrile, **a.** -300 mV to 600 mV, **b.** 600 mV to 950 mV.

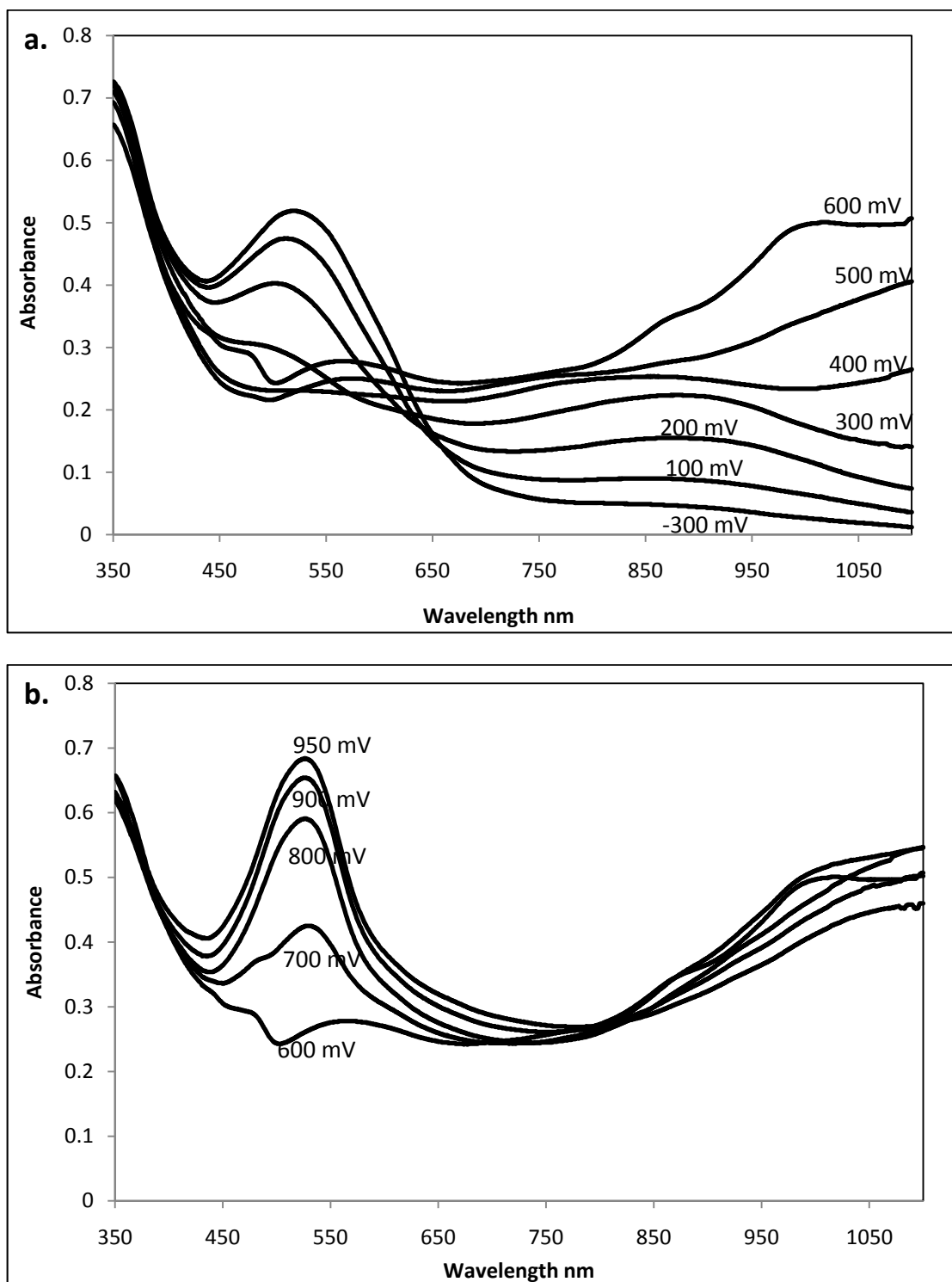


Figure 3.15. UV-visible spectroelectrochemistry of PTTSPA film on ITO glass in 0.1 M TBAP acetonitrile, **a.** -300 mV to 600 mV, **b.** 600 mV to 950 mV.

These polymers have potential to be used in bionic sensor applications and for such applications a flexible, cheap, transparent electrode substrate would be desirable. ITO coated PET is such a transparent flexible electrode, we sought to utilise it by designing a cheap disposable chip for sensing applications. Such a sensing chip could be coated with polymer and used to sense metal ions then be discarded. Dr Fernando Benito-Lopez (DCU) was kindly able to help with design and fabrication of an electrode chip from this material. This electrode chip, shown in Figure 3.16, was made by laminating two pieces of ITO PET together. The bottom piece acts as the working electrode and can be coated with polymer by constant potential growth. The upper piece acts as the counter electrode. We found that ITO coated PET has a slightly higher resistance than ITO glass electrodes; this caused an IR drop when growing the polymers. To get around the IR drop the chip was designed with a small growth area. A drop of electrolyte can be placed in the electrolyte well so that it covers both electrodes, a potential can then be applied to the polymer. This transparent electrode chip was designed for studying the UV-visible spectroelectrochemistry of polymer films using a fibre optic UV-visible probe.

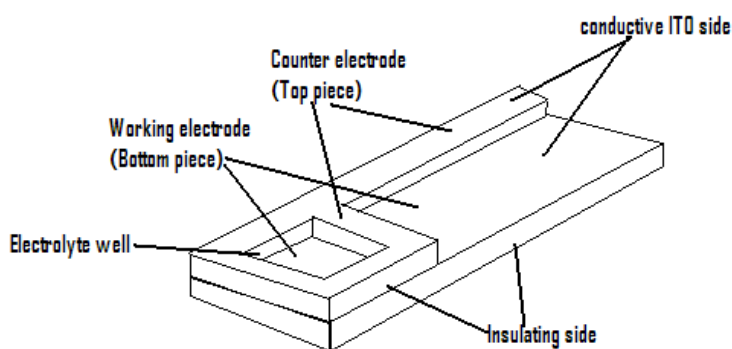


Figure 3.16. Schematic of ITO PET electrode chip.

The polymers PTTSPA and PTTSPC were then successfully deposited onto the substrate by applying a constant potential of 1 V a slightly higher potential than used with the ITO glass substrates due to the IR drop. The polymer films covered the working electrode window area well although were slightly uneven (Figure 3.17).

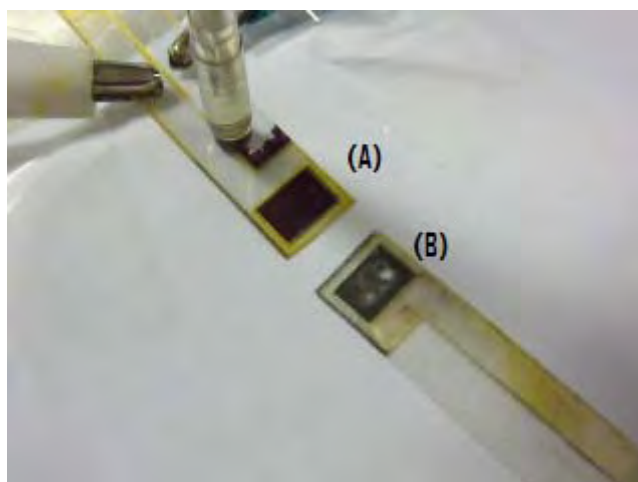


Figure 3.17. PTTSPA films on electrode chips. The upper polymer film (A) has a potential of -0.3 V applied (reduced form), the lower oxidised film (B) has no applied voltage. The blue/grey colour is indicative of oxidised polymer with the spiropyran form attached.

Firstly, the switching of the PTTSPA on the electrode chip was studied, a drop of electrolyte was placed on the chip and the potential was scanned from -300 mV to 1.5 V by cyclic voltammetry. The PTTSPA on the chip was observed to change colour from purple (-300 mV) to light blue/grey (600 mV) then back to purple (1.4 V) (Figure 3.17). A higher potential needed to be applied compared to ITO glass due to the IR drop in the substrate. We attempted to characterise the spectroelectrochemistry of the polymer on this electrode chip using a fibre optic UV probe. However, this probe gave a very high baseline and low signal quality and thus we did not pursue this any further. Time did not permit further work on this device.

This electrode chip and polymer system is promising for future *in situ* sensor applications although much optimisation is needed before it can be used as a prototype device. We were unable to incorporate a reference electrode into this chip and thus in its current form is only useful for qualitative analysis. The reference electrode needed to be placed on top of the chip. In the future, the incorporation of a reference electrode should be investigated as this would allow the chip to be used in quantitative applications without the use of an external reference.

3.4 Conclusions.

A range of terthiophenes materials containing alkoxy groups as well as other functionalities have been synthesised. These materials will be interesting as precursors for polythiophenes for bionic applications. The versatility of the Suzuki coupling used in the synthesis method as well as the building block approach used will allow for easy synthesis and optimisation of this type of materials to suit particular applications. For this section the focus was on the synthesis of terthiophenes containing acid functionality for use in further functionalisation. Acid functionalised terthiophenes were easily synthesised by the hydrolysis of ester functionalised materials.

Such terthiophene materials are promising building blocks for the synthesis of functionalised materials. Several functionalisations have been studied, the addition of barbituric acid, amino acid and spiropyran. These functionalised terthiophene materials were characterised and used to create functional polymers.

A barbituric acid functionalised terthiophene was synthesised. This novel material could be polymerised however the polymer produced was insoluble so was not amenable to further characterisation. Several ester linker terthiophene amino acids were synthesised by coupling, protected amino acids containing alcohol functionality to acid terthiophenes by DCC mediated esterification. These functional terthiophene materials were then polymerised by both chemical and electrochemical methods. The polymer properties were then characterised. These materials are interesting candidates for increasing the biocompatibility of polythiophene materials. This

procedure will be applicable for the functionalisation of materials with peptides and proteins in the future, paving the way for covalent attachment of growth factors to conducting polymers.

The functionalisation of terthiophene materials by spiropyrans was also investigated as this interesting class of molecule is well known to bind a range of ions or molecules. Spiropyran-functionalised terthiophenes were synthesised by DCC mediated esterification. The interaction of these functional molecules with a range of analytes was then studied. Electrochemical polymerisation of the functional terthiophene was carried out to avoid the solubility issues observed with chemical polymerisation. The polymer could be grown on a flexible electrode chip and the polymer could be switched on this chip. This chip has the potential to be optimised and could potentially be used in biosensing applications. Polymer coated electrodes were studied by spectroelectrochemistry, they exhibited very interesting spectra where at high potentials the spiropyran could be opened to the merocyanine form. The interaction of this polymer with several ions was investigated.

Overall functionalisation gives the ability of tailoring material properties for specific applications. Several terthiophenes were prepared, the acid functionalised terthiophenes in particular show much promise as building blocks for further functionalisation. The attachment of several molecules was investigated and these functional polymers have much promise as biocompatible materials and in biosensing applications.

3.5 References.

- [1] L. An, L. Liu, S. Wang, *Biomacromolecules* **2009**, *10*, 454.
- [2] H.-C. Kim, S.-K. Lee, W. B. Jeon, H.-K. Lyu, S. W. Lee, S. W. Jeong, *Ultramicroscopy* **2008**, *108*, 1379.
- [3] H. Meng, J. Zheng, A. J. Lovinger, B.-C. Wang, P. G. Van Patten, Z. Bao, *Chemistry of Materials* **2003**, *15*, 1778.
- [4] W. Huang, H. Meng, W.-L. Yu, J. Pei, Z.-K. Chen, Y.-H. Lai, *Macromolecules* **1999**, *32*, 118.
- [5] F. C. Krebs, H. Spanggaard, *Solar Energy Materials & Solar Cells* **2005**, *88*, 363.
- [6] A. Iraqi, D. F. Pickup, *Polymer International* **2006**, *55*, 780.
- [7] J. Cremer, E. Mena-Osteritz, N. G. Pschierer, K. Muellen, P. Baeuerle, *Organic & Biomolecular Chemistry* **2005**, *3*, 985.
- [8] N. K. Guimard, N. Gomez, C. E. Schmidt, *Progress in Polymer Science* **2007**, *32*, 876.
- [9] G. G. Wallace, L. A. P. Kane-Maguire, *Advanced Materials (Weinheim, Germany)* **2002**, *14*, 953.
- [10] J. Roncali, F. Garnier, M. Lemaire, R. Garreau, *Synthetic Metals* **1986**, *15*, 323.
- [11] P. Wagner, A. C. Partridge, K. W. Jolley, D. L. Officer, *Tetrahedron Letters* **2007**, *48*, 6245.
- [12] G. E. Collis, A. K. Burrell, E. J. Blandford, D. L. Officer, *Tetrahedron* **2007**, *63*, 11141.

- [13] J. Chen, G. Tsekouras, D. L. Officer, P. Wagner, C. Y. Wang, C. O. Too, G. G. Wallace, *Journal of Electroanalytical Chemistry* **2007**, 599, 79.
- [14] P. Wagner, D. L. Officer, *Synthetic Metals* **2005**, 154, 325.
- [15] D. K. Grant, D. L. Officer, *Synthetic Metals* **2005**, 154, 93.
- [16] S. Gambhir, K. Wagner, D. L. Officer, *Synthetic Metals* **2005**, 154, 117.
- [17] G. E. Collis, A. K. Burrell, S. M. Scott, D. L. Officer, *Journal of Organic Chemistry* **2003**, 68, 8974.
- [18] J. Chen, A. K. Burrell, G. E. Collis, D. L. Officer, G. F. Swiegers, C. O. Too, G. G. Wallace, *Electrochimica Acta* **2002**, 47, 2715.
- [19] G. E. Collis, A. K. Burrell, D. L. Officer, *Tetrahedron Letters* **2001**, 42, 8733.
- [20] G. Zotti, M. C. Gallazzi, G. Zerbi, S. V. Meille, *Synthetic Metals* **1995**, 73, 217.
- [21] I. Bolz, M. Bauer, A. Rollberg, S. Spange, *Macromolecular Symposia* **2010**, 287, 8.
- [22] A. Radu, S. Scarmagnani, R. Byrne, C. Slater, K. T. Lau, D. Diamond, *Journal of Physics D: Applied Physics* **2007**, 40, 7238.
- [23] F. Benito-Lopez, S. Scarmagnani, Z. Walsh, B. Paull, M. Macka, D. Diamond, *Sensors and Actuators, B: Chemical* **2009**, B140, 295.
- [24] R. Byrne, K. J. Fraser, E. Izgorodina, D. R. MacFarlane, M. Forsyth, D. Diamond, *Physical Chemistry Chemical Physics* **2008**, 10, 5919.
- [25] S. Scarmagnani, Z. Walsh, F. Benito Lopez, C. Slater, M. Macka, B. Paull, D. Diamond, *e-Journal of Surface Science and Nanotechnology* **2009**, 7, 649.
- [26] S. Scarmagnani, Z. Walsh, C. Slater, N. Alhashimy, B. Paull, M. Macka, D. Diamond, *Journal of Materials Chemistry* **2008**, 18, 5063.

- [27] R. J. Byrne, S. E. Stitzel, D. Diamond, *Journal of Materials Chemistry* **2006**, *16*, 1332.
- [28] J. D. Winkler, K. Deshayes, B. Shao, *Journal of the American Chemical Society* **1989**, *111*, 769.
- [29] J. Andersson, S. Li, P. Lincoln, J. Andreasson, *Journal of the American Chemical Society* **2008**, *130*, 11836.
- [30] B. I. Ipe, S. Mahima, K. G. Thomas, *Journal of the American Chemical Society* **2003**, *125*, 7174.
- [31] J. Sunamoto, K. Iwamoto, Y. Mohri, T. Kominato, *Journal of the American Chemical Society* **1982**, *104*, 5502.
- [32] M. Ino, H. Tanaka, J. Otsuki, K. Araki, M. Seno, *Colloid and Polymer Science* **1994**, *272*, 151.
- [33] R. Byrne, *Vol. 2010*, Dublin City University, Dublin, **2010**.
- [34] S. Kotha, K. Lahiri, D. Kashinath, *Tetrahedron* **2002**, *58*, 9633.
- [35] S. Gambhir, Massey University, **2006**, unpublished results.
- [36] S. K. Dewan, R. Singh, *Synthetic Communications* **2003**, *33*, 3081.
- [37] V. M. Niemi, P. Knuuttila, J. E. Osterholm, J. Korvola, *Polymer* **1992**, *33*, 1559.
- [38] J. Thyberg, *International Review of Cytology* **1996**, *169*, 183.
- [39] <http://www.faculty.virginia.edu/mcgarveylab/Carbsyn/AminoAcids.html> Mcgarvey, **2010**,
- [40] K. Wagner, R. Byrne, M. Zanoni, S. Gambhir, L. Dennany, R. Breukers, M. Higgins, P. Wagner, D. Diamond, G. G. Wallace, D. L. Officer, *Journal of the American Chemical Society* **2010**, submitted for publication.
- [41] H. Gorner, *Physical Chemistry Chemical Physics* **2001**, *3*, 416.

- [42] L. Angiolini, T. Benelli, L. Giorgini, F. M. Raymo, *Polymer* **2009**, *50*, 5638.
- [43] A. K. Chibisov, H. Gerner, *Chemical Physics* **1998**, *237*, 425.
- [44] K. E. Brancato-Buentello, S.-J. Kang, W. R. Scheidt, *Journal of the American Chemical Society* **1997**, *119*, 2839.

CHAPTER 4. THIOPHENE-BASED OLIGOMER MATERIALS AS A SOURCE OF BIODEGRADABLE CONDUCTING POLYMERS.

4.1 Introduction.

Many bionic applications require novel materials that are multi functional. One desirable combination of functionality would be conductivity and biodegradability.^[1] A conductive biodegradable material could be implanted, used to stimulate cell growth, then degrade and be removed from the body. However the synthesis of a material that is biodegradable and yet remains conductive represents a significant challenge in the design of novel bionic materials.^[2] In this work, biodegradability is referred to as the ability for the bionic implant having fulfilled its role to degrade and be eluted from the organism.

There are many examples of non conductive, naturally occurring, biodegradable polymers,^[3] as well as synthetic biodegradable polymers.^[4] To date, there have been few reports on the investigation of biodegradable conducting polymers. These mainly concentrate on small pyrrole oligomers that erode and can be renally cleared,^[5, 6] or on conductive oligomers linked by nonconjugated degradable segments.^[1, 7, 8]

In previously synthesised biodegradable conducting polymers, conductivity is typically sacrificed for biodegradability.^[2] Thus, the research in this section

investigates materials, which could potentially remain more conductive whilst being biodegradable. A functional biodegradable conducting polymer represents a significant challenge. The polymer needs to remain relatively stable for the period of time whilst it is fulfilling its function, often for a period of weeks, once the polymer has fulfilled its function it needs to break down and be eluted from the organism. The optimum bionic material would incorporate a switch whereby the biodegradability of the material could be turned on once the polymer had fulfilled its function.

Our aim was to synthesise a conducting polymer made up of conjugated units linked by conjugated yet degradable linkers. Our investigation focused on azomethine-linked thiophene oligomers as they are conductive^[9] and unstable under acidic conditions.^[10] The optical properties of azomethine materials have been studied however these materials have not been investigated for bionic applications.^[11] Tailoring the electronic structure of azomethines could be used to control degradation. We thus carried out preliminary studies on azomethine-linked thiophene oligomers and polymers to assess their suitability as biodegradable conducting polymer materials.

Some currently reported degradable conducting polymers are made up of conjugated oligomers linked by degradable linkers.^[2] For the synthesis of degradable conducting polymers made up of oligomer units, longer oligomers give increased conductivity (it has been reported that penta-thiophenes give conductivities of 0.4 S/cm).^[12] We thus investigated the synthesis of sexithiophenes as building blocks for biodegradable conducting polymers. In the process of sexithiophene synthesis, several terthiophene molecules (synthesised in Chapter 3) were brominated. However, it was found that

these brominated terthiophene molecules spontaneously autopolymerised. A review of the literature revealed that there has been some observation of similar behaviour with bromoEDOT monomers^[13-15] and bromopyrroles.^[16, 17] This behaviour has been previously observed with explosive results for 2-bromo-3-alkoxythiophene molecules in our laboratory.^[18] No previous reports of this phenomenon with terthiophene oligomers were found in the literature so we set out to further investigate this phenomenon with respect to terthiophene molecules.

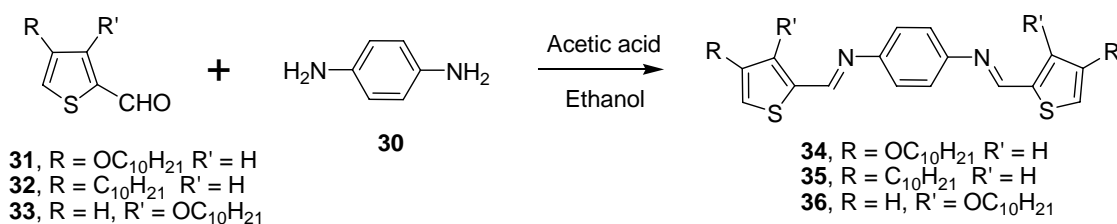
There are many examples in the literature of the synthesis of thiophene oligomers using a multitude of chemistries, each giving oligomers with different functionalities.^[12, 19-23] Here Stille coupling was investigated to give novel terthiophene molecules as precursors to sexithiophenes. Stille coupling reactions are compatible with a wide range of functionalities,^[23, 24] thus terthiophenes containing ester groups were investigated. These terthiophenes did not have alkoxy chains and therefore autopolymerisation was avoided.

4.2 Azomethines.

Polyazomethines are known to be conductive^[9] as well as being unstable under acidic conditions,^[10] making them candidate materials for biodegradable conducting polymers. Incorporating thiophene oligomers into azomethines is known,^[11, 21, 25-29] although their use in bionic applications has not been investigated.

Here several simple thiophene azomethine monomers were prepared for preliminary stability studies. These simple azomethine compounds were synthesised by coupling thiophene aldehyde molecules with *p*-phenylenediamine **30** (Scheme **4.1**). Firstly aldehydes, 4-decoxythiophene-2-carbaldehyde **31**, 3-decoxythiophene-2-carbaldehyde **32** and 4-decylthiophene-2-carbaldehyde **33** were synthesised from the corresponding alkyl and alkoxy thiophenes, by lithiation and treatment with DMF in a similar manner to the synthesis of 4-hexoxythiophene-2-carbaldehyde by Zollner *et al.*^[30] These molecules have long alkyl and alkoxy chains for improving solubility of their corresponding polymers.

Characterisation of the new **31** by ¹H NMR spectroscopy showed the expected aldehyde proton at 9.81 ppm and thiophene proton doublets at 7.41 (H3) and 6.22 (H5) when compared to the spectrum of the similar known 4-hexoxythiophene-2-carbaldehyde.^[30] The ¹H NMR spectra of the new **32** and **33** were also as expected showing aldehyde peaks at 10.01 ppm and 9.87 ppm respectively.



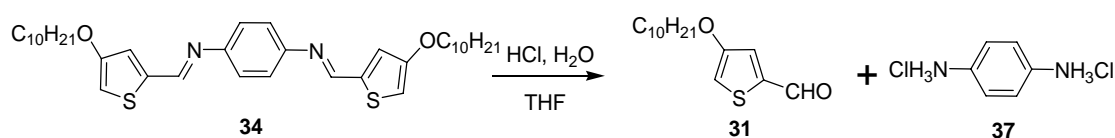
Scheme 4.1.

The azomethine coupling reactions proceeded at room temperature overnight by stirring the reactants in ethanol with a small quantity of acetic acid, which acted as a catalyst.^[31] The colourless reactions changed colour as the yellow products formed indicating azomethine synthesis. Bis((4-decoxythiophen-2-yl)methylene)benzene-1,4-diamine **34**, bis((3-decoxythiophen-2-yl)methylene)benzene-1,4-diamine **35** and bis((4-decylthiophen-2-yl)methylene)benzene-1,4-diamine **36** precipitated from the reactions and were collected by filtration.

These new azomethine compounds are similar to the known bis((thiophen-2-yl)methylene)benzene-1,4-diamine reported by Dubitsky *et al.*, which does not have alkoxy or alkyl substituents.^[32] For bis((4-decoxythiophen-2-yl)methylene)benzene-1,4-diamine **34**, MALDI MS gave the expected mass at 609.4 (MH⁺). The ¹H NMR spectrum did not show an aldehyde peak at 9.81 ppm but contained an azomethine peak at 8.50 ppm, a phenylene proton peak at 7.25 ppm and thiophene proton peaks at 7.14 ppm and 6.44 ppm. The ¹H NMR spectra of bis((3-decoxythiophen-2-yl)methylene)benzene-1,4-diamine **36** contained an azomethine peak at 8.69 ppm and showed doublets with a 5.7 Hz coupling constant for the H4 and H5 thiophene protons. Bis((4-decylthiophen-2-yl)methylene)benzene-1,4-diamine **35** similarly

showed an azomethine peak at 8.55 ppm, although the spectrum differed from that of the alkoxy monomer **34** in that the alkyl proton peak at 2.62 ppm replaced the alkoxy peak at 3.97 ppm.

Azomethine monomers **34**, **35**, and **36** were found to be unstable under acidic conditions. When a drop of HCl was added to a solution of monomer in THF the solution immediately clouded and within 5 minutes the yellow colour of the monomer had disappeared. This degradation is shown in Scheme 4.2 for **34**. It is thought the acid protonates the monomer, the azomethine bond is then hydrolysed and *p*-phenylenediamine dihydrochloride **37** precipitates from solution.



Scheme 4.2.

The degradation of didecoxy monomer **34** shown in Scheme 4.2 was studied in more detail by putting a drop of HCl in a NMR sample dissolved in d_6 -THF. A precipitate formed in the NMR tube that broadened the spectrum, however the degradation was evidenced by the formation of an aldehyde peak at 9.79 ppm. After leaving the NMR sample overnight, it had gone almost colourless and had a white precipitate at the bottom of the tube. The organic and aqueous phases were separated and the breakdown products analysed by ^1H NMR spectroscopy. Figure 4.1 compares the spectrum of monomer **34** with that of the organic extract after degradation and also the aqueous extract. The organic extract ^1H NMR spectrum showed only the peaks corresponding to the aldehyde **31** used to form the azomethine. The ^1H NMR

spectrum of the aqueous extract agreed with the spectrum of *p*-phenylenediamine dihydrochloride **37**.^[33]

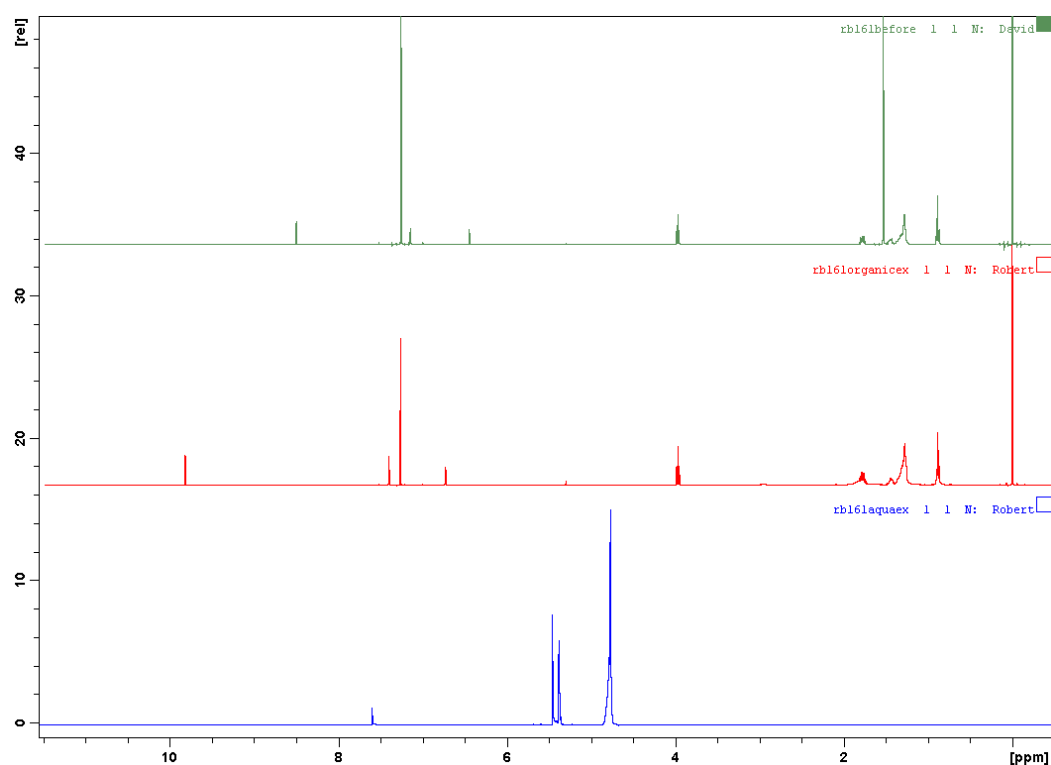
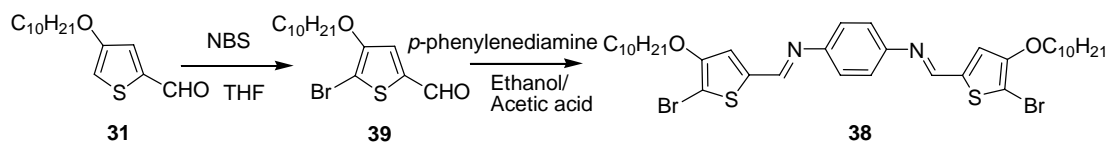


Figure 4.1. ¹H NMR spectra of **34** and its breakdown products after acid hydrolysis. Top, bis((4-decoxythiophen-2-yl)methylene)benzene-1,4-diamine **34**. Middle, organic extract of reaction mixture, which corresponds to the spectrum of aldehyde **31**. Bottom, aqueous extract of reaction mixture, which corresponds to the spectrum of *p*-phenylenediamine dihydrochloride **37** (one phenylene singlet at 7.56 ppm, the peaks at 5.47, 5.38 and 4.78 ppm are due to water and DCM contamination).^[33]

With these promising results offering the potential of degradable azomethine polymers, polymerisations of **34-36** were investigated. The electropolymerisation of azomethine monomers has previously been reported.^[34, 35] Preliminary trials of the electropolymerisation of monomer **34** found it only sparingly soluble in 0.1 M TBAP DCM/acetonitrile electrolyte and no polymer could be grown. The investigation of chemical polymerisation of **34** by iron chloride oxidant in chloroform also gave disappointing results, whereby a brown sludge formed and no polymer could be

isolated. This is consistent with observations by Dubitsky *et al.* for bis((thiophen-2-yl)methylene)benzene-1,4-diamine where a complex between the monomer and the iron salt was observed to form.^[32] An alternative oxidising agent copper *para*-toluenesulfonate was also trialled for polymerisation, however no polymer formed and TLC analysis revealed the monomer had degraded.

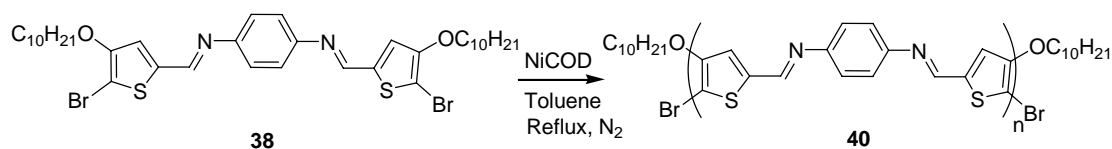
To prevent monomer degradation, a milder polymerisation method was investigated. This method involved a nickel COD catalysed polymerisation of the unknown bis((5-bromo-4-decoxythiophen-2-yl)methylene)benzene-1,4-diamine **38**. Aldehyde starting material **31** was easily brominated by NBS to give 2-bromo-3-decoxythiophene-5-carbaldehyde **39**. Bromination was evidenced by the absence of the H5 thiophene proton peak in the ¹H NMR spectrum (at 6.22 ppm in **31**). Aldehyde **39** was then coupled with *p*-phenylenediamine **30** to give azomethine **38** (Scheme 4.3). The ¹H NMR spectrum of the new compound **38** was similar to that of **34** containing an azomethine peak at 8.42 ppm, a phenylene proton peak at 7.24 ppm and a thiophene proton peak at 7.12 ppm, the main difference being the absence of the H5 peak (6.44 ppm in **34**).



Scheme 4.3.

A nickel COD catalysed polymerisation reaction of **38** was then performed under anhydrous conditions (Scheme 4.4). Poly(bis((4-decoxythiophen-2-

yl)methylene)benzene-1,4-diamine) **40** was isolated and characterised by MALDI mass spectroscopy, which showed that the material was mainly a mixture of short oligomers with peaks at 1373 (2Mer^+), 1979 (3Mer^+), 2586 (4Mer^+), and 3193 (5Mer^+) (Figure 4.2). Typically short chain polymers are unsuitable for processing into uniform films or fibres. Even though this is a promising material, its low molecular weight makes it unsuitable for the fabrication of structures to be used in bionic applications.



Scheme 4.4.

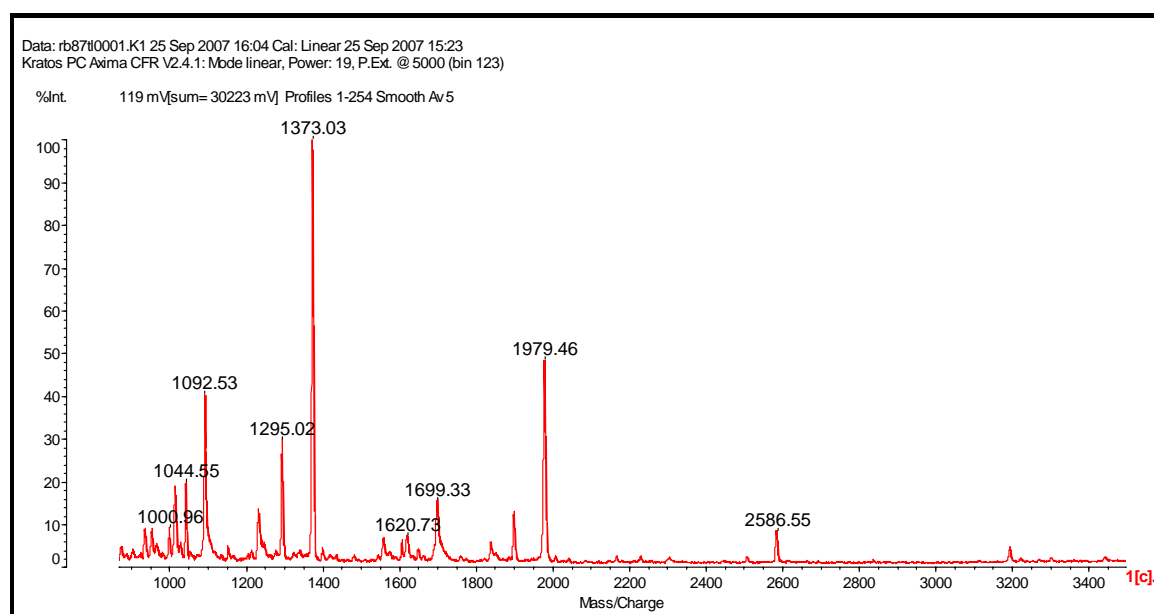
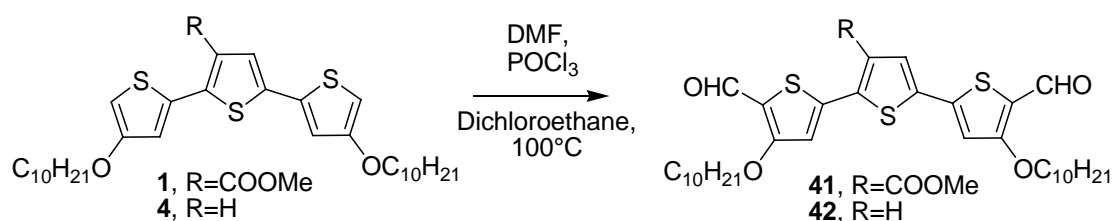


Figure 4.2. MALDI MS spectrum of poly(bis((4-decoxythiophen-2-yl)methylene)benzene-1,4-diamine) **40**. The main peaks at m/z 1373 (2Mer^+), 1979 (3Mer^+), 2586 (4Mer^+), and 3193 (5Mer^+) show the material is oligomeric.

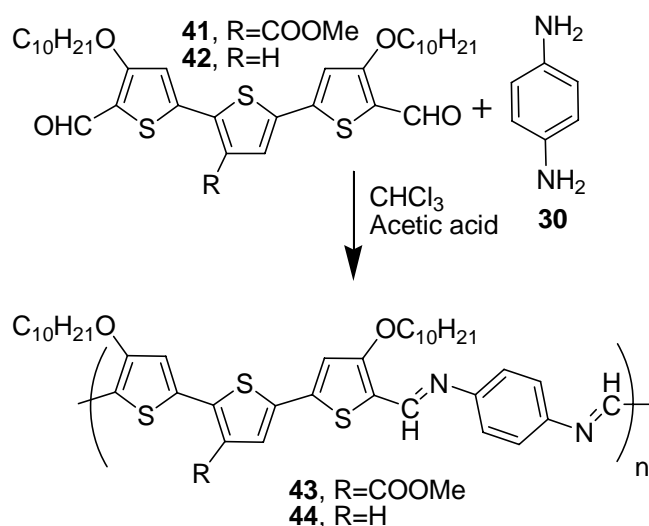
In order to synthesise higher molecular weight azomethine polymers, a polymerisation method involving the coupling of terthiophene dialdehydes and *p*-phenylenediamine **30** was investigated. The coupling of dialdehydes and diamines is a well known method of azomethine synthesis.^[28, 36] Since a range of terthiophene materials containing solubilising alkoxy substituents had previously been synthesised in Chapter **3**, it was hoped these would give soluble azomethine polymers when functionalised as aldehydes and coupled with *p*-phenylenediamine **30**.

Terthiophene dialdehydes, methyl 5,5''-diformyl-4,4''-didecoxy-2,2':5',2''-terthiophene-3'-carboxylate **41** and 5,5''-diformyl-4,4''-didecoxy-2,2':5',2''-terthiophene **42** were synthesised from terthiophenes **1** and **4** using Vilsmeier conditions (Scheme **4.5**). ¹H NMR spectroscopy confirmed the synthesis of the aldehydes, the spectrum of **42** had an aldehyde peak at 9.98 ppm and the aromatic thiophene peak at 6.12 ppm attributed to the C5,5'' protons in the terthiophene starting material **4** had disappeared. Similarly, the ¹H NMR spectrum of the unsymmetrical ester **41** showed peaks at 10.03 ppm and 9.99 ppm corresponding to aldehyde protons, replacing the peaks at 6.33 ppm and 6.16 ppm of the C5,5'' protons of **1**.



Scheme **4.5**.

Polymerisation of monomers **41** and **42** with *p*-phenylenediamine **30** was carried out in chloroform using acetic acid as a catalyst (Scheme 4.6). This yielded poly((methyl 5,5'-dimethylene -4,4''-didecoxy-2,2':5',2''-terthiophene-3'-carboxylate)benzene-1,4-diamine) **43** as a insoluble purple solid. Likewise poly((5,5'-dimethylene -4,4''-didecoxy-2,2':5',2''-terthiophene)benzene-1,4-diamine) **44** was synthesised and also found to be insoluble. The alkoxy chains in these polymers were clearly insufficient to solubilise these longer chain polymers.



Scheme 4.6.

The insoluble azomethine polymers **43** and **44** could not be processed, therefore producing films for degradability studies posed a challenge. The synthesis of azomethine films has been reported by Zotti *et al.* who used a layer-by-layer method involving sequential dipping of an aldehyde functionalised surface in diamine and dialdehyde solutions.^[25] Inspired by this layer-by-layer method, we sought to

investigate solid phase azomethine film synthesis. Preliminary experiments showed that polymer films could be produced, by casting an aldehyde **41** and *p*-phenylenediamine **30** mixture onto a substrate and allowing them to react. Polymerisation happened spontaneously overnight but the process could be accelerated by exposing the monomer film to acetic acid vapour. Spin coating the monomer mixture onto ITO glass substrates resulted in apparently uniform poly((methyl 5,5'-dimethylene -4,4''-didecoxy-2,2':5',2''-terthiophene-3'-carboxylate)benzene-1,4-diamine) **43** films.

These polymer **43** films were characterised by cyclic voltammetry to analyse their electrochemistry (Figure **4.3**). Both the non-acid catalysed and acid catalysed polymer films show an electroactive capacitive response typical for this class of materials,^[25, 29] the film exposed to acid vapour had an earlier onset of oxidation at 0.3 V compared to the non catalysed film, which had an onset of oxidation at 0.4 V indicating it was more electroactive, possibly with a greater degree of polymerisation. The non catalysed film also had a small peak at 0.6 V, which was not observed in the acid catalysed film and that could be indicative of unpolymerised monomer or short oligomers.

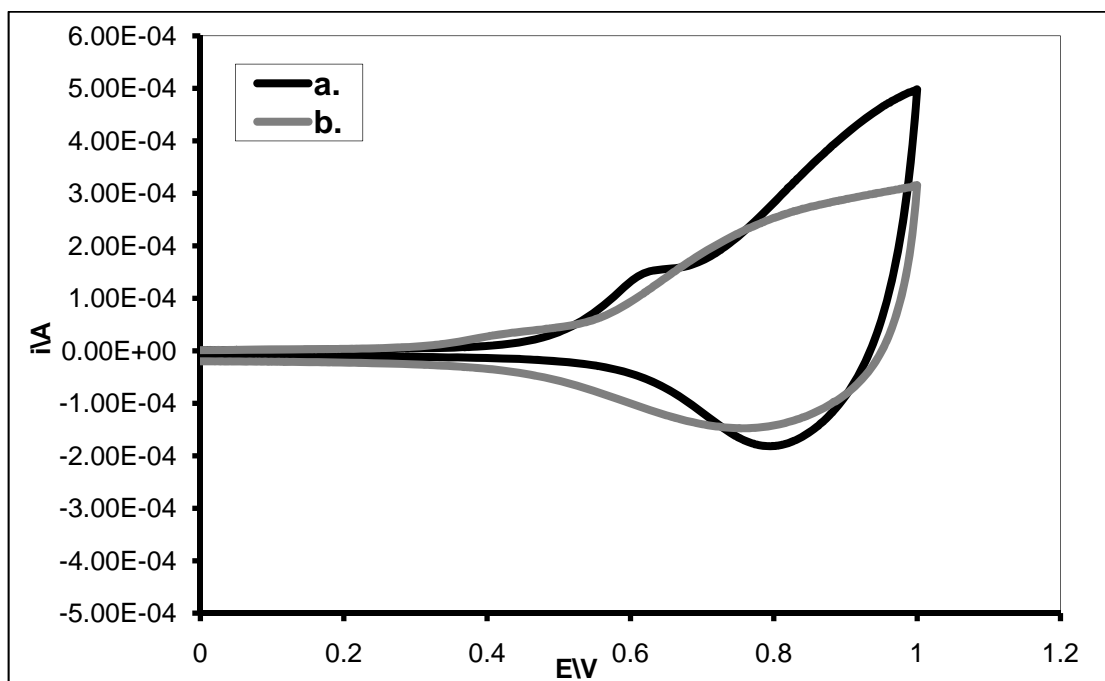


Figure 4.3. CV's showing the electrochemistry of azomethine films on ITO glass in 0.1 M TBAP acetonitrile electrolyte at 50 mV/s scan rate. **a.** Non-acid catalysed azomethine **43** film. **b.** Acid catalysed azomethine **43** film.

The degradation of an acid catalysed azomethine **43** polymer film on ITO glass was studied by UV-visible spectroscopy. This degradation study was carried out by placing the film in a THF solution containing 2 drops of HCl. The UV-visible absorbance spectrum (Figure 4.4) showed some interesting results. Initially the film had an absorbance peak at 500 nm but upon addition of acid, the spectrum immediately changed to give a peak at 600 nm with two shoulders, this absorbance change is presumably due to the protonation of the material. The protonation of a thiophene-based poly(azomethine) has previously been reported by Wang *et al.* who observed a shift in λ_{max} from 457 nm to 638 nm upon addition of acid.^[29] Wang *et al.* did not report any degradation of their material. For our polymer the intensity of the absorbance peak at 600 nm reduced over time and a small peak at 400 nm grew

and after approximately 7 hours the film was almost totally degraded. No insoluble material was left after 7 days.

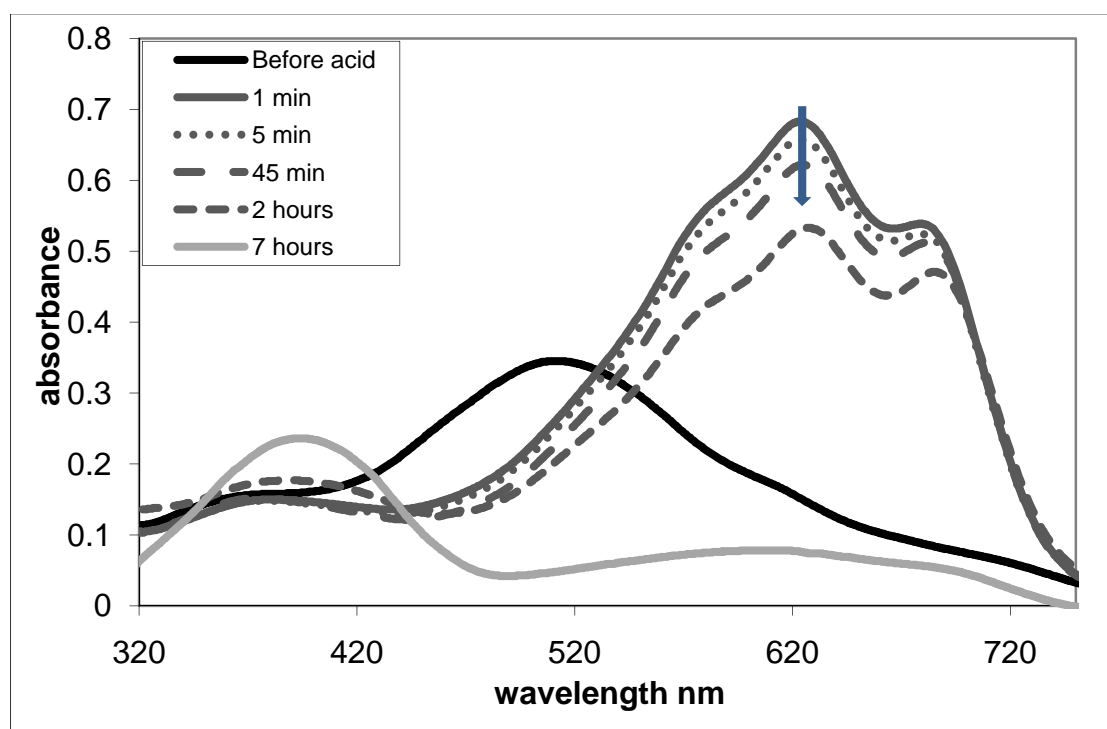


Figure 4.4. UV-visible absorption spectra of an acid catalysed azomethine **43** polymer film in acidic THF, showing the change in the spectra from before the acid was added to 7 hours after acid addition, illustrating film degradation. The arrow indicates the direction of the change in absorbance over time.

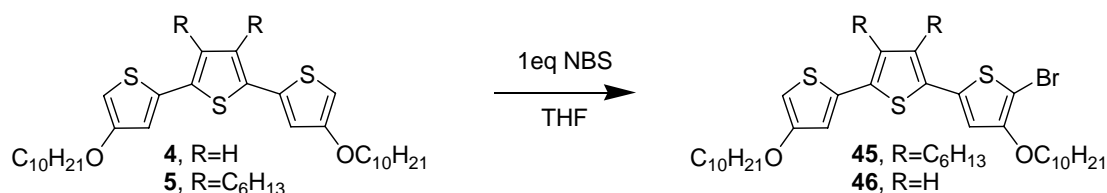
The preliminary degradation result in acidic THF was encouraging; however the degradability of the polymer in aqueous conditions is of more importance. A polymer **43** film was placed in pH 7.3 phosphate buffer, at this pH the film was stable for several weeks with no change observed in the UV-visible spectrum. A polymer **43** film was then placed into a dilute HCl solution (pH 1). The film was observed to undergo protonation and change colour from purple/red to blue/green similar to the initial change observed in acidic THF, however the film was still present after 2 weeks. It is speculated that the polymer **43** film does not degrade in aqueous solutions due to the insolubility of any breakdown products.

This research has identified thiophene-based azomethines as being promising electroactive, degradable materials, and has also identified many challenges to the application of these materials in bionics. Improvement of the electronic properties requires longer thiophene dialdehyde oligomers. For bionic applications soluble, processable materials that can easily be processed are required. These materials also need to be functionalised with hydrophilic groups to improve their wettability and interaction with biological environments. The breakdown products should be water soluble and non toxic. Azomethine degradation requires acidic conditions, materials could be tailored to degrade in the acidic lysosome within cells, which has an internal pH of approximately 4.5.^[37] Azomethine materials will require a great deal more investigation and optimisation before they can be applied to bionic applications.

4.3 Autopolymerisation.

In an effort to synthesise sexithiophenes as precursors for degradable conducting polymers, terthiophene materials **4** and **5** synthesised in Chapter 3 were brominated. These brominated terthiophene molecules spontaneously polymerised. This polymerisation was termed autopolymerisation as the monomers polymerised without the addition of any oxidant or catalyst. As noted in the introduction to this chapter several researchers have observed similar behaviour with bromopyrroles^[16, 17] and bromoEDOT monomers.^[13-15] As there has not been any previous reports of this phenomenon with terthiophene oligomers this was investigated further.

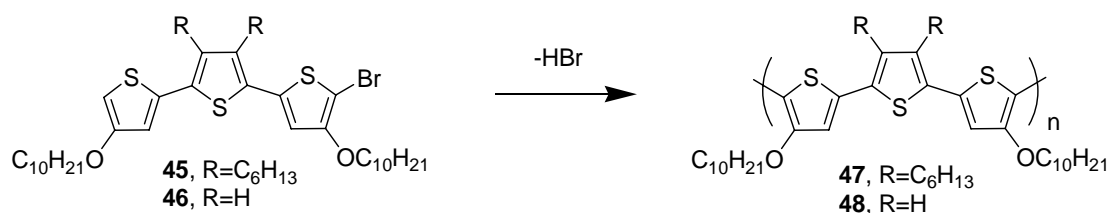
The bromination of terthiophene monomers **4** and **5** by 1 equivalent of NBS in THF was investigated (Scheme 4.7). Monomers 5-bromo-3',4'-dihexyl-4,4''-didecoxy-2,2':5',2''-terthiophene **45** and 5-bromo-4,4''-didecoxy-2,2':5',2''-terthiophene **46** were intended as precursors for sexithiophene synthesis.



Scheme 4.7.

These bromination reactions proved challenging, with much difficulty encountered in isolating pure **45** and **46**. The phenomenon of autopolymerisation was first observed when terthiophene **45** was left overnight as a neat oil. In the morning the oil had polymerised and evolved HBr as evidenced by a white gas over the resulting

poly(3',4'-dihexyl-4,4''-didecoxy-2,2':5',2''-terthiophene) **47** (Scheme 4.8). During the synthesis of monomer **46**, the crude monomer polymerised to poly(4,4''-didecoxy-2,2':5',2''-terthiophene) **48** whilst the solvent was being removed at 40°C on a rotary evaporator.



Scheme 4.8.

GPC was used to determine the molecular weight of these polymers, polymer **47** had a molecular weight of 13 kDa with a polydispersity of 2.1 (chemically polymerised polymer **47** in the literature has been reported with a molecular weight of 91 kDa),^[38] polymer **48** had a molecular weight of 12 kDa with a polydispersity of 3.4 (polymer **48** has been reported in the literature but was polymerised electrochemically).^[39] A solution of polymer **48** in chloroform was analysed by UV-visible spectroscopy (Figure 4.5), spectra were taken both in the reduced form and in the oxidised form after addition of copper perchlorate solution in acetonitrile (1 drop). The spectrum showed a peak at 540 nm in the reduced form typical of terthiophene based polymers and a free carrier tail in the oxidised form.^[38]

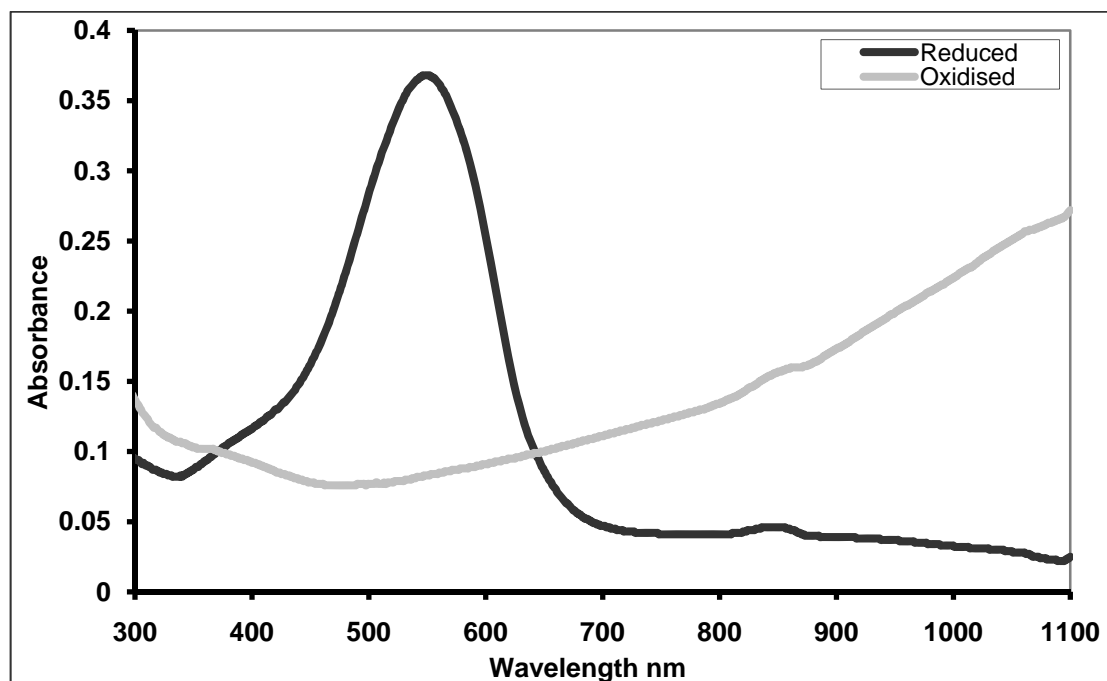


Figure 4.5. UV-visible spectrum of polymer **48** in reduced and oxidised forms.

To prevent autopolymerisation in subsequent reactions more care was taken not to expose the products to heat or leave neat oils at room temperature. Unfortunately, the isolation of pure **45** and **46** remained a challenge, although reactions were performed in a range of solvents (CHCl_3 /acetic acid, THF and DMF) at room temperature and 0°C . In all cases, NMR spectra of the reaction mixtures showed several peaks corresponding to the starting materials **4** and **5**, the monobromoterthiophene products **45** and **46** and also dibromoterthiophenes. This was confirmed by MALDI MS, which showed for **46**, for example, peaks at 560 (M^+ **4**), 639 (M^+ **46**) and 718 (M^+ 5,5''-dibromo-4,4''-didecoxy-2,2':5',2''-terthiophene).

If the phenomenon of autopolymerisation could be controlled, it could be used as a convenient method for polymer synthesis. The phenomenon was investigated in more detail, further bromo-terthiophene **46** was synthesised, carefully isolated and stored

at -20C to prevent polymerisation, ¹H NMR spectroscopy of this monomer showed that it was 90% pure containing traces of **4** and 5,5''-dibromo-4,4''-didecoxy-2,2':5',2''-terthiophene. The effects of heat and HBr on monomer **46** were then studied as these were identified as two potential triggers for autopolymerisation. Three lots of 20 mg monomer **46** in 10 mL chloroform were taken and treated with different conditions, stirring at room temperature, stirring at reflux and stirring with one drop of HBr added. It was observed that adding a drop of HBr to the solution resulted in the solution darkening and thus polymerising more rapidly than stirred and heated solutions. However, over a period of 12 hours, all three solutions darkened. GPC analysis was conducted on the polymers, whilst the stirred and heated solution had polymers with molecular weights of only 2 kDa the solution with the added HBr had a polymer with a molecular weight of 12.3 kDa.

The phenomenon of autopolymerisation was an interesting complication to the synthesis of sexithiophene oligomers, resulting in reasonable molecular weight polymers. A mechanism for autopolymerisation of 2-bromo-3-alkoxythiophenes has been proposed by Dr Pawel Wagner,^[18] this is shown below in Figure 4.6. In this mechanism, the polymerisation is initiated by acid protonating the alkoxy group adjacent to the bromine, the monomer is then able to rearrange and eliminate HBr and the original proton. Our studies agreed with this mechanism whereby autopolymerisation was promoted by HBr.

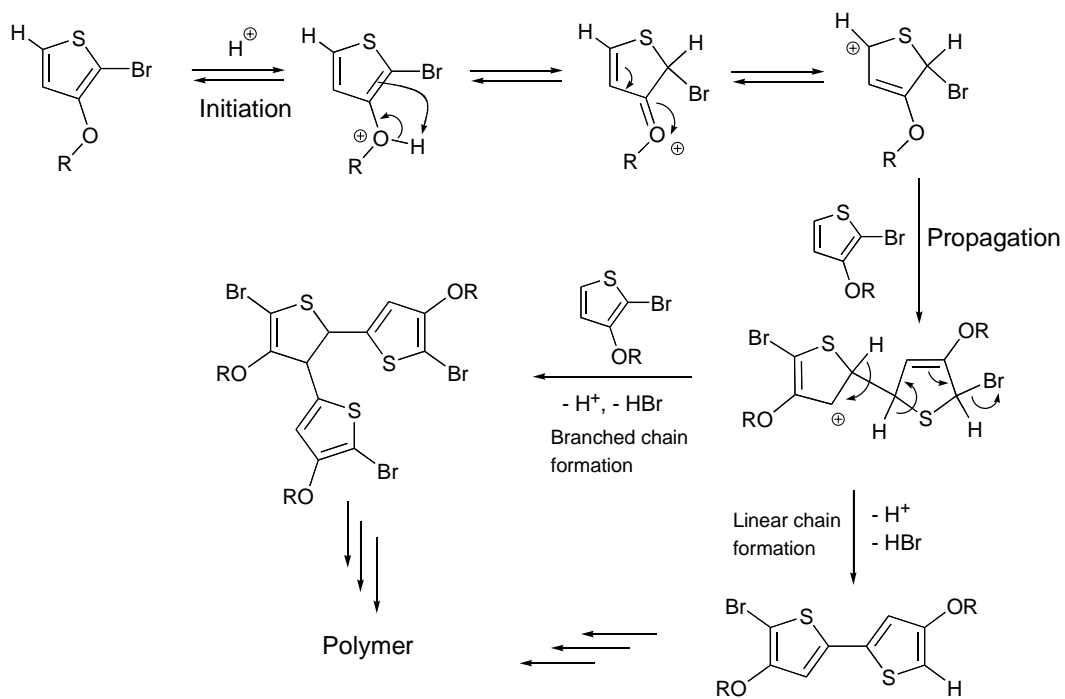


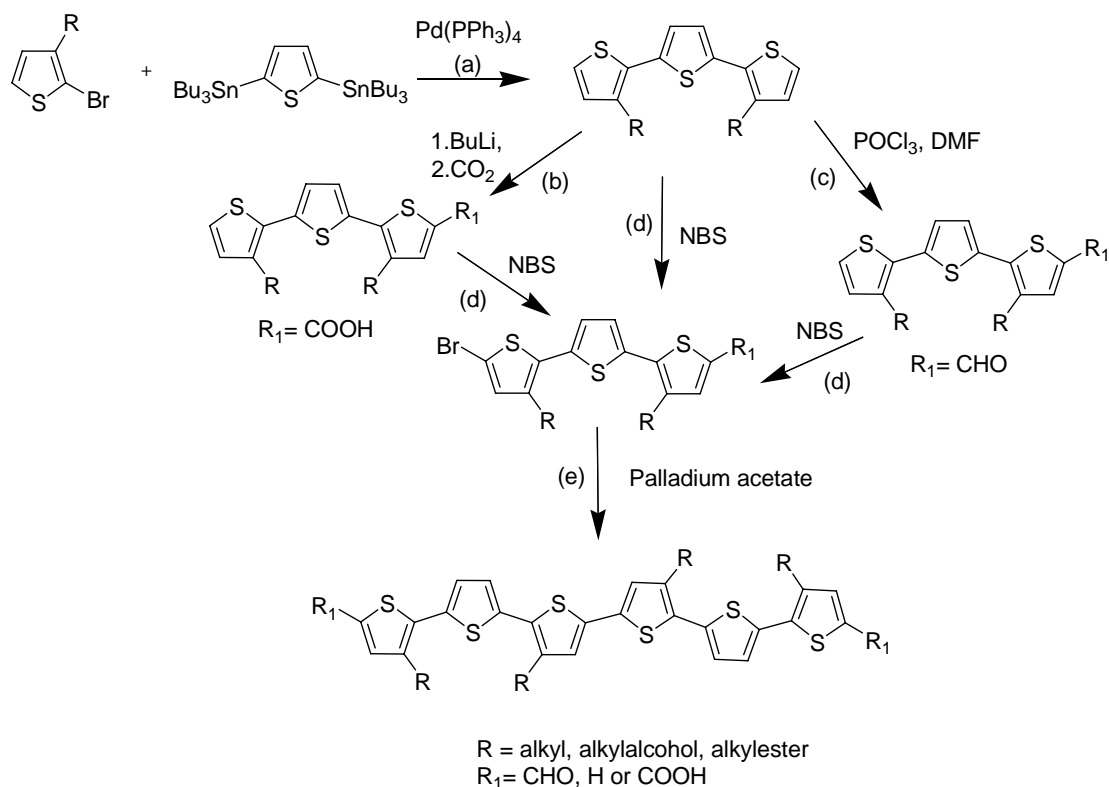
Figure 4.6. Proposed mechanism for the autopolymerisation of 2-bromo-3-alkoxythiophenes, courtesy of Dr Pawel Wagner.^[18]

4.4 Thiophene oligomers.

Our aim was to synthesis oligomers that could be used as precursors to the synthesis of biodegradable conducting polymers. One challenge, which was identified in the studies of azomethines, was the use of longer oligomers to improve the conductivity of the resulting polymer (thiophene oligomers with greater than 5 thiophene units are known to have conductivities of the order of 0.4 S/cm).^[12, 40] As our research group has had much experience with the synthesis of terthiophenes,^[38, 39, 41] we aimed to synthesise sexithiophene oligomers by coupling together two terthiophene monomers. The autopolymerisation of the bromoalkoxyterthiophenes (Section 4.3) made them unsuitable precursors for sexithiophene synthesis. Here, the synthesis of terthiophene molecules without alkoxy chains as precursors for sexithiophene synthesis was investigated.

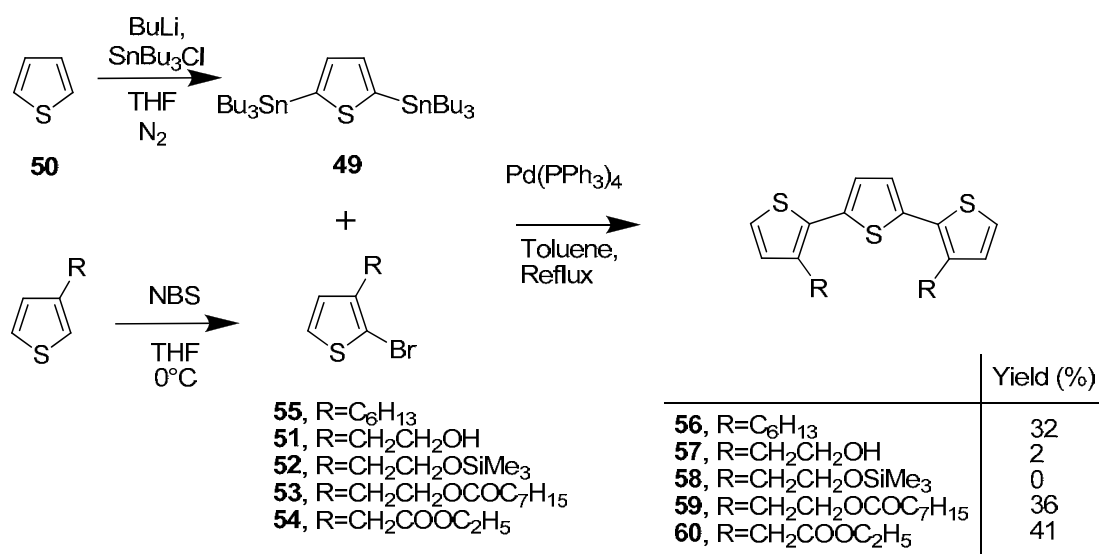
There are many examples in the literature of the synthesis of thiophene oligomers using a multitude of chemistries, each giving oligomers with different functionalities.^[12, 19-23] Whilst researching thiophene-based azomethine materials (Section 4.2), we identified that hydrophilic materials with functionalities that improve the wettability of the polymer and the solubility of any breakdown products are important for bionic applications. We thus set out to synthesise alcohol and acid functionalised oligomer materials to be used as precursors to biodegradable conducting polymers. Here, a method using a Stille coupling was investigated as this reaction is known to be compatible with functionalities such as alcohols and esters.^[23, 24]

The route we proposed for the synthesis of functionalised oligomers is shown below in Scheme 4.9. We proposed to synthesise the base terthiophenes by Stille coupling as indicated by (a) in Scheme 4.9, incorporating a range of functional groups (R) such as hexyl chains (as a simple test compound), an alkylalcohol functionality, and ester functionalities that can be later cleaved to give hydrophilic materials. In the case of the carboxylation, the alcohol functionality needed to be protected by a TMS protecting group. We aimed to end-functionalise these terthiophenes with carboxyl (b, $R_1 = \text{COOH}$) and aldehyde (c, $R_1 = \text{CHO}$) functional groups as well as leave the materials unfunctionalised ($R_1 = \text{H}$). The terthiophenes would then be brominated by NBS (d), and coupled using a palladium acetate catalyst (e) to give sexithiophenes. These sexithiophenes could be used as precursors to degradable conducting polymers.



Scheme 4.9.

The starting materials for terthiophene synthesis by Stille coupling were synthesised as shown in Scheme 4.10. 2,5-Bis(tributylstannyl)thiophene **49** was prepared from thiophene **50** by the procedure of Hou *et al.*^[42] and was obtained after vacuum distillation in 55% yield (lit.^[42] 53%). The various 2-bromothiophene starting materials that were needed later (as outlined below) were synthesised by bromination of the corresponding thiophenes with NBS. These bromination reactions generally went in good yields compared to the literature (Table 4.1).



Scheme 4.10.

Table 4.1. A comparison of the yields for 2-bromothiophene starting materials compared to literature yields.

Compound.	Yield.	Lit. yield.
2-(2-Bromothiophen-3-yl)ethanol 51	77%	98% ^[43]
(2-(2-Bromothiophen-3-yl)ethoxy)trimethylsilane 52	96%	92% ^[44]
2-(2-Bromothiophen-3-yl)ethyl octanoate 53	83%	-
Ethyl 2-(2-bromothiophen-3-yl)acetate 54	53%	88% ^[45]
2-Bromo-3-hexylthiophene 55	87%	81% ^[46]

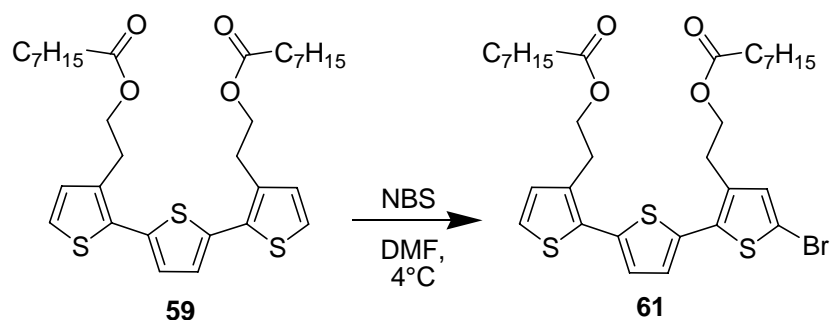
The lower yield of ethyl 2-(2-bromothiophen-3-yl)acetate **54** when compared to the literature is due to this monomer being synthesised in two steps (bromination and esterification) from 3-thiophene acetic acid also before purification. 2-(2-Bromothiophen-3-yl)ethyl octanoate **53** has not been previously reported ¹H NMR of this compound showed thiophene proton doublets at 7.21 ppm (H5) and 6.98 ppm (H4), which were as expected when compared to the spectrum of the similar 2-(2-bromothiophen-3-yl)ethyl acetate.^[47]

As a model reaction, the alkyl thiophene **55** was coupled to **49** using a Pd catalyst to give 3,3''-dihexyl-2,2':5',2''-terthiophene **56**, which had previously been made by a Kumada coupling reaction that was unsuitable for ester functionalised derivatives.^[21] Using this Stille method, the yield was substantially lower (32%) (lit.^[21] 94%) but sufficient to explore further couplings. The ¹H NMR spectrum of **56** agreed with the literature showing aromatic thiophene peaks at 7.17, 7.05 and 6.93 ppm. The synthesis of 2,2':5',2''-(terthiophene-3,3''-yl)ethanol **57** gave a much lower yield of 2% primarily due to difficulties in purification causing a loss of product. In an effort to overcome the purification difficulties experienced in the synthesis of **57**, the synthesis of TMS protected 2,2':5',2''-(terthiophene-3,3''-yl)ethoxy)trimethylsilane **58** was undertaken (the TMS group was also needed to protect the alcohol functionality in subsequent reactions). The synthesis of TMS protected **58** was similarly unsuccessful, with the acid sensitive TMS groups deprotecting during washing of the product even with mildly acidic ammonium chloride. Therefore the use of esters was investigated.

The synthesis of terthiophene esters 2,2':5',2''-(terthiophene-3,3''-diyl)bis(ethane-2,1-diyl) dioctanoate **59** and diethyl 2,2':5',2''-(terthiophene-3,3''-diyl) diacetate **60** were synthesised in yields of 36% and 41% respectively, and although these yields were low, they were deemed reasonable enough to give the required polymers.

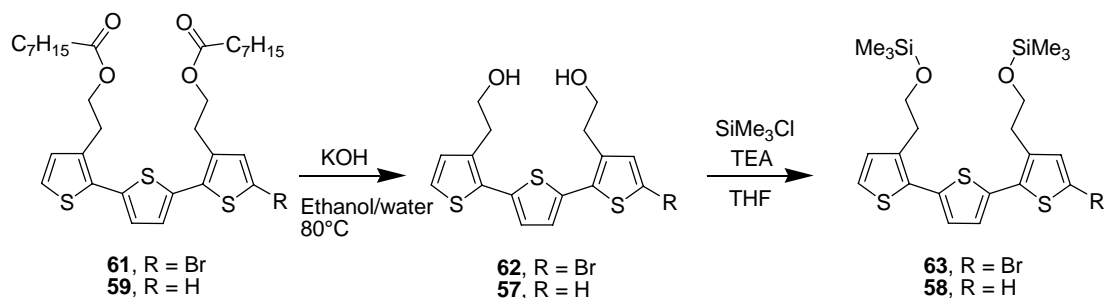
MALDI MS of terthiophene **59** gave a mass of 589, which was as expected for MH^+ and the 1H NMR spectrum showed 3 aromatic proton peaks at 7.21, 7.10 and 6.98 ppm, similar to terthiophene **56**. The 1H NMR spectrum of terthiophene **60** analogously had proton peaks at 7.24, 7.15 and 7.06 ppm.

Given our experience in this research program with thienyl esters, we decided to focus on dioctanoate **59**. This terthiophene has ester functionality similar to that of the materials discussed in Chapter 5, which makes the molecule organic solvent soluble and processable whilst allowing hydrolysis to more hydrophilic materials that are desirable for bionic applications. As outlined in Scheme 4.9, the terthiophenes needed to be brominated before they could be coupled to form sexithiophenes. The bromination of terthiophene **59** was carried out by NBS (Scheme 4.11). 5-Bromo-2,2':5',2''-(terthiophene-3,3''-diyl)bis(ethane-2,1-diyl) dioctanoate **61** was synthesised in 84% yield and characterised by 1H NMR spectroscopy. Adding the bromine broke the symmetry in the terthiophene and thus 5 aromatic proton peaks are now observed at 7.23, 7.09, 7.05, 6.98 and 6.95 ppm.



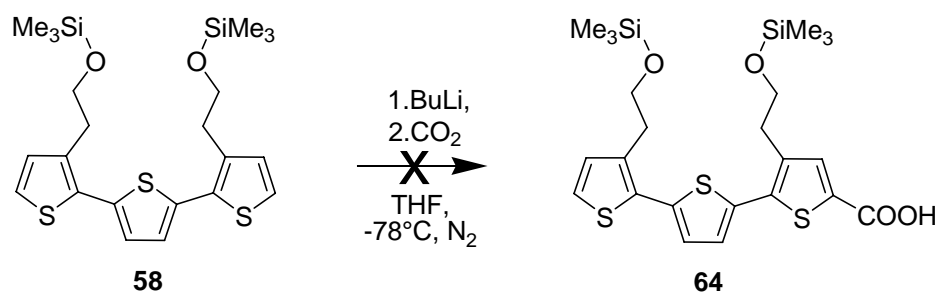
Scheme 4.11.

Since the ester functionality in **59** is susceptible to attack by butyl lithium, we needed to introduce a suitable protecting group such as TMS before a carboxyl group could be added, first hydrolysing the ester. Treatment of both unsubstituted ester **59** and brominated ester **61** with potassium hydroxide gave the alcohols, 2,2':5',2''-(terthiophene-3,3''-yl)ethanol **57** and 5-bromo-2,2':5',2''-(terthiophene-3,3''-yl)ethanol **62** (Scheme 4.12). These alcohols were then protected by treatment with trimethylsilyl chloride giving 5-bromo-2,2':5',2''-(terthiophene-3,3''-yl)ethoxy)trimethylsilane **63** and 2,2':5',2''-(terthiophene-3,3''-yl)ethoxy)trimethylsilane **58** in 95% and 97% yields respectively. This protection was followed by ^1H NMR, where the broad OH peaks at 1.8 ppm (for **57**) and 2.05 ppm (for **62**) disappeared and a peak at 0.07 ppm was observed for the trimethylsilyl protons.



Scheme 4.12.

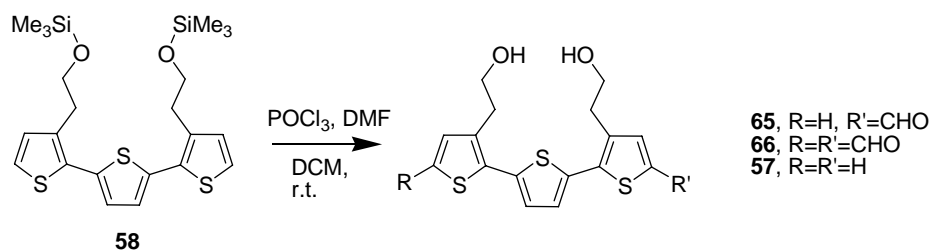
The introduction of a carboxyl group to the terminal position of terthiophene **58** was investigated, so that it could be used as a precursor for an ester-linked biodegradable polymer. Terthiophene **58** was treated with 1 equivalent of *n*-butyllithium and carbon dioxide was then bubbled through the reaction (Scheme 4.13). This reaction was unsuccessful and no 2,2':5',2''-(terthiophene-3,3''-yl)ethoxy(trimethylsilane)-5-carboxylic acid **64** was obtained with some starting material **58** recovered. The sensitive nature of reaction involving butyl lithium makes them difficult on small scales as a small amount of water will destroy the generated anion.



Scheme 4.13.

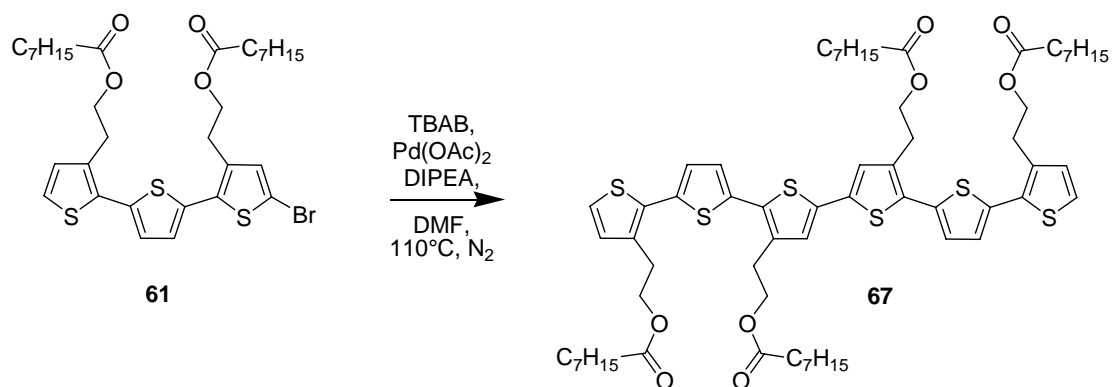
With the failure to introduce a carboxyl functionality, the synthesis of a 5-formyl-2,2':5',2''-(terthiophene-3,3''-yl)ethoxy(trimethylsilane) was undertaken.

Terthiophene **58** was treated under Vilsmeier conditions (Scheme **4.14**). The reaction gave a mixture of products. MALDI MS showed masses of 364 (M^+) indicative of 5-formyl-2,2':5',2''-(terthiophene-3,3''-yl)ethanol **65**, 392 (M^+) for 5,5''-diformyl-2,2':5',2''-(terthiophene-3,3''-yl)ethanol **66** and 336 (M^+) for the unsubstituted 2,2':5',2''-(terthiophene-3,3''-yl)ethanol **57**. The TMS protecting groups were hydrolysed by the acidic reaction conditions such that the mixture of products could not be purified by column chromatography. Consequently, it was decided to form the sexithiophene before hydrolysis of the ester groups so the synthesis of the ester functionalised sexithiophene, 2,2':5',2'': 5'',2''': 5''',2''''': 5''''',2'''''' - (sexithiophene-3,3'',4''',3''''')-tetrayl)tetrakis(ethane-2,1-diyl) tetraoctanoate **67** was investigated (Scheme **4.15**).



Scheme **4.14**.

Bromoterthiophene **61** was coupled by palladium acetate catalysis (Scheme **4.15**) to give sexithiophene **67** in 27% yield. The synthesis of **67** was confirmed by MALDI MS, which gave 1175 as the expected mass of M^+ . The ^1H NMR spectrum of this symmetrical sexithiophene showed the expected 5 aromatic proton peaks at 7.23, 7.14, 7.12, 7.05 and 6.99 ppm, as well as the expected signals for the side chains.



Scheme 4.15.

To investigate the ability of these oligothiophene materials to be electrochemically polymerised, we studied the polymerisation of terthiophene **59**. Growth of a poly(2,2':5',2''-(terthiophene-3,3''-diyl)bis(ethane-2,1-diyl) dioctanoate) (PTBEO) film on an ITO glass substrate was investigated by cyclic voltammetry (Figure 4.7). Here a 20 mmol/L monomer solution in 0.1M TBAP acetonitrile electrolyte was used, and the onset of monomer oxidation was observed to be at 0.7 V. PTBEO films grown at constant potential of 0.8 V for 40 seconds showed even coverage of the ITO glass electrode and appeared very smooth. The post CV (Figure 4.8) of such a PTBEO film showed an onset of polymer oxidation at 0.25 V and gave a capacitive response, typical of an electroactive polythiophene. Interestingly this CV showed two oxidation peaks. This could be due to side chain interactions resulting in some segments of the polymer backbone being oxidised preferentially.

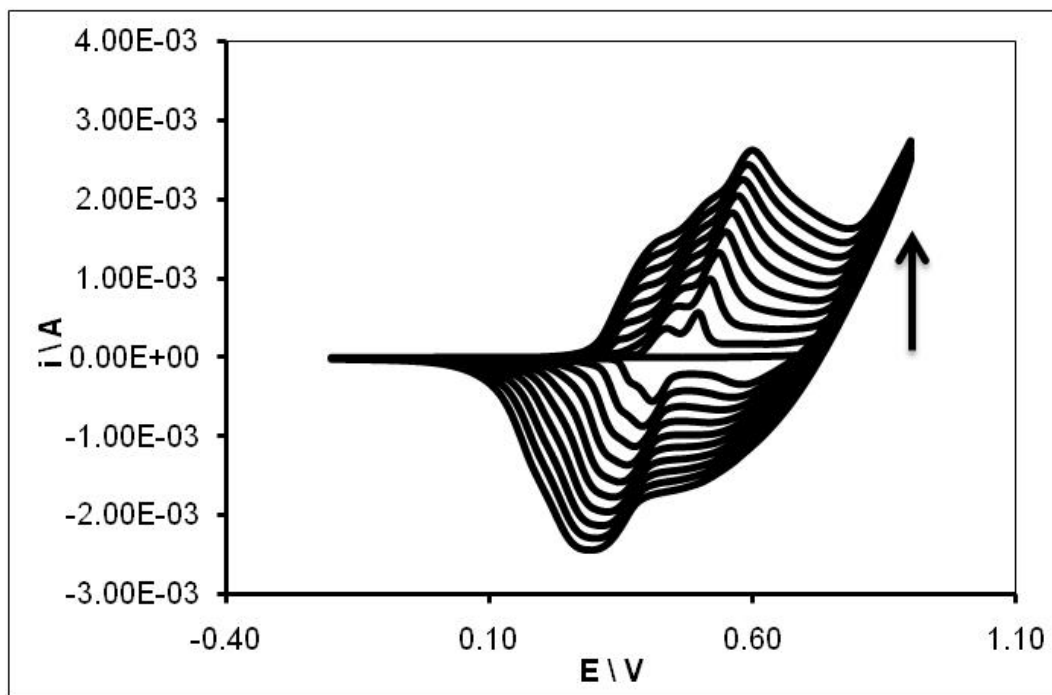


Figure 4.7. Cyclic voltammetric growth of PTBEO on a 1 cm² ITO glass electrode, scan rate 50 mV/s. The arrow indicates the growth in current with subsequent scans.

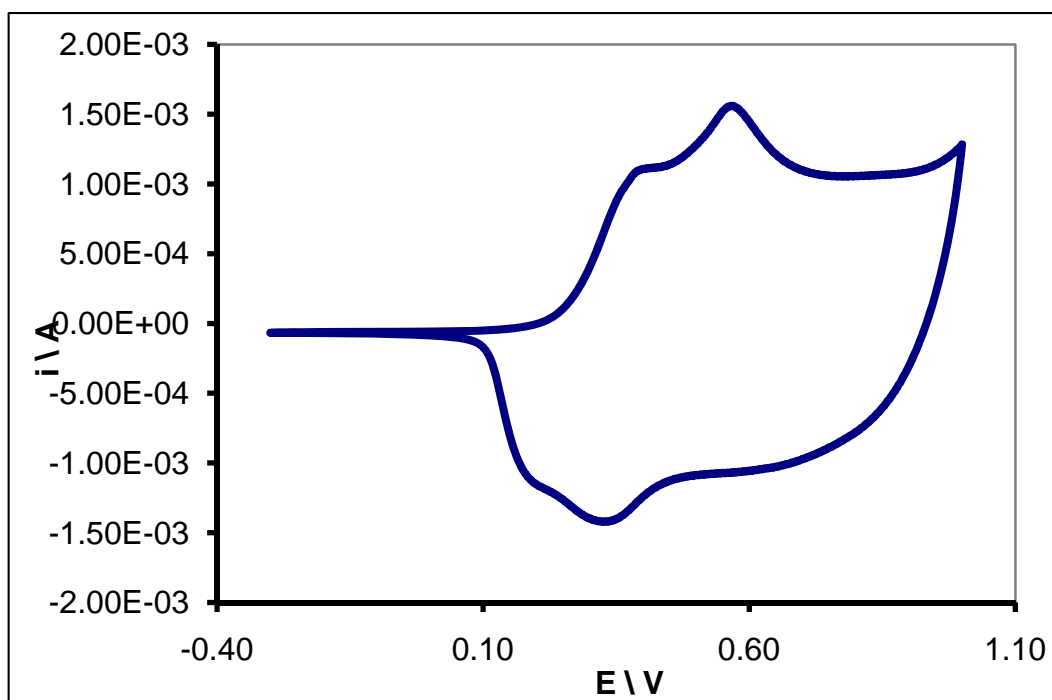


Figure 4.8. Post growth CV of PTBEO film grown at constant potential, scan rate 50 mV/s, -0.3 V to 1.0 V.

Time did not allow us to investigate the electropolymerisation of the analogous sexithiophene **61** or continue further synthetic work in this area. However, the thiophene-oligomers containing ester functionalities, synthesised in this work will make promising building blocks for biodegradable conducting polymers. From this research we have learned a lot about the chemistries involved in the synthesis of thiophene-oligomers. This knowledge will help other researchers within our laboratories to continue this research in the future.

4.5 Conclusions.

Here novel thiophene oligomer materials for bionic applications have been investigated. The incorporation of linkers into these materials to make them biodegradable was investigated to make the materials more suitable for *in vivo* applications. Several azomethine linked thiophene oligomer materials were synthesised. Preliminary results showed these azomethines are unstable under acidic conditions but stable in physiological conditions such as cell culture media. There remains the possibility of tailoring these materials to be degraded in the lysosome, which has an internal pH of 4.5. However, for this to occur, the polymer structure would need to bioerode and be targeted to this inter cellular compartment.

The synthesis of novel thiophene oligomers was also investigated, with sexithiophenes being of particular interest. The bromination of terthiophene molecules **4** and **5** resulted in autopolymerisation. This unforeseen complication was studied in more detail as a method of polymer synthesis. Our observations that autopolymerisation is activated by HBr and occurs much faster with neat monomer agree with a mechanism previously proposed for the autopolymerisation of 2-bromo-3-alkoxythiophenes.^[18]

Several novel terthiophene molecules were synthesised by a Stille coupling method. The terthiophene ester **59** was of particular interest for bionic applications. Further functionalisation of **59** was investigated however this was relatively unsuccessful and more investigation is needed to develop this as a precursor to biodegradable polymers. The terthiophene material **59** was successfully dimerised to create a sexithiophene **67**.

4.6 References.

- [1] T. J. Rivers, T. W. Hudson, C. E. Schmidt, *Advanced Functional Materials* **2002**, *12*, 33.
- [2] N. K. Guimard, N. Gomez, C. E. Schmidt, *Progress in Polymer Science* **2007**, *32*, 876.
- [3] D. W. Hutmacher, J. C. Goh, S. H. Teoh, *Annals of the Academy of Medicine, Singapore* **2001**, *30*, 183.
- [4] M. Martina, D. W. Hutmacher, *Polymer International* **2007**, *56*, 145.
- [5] G. Shi, M. Rouabhia, Z. Wang, L. H. Dao, Z. Zhang, *Biomaterials* **2004**, *25*, 2477.
- [6] G. Shustak, M. Gadzinowski, S. Slomkowski, A. J. Domb, D. Mandler, *New Journal of Chemistry* **2007**, *31*, 163.
- [7] L. Huang, J. Hu, L. Lang, X. Wang, P. Zhang, X. Jing, X. Wang, X. Chen, I. Lelkes Peter, G. MacDiarmid Alan, Y. Wei, *Biomaterials* **2007**, *28*, 1741.
- [8] N. K. Guimard, J. L. Sessler, C. E. Schmidt, *Materials Research Society Symposium Proceedings* **2007**, *950E*, No pp given.
- [9] C. R. Hauer, G. S. King, E. L. McCool, W. B. Euler, J. D. Ferrara, W. J. Youngs, *Journal of the American Chemical Society* **1987**, *109*, 5760.
- [10] M. Grigoras, O. Catanescu, C. I. Simionescu, *Revue Roumaine de Chimie* **2002**, *46*, 927.
- [11] S. Destri, I. A. Khotina, W. Porzio, C. Botta, *Optical Materials (Amsterdam)* **1998**, *9*, 411.
- [12] A. Donat-Bouillud, L. Mazerolle, P. Gagnon, L. Goldenberg, M. C. Petty, M. Leclerc, *Chemistry of Materials* **1997**, *9*, 2815.

- [13] H. Meng, D. F. Perepichka, F. Wudl, *Angewandte Chemie, International Edition* **2003**, *42*, 658.
- [14] H. Meng, D. F. Perepichka, M. Bendikov, F. Wudl, G. Z. Pan, W. Yu, W. Dong, S. Brown, *Journal of the American Chemical Society* **2003**, *125*, 15151.
- [15] H. J. Spencer, R. Berridge, D. J. Crouch, S. P. Wright, M. Giles, I. McCulloch, S. J. Coles, M. B. Hursthouse, P. J. Skabara, *Journal of Materials Chemistry* **2003**, *13*, 2075.
- [16] P. Audebert, G. Bidan, *Synthetic Metals* **1986**, *15*, 9.
- [17] P. Audebert, G. Bidan, *Molecular Crystals and Liquid Crystals* **1985**, *118*, 187.
- [18] P. Wagner, University of Wollongong, Wollongong, **2007**.
- [19] H. Higuchi, T. Nakayama, H. Koyama, J. Ojima, T. Wada, H. Sasabe, *Bulletin of the Chemical Society of Japan* **1995**, *68*, 2363.
- [20] J. Hassan, C. Gozzi, E. Schulz, M. Lemaire, *Journal of Organometallic Chemistry* **2003**, *687*, 280.
- [21] T. Olinga, S. Destri, W. Porzio, A. Selva, *Macromolecular Chemistry and Physics* **1997**, *198*, 1091.
- [22] G. Cik, Z. Vegh, F. Sersen, J. Kristin, B. Lakatos, P. Fejdi, *Synthetic Metals* **2005**, *149*, 31.
- [23] T. Pinault, F. Cherioux, B. Therrien, G. Suess-Fink, *Heteroatom Chemistry* **2004**, *15*, 121.
- [24] F. C. Krebs, H. Spanggaard, *Solar Energy Materials & Solar Cells* **2005**, *88*, 363.

- [25] G. Zotti, A. Randi, S. Destri, W. Porzio, G. Schiavon, *Chemistry of Materials* **2002**, *14*, 4550.
- [26] S. Destri, I. A. Khotina, W. Porzio, *Macromolecules* **1998**, *31*, 1079.
- [27] C. Botta, S. Destri, W. Porzio, L. Rossi, R. Tubino, *Synthetic Metals* **1998**, *95*, 53.
- [28] S. Destri, W. Porzio, I. Khotina, T. E. Olinga, *Synthetic Metals* **1997**, *84*, 219.
- [29] C. Wang, S. Shieh, E. LeGoff, M. G. Kanatzidis, *Macromolecules* **1996**, *29*, 3147.
- [30] M. J. Zoellner, U. Jahn, E. Becker, W. Kowalsky, H.-H. Johannes, *Chemical Communications (Cambridge, United Kingdom)* **2009**, 565.
- [31] M. Bourgeaux, W. G. Skene, *PMSE Preprints* **2005**, *93*, 1002.
- [32] Y. A. Dubitsky, M. Catellani, A. Bolognesi, S. Destri, W. Porzio, *Synthetic Metals* **1993**, *55*, 1266.
- [33] <http://riodb01.ibase.aist.go.jp/sdbs/> T. Yamaji, T. Saito, K. Hayamizu, M. Yanagisawa, O. Yamamoto, National Institute of Advanced Industrial Science and Technology, Japan, **2010**.
- [34] F. R. Diaz, M. A. del Valle, F. Brovelli, L. H. Tagle, J. C. Bernede, *Journal of Applied Polymer Science* **2003**, *89*, 1614.
- [35] M. Bourgeaux, S. A. P. Guarin, W. G. Skene, *Journal of Materials Chemistry* **2007**, *17*, 972.
- [36] T. E. Olinga, S. Destri, C. Botta, W. Porzio, R. Consonni, *Macromolecules* **1998**, *31*, 1070.
- [37] G. M. Cooper, *The Cell : A Molecular Approach*, 5th ed., Sinauer Associates, Sunderland, Mass., **2009**.

- [38] K. Wagner, L. L. Crowe, P. Wagner, S. Gambhir, A. C. Partridge, J. C. Earles, T. M. Clarke, K. C. Gordon, D. L. Officer, *Macromolecules (Washington, DC, United States)* **2010**, *43*, 3817.
- [39] C. Y. Wang, G. Tsekouras, P. Wagner, S. Gambhir, C. O. Too, D. Officer, G. G. Wallace, *Synthetic Metals* **2010**, *160*, 76.
- [40] G. Zotti, S. Zecchin, B. Vercelli, A. Berlin, S. Grimoldi, M. C. Pasini, M. M. M. Raposo, *Chemistry of Materials* **2005**, *17*, 6492.
- [41] S. Gambhir, K. Wagner, D. L. Officer, *Synthetic Metals* **2005**, *154*, 117.
- [42] J. Hou, Z. a. Tan, Y. Yan, Y. He, C. Yang, Y. Li, *Journal of the American Chemical Society* **2006**, *128*, 4911.
- [43] J. Yu, S. Holdcroft, *Macromolecules* **2000**, *33*, 5073.
- [44] P. J. Costanzo, K. K. Stokes, *Macromolecules* **2002**, *35*, 6804.
- [45] S.-Y. Jang, G. A. Sotzing, M. Marquez, *Macromolecules* **2004**, *37*, 4351.
- [46] T. Dohi, M. Ito, N. Yamaoka, K. Morimoto, H. Fujioka, Y. Kita, *Tetrahedron* **2009**, *65*, 10797.
- [47] S. Zrig, P. Remy, B. Andrioletti, E. Rose, I. Asselberghs, K. Clays, *The Journal of Organic Chemistry* **2008**, *73*, 1563.

CHAPTER 5. POLYTHIOPHENE SCAFFOLD

FABRICATION.

5.1 Introduction.

One consideration for the development of new materials is their ability to be processed to form useful structures.^[1] In this case, we focus on the investigation of novel scaffold materials to support the growth and differentiation of muscle cells. There have been several reports of investigations into scaffold materials for muscle cells. These reports have shown that muscle cells are able to respond to electrical stimulation and this can be used to improve the growth of these cells,^[2-4] thus the use of a conducting polymer would give a flexible substrate capable of providing electrical stimulation. As muscle cells are predominantly fibrous, the use of fibre mats has been investigated^[5] and aligned fibre mats have been shown to promote cell alignment.^[6, 7] Polymer films are of value for initial studies, however the overall goal is to combine a conducting polymer with hydrophilic surface groups into a fibrous scaffold. There are a wide variety of techniques available for polythiophene structure fabrication, provided we have soluble materials.^[8]

This research aims to incorporate ester linkages into the side chains of the polythiophenes, providing organic solvent solubility, whilst allowing the hydrolysis of the ester groups to give polymer structures with increased hydrophilicity, as well as allowing the possibility of further functionalisation. After a review of the literature, 3-thiophene ethanol was chosen as the starting material for the synthesis of ester polymers as its esters can be polymerised to give conductive polymers of high

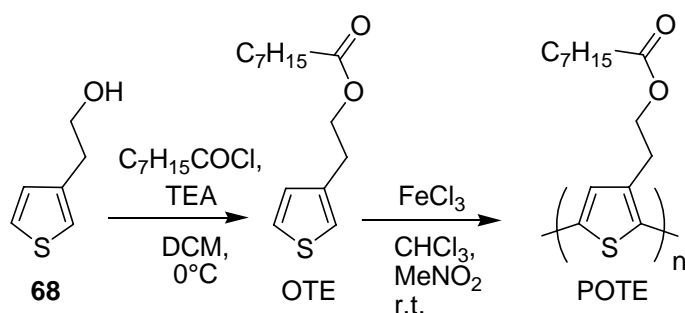
molecular weight.^[9] Polymers of 3-thiophene acetic acid, although readily available are reported to have a low conductivity^[10] and thus were deemed unsuitable as a material for a conducting polymer scaffold. There have been several reports on the polymerisation of 3-thiophene ethanol in ester form, with esters of varying chain lengths.^[9, 11-13] Various polymerisation conditions are reported; chemical and electrochemical^[13] as well as copolymerisation with alkyl thiophenes.^[14] The current literature does not report fabrication of these materials into film and fibre structures and the chemical modification of these structures as scaffolds to support cell growth.

We utilised the method of spin coating to produce simple polymer films for preliminary studies. Spin coating was chosen as it is a fabrication method capable of consistently producing uniform polymer films. This fabrication technique involves application of a polymer solution onto a rotating substrate. The centrifugal force spreads the polymer solution evenly over the substrate. Spin coating is advantageous over other methods of film fabrication such as drop casting as it gives a thinner more uniform film. Reasonably large areas are able to be coated and multiple films can be repeatedly produced. There are several spin coating parameters that can be adjusted to give optimum films, these include polymer concentration, solvent and rotation speed.^[15]

Electrospinning was chosen for producing fibrous polymer scaffolds as it is a simple technique that is well known to produce small fibres ranging from 0.01 micron to a few microns in diameter.^[16] Electrospinning can be used to produce entangled fibre mats, and also gives the possibility of fibre alignment, which would give topographical cues for directional growth in a bionic scaffold.^[17]

5.2 Polymer synthesis.

The synthesis of an organic solvent-soluble ester functionalised polythiophene based on 3-thiophene ethanol **68** was undertaken using knowledge gained from the literature.^[9, 11-13] As well as increasing the solubility of the resulting polymer, esters also protect the hydroxyl functionality (poly(3-thiophene ethanol) has been reported in the literature to get significant chlorine substitution when the unesterified monomer **68** is oxidatively polymerised by iron chloride).^[12] Here octanoic acid 2-thiophen-3-yl ethyl ester (OTE) was synthesised by reaction of **68** with octanoyl chloride (Scheme 5.1) following the procedure of Camurlu *et al.*^[13] Octanoyl chloride was chosen over other acid chlorides as this relatively long alkyl chain gives processable materials with good solubility in common organic solvents.^[11]

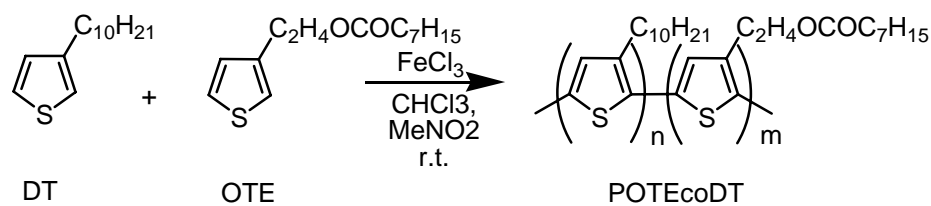


Scheme 5.1.

The polymerisation conditions of Camurlu *et al.*^[13] were modified and used for the oxidative polymerisation of OTE by iron chloride. Chloroform was used to replace the carbon tetrachloride as reaction solvent as chloroform is less toxic but still able to act as a non-solvent for iron chloride. The non-solvent causes precipitation of the iron chloride from the nitromethane solution. This method, which involves adding a nitromethane solution of iron chloride oxidant to a non-solvent in this case

chloroform, has been reported to give improved yields over the use of an iron chloride slurry in chloroform.^[18] ¹H NMR data for the polymer was consistent with the literature showing a broad singlet at 7.14 ppm.^[14] The molecular weight of the polymer as determined by GPC was 61 kDa with a polydispersity of 1.44, by comparison with polystyrene standards. Poly(octanoic acid 2-thiophen-3-yl ethyl ester) (POTE) was soluble in common organic solvents, such as DMF and chloroform, and so was amenable to subsequent processing using spin coating to produce thin films or electrospinning to produce nanofibres.^[16]

Copolymerisation is a convenient method that is known to increase the molecular weight and processability of polymers. It is also able to tailor the material for particular applications by optimising the number of functional groups in the polymer.^[19] Copolymerisation of OTE was investigated with 3-decylthiophene (DT) to determine the effect on the material properties, as copolymer materials may be more suited to scaffold fabrication since they may have increased molecular weights and processability. A similar polymerisation method to that of the OTE homopolymerisation was used to synthesise poly(octanoic acid 2-thiophen-3-yl ethyl ester)-co-(3-decylthiophene) (POTEcoDT) (Scheme 5.2). POTEcoDT was then characterised by NMR spectroscopy, which showed a ratio of 2:1 3DT:OTE. This is less than the ratio used in polymerisation of 1:1 reflecting a possible difference in reactivity of the two monomers. GPC analysis gave a molecular weight of 61 kDa and polydispersity of 1.42 for POTEcoDT, this is the same as the molecular weight of POTE and thus copolymerisation does not give an increase in molecular weight in this case.



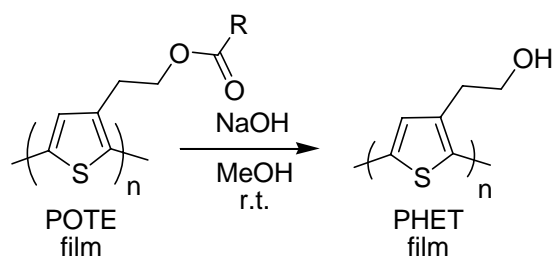
Scheme 5.2.

Copolymerisation can be an easy way of tailoring polymer material properties for particular applications, however in this case it did not give an increase in the molecular weight of the polymer. There is scope for further research into the polymerisation conditions and the use of copolymerisation to optimise material properties for particular applications. However, structure fabrication from POTE is the focus of this preliminary research.

5.3 Polymer film fabrication and characterisation.

POTE is highly soluble in chloroform and thus this solvent was used to prepare a polymer solution of 10 mg/mL for spin coating. The solution was filtered to remove any insoluble particles, as these are known to cause imperfections in the films. ITO glass, gold Mylar and glass were chosen as substrates, 1 cm x 5 cm pieces were prepared and washed thoroughly using aqueous detergent, water, methanol and isopropanol. Trials showed that 0.1 mL was sufficient polymer solution to give full coverage of the substrate. A range of rotation speeds were investigated and 1000 rpm was found to give uniform films without macroscopic imperfections (by optical inspection) with an average thickness of 2 μm .

Multiple films were consistently prepared using these conditions. Ester hydrolysis of the polymer films was then investigated (Scheme 5.3). In trial experiments, the POTE had been hydrolysed in solution by treating a THF solution with sodium hydroxide. This resulted in a sparingly soluble hydroxyl material as determined by FTIR, which was unsuitable for structure fabrication. Nonetheless, THF was not going to be a suitable solvent for film hydrolysis since it was likely to affect the macroscopic structure of the polymer film, due to the solubility of the POTE material in this solvent. Thus, methanol was chosen as an appropriate solvent due to the insolubility of the polymer film in this solvent (methanol is routinely used as a solvent to precipitate polythiophenes). A saturated solution of sodium hydroxide in methanol was prepared and the polymer films placed in this solution. After 1 hour, polymer films were removed and washed, first by water, then methanol, and followed by drying under vacuum to remove residual solvent.



Scheme 5.3.

The FTIR spectrum (Figure 5.1) of the POTE film was compared to that of the poly(3'-(2-hydroxyethyl) thiophene) (PHET) (hydrolysed) film. The characteristic carbonyl (1730 cm^{-1}) and C-O (1170 cm^{-1}) absorption bands observed for the ester form were no longer apparent following hydrolysis and the PHET film's FTIR spectrum displayed an OH absorption band at 3300 cm^{-1} .

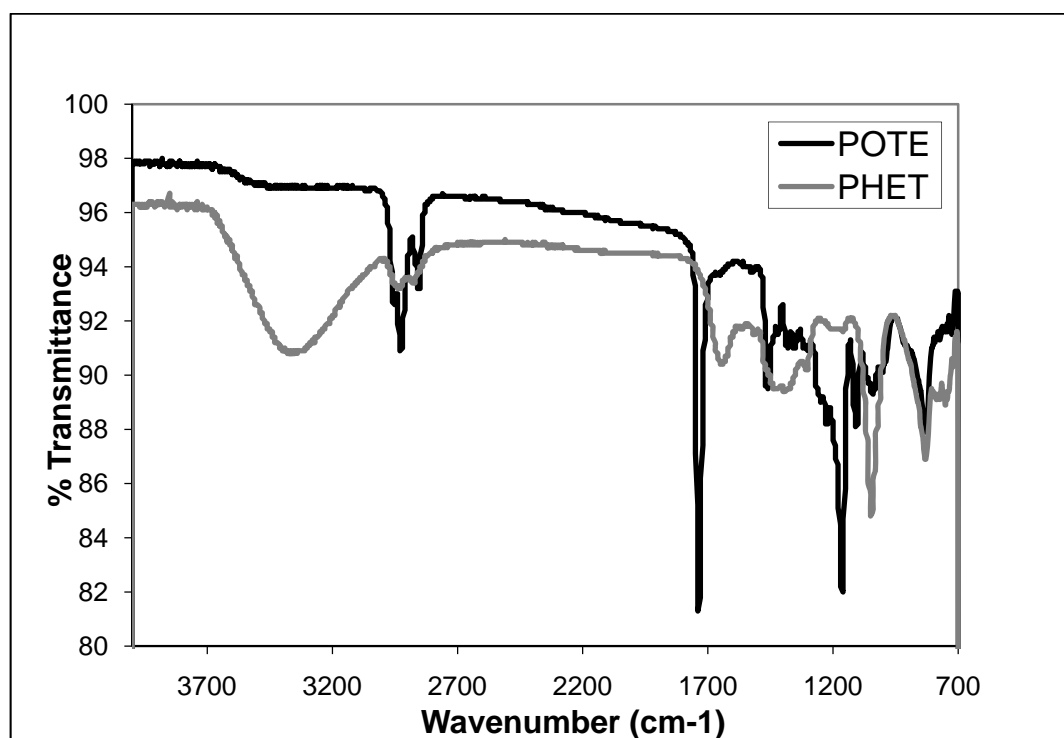


Figure 5.1. FTIR spectra of POTE and PHET films.

The FTIR spectrum for the PHET film was obtained using an ATR attachment and as such is only indicative of the polymer surface to a maximum depth of a few microns depending on the wavelength.^[20] Therefore, FTIR spectroscopy can not confirm that the film has been completely hydrolysed. It does show however that the polymer surface has been hydrolysed. Since the surface of the polymer is what interacts with the environment, it is the surface of the polymer that is important for determining the properties of the bio scaffold, as indicated in Figure 5.2 below.

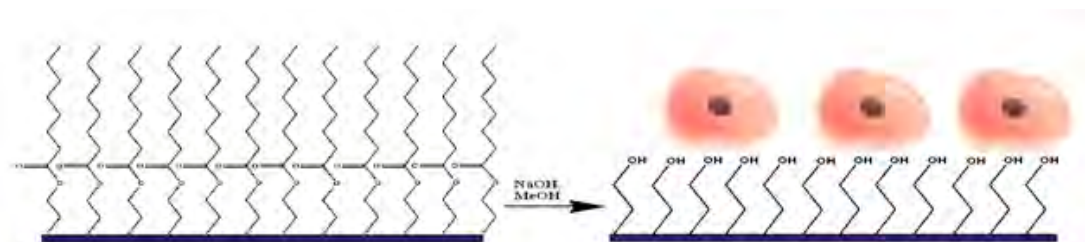


Figure 5.2. Schematic of POTE (left) and PHET (right) surfaces (cells attached to hydrophilic PHET surface).

SEM images of the films were obtained by Dr Tony Romeo. These images show that even though the films appear optically smooth, they have regular imperfections (Figure 5.3). These imperfections may have been caused by air bubbles as the films were spin coated, leading to lines of small holes across the films. The PHET film shows pitting and cracking, which has been caused by the sodium hydroxide on the exposed gold. The SEM analysis compares well with AFM characterisation, performed by Dr Michael Higgins, on these materials where the PHET film shows many small holes (Figure 5.4).

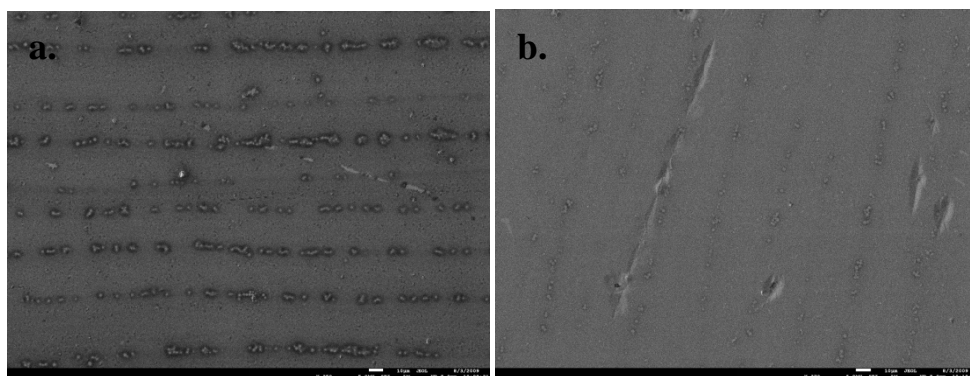


Figure 5.3. SEM images of spin coated films (10 µm scale bars) **a.** POTE and **b.** PHET.

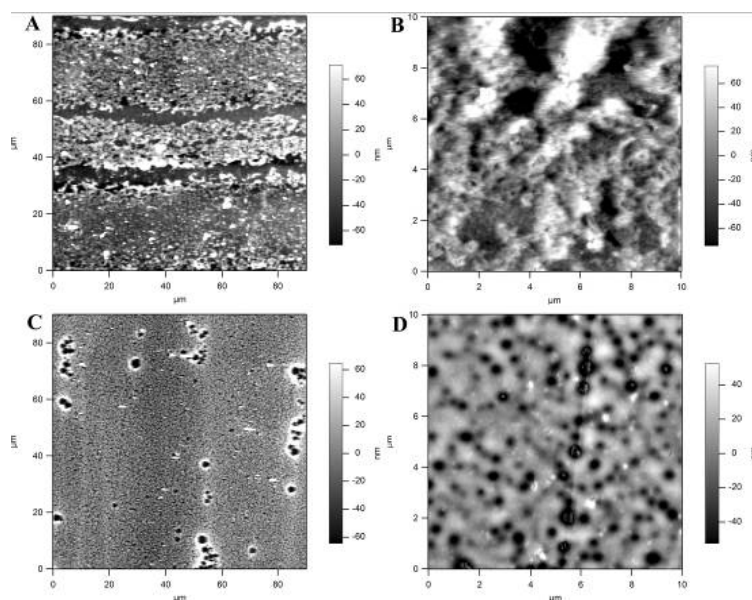


Figure 5.4. AFM topographic images of POTE (**a.** and **b.**) and PHET (**c.** and **d.**). Polymers were scanned over 90 x 90 µm areas (**a,c**) and higher resolution images obtained from the same polymers over 10 x 10 µm areas (**b,d**).

The polymer films were then characterised to compare their material properties such as electroactivity and wettability. This data is able to give an indication of the materials suitability for bionic applications. The electrochemistry of these materials was studied by running CV's of these materials in both organic acetonitrile (0.1 M) TBAP electrolyte and aqueous (0.1 M) KNO_3 electrolyte. Cyclic voltammetry is a

useful technique for studying the current from oxidation and reduction of the polymer as the voltage is scanned through a potential range. Much information can be gained from this technique including the stability of the conducting polymer (Figure 5.5). In the acetonitrile electrolyte (Figure 5.5a) it can be seen that the POTE shows a more stable response, over the course of several scans. The PHET shows an earlier onset of oxidation and also some degradation with successive scans reaching lower currents. These CV's were carried out at a scan rate of 50 mV/s, and as these films were thin (2 μ m), they gave a nice electrochemical response at this scan rate. A detailed study of scan rate dependence was not carried out, however at scan rates of 200 mV/s and above, the oxidation peak of the POTE material was at a higher potential and broader. At higher scan rates, there is less time for dopant anions to diffuse into the polymer film resulting in this behaviour.

Interestingly, when the electrochemistry of the polymer films in aqueous electrolyte was compared, there is a major difference between the two forms (Figure 5.5b). The POTE has very low activity. The alcohol PHET, on the other hand, shows a response in the aqueous electrolyte. This presumably reflects the hydrophilic nature of the PHET film (surface at least) and the resulting wettability. This is a significant result as if these materials are to be used as cell culture scaffolds where they will be used to electrically stimulate cells, they will need to be electrochemically active in aqueous environments.

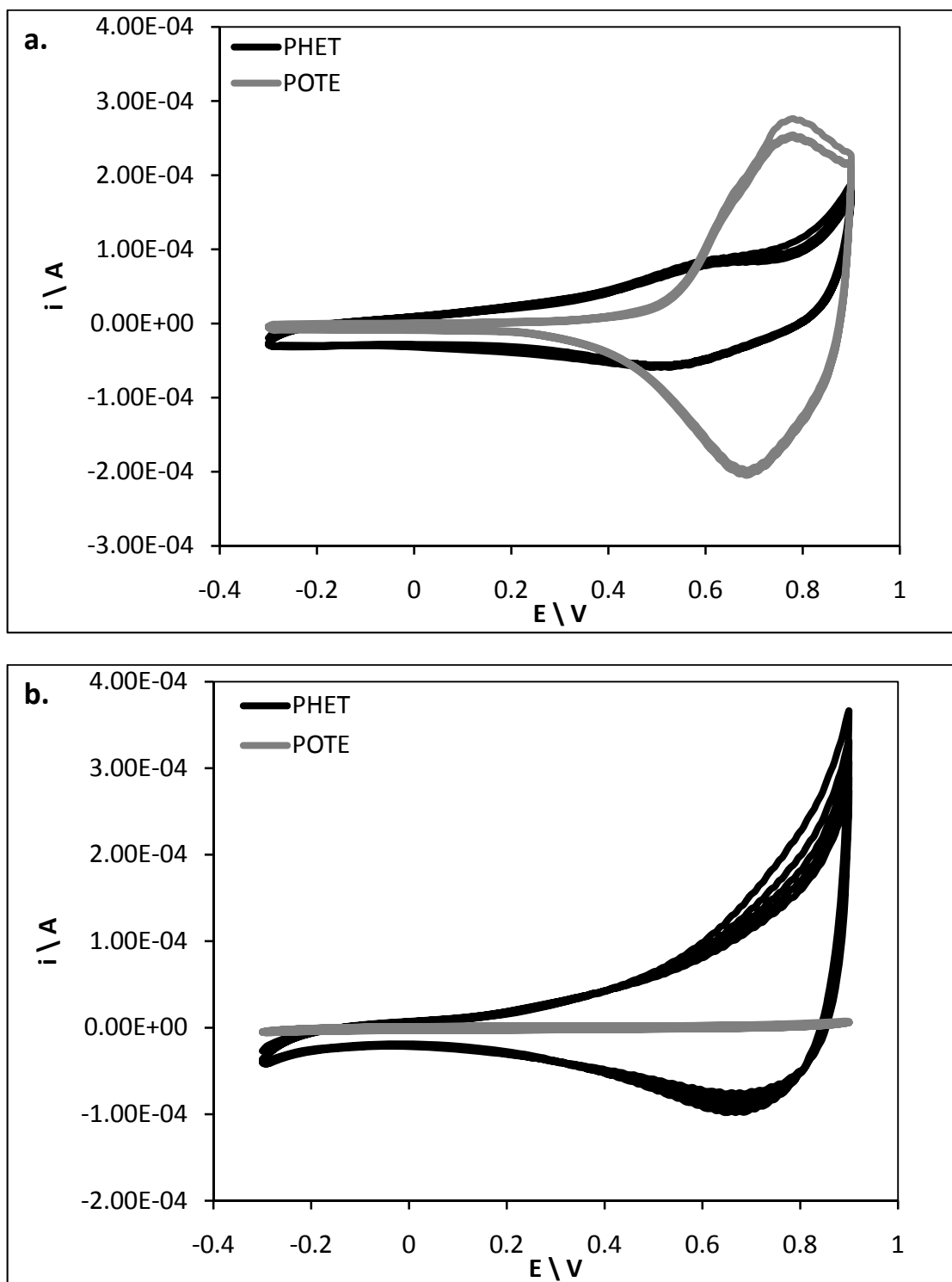


Figure 5.5. CV's of POTE and PHET films at 50 mV/s: **a.** acetonitrile electrolyte (0.1M TBAP) **b.** aqueous electrolyte (0.1M KNO_3).

The films were compared using UV-visible spectroelectrochemistry, which shows the shift in the UV spectrum as a polymer changes from being reduced to oxidised

(Figure 5.6).^[21] These spectra were recorded on a film spin coated onto ITO glass with a platinum sputtered ITO counter electrode (platinum was sputtered on the counter electrode to increase the rate of charge transfer). Comparing the two films, both show characteristic polythiophene spectra at negative potentials. The polymers are in the reduced state and thus show a single peak at a wavelength around 450 nm. As the polymer films are oxidised, this peak begins to get smaller and a peak around 750 nm begins to grow. This starts happening at 0.4 V for the POTE film and represents polaron formation. As the potential is further increased the polaron peak gets smaller and a bipolaron free carrier tail is formed, this compares with what is observed in the CV (Figure 5.5) where the polymer oxidation onset is around 0.4 V. The spectroelectrochemistry of the PHET film shows an earlier onset of oxidation with the spectrum at 0.1 V showing some oxidation. There is little difference between the two forms of the polymer films but it can be seen that the peaks in the spectrum have shifted and become broader for PHET, moving from 430 nm and 780 nm for the POTE film to 460 nm and 750 nm for the PHET film. This may possibly be due to changes in the crystallinity of the polymer as the hydroxyl polymer is more capable of hydrogen bonding. This difference in probable polymer conformation may be reflected in the fact that at 1.0 V the PHET film still shows a considerable polaron band in comparison to the POTE spectrum, suggesting that parts of the polymer chain are more resistant to bipolaron formation.

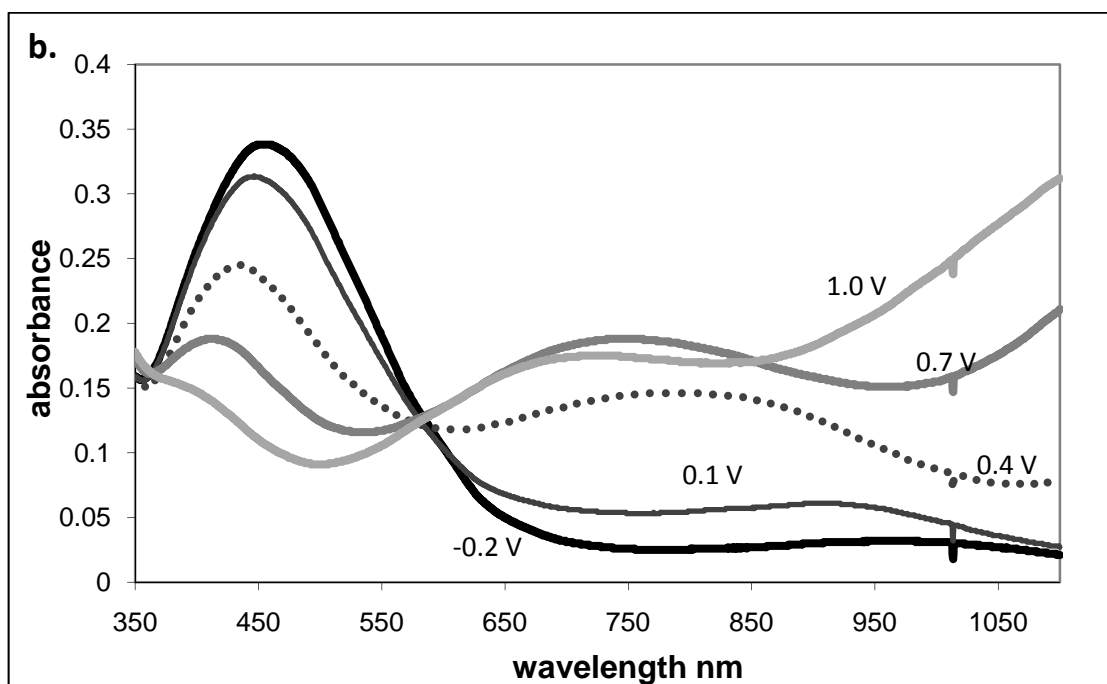
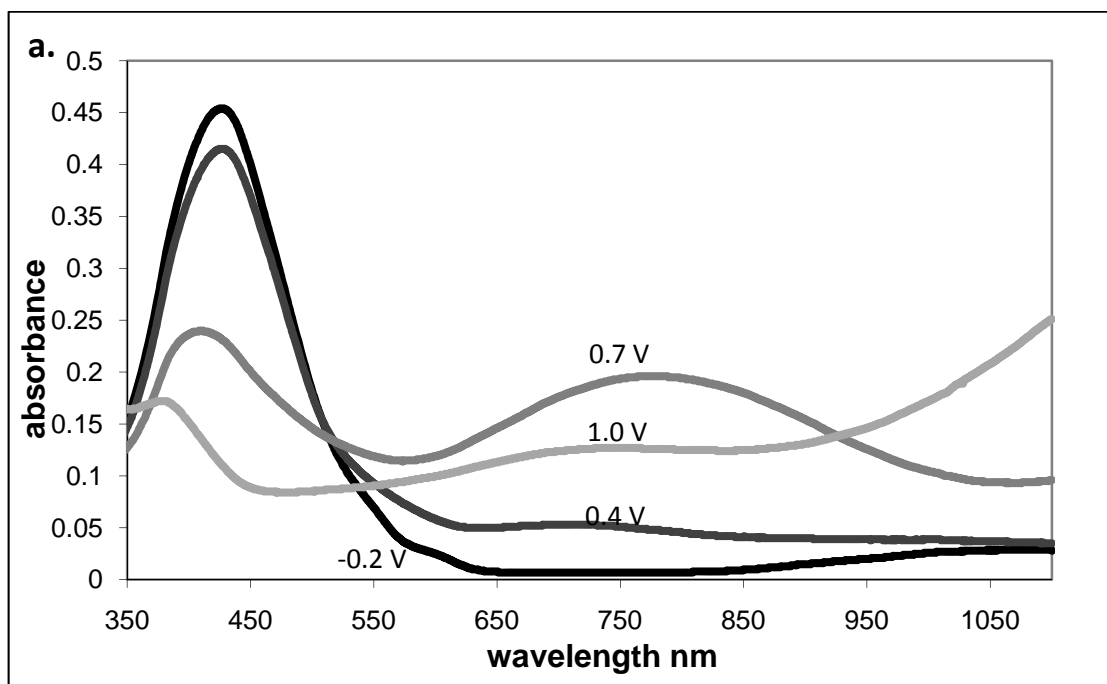


Figure 5.6. UV-visible spectroelectrochemistry of polymer films in 0.1 M TBAP acetonitrile electrolyte, each spectrum is labelled with the applied potential: **a.** POTE film on ITO glass, **b.** PHET film on ITO glass.

One way that this difference in the electroactivity of the polymers can be explained is by comparing the contact angle of the two polymer films. Contact angles can be

measured relatively easily using a goniometer. A 10 microliter droplet of water is dispensed onto the film. The instrument then measures the contact angle of this droplet on the polymer surface. A series of readings are taken for both surfaces and the readings averaged to find an average contact angle for each surface. The contact angle of the POTE film was 104° , which changed to 50° degrees upon hydrolysis to the PHET film (Figure 5.7). Since the water droplet interacts better with the PHET surface, reducing the contact angle, this indicates that the PHET film surface is significantly more hydrophilic than that of the POTE film.

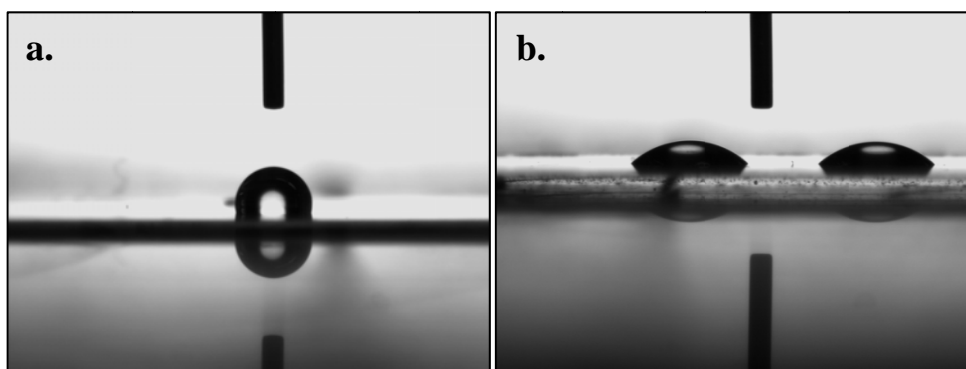


Figure 5.7. Water droplets on polymer films **a.** POTE film with contact angle 104° **b.** PHET film with contact angle 50° .

The conductivity of these materials is also of interest, although conductivities can not be measured on conductive substrates. However, accurate readings of the conductivity of the spin coated POTE and PHET films on glass substrates could not be measured as a result of the thin nature of the films leading to poor contact by the four point conductivity probe, producing widely varied readings. To obtain thicker films of material, POTE was drop cast from 10 mg/mL solutions of both chloroform and THF onto glass microscope slides. These solvents gave different looking films with the chloroform film thicker in the middle of the film and being on average 46

μm thick. The THF film looked thicker around the outside and was on average 24 μm thick. As these polymers were cast in the reduced state they needed to be oxidised to become conductive. The films were oxidised by exposure to an iodine atmosphere for 1 hour. The conductivities were then measured using the four point probe method. The voltage at a series of currents was measured and an average reading for voltage divided by current calculated. This average V/I was then applied to Equation 5.1 to calculate sheet resistance, which was converted to bulk resistivity by Equation 5.2 and this in turn was used to calculate conductivity using Equation 5.3. Average conductivities for these films after iodine doping were calculated as 0.03 S/cm for the film cast from THF and 0.3 S/cm for the film cast from chloroform. The conductivities of thin films were difficult to accurately measure and therefore the conductivity of the thicker chloroform cast film is a more accurate representation of the bulk POTE polymer.

$$R_s = 4.532 \times \frac{V}{I} \quad \text{Equation 5.1}$$

where R_s (Ω/square) is the sheet resistance, V the average of voltage, I the current and 4.532 the correlation factor of the probe taken from the Jandel-RM3 manual.^[22]

$$\rho = R_s \times T \quad \text{Equation 5.2}$$

where ρ ($\Omega \cdot \text{cm}$) is the bulk resistivity, R_s the sheet resistance and T the thickness of the film in cm.

$$C = \frac{1}{\rho} \quad \text{Equation 5.3}$$

where C (S/cm) is the conductivity and ρ the bulk resistivity.

One of the POTE films cast from chloroform was hydrolysed as described above for the spin coated films by immersion in a methanolic sodium hydroxide solution. The conductivity after iodine doping of this PHET film was 0.5 S/cm (calculated using Equations **5.1-3** as above). The slightly improved conductivity, consistent with the apparent increase in free carrier tail in the PHET UV-visible spectroelectrochemistry spectrum (Figure **5.6b**), could possibly be due to the removal of the alkyl chains as the esters were hydrolysed. This could allow the thiophene backbones to come in closer contact, be more crystalline in nature and thus cause this increase in conductivity.

5.4 Fibre fabrication by electrospinning.

5.4.1 Electrospinning poly(3-hexylthiophene).

The electrospinning of poly(3-alkylthiophenes) has been previously reported,^[8, 23-27] thus poly(3-hexylthiophene) (P3HT) was chosen as a model compound to optimise the electrospinning conditions before POTE fibres were spun. To increase the ability to electrospin from solutions, PEO is often added as this high molecular weight polymer is reported to increase chain entanglements.^[23] Although Bianco *et al.* reported the electrospinning of poly(3-dodecylthiophene) with 40 wt% PEO,^[23] we decided to only incorporate 5 wt% PEO as this polymer is insulating and would significantly affect the electronic properties of the resulting fibres.

3-Hexylthiophene (3HT) was prepared following the method of Pham *et al.*^[28] This 3HT monomer was then polymerised to P3HT by a standard iron chloride polymerisation giving a polymer with a molecular weight of 89 kDa as determined by GPC. A stock spinning solution was then prepared by dissolving P3HT (38 mg) and PEO (Mw 5×10^3 kDa, 1 mg) in 1 mL chloroform. The electrospinning was performed in a box flushed with dry air as humidity is known to have a negative effect on electrospinning.^[16]

The P3HT solution was electrospun starting at a flow rate of 1 mL/hour, and the applied voltage varied until a stable polymer jet was observed to come from the electrospinning needle, which was found to occur at 5 kV. The fibres however were highly beaded. The flow rate was gradually reduced, although no improvement in fibre morphology was observed. The polymer concentration was then halved by

diluting 0.5 mL of the stock solution with 0.5 mL of chloroform. This solution was observed to also form a stable jet at 5 kV. The flow rate was slowly reduced and the fibre morphology was observed to be optimal at 0.5 mL/hour at which the fibres were smooth and unbeaded (Figure **5.8a**).

Reducing the polymer concentration further to 10 mg/mL resulted in fibre beading. A polymer concentration of 12.5 mg/mL was observed to give good fibres at a flow rate of 0.3 mL/hour and 5 kV applied voltage (Figure **5.8b**). The fibres were collected for a 2 minute period onto clean gold Mylar, ITO glass, and glass substrates attached to the electrospinning apparatus target electrode. The addition of 10% DMF to the spinning solution was found to reduce the volatility of the spinning solution so that fibres could be spun reproducibly.

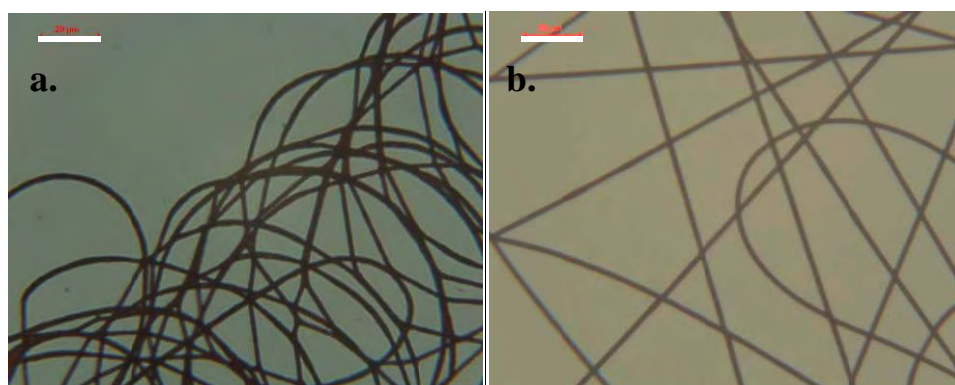


Figure **5.8**. Microscope images of P3HT electrospun fibres: **a.** P3HT fibres (spun from a 20 mg/mL soln.) **b.** P3HT fibres (spun from a 12.5 mg/mL soln.) The scale bar represents 20 μm .

5.4.2 Electrospinning of POTE.

The experience gained from the electrospinning of P3HT was then applied to the electrospinning of POTE. A spinning solution was prepared by dissolving POTE (19 mg) and PEO (Mw 5×10^3 kDa, 1 mg) in chloroform (0.9 mL) and DMF (0.1 mL), followed by filtration. The solution was electrospun with a flow rate of 0.5 mL/hour at an applied voltage of 5 kV with 15 cm separation between needle and collector in an atmosphere flushed with dry air. The fibres were collected for a 2 minute period onto clean gold Mylar, ITO glass, or glass substrates attached to the target. As can be seen in Figure 5.9, this resulted in deposition of a fibre mat with good fibre coverage, minimal beading and fibres approximately 1 micron in diameter.

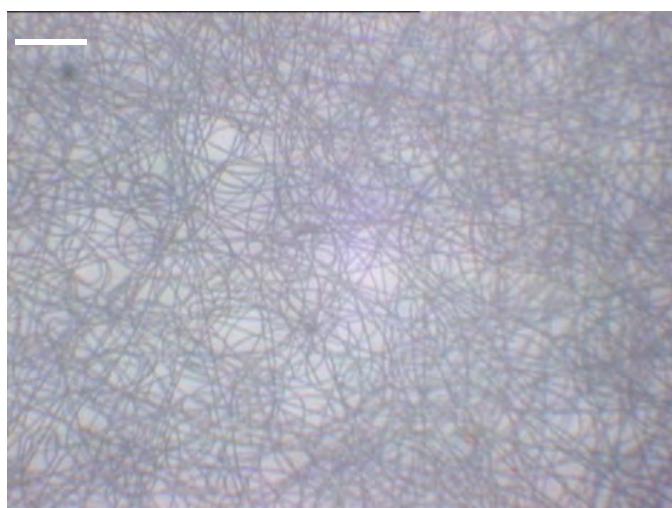


Figure 5.9. Microscope image of a POTE electrospun fibre mat. The scale bar represents 40 μm .

Once the conditions for the spinning of random fibre mats were optimised, the method was modified for the production of aligned fibre mats. Aligned mats are potentially useful for applications such as sensing or bionics where directionality is desirable.^[17] There are two common methods for fibre alignment the use of a parallel electrodes or a rotary drum collector.^[16] Both methods were trialled but the use of parallel electrodes was unsuccessful possibly due to the conductivity of the fibres dispersing the electrostatic charge, which normally drives this sort of alignment.^[29] The rotary drum method was more successful and was optimised to give well aligned fibre mats.

The aligned fibre mats were formed using the same spinning conditions as above for the non-aligned mats. The fibres were collected on a rotating drum of 5 cm diameter, the rotation speed of the collecting drum was varied and the alignment of the collected fibres analysed by optical microscopy. It was observed on increasing the rotation speed of the drum gradually from 500 rpm to 2000 rpm that the fibres went from a random mat configuration to a highly aligned morphology. The fibres were collected for a 2 minute period onto gold Mylar attached to the rotating target drum.

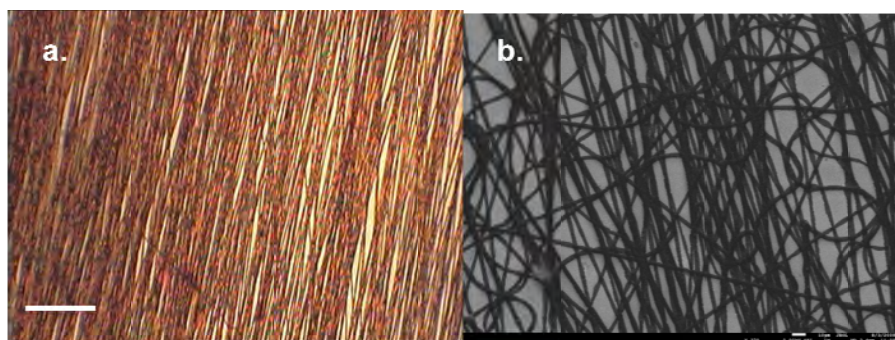


Figure 5.10. Aligned POTE fibres: **a.** microscope image, scale bar represents 20 μm ; **b.** SEM image, scale bar represents 10 μm .

The alignment of the fibres could be quantified by using Image-Pro Plus 6.0 and SPSS 15.0 software. A histogram of the alignment for a sample of fibres aligned at 2000 rpm is shown below (Figure 5.11). These fibres were aligned with a standard deviation of 2 degrees and 93% of the fibres were within 4 degrees of the axis of alignment.

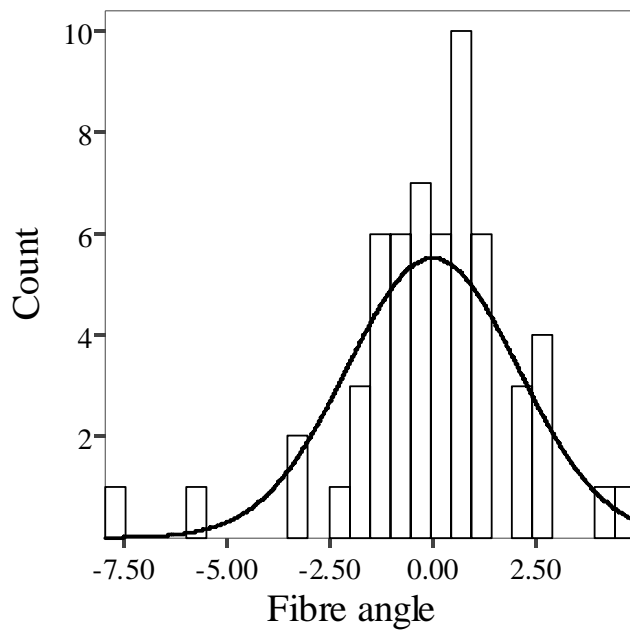


Figure 5.11. Histogram showing the distribution of fibre angles for a POTE fibre mat aligned at 2000 rpm.

5.4.3 Hydrolysis and characterisation of POTE aligned electrospun fibres.

As was carried out for the POTE spin coated films, the aligned and random POTE fibres could be hydrolysed to form PHET fibres. A saturated solution of sodium hydroxide in methanol was prepared and the ester containing fibre mats on gold Mylar placed in this solution. After 1 hour polymer fibre mats were removed and washed by water and methanol, then dried under vacuum to remove residual solvent. FTIR again confirmed the ester hydrolysis with the characteristic carbonyl (1730 cm^{-1}) and C-O (1170 cm^{-1}) absorption bands of POTE no longer apparent and the OH absorption band at 3300 cm^{-1} appearing.

Fibres were then characterised to assess and compare their material properties.

However, due to the porous nature of fibre mats, their conductivity could not be measured by the 4 point probe method. A method was devised to get an approximate measure of conductivity, where the resistance of a known number of fibres was measured between two platinum wires spaced 1 mm apart. This two point method is not as accurate as using a four point probe method as the contact resistance between the fibres and the wire is not accounted for. It does, however, give an indication of sample conductivity. Thus the method was used to calculate the conductivity of a sample of POTE fibres as follows. A fibre sample was collected between two platinum wires (Figure 5.12), the fibres spanning the wires were counted under a microscope to be 300.

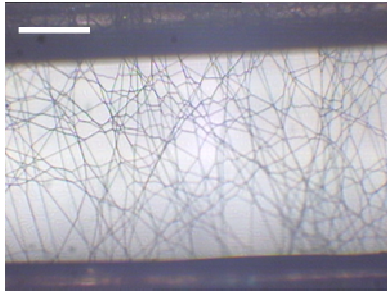


Figure 5.12. Microscope image of POTE fibres between platinum electrodes. Scale bar represents 100 μm .

The resistance of the sample was measured after doping it with iodine. When the fibres were in iodine atmosphere they had a stable resistance. However once the sample was removed from the doping chamber, the resistance was unstable, continually increasing. This was due to the high surface area fibres undergoing rapid autoreduction,^[30] as discussed later in more detail for these fibres and for polymer films in Section 6.4. The measurement of resistance from the doping chamber of 257 $\text{k}\Omega$ was thus used for the calculation. The diameter of the fibres was taken as 1 micron and the distance between the electrodes 1mm. These parameters were then applied to Equation 5.4, ρ was found to be 0.0771 $\Omega \text{ m}$.

$$\rho = \frac{R \times N_f \times A_f}{d} \quad \text{Equation 5.4}$$

where ρ ($\Omega \text{ cm}$) is the bulk resistivity of the fibres, R the measured resistance, N_f the number of fibres, A_f the cross sectional area of the fibres and d the distance between the two wires.

Conductivity was then calculated using Equation 5.3. The conductivity of the fibres was 0.13 S/cm. This is a rather crude method of conductivity calculation, especially

as the small size of the fibres makes getting an accurate reading difficult. The calculated figure of 0.13 S/cm is lower than the figure of 0.3 S/cm calculated for the POTE film. The conductivity of the fibres could be lower due to the inclusion of PEO or it could be due to this two point probe measurement not taking into account the contact resistance, which is factored in to a four point probe measurement. Attempting to hydrolyse a web of POTE fibres supported between two wires resulted in the fibres detaching in solution as they are not strong enough and contracted slightly in the methanol. Thus, the conductivity of PHET fibres could not be measured.

The electrochemistry of fibre mats on gold Mylar substrates was then studied in both organic and aqueous electrolytes. The CV's were similar to those obtained using the polymer film electrodes. Again the POTE fibres showed a more stable response in the organic electrolyte than the PHET fibres, and the PHET fibres showed a much greater electroactivity in aqueous electrolyte. The electrochemistry of these materials in comparison to the films is discussed further in section 5.5 where films and fibres are functionalised by ferrocene and the electrochemistry of the functionalised films and fibres compared with the unfunctionalised versions. Overall the fibre structures show similar properties to the films. However, they are more appropriate structures for bionic applications, with the aligned fibres being of particular interest.

5.5 Ferrocene functionalisation.

To further tune the properties of conducting polymers for particular bionic applications, the polymers may be functionalised.^[31] There have been many examples of functionalised polythiophenes in the literature.^[32] Ideally the incorporation of molecules such as peptides, which are growth factors that naturally support cell growth *in vivo*, would be used. These molecules, however, are expensive and the chemistries involved in their covalent attachment difficult. In addition, it can often be difficult to detect these molecules and confirm their attachment if they are used in small quantities.

Adding functional groups after polymerisation is known as post polymerisation functionalisation. This method is best suited to adding reactive groups that may interfere with polymerisation or if the introduction of the functional group dramatically changes the solubility of the polymer; for example, the hydrolysis of an ester group to an acid gives a much more hydrophilic polymer and thus the solubility of the material changes dramatically.^[33] To avoid changes in solubility, polymers can be surface functionalised. Thus a polymer film or fibre can be functionalised and as long as it remains insoluble in the reaction solvent the overall structure will remain unchanged.

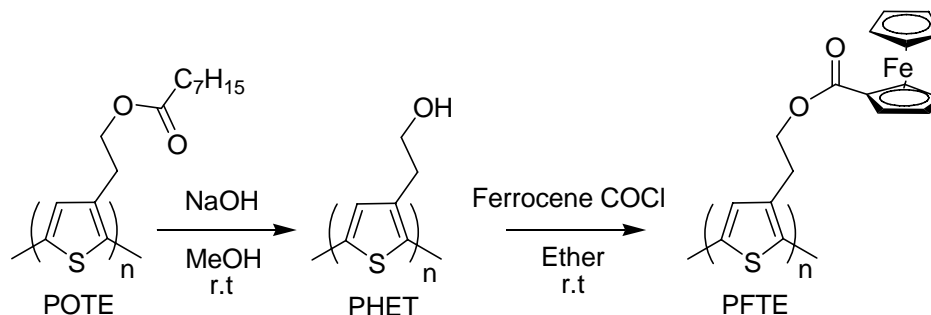
This PHET material acts as a versatile platform for further functionalisation of the surface as almost any molecule containing a carboxylic group can theoretically be coupled to the polymer by forming any ester linkage. Ferrocene carboxylic acid was chosen as a good starting point to demonstrate the utility of this hydroxyl surface for

further functionalisation as ferrocene can easily be detected electrochemically due to its strong redox activity. The chemistry was also thought to be relatively straight forward as there are examples in the literature where ferrocene acid chloride is used to form esters easily and quickly when reacting with alcohols.^[34-36] This functionalisation method is applicable to the covalent attachment of any acid group to the PHET and thus a diverse range of peptides, proteins or sensor molecules could potentially be added to tailor the material for particular applications in bionics and other research areas.

When carrying out surface functionalisation of polymer structures, several factors need to be taken into account that makes it more difficult than solution chemistry. Here a solvent must be chosen that does not solubilise the starting polymer structure, any intermediates or the resulting functionalised polymer. The solvent, however, needs to wet the polymer and facilitate reaction as well as dissolving the reactants. This is in contrast to conventional solution chemistry where a solvent is generally chosen in which the starting materials have good solubility. Here, ether was chosen as a suitable solvent as it suitably dissolved the reactants, its organic nature gave good contact with the polymer and it did not dissolve the starting polymer structure or the product after functionalisation.

As the reactant polymer is not dissolved in the solvent, the surface functionalisation reactions often proceed slower than reactions in solution. Thus, the functionalisation reaction was left overnight so that the polymer surface could be given time to react. The polymer films and fibres were successfully functionalised with ferrocene to give poly(ferrocene carboxylate 2-thiophen-3-yl ethyl ester) (PFTE) (Scheme 5.4). This

functionalisation was confirmed, by FTIR with the presence of characteristic ferrocene peaks at 1100 cm^{-1} and 1000 cm^{-1} observed, and electrochemistry, which will be discussed in more detail.



Scheme 5.4.

PFTE films and fibres were characterised electrochemically by cyclic voltammetry. The electrochemistry of the materials showed a characteristic shift from the original ester to the alcohol along with the appearance of a fully reversible oxidation peak at 0.45 V corresponding to the covalently-attached ferrocene. This is seen in both Figures 5.13a and 5.13b for fibres and films, respectively, at scan rates of 50 mV/s . It is interesting that the fibre ferrocene redox peaks are much sharper than those of the film, which is undoubtedly due to the higher relative surface area of this structure compared to the films.

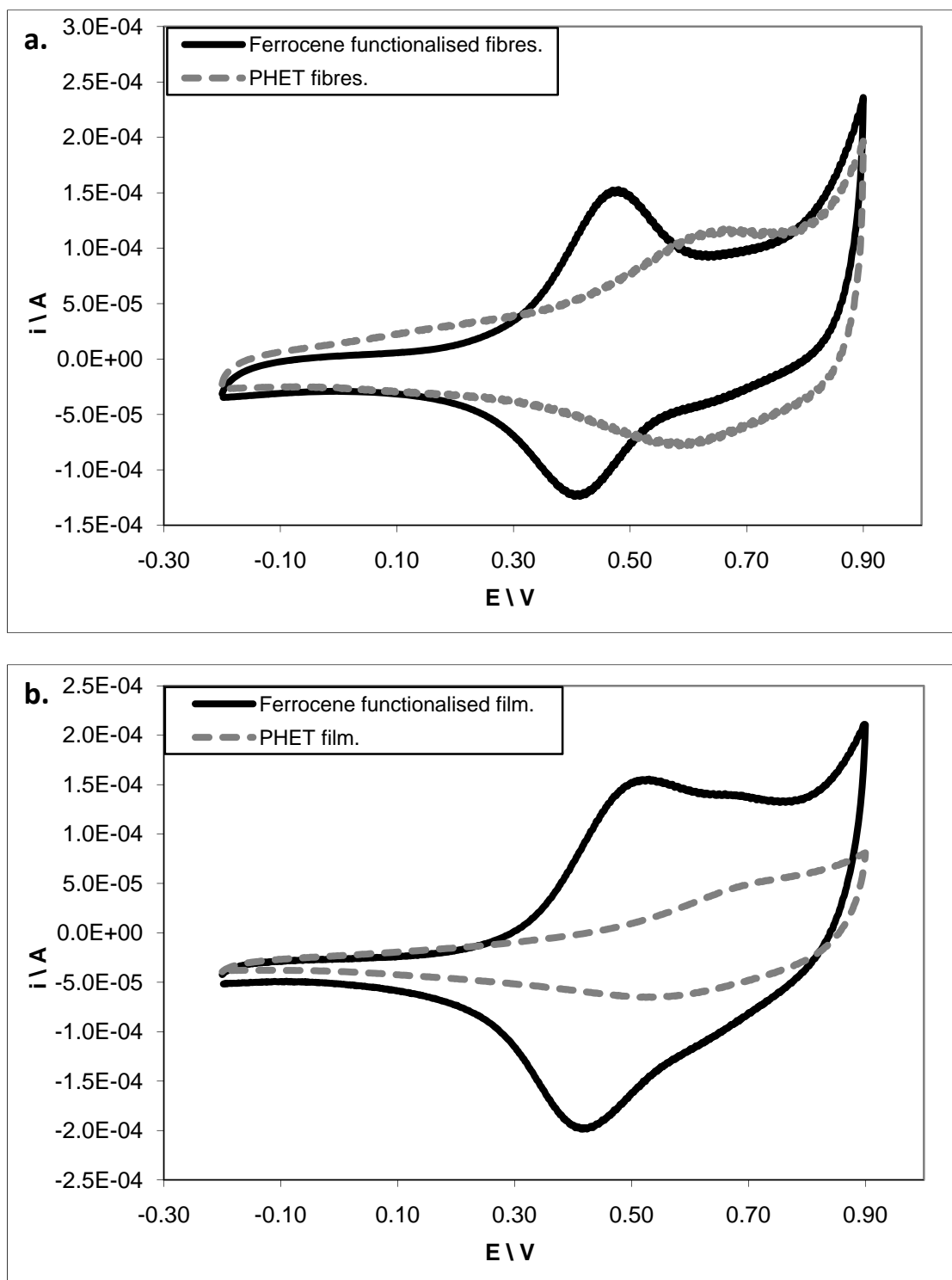


Figure 5.13. CV's showing the electrochemistry at 50 mV/s in 0.1 M TBAP acetonitrile electrolyte of PHET and PFTE on gold Mylar electrodes: **a.** Polymer fibres, **b.** Polymer films.

The position of the oxidation (**B**) and reduction (**B'**) peaks of the bound ferrocene is at a higher potential than free ferrocene. When free ferrocene is added into the electrolyte it was seen that an additional oxidation (**A**) and reduction (**A'**) peaks occur in the CV (Figure 5.14).

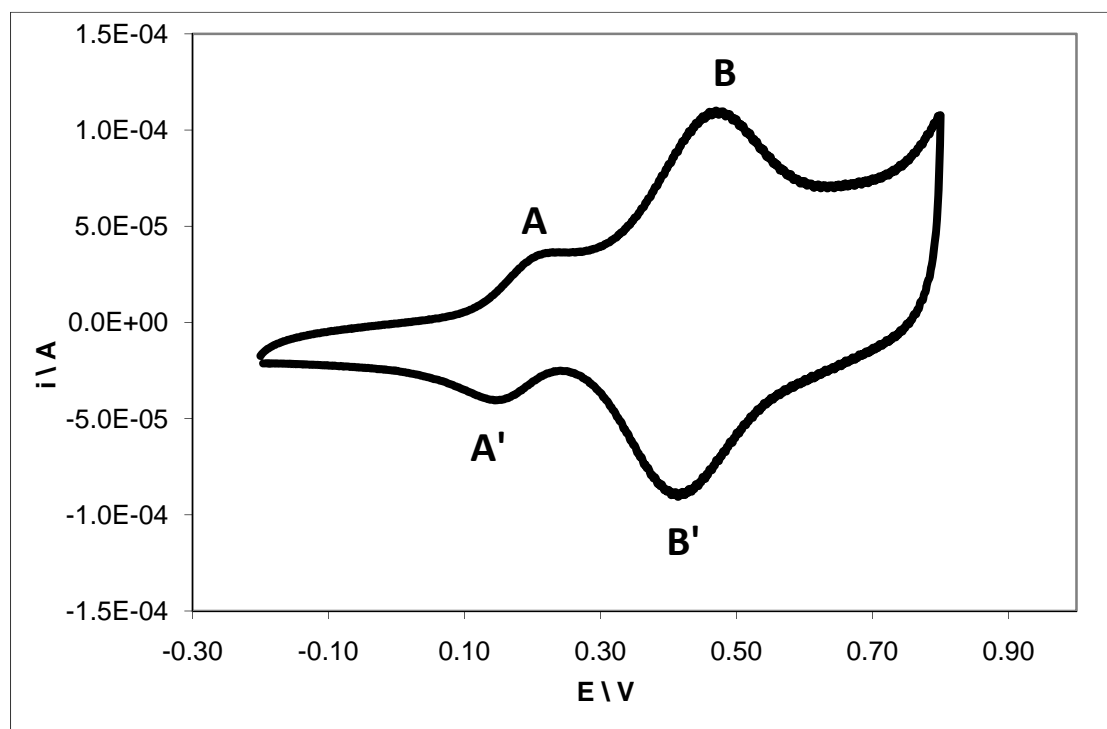


Figure 5.14. CV showing the electrochemistry at 50 mV/s in 0.1 M TBAP acetonitrile electrolyte of PFTE fibres. **A** Oxidation and **A'** reduction peaks for ferrocene added to the electrolyte, **B** oxidation and **B'** reduction peaks for ferrocene bound to the fibres.

In aqueous electrolyte, the ferrocene peak was not strongly observed with only a very small oxidation peak observed at 0.55 V for the PFTE film such that the responses of all the materials, whether film or fibre with or without ferrocene, are similar (Figure 5.15). This is in contrast to the observations of Chen *et al.* who found that for a ferrocene functionalised polythiophene, albeit one in which the ferrocene is conjugated to the polymer backbone, only the oxidation of ferrocene was observed.^[37] The difference is likely due to the hydrophilic nature of the PHET

material that may form a highly solvated polymer surface layer. This may prevent effective communication between the oxidised ferrocene and the polymer backbone, thus making the ferrocene redox behaviour “invisible”.

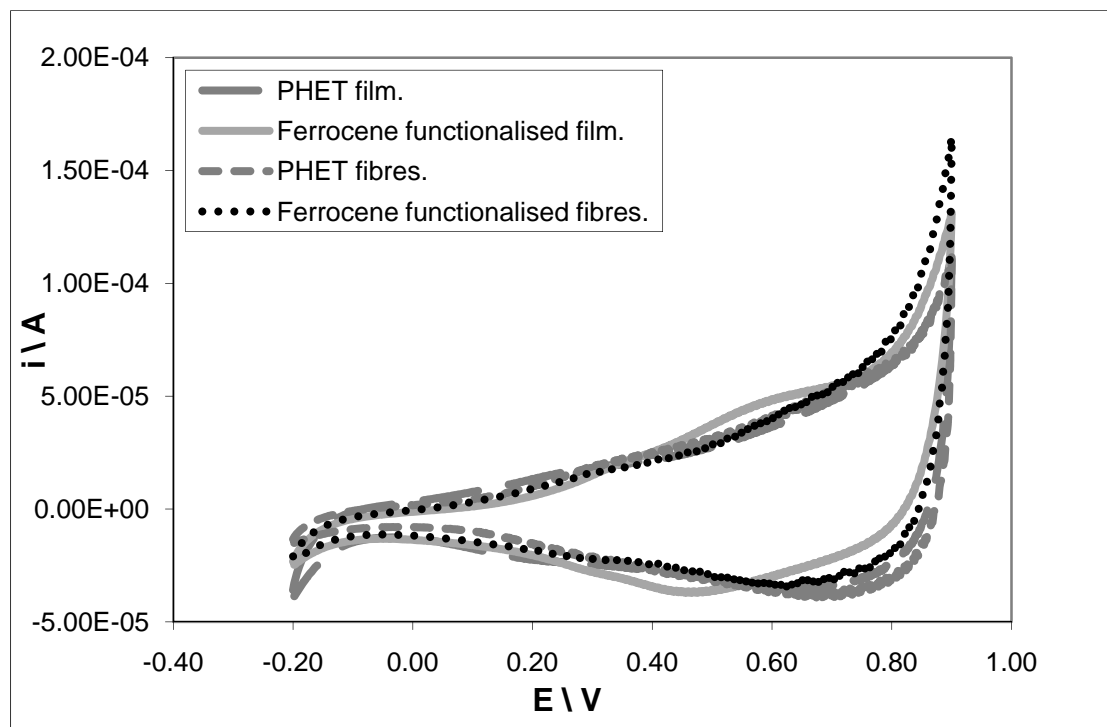


Figure 5.15. CV's comparing the electrochemistry at 50 mV/s, of PHET and PFTE films and fibres in aqueous 0.1 M KNO_3 electrolyte.

To test if the fibre mats had a faster electrochemical response compared to the films, PFTE materials were studied at a range of scan rates. The higher surface area of the fibre mats was hypothesised to give an increase in rate of charge transfer and be stable over a wider range of scan rates as the material should have a faster electrochemical response. For both materials, electrodes of surface area 1 cm^2 were used. Firstly the peak current (i_p) of the bound ferrocene peak was plotted at a range of scan rates (Figure 5.16a). The peak current of the bound ferrocene on the fibres increased at a faster rate than that of the films. It is likely that this is due to the higher

relative surface area of these fibres compared to the films allowing better contact between the material and the electrolyte.

Next, the difference between the peak voltage of bound and free ferrocene (ΔE_p) was plotted versus scan rate (Figure **5.16b**). Here there was an observable difference, as the scan rate increased from 10 mV/s to 50 mV/s the response of the film became more sluggish and ΔE_p increased more rapidly than for the fibres. The fibres have a relatively higher surface area than the films therefore the peak positions are more stable at higher scan rates. In the future, thicker films and fibre mats could be studied and the faster electrochemical response of the fibres will become more apparent.

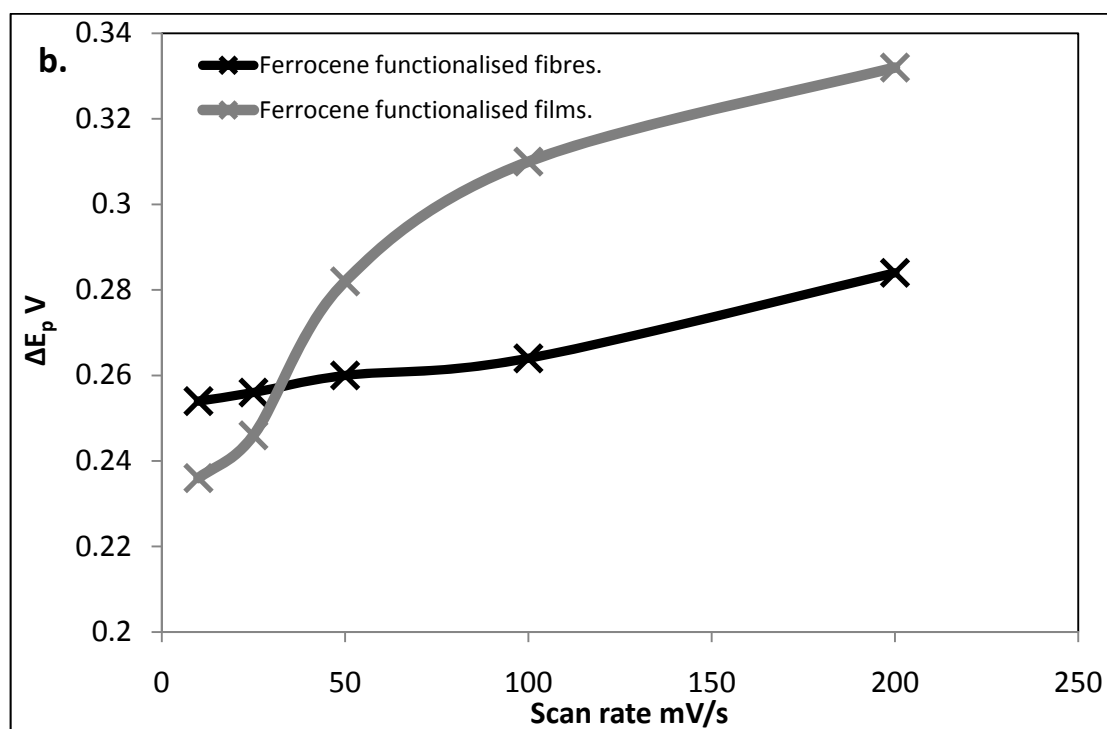
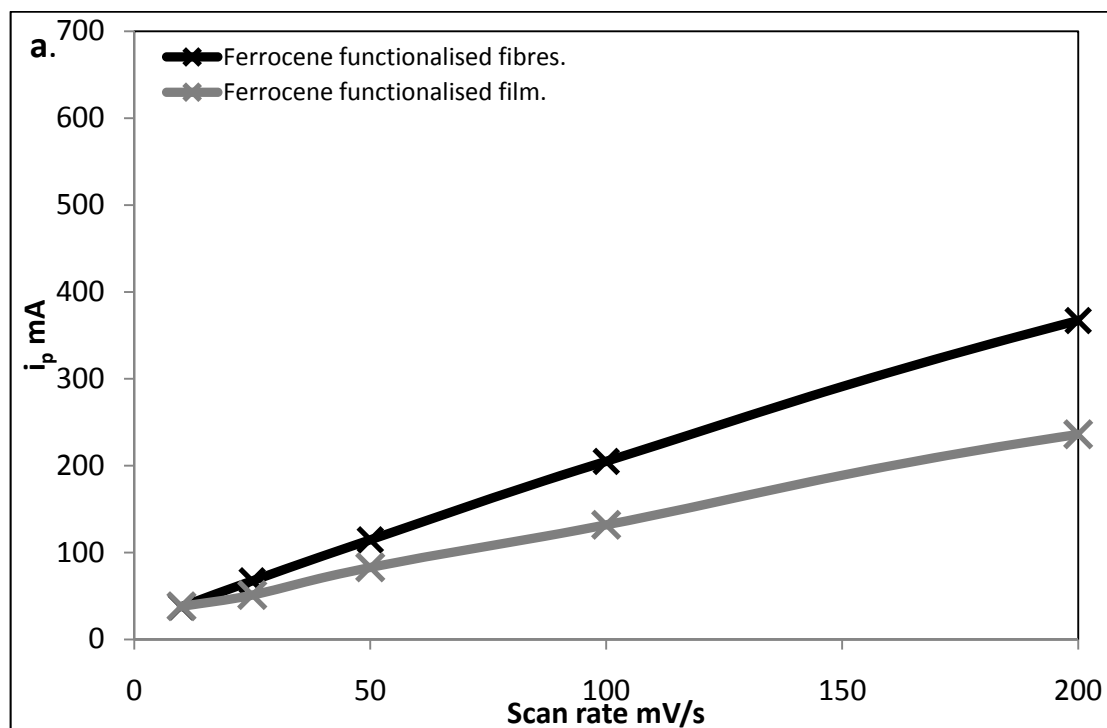


Figure 5.16. Comparison of the electrochemistry of PFTE films and fibres at different scan rates. **a.** The peak current (i_p) measured from the bound ferrocene peak versus scan rate for PFTE films and fibres. **b.** The difference between the peak voltage of bound and free ferrocene from the CV (ΔE_p) versus scan rate for PFTE films and fibres.

5.6 Conclusions.

A highly processable polythiophene ester material (POTE) was synthesised and its utility in fabricating bionic scaffolds demonstrated. The versatility of POTE was demonstrated by using it to create novel film and fibre structures. The ester groups in POTE structures could be hydrolysed to yield PHET a material with promising surface properties for bionics. These materials were characterised by a range of techniques showing a promising increase in the electrochemical response of the PHET in aqueous electrolyte, possibly due to the lower water contact angle. The fabrication of aligned structures is a promising result as this will allow control of the morphology of cells within bionic devices.

Further functionalisation of these materials was also demonstrated with the addition of ferrocene through an ester linkage to give PFTE structures. This illustrates the versatility of this platform and its amiability to further functionalisation through similar chemistries.

Ferrocene is an important redox mediator and as such these functionalised structures are promising as bionic materials for interaction with enzymes or in sensor applications. The interaction of these scaffold materials will be further investigated in Chapter 6. This research has developed useful polythiophene scaffold materials, proven the utility of ester functionalised polythiophenes for fabrication of structures and demonstrated alignment of electrospun polythiophene fibres through use of a rotating collector.

5.7 References.

- [1] M. R. Abidian, D.-H. Kim, D. C. Martin, *Advanced Materials (Weinheim, Germany)* **2006**, *18*, 405.
- [2] U. Wehrle, S. Duesterhoeft, D. Pette, *Differentiation (Berlin, Germany)* **1994**, *58*, 37.
- [3] S. Dusterhoft, D. Pette, *Differentiation; Research in Biological Diversity* **1990**, *44*, 178.
- [4] R. G. Dennis, P. E. Kosnik, II, M. E. Gilbert, J. A. Faulkner, *American Journal of Physiology* **2001**, *280*, C288.
- [5] I. Jun, S. Jeong, H. Shin, *Biomaterials* **2009**, *30*, 2038.
- [6] S. C. Jin, J. L. Sang, J. C. George, A. Atala, J. Y. James, *Biomaterials* **2008**, *29*, 2899.
- [7] X. Zong, H. Bien, C.-Y. Chung, L. Yin, D. Fang, B. S. Hsiao, B. Chu, E. Entcheva, *Biomaterials* **2005**, *26*, 5330.
- [8] H. Liu, C. H. Reccius, H. G. Craighead, *Applied Physics Letters* **2005**, *87*, 253106/1.
- [9] H.-C. Kim, J.-S. Kim, S. Baek, M. Ree, *Macromolecular Research* **2006**, *14*, 173.
- [10] T. Kuwahara, K. Oshima, M. Shimomura, S. Miyauchi, *Synthetic Metals* **2005**, *152*, 29.
- [11] C. Lee, K. J. Kim, S. B. Rhee, *Synthetic Metals* **1995**, *69*, 295.
- [12] F. Andreani, P. Costa Bizzari, C. Della Casa, E. Salatelli, *Polymer Bulletin (Berlin, Germany)* **1991**, *27*, 117.

- [13] P. Camurlu, A. Cirpan, L. Toppare, *Materials Chemistry and Physics* **2005**, 92, 413.
- [14] J. Lowe, S. Holdcroft, *Macromolecules* **1995**, 28, 4608.
- [15] K. Norrman, A. Ghanbari-Siahkali, N. B. Larsen, *Annual Reports on the Progress of Chemistry, Section C: Physical Chemistry* **2005**, 101, 174.
- [16] D. Li, Y. Xia, *Advanced Materials (Weinheim, Germany)* **2004**, 16, 1151.
- [17] A. Huber, A. Pickett, K. M. Shakesheff, *European Cells and Materials* **2007**, 14, 56.
- [18] P. Costa Bizzarri, F. Andreani, C. Della Casa, M. Lanzi, E. Salatelli, *Synthetic Metals* **1995**, 75, 141.
- [19] A. Fraleoni-Morgera, C. Della-Casa, M. Lanzi, P. Costa-Bizzarri, *Macromolecules* **2003**, 36, 8617.
- [20] L. A. Averett, P. R. Griffiths, K. Nishikida, *Analytical Chemistry* **2008**, 80, 3045.
- [21] R. J. Gale, Editor, *Spectroelectrochemistry: Theory and Practice*, **1988**.
Plenum Press, New York
- [22] Jandel-Engineering, *Jandel-RM3 Manual*, **2004**.
- [23] A. Bianco, C. Bertarelli, S. Frisk, J. F. Rabolt, M. C. Gallazzi, G. Zerbi, *Synthetic Metals* **2007**, 157, 276.
- [24] A. Babel, D. Li, Y. Xia, S. A. Jenekhe, *Macromolecules* **2005**, 38, 4705.
- [25] R. Gonzalez, N. J. Pinto, *Synthetic Metals* **2005**, 151, 275.
- [26] D. Li, A. Babel, S. A. Jenekhe, Y. Xia, *Advanced Materials (Weinheim, Germany)* **2004**, 16, 2062.
- [27] A. Laforgue, L. Robitaille, *Synthetic Metals* **2008**, 158, 577.

- [28] C. V. Pham, H. B. Mark, Jr., H. Zimmer, *Synthetic Communications* **1986**, *16*, 689.
- [29] D. Li, Y. Wang, Y. Xia, *Advanced Materials (Weinheim, Germany)* **2004**, *16*, 361.
- [30] C. G. Wu, Y. R. Yeh, L. N. Chien, *Polymer* **2000**, *41*, 5839.
- [31] G. G. Wallace, L. A. P. Kane-Maguire, *Advanced Materials (Weinheim, Germany)* **2002**, *14*, 953.
- [32] S. Gambhir, K. Wagner, D. L. Officer, *Synthetic Metals* **2005**, *154*, 117.
- [33] M. A. Gauthier, M. I. Gibson, H.-A. Klok, *Angewandte Chemie, International Edition* **2009**, *48*, 48.
- [34] J. A. Helwig, X. Chen, K. E. Gonsalves, *Polymeric Materials Science and Engineering* **1995**, *73*, 306.
- [35] J. Rolfes, J. T. Andersson, *Analytical Communications* **1996**, *33*, 429.
- [36] G. Diehl, A. Liesener, U. Karst, *The Analyst* **2001**, *126*, 288.
- [37] J. Chen, A. K. Burrell, G. E. Collis, D. L. Officer, G. F. Swiegers, C. O. Too, G. G. Wallace, *Electrochimica Acta* **2002**, *47*, 2715.

CHAPTER 6. BIOCOMPATIBILITY OF POLYTHIOPHENE MATERIALS.

6.1 Introduction.

To be useful for bionic applications, conducting polymers need to be biocompatible.^[1] Biocompatibility is a measure of the extent to which a foreign, usually implanted, material elicits an immune or other response in a recipient living organism.^[2] Initial biocompatibility tests involve testing for cytotoxicity and are often carried out *in vitro* with an immortal cell line from the target cell type, this is often followed by tests with primary cells, which are more sensitive to their environment, then finally by implanting the material into animal models.^[3]

We set out to assess the biocompatibility of a range of simple polythiophene materials with muscle cells to ascertain their suitability for applications in muscle regeneration applications. This work was carried out collaboratively with the help of Dr Klaudia Wagner, who performed some of the electrochemistry as acknowledged below, and Dr Kerry Gilmore, Dr Anita Quigley, and Ms. Magdalena Kita, who are acknowledged for their work in the biocompatibility studies.

Currently in the literature most of the research into the biocompatibility of conducting polymers has focused on polypyrroles,^[4] with polyanilines^[5-7] and polythiophenes^[4] receiving less attention. We are most interested in the biocompatibility of polythiophene materials as their ability to be readily

functionalised and tailored to particular applications is advantageous over other types of conducting polymers. Reported studies on the biocompatibility of polythiophenes, an oligosiloxane-modified polythiophene with HeLa cells,^[8] PEDOT with epithelial Hep-2 cells,^[1] and poly(3-alkylthiophenes) with PC-12 cells,^[9] all show promising cell growth results. However, there is no consistency to these studies in terms of the materials and cell types used.

We chose several polythiophene materials for our study that could easily be synthesised and polymerised. Polymer films were then produced on gold Mylar electrodes as this is a flexible conducting substrate that can be easily handled and used in biocompatibility studies. Optimally polymers would have been synthesised both chemically and electrochemically then the biocompatibility results compared. However, some monomers could only be electrochemically polymerised due to the low solubility of the polymers preventing easy processing. Other monomers could not be electrochemically polymerised due to their high oxidation potential and were thus only synthesised chemically. We also decided to compare our materials to poly(3-octylpyrrole) as this polymer had previously given promising biocompatibility results within our laboratories.^[10] As discussed in Chapter 5, fibre substrates are able to promote cell alignment. Thus, electrospun POTE and PHET fibre substrates (produced in Chapter 5) were also investigated.

Once the polymer films and fibres had been prepared, their biocompatibility was assessed. An initial assessment of biocompatibility can be carried out *in vitro* by culturing cells on the material and quantifying the growth and proliferation of these cells compared to control materials.^[4] Muscle cells were chosen as our target cell

type as they are known to be electrically responsive and therefore for future applications could benefit from a conductive substrate.^[11-13] Initially we tested biocompatibility of our materials with a robust muscle cell line (C2C12 cells) and then with more sensitive primary muscle cells (ROSA cells).

During the course of the biocompatibility studies, the polymers were characterised using contact angle measurements, SEM and electrochemistry in order to determine whether properties such as the hydrophobicity, surface morphology and electroactivity had an impact on the biocompatibility of these materials.

6.2 Monomer synthesis and polymerisation.

For this study, we selected polymers, shown in Figure 6.1, that would have different contact angles and surface morphologies and therefore a likely different impact on biocompatibility. The POTE and PHET (film and fibre structures synthesised and discussed in Chapter 5) gave easy access to hydrophobic and hydrophilic materials. Bithiophene, readily commercially available, was chosen as a suitable monomer for electropolymerisation to make a simple unfunctionalised model polythiophene (PBT) for comparison. Alkoxy-functionalised PDOT and PDDTTC (from monomers 9 and 3 synthesised in Chapter 3) were chosen since alkoxy-substituted polymers are more stable in the oxidised form. In addition, the alkoxy chains enhance the solubility of the polymers giving access to chemically and electrochemically produced materials with differing morphologies. POP was chosen for comparison as this polymer has previously been shown to be biocompatible. However, its monomer 3-octylpyrrole 69 needed to be synthesised. The polymer films were deposited on gold Mylar substrates as this flexible electromaterial was ideal for use in biocompatibility studies.

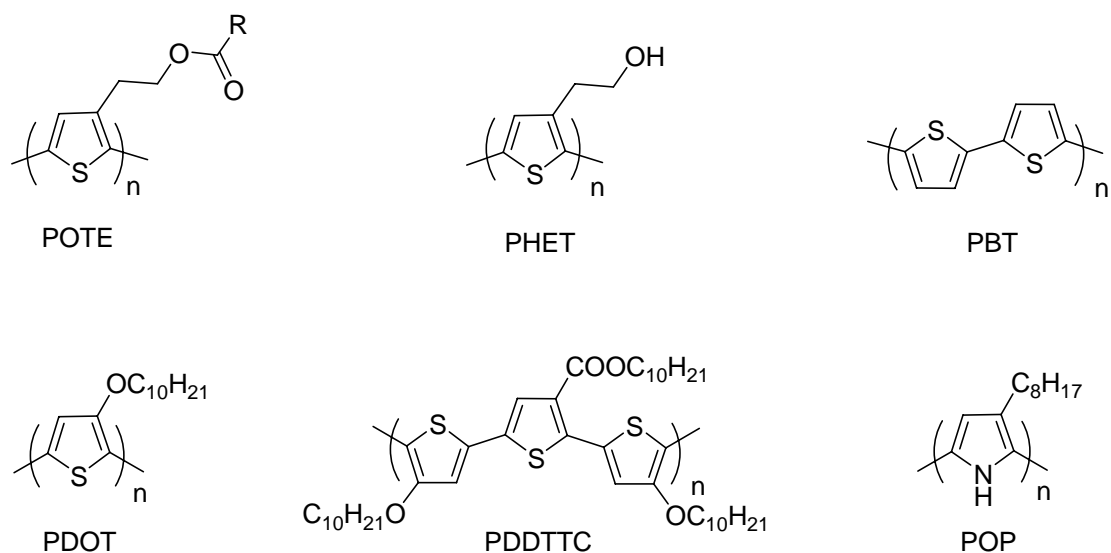
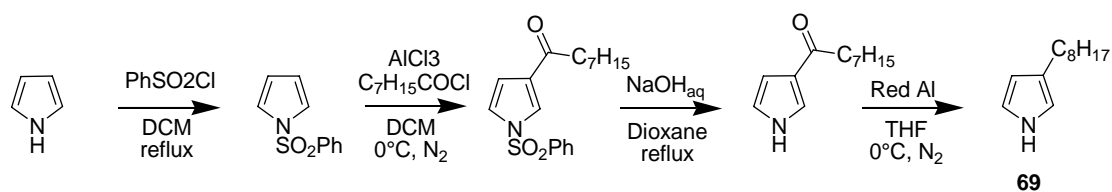


Figure 6.1. The structures of the polymers chosen for biocompatibility studies; poly(octanoic acid 2-thiophen-3-yl ethyl ester) (POTE), poly(3'-(2-hydroxyethyl) thiophene) (PHET), polybithiophene (PBT), poly(3-decoxythiophene) (PDOT), poly(decyl 4,4''-didecoxy-2,2':5',2''-terthiophene-3'-carboxylate) (PDDTTC) and poly(3-octylpyrrole) (POP).

3-Octylpyrrole **69** was synthesised following the procedure of Ashraf *et al.*^[14]

(Scheme 6.1). This procedure was relatively straight forward and **69** was obtained in 36% yield over the 4 steps. This yield is an improvement over that given in the literature (7%).^[15]



Scheme 6.1.

Once the 3-octylpyrrole **69** had been synthesised, it was polymerised electrochemically by Dr Klaudia Wagner following a procedure modified from the literature using constant current conditions.^[14] This method produced uniform poly(3-octylpyrrole) (POP) films, which were taken for further studies.

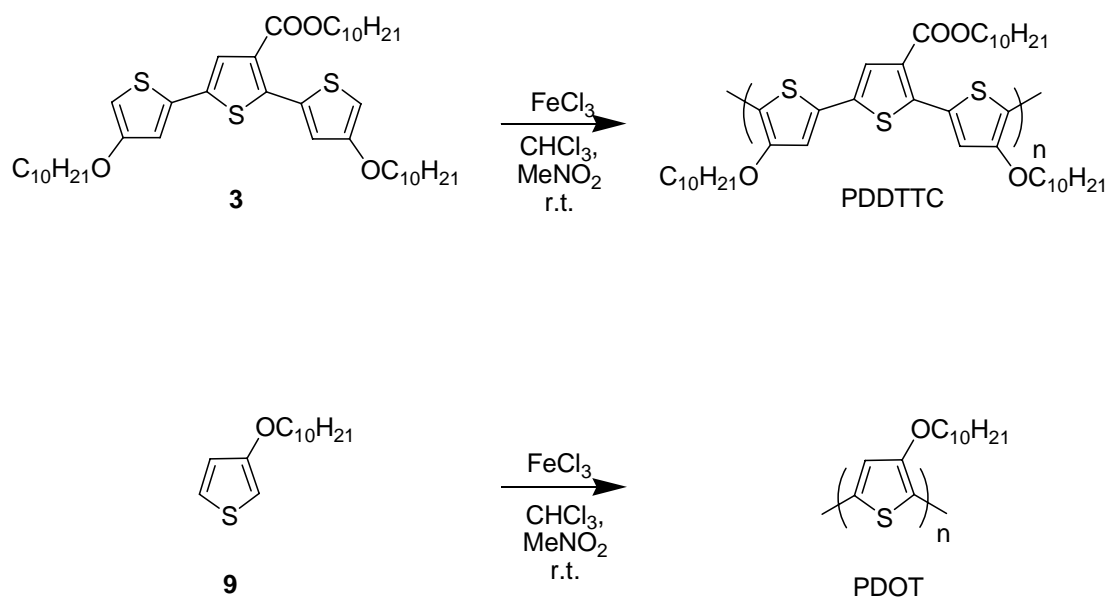
The electropolymerisation of the 3-decoxythiophene **9** (synthesised in Chapter **3**) was also performed by Dr Klaudia Wagner using 1 mA/cm² constant current. Similar electropolymerisations of 3-alkoxythiophene monomers have previously been reported in the literature.^[16] Uniform poly(3-decoxythiophene) (PDOT_e) films were produced by this method.

The electropolymerisation of bithiophene is well known and relatively straight forward.^[17] The commercially available bithiophene monomer was polymerised electrochemically by both Dr Klaudia Wagner and this researcher from a growth solution containing 0.1 M bithiophene in 0.1 M TBAP acetonitrile electrolyte. Uniform polybithiophene (PBT) films were grown at constant current 1 mA/cm² for 40 seconds.

The electropolymerisation of decyl 4,4''-didecoxy-2,2':5',2''-terthiophene-3'-carboxylate **3** has previously been reported by a constant potential method.^[18] We chose to maintain consistency with the other polymerisations, thus a constant current polymerisation method was chosen over the previously reported constant potential method. The terthiophene monomer **3** (synthesised in Chapter **3**) was polymerised at 1 mA/cm² constant current in a 1:1 DCM:acetonitrile electrolyte solution containing

0.1 M TBAP, and this gave uniform poly(decyl 4,4''-didecoxy-2,2':5',2''-terthiophene-3'-carboxylate) (PDDTTC_e) films.

One of the aims of this study was to compare electrochemically produced polymer films with chemically synthesised polymers that could be fabricated into films by spin coating. Both PDOT and PDDTTC have long alkoxy chains affording them significant solubility in organic solvents and allowing them to be spin coated to make polymer films for biocompatibility studies. The appropriate monomers were polymerised by oxidation with anhydrous iron chloride (Scheme 6.2) for 24 hours, then reduced by hydrazine and the soluble fraction of polymer was extracted by Soxhlet extraction. This polymerisation method of adding a nitromethane solution of iron chloride oxidant to chloroform (which has been reported to improve the yield of polymer^[19]) is consistent with the method used to synthesise POTE in Chapter 5. Whilst the synthesis of PDDTTC by chemical polymerisation has not been previously reported, the synthesis of PDOT by chemical polymerisation has been carried out by a GRIM method.^[20] This GRIM method involves the use of Grignard reagents and is not suitable for the polymerisation of monomers containing ester groups. Thus, to maintain consistency with the other polymerisations, only oxidative polymerisation by iron chloride was investigated.



Scheme 6.2.

GPC was used to determine the molecular weight of the polymers. Poly(3-decoxythiophene) (PDOT_c) had a low molecular weight of 2 kDa compared to poly(decyl 4,4''-didecoxy-2,2':5',2''-terthiophene-3'-carboxylate) (PDDTTC_c), which had a molecular weight of 125 kDa. It is unclear why there was such a large difference in molecular weight between the two materials, however similar poly(3-alkoxythiophenes) polymerised by iron chloride are reported to have molecular weights of only 1.8-2.2 kDa.^[21, 22] The polymers PDOT_c and PDDTTC_c were dissolved in chloroform and spin coated onto gold Mylar by the same method as described for POTE in Chapter 5. PDDTTC_c gave uniform polymer films with no visible defects; while the PDOT_c films gave uneven coverage of the gold Mylar substrate. The poor quality of the PDOT_c films is due to the very low molecular weight of this polymer. Thus only the PDDTTC_c spin coated films were taken for further studies.

We hypothesised that differences in hydrophilicity and surface morphology between the polymer films would affect their biocompatibility. We also considered that differences in electrochemistry would become important if these materials were to be used to electrically stimulate cells in the future. In order to correlate these material properties with the biocompatibility of the polymer films, the materials were characterised by contact angle measurements, electrochemistry and SEM. To aid in the discussion and comparison of material properties to biocompatibility, we first present here the biocompatibility results for these polymer materials (Section **6.3**). In Section **6.4** we then present the characterisation of these materials and compare this to the obtained biocompatibility results.

6.3 Biocompatibility results.

With the polymer films POP, PBT, PDOT and PDDTTC prepared in Section 6.2 in hand, as well as POTE and PHET films and fibres prepared in Chapter 5 we had a range of polymers upon which we could perform a consistent biocompatibility study.

Initial biocompatibility tests were carried out on polymer films in cell culture medium *in vitro* with immortal C2C12 cells. The cells were seeded onto the polymer films and grown for 48 hours, the number of cells growing on these polymers was then quantified by measuring the absorbance at 490 nm (Figure 6.2). These cells grew well on each of the polymer films with the number of cells on the polythiophene films (Thio A-F) being only slightly less than on the polystyrene (PS) control. Polystyrene is typically used as a control in cell culture as it is well known to support the growth and differentiation of many cell types.^[23] As can be seen in Figure 6.2, there was almost no significant difference between the materials indicating these conducting polymers are all capable of supporting growth of this robust cell type.

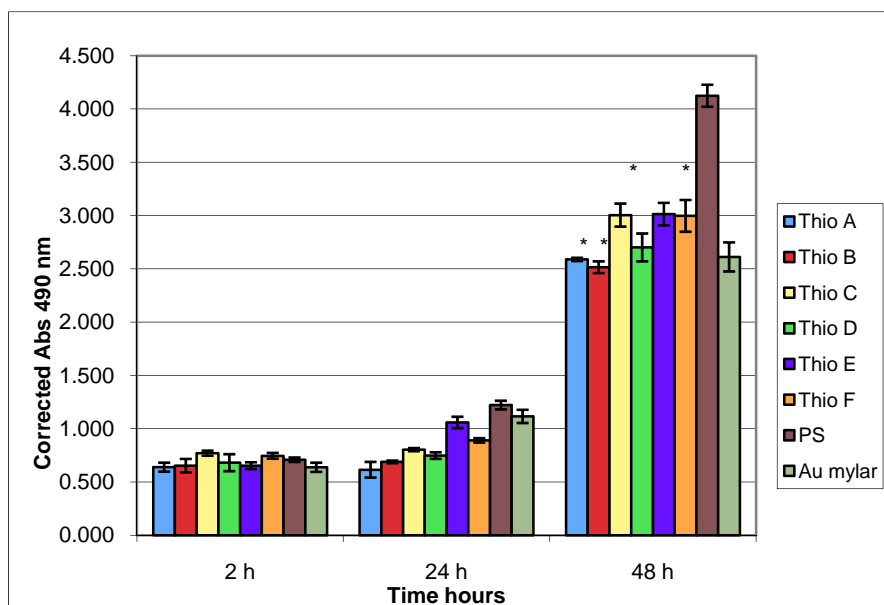


Figure 6.2. Quantitation of C2C12 cell adhesion and proliferation on polymer films by absorbance measurements at three time intervals. Thio A: POP, Thio B: PBT, Thio C: PDOT_e, Thio D: PDDTTC_e, Thio E: POTE, Thio F: PHET, PS: polystyrene control, Au Mylar: gold Mylar control.

Once the initial biocompatibility of these materials had been established by culture with C2C12 cells, the polymer films were then studied with the more sensitive ROSA primary cell line. These ROSA cells were seeded onto the polymer films and left for 24 hours to allow attachment. After this time, the cell culture media was changed to promote differentiation (differentiation of ROSA cells to myotubes is promoted in low serum medium containing growth factors which promote differentiation). Differentiation is the process whereby muscle cells form functional myotube tissue. ROSA cells are sensitive to their environment and will only differentiate to myotubes on favourable substrates. Figure 6.3 shows ROSA cells differentiated on the polythiophene films (a-f) compared to the positive controls gold Mylar (g) and polystyrene (h). The cells growing on the polystyrene are well differentiated and have formed long myotube structures. The conducting polymer films show varying degrees of differentiation, the PDDTTC_e film (d) showed poor

differentiation with most of the cells remaining rounded, the POTE (e) and PHET (f) films showed very good differentiation.

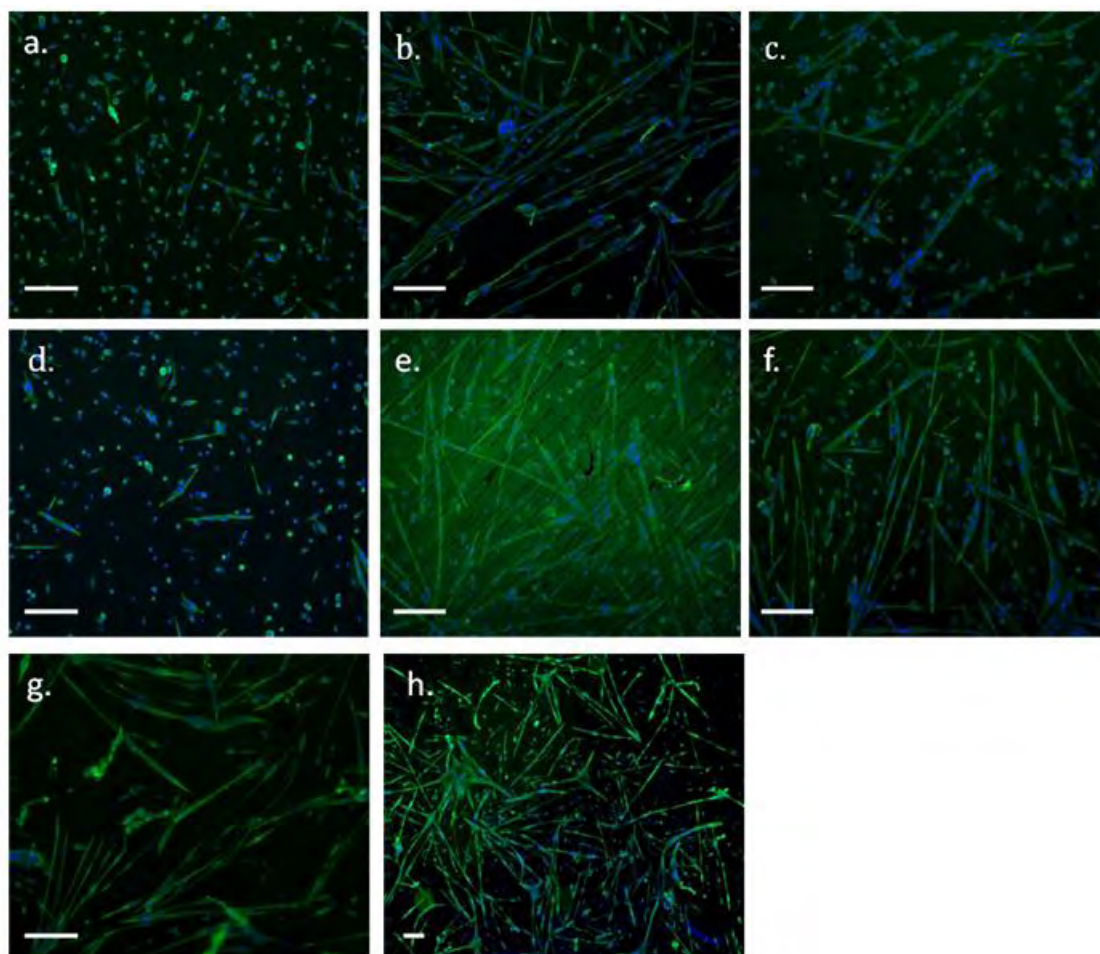


Figure 6.3. Polymer films with ROSA cells after 3 days of differentiation, blue DAPI (nuclear stain), green desmin (myogenic protein): **a.** POP, **b.** PBT, **c.** PDOT_e, **d.** PDDTTC_e, **e.** POTE, **f.** PHET, **g.** gold Mylar control, **h.** polystyrene control. Scale bars represent 100 μm .

The number of cells on each of the polymers is compared in Figure 6.4b. This indicates how well the cells survive and grow on the materials. The cells clearly grew much better on the spin coated PHET and POTE films (with a nuclei density of over 3000/mm²) than on the electrochemically produced films, which had approximately two third of the cell density.

Differentiation could be quantified by counting the number of nuclei that were multinucleated out of the total number of nuclei, and calculating the percentage that were multinucleated and differentiated (Figure 6.4a). Here the spin coated POTE and PHET polymer films had the greatest multinucleation densities (60% and 68%). The multinucleation density on the PDDTTC_e and POP films was comparably poor (under 20%).

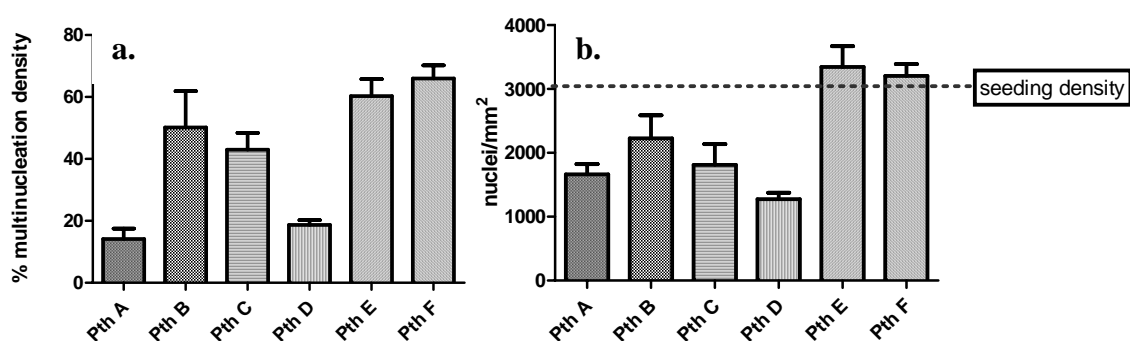


Figure 6.4. Quantitation of ROSA cell differentiation: **a.** percent multinucleation density, **b.** nuclei density per square millimetre. Pth A: POP, Pth B: PBT, Pth C: PDOT_e, Pth D: PDDTTC_e, Pth E: POTE, Pth F: PHET,

Chemically polymerised PDDTTC_c had been synthesised after the six polymers used in the initial study and therefore, was not included. We subsequently compared the biocompatibility of PDDTTC_c to the electrochemically polymerised PDDTTC_e. The biocompatibilities of these two polymers were assessed by quantifying the proliferation of ROSA cells in cell culture medium on the polymer films (Figure 6.5). The chemically synthesised and spin coated PDDTTC_c polymer films showed an increased cell growth after 48hrs when compared to the PDDTTC_e film. Since the error calculated from the standard deviation of the three cell growth experiments was large, there would appear to be little difference between the behaviour of these three

materials towards ROSA cells. However, more replicate experiments should be done in the future to confirm this.

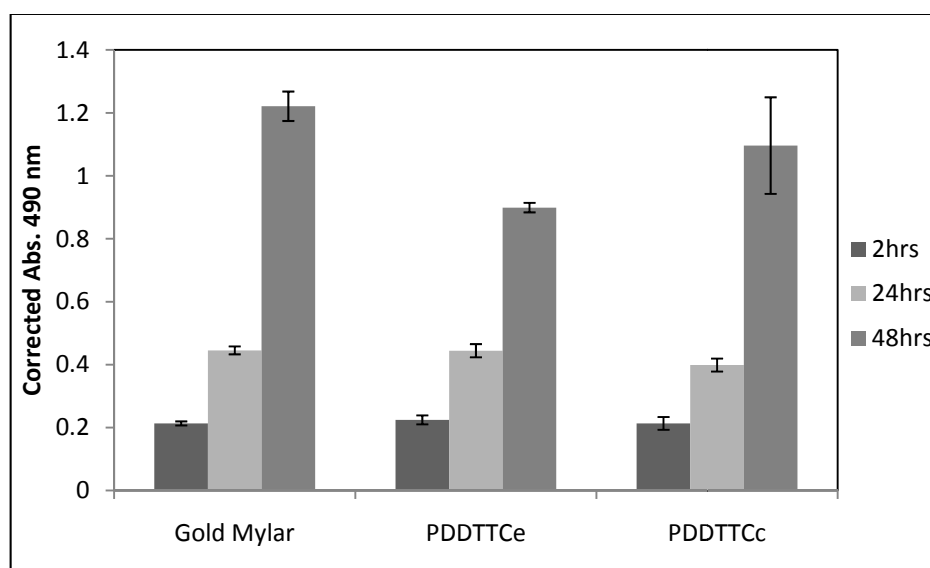


Figure 6.5. Quantitation of ROSA cell growth on PDDTTC_e and PDDTTC_c films at several time intervals compared to a gold Mylar control.

Differentiation of the ROSA cells was promoted by placing them in the low serum differentiation medium. As a result, there was a large difference between the two polymer films (Figure 6.6). On the PDDTTC_e polymer films (a) the cells remained rounded and very little differentiation was observed (this was consistent with the previous experiment shown in Figure 6.3d). In contrast, the smoother PDDTTC_c polymer film (b) showed differentiation comparable to the gold Mylar control (c).

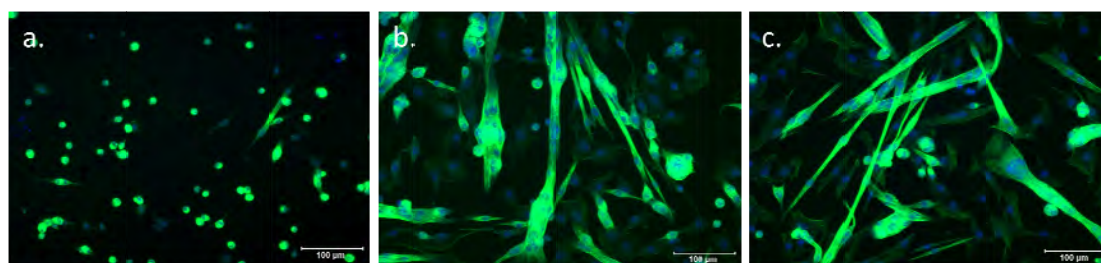


Figure 6.6. Polymer films with ROSA cells after 3 days of differentiation, blue DAPI (nuclear stain), green phalloidin (stain which binds actin filaments in muscle cells): a. PDDTTC_e, b. PDDTTC_c, c. gold Mylar control. Scale bars represent 100 µm.

In Chapter 5 POTE and PHET fibre mats were produced by electrospinning, two types of mats were produced, random unaligned fibre mats collected on a stationary target and aligned fibre mats collected on a rotating target. The ability of PHET and POTE fibre mats to support cell growth and differentiation was investigated. C2C12 cells were grown on these random mats in cell culture medium. These cells grew very well on the mats with cell growth at least as good as on the underlying gold Mylar substrate (Figure 6.7c). The C2C12 cells did not show a preference between the POTE (a) and PHET (b) fibre mats (Figure 6.7).

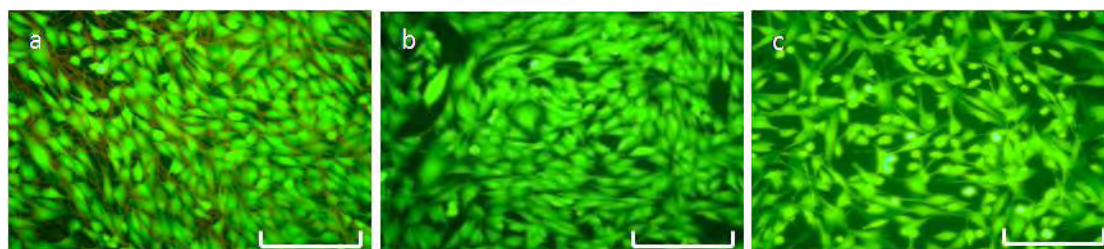


Figure 6.7. Calcein-stained C2C12 cells adhering and proliferating on **a.** POTE and **b.** PHET polymer fibres, **c.** underlying gold Mylar substrate. Scale bar represents 100 μm .

ROSA cells were then grown on aligned POTE and PHET fibre mats in an effort to induce aligned differentiation. Several aligned fibre densities were investigated; high density (no exposed gold Mylar between fibres), medium density (15-100 μm spacing between fibres), and low density (100-300 μm spacing between fibres). The cells were grown for 24 hours on the fibre mats in growth medium. The medium was changed as before to induce differentiation, and the cells allowed to differentiate into myotubes for 3 days. After this time, the degree of differentiation and the direction of cell growth were compared (Figure 6.8). On high density fibre mats the cells did not differentiate but remained rounded up and viable. At medium density with exposed gold Mylar of 15- 100 μm , the fibres could direct the cells to align and differentiate

in a directional fashion, with 83% of myotubes orientated within 10° of the fibre axis (Figure 6.8b). At lower densities, the myotubes were branched with no alignment (Figure 6.8d). There was no significant difference observed in the ability of ester POTE (a and c) and hydroxyl PHET (b and d) fibres to promote aligned differentiation.

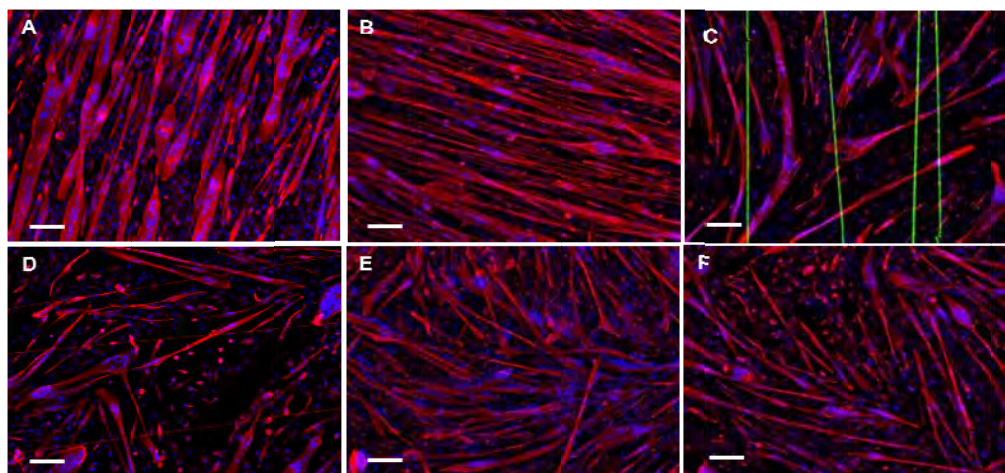


Figure 6.8. Fluorescence images of differentiated ROSA cells, stained with DAPI and desmin, aligned along medium (a. and b.) or low (c. and d.) densities of ester POTE (a. and c.) or hydroxyl PHET (b. and d.) fibres, or on gold Mylar in the absence of polymer fibres (e. and f.). Scale bars represent 80 μm .

Therefore, while the physical nature of the polymer fibres did not seem to have a significant impact on growth and differentiation, there appeared to be an advantage in using an aligned fibre substrate for cell growth and differentiation over that of a smooth film (compare Figures 6.3e,f and 6.8a,b). In addition, the medium density fibres appeared optimal for providing directional cues for the cells.

6.4 Characterisation of polymer film properties.

The polymer films produced in Section 6.2 were characterised by a range of techniques in an effort to correlate material properties to changes in biocompatibility. Changes in the hydrophilicity (contact angle) and morphology (SEM) of polymer films were hypothesised to be important in determining the biocompatibility of polymer films. The electrochemistry (oxidation onset potential) of the polymers was also considered important for determining the suitability of materials to electrically stimulate cells in the future. These properties are summarised and compared to a measure of biocompatibility in Table 6.1 below and discussed in more detail in the following section.

Table 6.1. Contact angles, onset potential from post growth CV's, morphology from SEM and biocompatibility (% multinucleation (MN) with ROSA cells) for polymer films. *Dr Klaudia Wagner is acknowledged for gathering this data.

Polymer	Contact angle	Oxidation Onset (V)	Morphology	Biocompatibility % MN
POP	84°*	-0.54*	Craters.	17
PBT	40°	0.42	Some rough areas.	51
PDOT	105°*	-0.22*	Small bumps.	44
PDDTTC _e	90°	0.08	Very rough many bumps.	20
PDDTTC _c	98°	-0.03	Smooth, some holes.	Not available.
POTE	104°	0.39	Smooth, some holes.	60
PHET	50°	0.04	Smooth, some holes/cracks.	68

The hydrophilicity of polymer films was thought to be important in determining their biocompatibility as more hydrophilic materials allow closer interactions with aqueous environments. An indication of how hydrophilic a material is can be gain from measuring the contact angle of a water drop on the surface of the material. The contact angles of a water drop on these polymer films were measured by using a goniometer and applying the sessile drop technique with a 2 μ L drop of RO water.^[24]

The PBT film was the most hydrophilic of the electrochemically produced polymers, which is not surprising as it does not have a hydrophobic alkyl or alkoxy chain that are present in the other polymers. The PDOT film was most hydrophobic, which is likely due to only hydrophobic decoxy chains being present, the PDDTTC has ester functionalities which cause a slight increase in the hydrophilicity. The chemically polymerised and spin coated materials have comparably higher contact angles compared to the electropolymerised materials, with an 8° difference between the PDDTTC_e and PDDTTC_c. This increase is due to the presence of dopant within the electrochemically produced polymer films making them more hydrophilic.

The morphologies of the polymer films were compared by taking SEM images (Figure 6.9), which were obtained by Dr Tony Romeo. The polymer films each had vastly different morphologies. The POP film (a) had crater like structures, the PDOT film (c) had small bumps, the PBT film (b) had rough (fluffy) areas, the PDDTTC_e film (d) was very rough and bumpy all over. Bumpy or cauliflower-type structures are typical of electrochemically grown conducting polymers, as polymer films grow by a nucleation and growth mechanism.^[25] The spin coated films (shown in Chapter

5) were not surprisingly smooth in comparison to the electrochemically produced films with only a few pinholes.

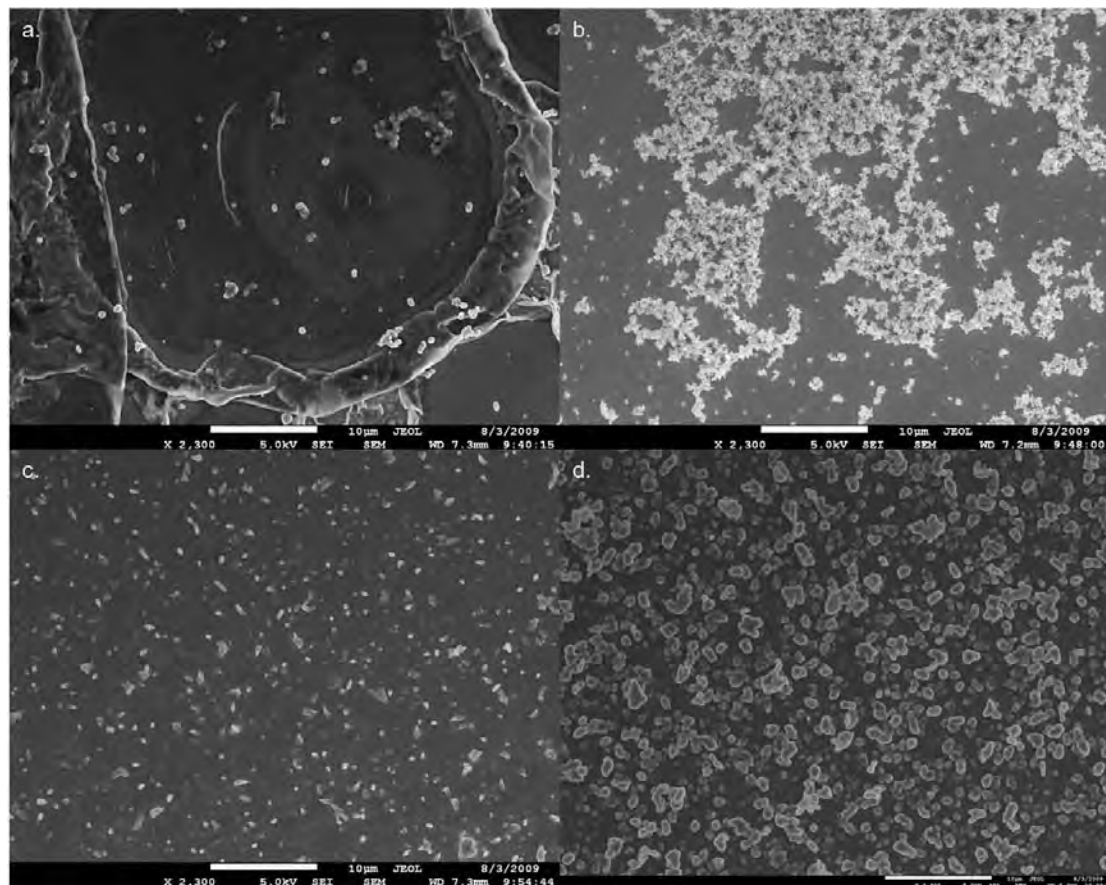


Figure 6.9. SEM images of polymer films: **a.** POP, **b.** PBT, **c.** PDOT, **d.** PDDTTC_e. Scale bars represent 10 μ m.

Overall, comparing the data for morphology and contact angle with the biocompatibility, it appears that the morphology of the materials has the greatest effect on the biocompatibility. The smoother spin coated POTE and PHET films showed the highest percentage of multinucleation, the moderately rough PBT and PDOT had the next best biocompatibility. The worst biocompatibility was observed with the cratered PBT and the very rough PDDTTC_e.

It appears from the contact angle measurements that the hydrophilicity/phobicity may have a small effect on biocompatibility. The POTE and PHET had very similar morphologies but increased biocompatibility was observed on the more hydrophilic PHET material, which gave 68% MN compared to 60% MN for the POTE. The hydrophilic PBT, with a contact angle 40° , had a biocompatibility of 51%. This is higher than that of the other electrochemically prepared samples such as PDOT, which had a biocompatibility of 44% with a similar slightly bumpy morphology but a much greater contact angle of 105° . Consequently, the dominant effect on cell growth would appear to be morphology with the polarity of the material having a much smaller influence.

A measure of the electroactivity of the polymer films could be gained by determining the onset of oxidation from post growth CV's of the materials. Post growth CV's of the polymer films were performed in an acetonitrile electrolyte containing 0.1 M TBAP. The CV for a chemically polymerised PDDTTC_c film on gold Mylar is shown below in Figure **6.10** with the arrow indicating the onset of oxidation. Zotti *et al.* have established a linear relationship between oxidation potential and conductivity in polypyrroles and polythiophenes, with lower oxidation potentials being associated with higher conductivities.^[26]

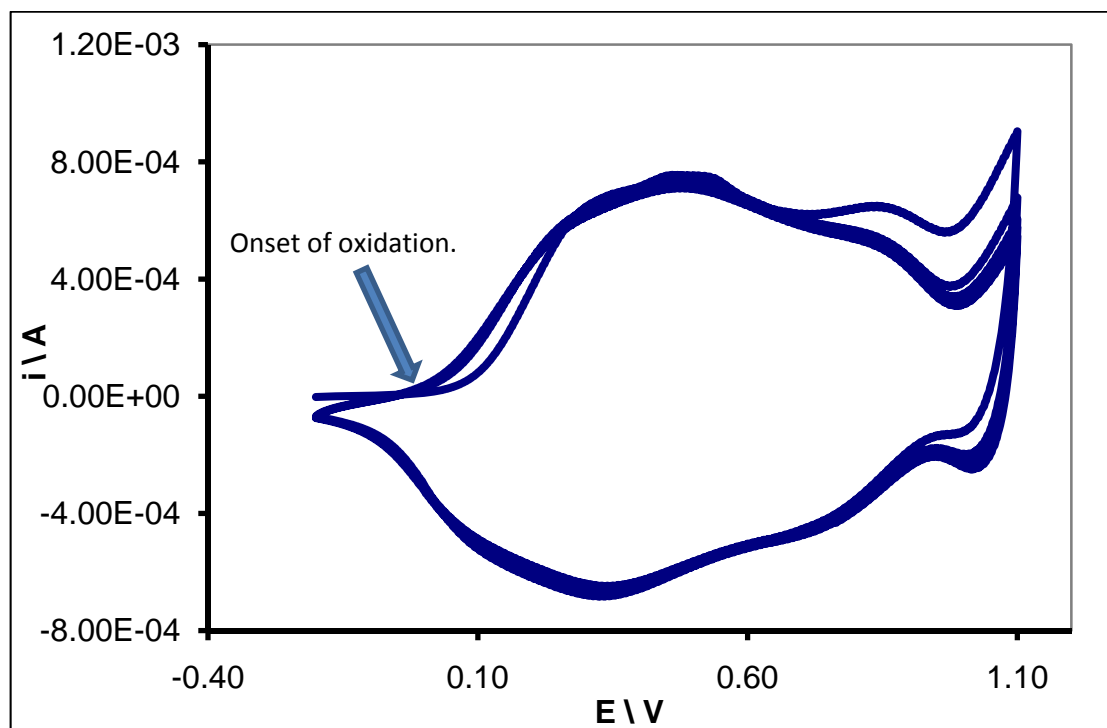


Figure 6.10. CV of a PDDTTC_c film on gold Mylar in 0.1 M TBAP acetonitrile electrolyte (50 mV/S scan rate). The arrow indicates the onset of oxidation.

From the onset of oxidation data in Table 6.1, POP has the lowest onset of oxidation followed by PDOT, then the PDDTTC polymer films. There is only a small difference between the chemically and electrochemically synthesised PDDTTC films, with the chemically produced polymer having a slightly lower oxidation potential. The PBT had the highest onset of oxidation of the polymer films. As these films were thin and coated on conductive substrates, conventional four point probe conductivity measurements could not be performed. It is difficult to see any correlation between onset of oxidation and biocompatibility. The electroactivity of these materials will become more important in the future if these materials are used to electrically stimulate cells. The hydrophilic PHET material will be most suitable for such future applications as not only did it have the highest multinucleation percentage but also had a relatively low onset potential of 0.04 V.

For cell stimulation studies, polymers will need to be in their conductive doped state. We had previously observed the resistance of a POTE fibre mat increasing when the sample was removed from the doping chamber during a conductivity measurement conducted in Chapter 5. This increase in resistance was attributed to the fibres dedoping. We thus set out to further investigate doping stability in our materials. A study of the doping stability of a POTE fibre mat was carried out by UV-visible spectroscopy of a fibre mat on an ITO glass electrode. The fibre mat was doped electrochemically at 900 mV and a spectrum was taken at this potential. The oxidised fibres were left immersed in electrolyte (0.1 M TBAP, acetonitrile) with no applied potential. UV-visible absorption spectra were taken at intervals over a 30 minutes period (Figure 6.11). Over this time the polymer underwent spontaneous reduction and the spectrum was observed to revert back to that of the reduced form of the polymer.

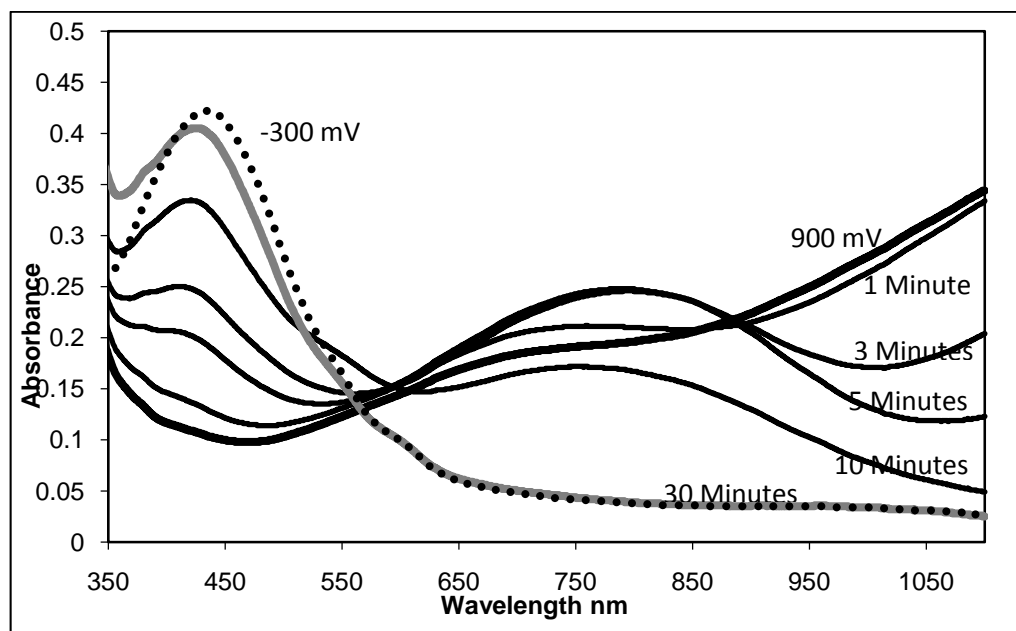


Figure 6.11. The UV-visible absorbance spectrum of a POTE fibre mat on ITO glass in 0.1 M TBAP acetonitrile, showing the spectrum at -300 mV, 900 mV and several time intervals after application of 900 mV to oxidise the fibres, leaving them in electrolyte.

A review of the literature revealed several reports on the dedoping of polythiophenes. These reports mainly concentrate on poly(3-alkylthiophenes) (P3AT's) and show the dedoping of these polymers under a range of conditions.^[27-29] The dedoping of P3AT's is reported to occur faster at higher temperatures^[30] and under illumination by UV light.^[29] Dedoping of P3AT's is also reported to be anion dependant.^[28, 31] Water is known to increase the rate of dedoping as it is able to reduce the polymer with hydroxide acting as an electron donor.^[27, 32] In the absence of water, dedoping still occurs however the rate is slower.^[33] Changing the structure and regioregularity of the polymer, giving space for closer interaction between the dopant and the polymer backbone, is reported to increase doping stability.^[34] Poly(3-alkoxythiophenes) are significantly more stable than P3AT's due to the absence of a benzylic proton donor atom connected to the polymer backbone.^[35]

The dedoping of polythiophenes is a significant issue for the application of these materials.^[31] We thus sought to investigate the doping stability of our polymer films in cell culture medium, which is similar to the conditions that materials will encounter in bionic applications. The chemically produced polymers POTE, PHET and PDDTTC_c were deemed most suitable for investigation, as these materials could be spin coated onto ITO glass to give thin uniform films that are ideal for studying by UV-visible spectroscopy. The study was performed as follows. Polymer films were oxidised in an acetonitrile electrolyte containing 0.1 M TBAP, by applying a potential of 0.8 V for 2 minutes. The oxidised films were quickly washed and placed in a cuvette containing cell culture medium, and the UV-visible spectra monitored over time.

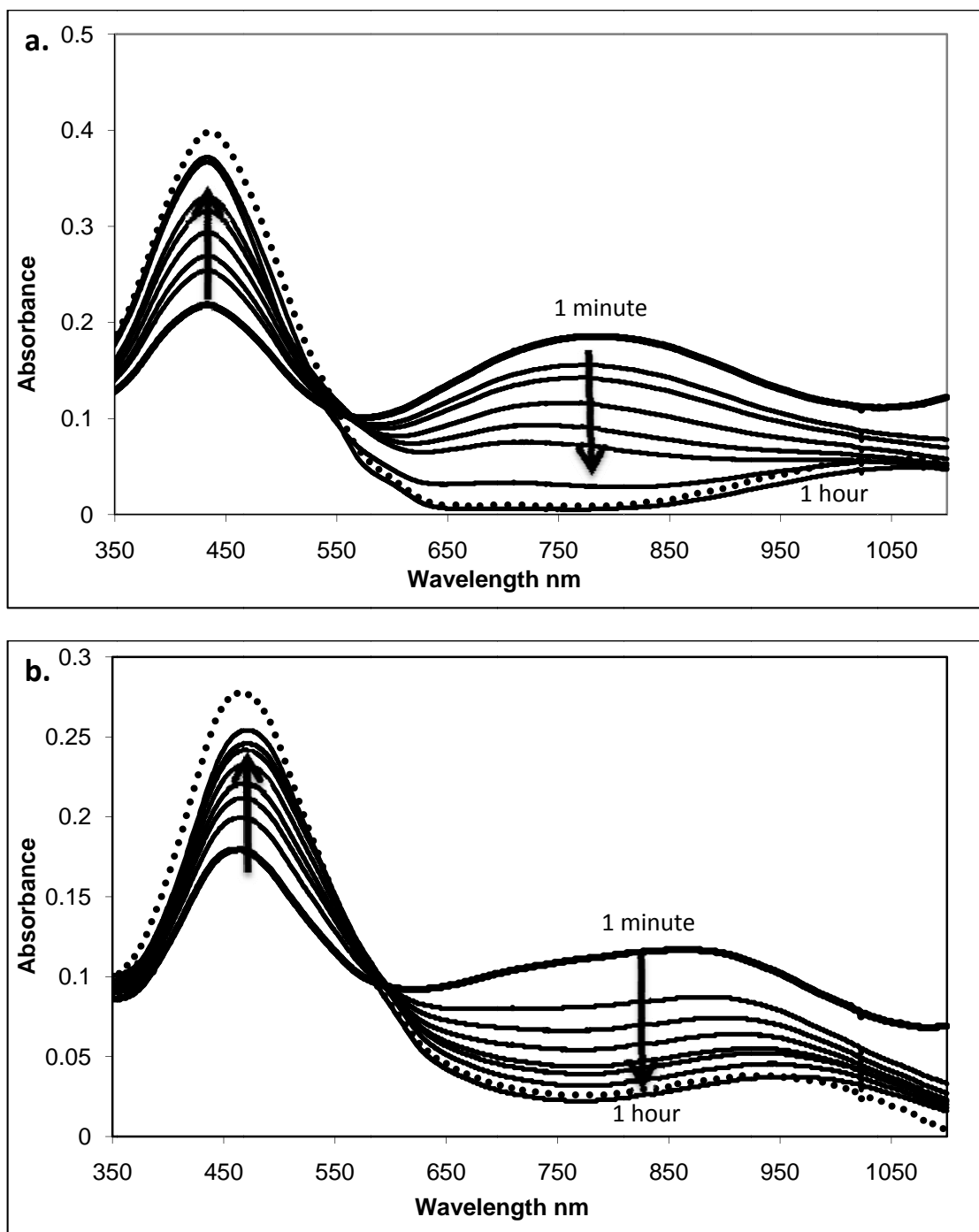


Figure 6.12. UV-visible spectra showing the reduction of perchlorate doped polymer films over time in cell culture medium: **a.** POTE **b.** PHET. The arrows show the changes in the spectra over time between 1 minute and 1 hour with the dotted lines showing the spectra for the reduced form of the polymer.

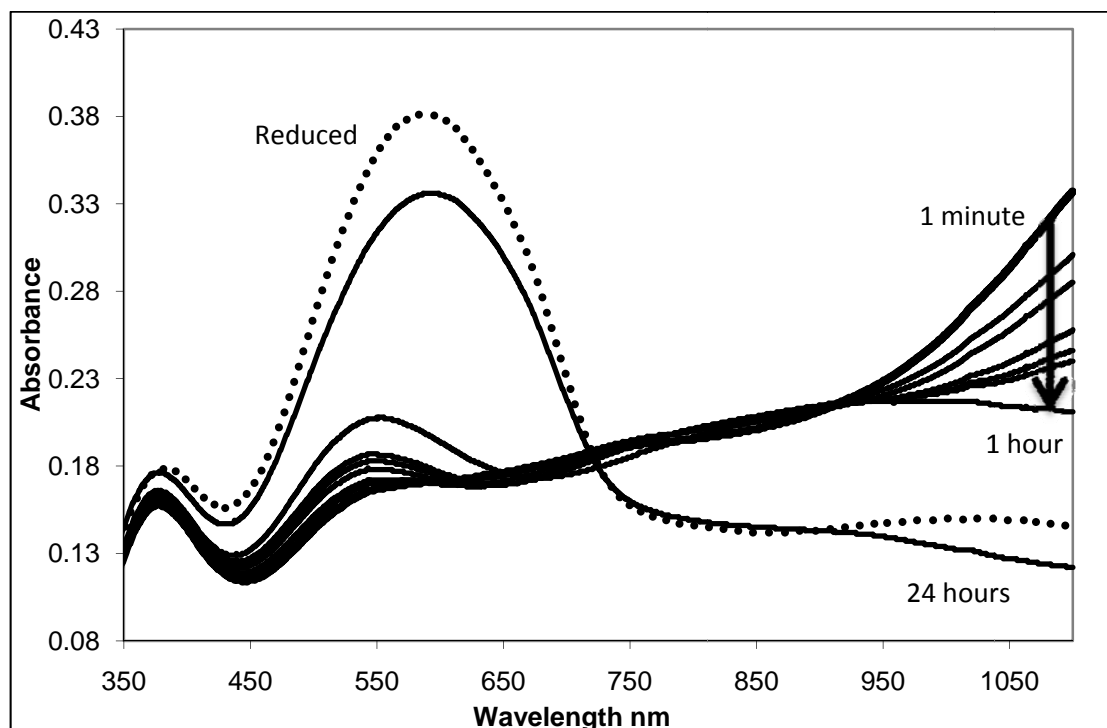


Figure 6.13. UV-visible spectra showing the reduction of a perchlorate doped PDDTTC_c polymer film over time in cell culture medium. The arrow shows the change in the spectra over time between 1 minute and 1 hour, the spectrum after 24 hours is also shown, the dotted lines showing the spectrum for the reduced form of the polymer.

All three polymer film samples that were tested showed autoreduction, the POTE and PHET were seen to reduce very quickly with a large drop in the free carrier tail observed in the first few minutes (Figure 6.12). The polymer films are clearly reduced even before the first one minute measurement (compare 900 mV POTE spectrum in Figure 6.11 with one minute scan in Figure 6.12a). After approximately one hour these samples were almost completely reduced. The fast rate of reduction is not surprising given that the polymer films are in aqueous medium and water is known to increase the rate of polymer reduction.^[27, 32] The PDDTTC_c (Figure 6.13) was slower to reduce with the UV-visible spectrum showing that the polymer is still predominantly in the oxidised form after one hour, however after 24 hours, the

sample was in the reduced form. The increased stability of the PDDTTC_c is consistent with observations in the literature where poly(3-alkoxythiophenes) were seen to be stably doped.^[35] The maximum absorbance of the peak due to the reduced polymer (450 nm or 550 nm) was not reached (Figure 6.12). This is likely because some polarons are trapped within defect sites of the polymers making it difficult to fully reduce the polymers under mild conditions.^[27]

Another dopant commonly used in our laboratories to dope polythiophenes is *para*-toluenesulfonate. The stability of polymers in their oxidised state is reported to vary between dopants,^[28, 31] and, thus, we investigated the doping stability of POTE and PHET films with the *para*-toluenesulfonate dopant. The doping stability was investigated by the same method as above for the perchlorate dopant. As can be seen in Figure 6.14, the *para*-toluenesulfonate dopant gave less stably doped films for both polymers. The films were observed to revert to the oxidised form within 30 minutes.

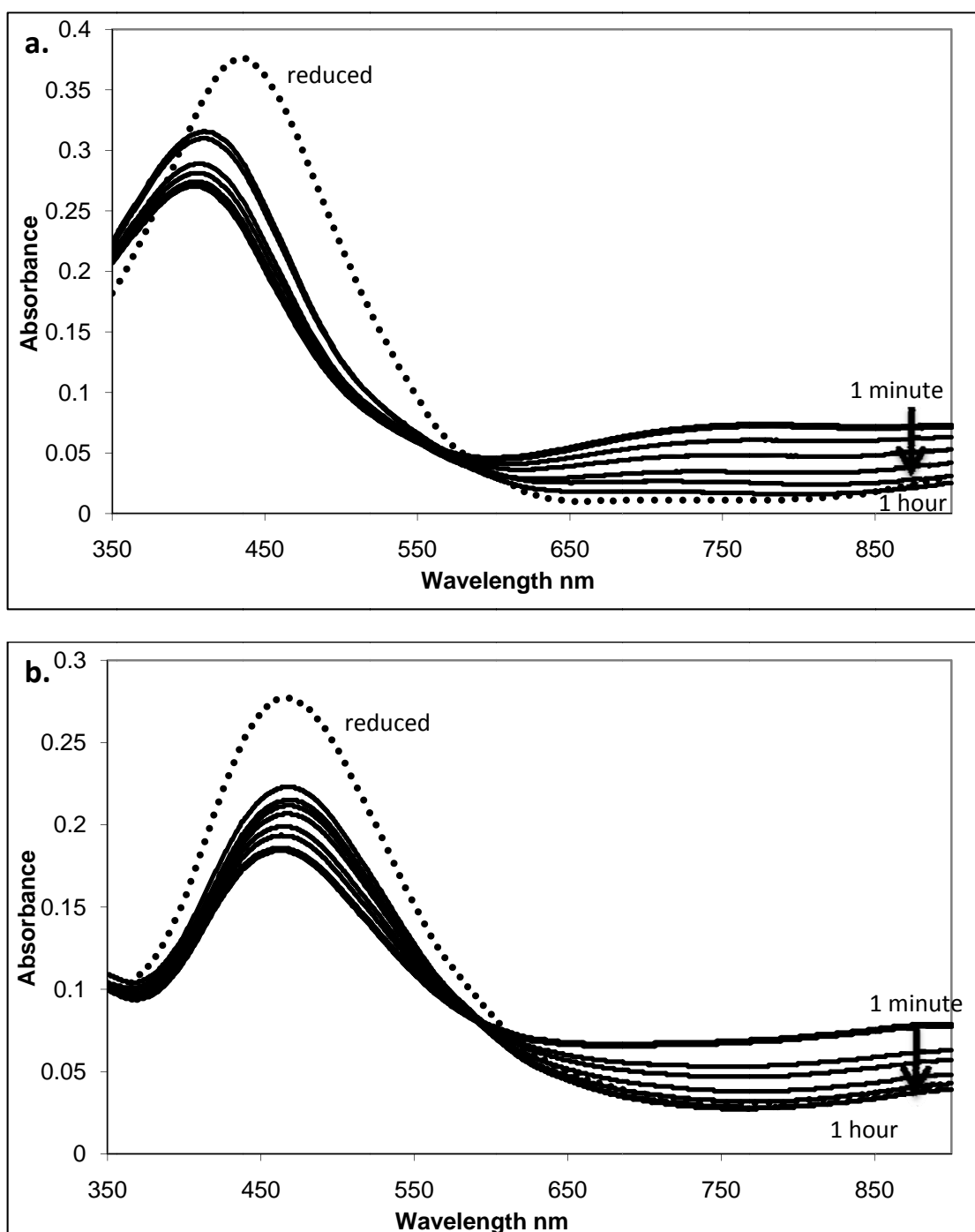


Figure 6.14. UV-visible spectra showing the reduction of *para*-toluenesulfonate doped polymer films over time in cell culture medium: **a.** POTE **b.** PHET. The arrows show the changes in the spectra over time between 1 minute and 1 hour with the dotted lines showing the spectra for the reduced form of the polymer.

The autoreduction of polythiophenes is a significant challenge that needs to be overcome if these materials are to be used for *in vivo* electrical stimulation applications. In some instances, the polymers may be held at an oxidising potential, which would keep them in the conductive form. However, in other applications, continuously applying an oxidising potential is not feasible. There remains the possibility that polymeric dopants incorporated during polymer growth or film fabrication could improve oxidised polymer stability, an investigation for future researchers in this field. The increase in the stability of the PDDTTC_c is a promising result, and shows how different substituents can be incorporated to enhance the stability of the oxidised state of the polymer.

6.5 Conclusions.

Polythiophene films were synthesised both chemically and electrochemically and characterised by a range of techniques contact angle measurements, electrochemistry and SEM. The doping stability of the chemically produced polymers was assessed by UV-visible spectroscopy, which showed that polythiophene materials do not stay oxidised in cell culture medium, posing a challenge to the application of polythiophenes in this area. PDDTTC remained oxidised longer than POTE and PHET, which offers promise for improving the doping stability of materials in the future. More work is needed in the future to optimise the structure and dopant of polythiophene materials to prevent dedoping in aqueous environments.

The biocompatibility of the polymer films was assessed; all the materials were seen to be compatible with the robust C2C12 cell line. Differentiation of ROSA cells was also assessed on these materials, these cells are more particular and differences were noted between the polymers. Cells were seen to be more biocompatible with the smoother spin coated films than the electrochemically produced films. To a lesser degree the cells were also more biocompatible with hydrophilic films such as the alcohol functionalised POTE.

Fibre structures were shown to be biocompatible; random fibre mats supported the growth of C2C12 cells. Aligned fibre mats were shown to guide ROSA cell differentiation. Medium density aligned fibre mats gave the best degree of alignment, with enough fibres present to give directional cues but not so many fibres that the surface is overly rough. No difference was seen between the POTE and PHET fibres.

6. 6 References.

- [1] L. J. del Valle, D. Aradilla, R. Oliver, F. Sepulcre, A. Gamez, E. Armelin, C. Aleman, F. Estrany, *European Polymer Journal* **2007**, *43*, 2342.
- [2] *McGraw-Hill Concise Dictionary of Modern Medicine.*, The McGraw-Hill Companies, Inc., **2002**. New York.
- [3] D. Williams, *Biocompatibility of Implant Materials*, **1976**. London.
- [4] N. K. Guimard, N. Gomez, C. E. Schmidt, *Progress in Polymer Science* **2007**, *32*, 876.
- [5] M.-Y. Li, P. Bidez, E. Guterman-Tretter, Y. Guo, A. G. MacDiarmid, P. I. Lelkes, X.-B. Yuan, X.-Y. Yuan, J. Sheng, H. Li, C.-X. Song, Y. Wei, *Chinese Journal of Polymer Science* **2007**, *25*, 331.
- [6] P. R. Bidez, III, S. Li, A. G. MacDiarmid, E. C. Venancio, Y. Wei, P. I. Lelkes, *Journal of Biomaterials Science, Polymer Edition* **2006**, *17*, 199.
- [7] E. Guterman, S. Cheng, K. Palouian, P. Bidez, P. Lelkes, Y. Wei, *Abstracts of Papers, 224th ACS National Meeting, Boston, MA, United States, August 18-22, 2002*,
- [8] M. Waugaman, B. Sannigrahi, P. McGeady, I. M. Khan, *European Polymer Journal* **2003**, *39*, 1405.
- [9] D.-F. Li, H.-J. Wang, J.-X. Fu, W. Wang, X.-S. Jia, J.-Y. Wang, *Journal of Physical Chemistry B* **2008**, *112*, 16290.
- [10] K. J. Gilmore, unpublished results, University of Wollongong, **2008**.
- [11] U. Wehrle, S. Duesterhoeft, D. Pette, *Differentiation (Berlin, Germany)* **1994**, *58*, 37.

- [12] S. Dusterhoft, D. Pette, *Differentiation; research in biological diversity* **1990**, 44, 178.
- [13] R. G. Dennis, P. E. Kosnik, II, M. E. Gilbert, J. A. Faulkner, *American Journal of Physiology* **2001**, 280, C288.
- [14] S. A. Ashraf, F. Chen, C. O. Too, G. G. Wallace, *Polymer* **1996**, 37, 2811.
- [15] H. Masuda, S. Tanaka, K. Kaeriyama, *Synthetic Metals* **1989**, 33, 365.
- [16] M. Feldhues, G. Kaempf, H. Litterer, T. Mecklenburg, P. Wegener, *Synthetic Metals* **1989**, 28, C487.
- [17] J. Roncali, *Chemical Reviews (Washington, DC, United States)* **1992**, 92, 711.
- [18] S. Gambhir, K. Wagner, D. L. Officer, *Synthetic Metals* **2005**, 154, 117.
- [19] P. Costa Bizzarri, F. Andreani, C. Della Casa, M. Lanzi, E. Salatelli, *Synthetic Metals* **1995**, 75, 141.
- [20] C. Shi, Y. Yao, Y. Yang, Q. Pei, *Journal of the American Chemical Society* **2006**, 128, 8980.
- [21] G. Koeckelberghs, M. Vangheluwe, K. Van Doorselaere, E. Robijns, A. Persoons, T. Verbiest, *Macromolecular Rapid Communications* **2006**, 27, 1920.
- [22] G. Koeckelberghs, M. Vangheluwe, C. Samyn, A. Persoons, T. Verbiest, *Macromolecules* **2005**, 38, 5554.
- [23] A. S. Curtis, J. V. Forrester, C. McInnes, F. Lawrie, *The Journal of cell biology* **1983**, 97, 1500.
- [24] C. D. Bain, G. M. Whitesides, *Science (Washington, DC, United States)* **1988**, 240, 62.

- [25] W. F. Zhang, P. Schmidt-Zhang, G. Kossmehl, *Journal of Solid State Electrochemistry* **2001**, *5*, 74.
- [26] G. Zotti, G. Schiavon, A. Berlin, G. Pagani, *Synthetic Metals* **1991**, *40*, 299.
- [27] W. Chun-Guey, C. Mei-Jui, L. Yii-Chung, *Journal of Materials Chemistry* **1998**, *8*, 2657.
- [28] Y. Wang, M. F. Rubner, *Synthetic Metals* **1990**, *39*, 153.
- [29] M. S. A. Abdou, S. Holdcroft, *Chemistry of Materials* **1994**, *6*, 962.
- [30] M. T. Lopenen, T. Taka, J. Laakso, K. Vakiparta, K. Suuronen, P. Valkeinen, J. E. Osterholm, *Synthetic Metals* **1991**, *41*, 479.
- [31] J. L. Ciprelli, C. Clarisse, D. Delabouglise, *Synthetic Metals* **1995**, *74*, 217.
- [32] Y. Li, R. Qian, *Synthetic Metals* **1993**, *53*, 149.
- [33] H. Koizumi, H. Dougauchi, T. Ichikawa, *Journal of Physical Chemistry B* **2005**, *109*, 15288.
- [34] M. C. Magnoni, M. C. Gallazzi, G. Zerbi, *Acta Polymerica* **1996**, *47*, 228.
- [35] K. Hatakeyama, H. Koizumi, T. Ichikawa, *Bulletin of the Chemical Society of Japan* **2009**, *82*, 202.

CHAPTER 7. GENERAL CONCLUSIONS.

The aim of this project was to investigate novel conductive polythiophenes for bionic applications. As many bionic applications require materials which are processable, biodegradable, biocompatible and multifunctional, the incorporation of these aspects into functionalised polythiophene materials was investigated.

Chapter 3 describes the synthesis of basic terthiophene building blocks and their further functionalisation to optimise the materials for bionic applications. Suzuki coupling was utilised to synthesise a range of basic terthiophenes containing alkoxy chains and ester functionalities. Terthiophene acids 4,4''-didecoxy-2,2':5',2''-terthiophene-3'-carboxylic acid **15** and 4,4''-didecoxy-2,2':5',2''-terthiophene-3'-acetic acid **16** were synthesised by ester hydrolysis and used for further functionalisation.

The attachment of barbituric acid, amino acids and spiropyran to acids **15** and **16** as well as other suitable terthiophenes was investigated. The barbituric acid functionalised polymer was found to be insoluble and thus could not be processed for use in bionic applications. This highlighted the importance of solubility in producing processable materials. Amino acid functionalised polymers were successfully synthesised. The DCC coupling chemistry used to create these functional polymers could be utilised in the future for the attachment of peptides and proteins, to further enhance the biocompatibility of such conducting polymers. Two spiropyran functionalised terthiophene monomers TTSPA and TTSPC were successfully

synthesised. These molecules were observed to bind metal ions in their open merocyanine form. The analogous functional polymers PTTSPA and PTTSPC could be stimulated to open to their merocyanine forms by applying 0.9 V. Such functional polymers could be utilised in bionics for controlled release and sensing applications.

The synthesis of novel thiophene oligomers was investigated in Chapter 4 for the development of biodegradable conducting polymers. Azomethine linked thiophene oligomers were investigated and these were found to be degradable under acidic conditions as well as being electroactive. The synthesis of novel sexithiophenes was also investigated, with the alkoxy functionalised bromoterthiophenes precursors showing autopolymerisation. Autopolymerisation of these terthiophenes is an interesting phenomenon which warrants further investigation in the future. Several novel ester functionalised terthiophene and sexithiophene materials were synthesised and these materials will be useful as building blocks when making polymers for bionic applications in the future.

Chapter 5 describes investigations into the fabrication of polythiophene scaffolds. A simple ester functionalised polymer, POTE, was synthesised and could be fabricated into both films and electrospun fibres. The electrospun fibres were produced as both random and aligned mats. Such aligned fibre mats are ideal scaffolds to support the regeneration and guide alignment of tissues. Significantly, these structures could be hydrolysed to PHET making more hydrophilic structures. This hydrolysis improved the electroactivity of the polythiophene structures in aqueous electrolyte. Further surface modification of these polymer structures was investigated by esterification of the material with ferrocene acid chloride. This functionalisation by ferrocene

demonstrated the versatility of these structures to further modification; thus they can be tailored to a range of bionic applications.

In Chapter 6, the biocompatibility of a range of polythiophene materials was investigated. A range of simple polythiophenes films were prepared by electrochemical polymerisation as well as chemical polymerisation and spin coating. The POTE and PHET film and fibre structures were also investigated. The doping stability of several of the spin coated polythiophene films was investigated by UV-visible spectroscopy. The films were observed to dedope when placed in an aqueous environment. The alkoxy functionalised PDDTTC_c was found to be more stably doped than the POTE and PHET materials, however still dedoped over a 24 hour period. The doping stability of these polythiophene materials needs to be investigated further if they are to be applied to stimulate tissue in bionic applications.

All polythiophene films investigated were able to support the growth and differentiation of the robust, C2C12 cell line. Polymer films were also able to promote the differentiation of the more sensitive ROSA cell line to varying degrees with POTE being the best polymer and POP the worst. The degree of differentiation was compared against the physical properties of the polymer films. It was observed that the smoother spin coated films acted as better scaffolds to support differentiation. To a lesser degree, the cells were also more biocompatible with hydrophilic films. POTE and PHET electrospun fibre mats were also used as scaffolds for cell growth. These mats were able to support the growth of cells. Medium density aligned mats with spacings around 15 µm between fibres were best able to control the direction of differentiation of ROSA cells.

Overall, polythiophenes are promising materials for bionic applications. Here the ability of these materials to be optimised for applications through functionalisation has been demonstrated through the synthesis of spiropyran and amino acid functionalised materials. Novel thiophene oligomers were synthesised and shown to be useful building blocks for potentially biodegradable conducting polymers. The soluble ester functionalised POTE demonstrated the suitability of such materials to structure fabrication as well as further modification of structures through surface chemistry.

This research also identified significant challenges that need further investigation before polythiophenes can be applied in real world bionic applications. These include the dedoping of polythiophene materials in aqueous environments, the low solubility of functionalised materials leading to difficulty in processing and the difficult balance between stability and degradability for creating biodegradable conductive systems. This work has shown that polythiophenes have great promise in bionic applications, being biocompatible (able to support the growth and differentiation of muscle cells), processable and highly amenable to functionalisation. No doubt the ease of functionalisation of these materials will lead to many diverse applications in the future.